Vol. 151, No. 2, August 1, 1983
Completing Vol. 151
ISSN 0003-2670

ANALYTICA CHIMICA ACTA

International journal devoted to all branches of analytical chemistry

ELSEVIER SCIENTIFIC PUBLISHING COMPANY

ANALYTICA CHIMICA ACTA

International journal devoted to all branches of analytical chemistry
Revue internationale consacrée à tous les domaines de la chimie analytique
Internationale Zeitschrift für alle Gebiete der analytischen Chemie

PUBLICATION SCHEDULE FOR 1983

	J	F	M	A	M	J	J	A	S	O	N	D
Analytica Chimica Acta	145	146	147	148	149	150/1 150/2	151/1	151/2	152	153	154	155

Scope. *Analytica Chimica Acta* publishes original papers, short communications, and reviews dealing with ev aspect of modern chemical analysis, both fundamental and applied.

Submission of Papers. Manuscripts (three copies) should be submitted as designated below for rapid and effici handling:

Papers from the Americas to: Professor Harry L. Pardue, Department of Chemistry, Purdue University, West Lafaye IN 47907, U.S.A.

Papers from all other countries to: Dr. A. M. G. Macdonald, Department of Chemistry, The University, P.O. Box 3 Birmingham B15 2TT, England. Papers dealing particularly with computer techniques to: Professor J. T. Cle Universität Bern, Pharmazeutisches Institut, Baltzerstrasse 5, CH-3012 Bern, Switzerland.

Submission of an article is understood to imply that the article is original and unpublished and is not being consider for publication elsewhere. Upon acceptance of an article by the journal, authors resident in the U.S.A. will be asked transfer the copyright of the article to the publisher. This transfer will ensure the widest dissemination of informati under the U.S. Copyright Law.

Information for Authors. Papers in English, French and German are published. There are no page charg Manuscripts should conform in layout and style to the papers published in this Volume. Authors should cons Vol. 132, p. 239 for detailed information. Reprints of this information are available from the Editors or from: Elsev Editorial Services Ltd., Mayfield House, 256 Banbury Road, Oxford OX2 7DH (Great Britain).

Reprints. Fifty reprints will be supplied free of charge. Additional reprints (minimum 100) can be ordered. An or form containing price quotations will be sent to the authors together with the proofs of their article.

Advertisements. Advertisement rates are available from the publisher.

Subscriptions. Subscriptions should be sent to: Elsevier Science Publishers B.V., P.O. Box 211, 1000 Amsterdam, The Netherlands.

Publication. *Analytica Chimica Acta* appears in 11 volumes in 1983. The subscription for 1983 (Vols. 145–155) Dfl. 1980.00 plus Dfl. 220.00 (postage) (total approx. U.S. $880.00). Journals are sent automatically by airmail to t U.S.A. and Canada at no extra cost and to Japan, Australia and New Zealand for a small additional postal charge. earlier volumes (Vols. 1–144) except Vols. 23 and 28 are available at Dfl. 200.00 (U.S. $80.00), plus Dfl. 15.00 (U $6.00) postage and handling, per volume.

Claims for issues not received should be made within three months of publication of the issue, otherwise they cann be honoured free of charge.

Customers in the U.S.A. and Canada who wish to obtain additional bibliographic information on this and otl Elsevier journals should contact Elsevier Science Publishing Company Inc., Journal Information Center, 52 Vanderl Avenue, New York, NY 10017. Tel: (212) 867-9040.

Analytica Chimica Acta, 151 (1983) 281—295
Elsevier Science Publishers B.V., Amsterdam — Printed in The Netherlands

EVALUATION OF SOME PHYSICO-CHEMICAL TECHNIQUES FOR THE DETERMINATION OF THE FRACTION OF DISSOLVED COPPER TOXIC TO THE MARINE DIATOM *NITZSCHIA CLOSTERIUM*

T. M. FLORENCE*, B. G. LUMSDEN[a] and J. J. FARDY

CSIRO Division of Energy Chemistry, Private Mail Bag 7, Sutherland, N.S.W. 2232 (Australia)

(Received 15th February 1983)

SUMMARY

The toxicity of copper to the marine diatom *Nitzschia closterium* was determined by growth rate measurements in the presence of a range of copper complexing agents, both natural and synthetic. The measurements were made in raw, unenriched sea water to avoid the reaction of copper with silicate or colloidal hydrated iron(III) oxide which occurs in standard culture media. The algae remained in exponential growth for at least 72 h in unenriched sea water and, in the presence of copper, produced an exudate which decreased the concentration of labile copper. Labile copper was measured in the algal assay solutions by using anodic stripping voltammetry (a.s.v.) at different deposition potentials, by separation on iminodiacetate (Chelex-100) and thiol resins, and by extraction with hexane/n-butanol (9:1) to simulate lipid solubility. No consistent correlation was observed between the toxic fraction of copper measured by algal assay, and the labile copper determined by the physico-chemical techniques. Although some of the naturally-occurring ligands (e.g., fulvic acid and iron—humic acid colloid) gave reasonable agreement between the toxic fraction and a.s.v.-labile copper, the chelating resins usually grossly overestimated toxicity. Lipid-soluble complexes of copper with synthetic ligands (e.g., 8-quinolinol and diethyldithiocarbamate) were highly toxic; as little as 2 μg Cu l^{-1} in the presence of 5×10^{-8} M 8-quinolinol caused complete depression of algal growth. It is proposed that the extreme toxicity of lipid-soluble copper complexes results from their ability to catalyse the intercellular formation of highly destructive hydroxyl free radicals (OH·) from molecular oxygen, in a Fenton-type reaction.

A recent study [1] of the effect of model ligands on the speciation of copper, lead, cadmium and zinc, led to the conclusion that in most natural waters a large fraction of each of these metals is bound in highly stable complexes by unidentified organic ligands. In addition, some water samples were found to contain a significant percentage of lipid-soluble metal. Anodic stripping voltammetry (a.s.v.), and treatment with iminodiacetate, 8-quinolinol and thiol chelating resins yielded quite different values for the labile metal fraction.

Stephan [2], Young et al. [3], Srna et al. [4] and Borgmann [5] found

[a]Present address: OKTEDI Mining Corp., Port Moresby, Papua-New Guinea.

0003-2670/83/$03.00

correlations between a.s.v.-labile metal and biotoxicity, although the a.s.v. conditions used varied considerably. The a.s.v. technique measures several other labile metal forms in addition to the free metal ion, which has been identified by many investigators, using computer modelling, as the species most toxic to aquatic biota [6—12]. The hydroxy complexes of copper are also believed to be toxic [13]. Florence [1, 14] pointed out that lipid-soluble metal complexes are often neglected in biotoxicity studies, even though some such compounds are known to be strongly bio-accumulated and highly toxic [15—17].

Algal assays are usually conducted in the media in which the algae are cultured [18, 19]. For marine studies, the most commonly-used media are the *f* and *f*/2 enriched sea-water mixtures of Guillard and Ryther [20], or the chemically-defined synthetic medium, Aquil [21]. These media contain substances such as phosphate, citrate and EDTA which complex the heavy metal ions being tested for toxicity. Aquil was designed for accurate computation of free metal ion activity from knowledge of total metal added, although important active agents such as colloidal hydrated iron(III) oxide and silicic acid were not taken into account in the equilibrium calculations because the relevant equilibrium constants are unknown [22]. It was shown recently that both silicic acid and hydrated iron(III) oxide decreased a.s.v.-labile copper in sea water [23]. To overcome this problem, which complicates the interpretation of metal—ligand interactions with algae, an algal assay procedure was devised in which the alga was cultured in a modified *f* medium, but assays were conducted in raw, unenriched sea water [23]. As reported previously by Erickson [24], raw sea water can maintain algae in exponential growth for at least 72 h.

This investigation with copper in sea water was undertaken to establish the relationship between labile copper, measured by various physico-chemical techniques, and the toxic fraction of copper determined by algal assay. A range of model copper-complexing agents was studied, to identify those which either ameliorate or enhance the toxicity.

EXPERIMENTAL

Apparatus and reagents

An E.G. and G. Princeton Applied Research Model 384 Polarographic Analyzer, with a Model 303 static mercury drop electrode assembly, was used for all a.s.v. measurements. The a.s.v. conditions were: deposition time, 300 s; pulse amplitude, 25 mV; scan rate, 2 mV s^{-1}; drop size, medium. Electrode potentials refer to the silver—silver chloride reference.

All water filtration, ion exchange, and analytical procedures were done in a class-100 clean room at 25 ± 0.5°C.

The Chelex-100 and thiol resin [25] columns were prepared and maintained as described previously [1], as were the soil-derived fulvic acid and the iron(III)—humic acid colloids. Sodium acetate, nitric acid, and perchloric acid were Merck Suprapur. Water was reverse-osmosis Milli-Q.

Surface sea water was collected [1] 2 km off Port Hacking, New South Wales, in polyethylene bottles, and filtered on the day of collection through a layer of activated charcoal on a 0.45-μm membrane filter. The filtered sea water was stored at 4°C, and typically contained 0.6 $\mu g\ l^{-1}$ total copper, 0.2 $\mu g\ l^{-1}$ a.s.v.-labile copper, and 1.8 $\mu g\ l^{-1}$ total iron, determined as described by Martin [26]. After the water had passed through a column of Chelex-100 resin, the equivalent concentrations were 0.5 $\mu g\ l^{-1}$, 0.1 $\mu g\ l^{-1}$, and $<0.5\ \mu g\ l^{-1}$, respectively.

Determination of copper

The labile and total copper contents in the sea-water samples were determined by a.s.v. Labile measurements were made at the natural pH (pH 8.2), using deposition potentials of −0.6 V and −1.3 V (peak potential was −0.28 V), and in acetate buffer pH 4.7 (0.2 ml of 3 M buffer per 10 ml of sea water). Total copper was determined [1] after adding 0.2 ml of 4 M HNO_3 and 0.05 ml of 30% H_2O_2 to 10 ml of sea water, irradiating with a 550 W mercury lamp for 12 h, and then adding 0.4 ml of 4 M sodium acetate. Copper in the algae was determined by filtering 60 ml of the algal suspension through an acid-washed membrane filter (25 mm diameter, 0.45 μm). Tests showed that no dissolved copper was adsorbed by the filter and, to avoid surface adsorption, all glass surfaces were siliconized. The membrane filter was digested in a 25-ml covered beaker with 2 ml of water, 1 ml of 15 M HNO_3, and 0.5 ml of 72% $HClO_4$ to strong fumes of perchloric acid. This solution was diluted with water to 10 ml and copper was determined directly in it by a.s.v., using a standard addition procedure. An acid-washed membrane filter was used as a blank. The blank copper value varied considerably between batches of filters, but was constant within a batch.

Separations with Bio-Rad Chelex-100 resin and with thiol resin [25] were conducted in 10 cm × 0.7 cm diameter columns as described previously [1]. Total copper was measured in the column feed and effluent solutions, and resin-labile copper was determined by difference. Lipid-soluble copper was measured by extracting 10 ml of sea water with 5 ml of n-hexane/n-butanol (9:1), and determining copper in the aqueous phase [1]. It is commoner to use n-octanol as a model for lipid solubility [27], but a much lower copper blank was obtained [1] with spectroscopic-grade n-hexane.

Algal assays

An inoculum of the marine diatom *Nitzschia closterium* was obtained from the culture bank of Dr. S. W. Jeffrey, CSIRO Division of Fisheries, Cronulla. The alga was cultured in filtered sea water (100 ml in 500-ml conical flasks) enriched with the following nutrients: $NaNO_3$, 0.15 g l^{-1}; $NaH_2PO_4 \cdot 2H_2O$, 0.01 g l^{-1}; SiO_2, 6.0 mg l^{-1}; iron(III) citrate, 9 $\mu g\ l^{-1}$; citric acid, 9 $\mu g\ l^{-1}$; thiamine hydrochloride, 200 $\mu g\ l^{-1}$; biotin, 1 $\mu g\ l^{-1}$; vitamin B_{12}, 1 $\mu g\ l^{-1}$. The stock silicon solution (2.8 g l^{-1}) was prepared from spectroscopic-grade silica and the minimum amount of sodium hydroxide. No other

trace elements were added, and the iron(III) concentration was a factor of 10^3 lower than that used by Guillard and Ryther in their *f* medium [20]. The algal cultures were maintained at 21°C as described previously [23], on a light box (6,400 lux) and a 12 h/12 h light/dark cycle. Transfers under axenic conditions were done every seven days into autoclaved culture medium. Algal suspensions 4—5 days after transfer (exponential growth phase) were used for algal assays.

Algal assays were conducted in 50-ml culture tubes, using 30 ml of sea water and an initial cell density of $2—4 \times 10^4$ cells per ml [23]. Cell density was measured after preparation and on three subsequent days, using a haemocytometer. A regression line was fitted to a plot of $\log_{10}$ (cell density/initial cell density) versus time (in hours) for each sample, and growth rate (h^{-1}) was determined from the slope. For copper—ligand mixtures, aliquots of a standard copper(II) sulphate solution (5 mg Cu l^{-1}) were mixed with 0.1 ml of ligand solution and 30 ml of sea water in culture tubes. An aliquot of the algal suspension, washed with sea water, was added after one hour. Each solution was prepared in duplicate, and additional tubes were used for daily speciation measurements. The "toxic" concentration of copper was determined from the measured growth rate and a calibration curve of per cent depression of blank growth rate versus added (ionic) copper. Correction was made when necessary for the effect of ligand alone on growth rate. Ethanol, up to 0.2 ml per 30 ml of sea water, had no effect on growth rate.

RESULTS AND DISCUSSION

The Guillard and Ryther [20] culture media were found [23] to have significant copper-reacting capacity, resulting principally from colloidal hydrated iron(III) oxide and silicic acid. Rueter et al. [22], using a copper ion-selective electrode, found no reaction in sea water between copper(II) and millimolar concentrations of silicic acid. However, a.s.v. measurements showed that $Si(OH)_4$ does react with copper(II) in sea water (Fig. 1). It is not clear if the reaction involves a molecular silicato copper complex, as has been reported for calcium and iron(III) [28], or if copper ions are sorbed on colloidal silica. The non-proportionality of the percent depression of the copper peak versus silicon concentration (Fig. 1a) suggests that an adsorption mechanism is operative. Reactive silicon in the oceans is unlikely to be sufficiently high to affect labile copper, but it could have some influence in estuaries [29].

The effect of algae on a.s.v.-labile copper was determined in sea water in which algae had been grown for 72 h. Both filtered and unfiltered samples were examined by a.s.v., and the copper content of the algae was measured (Table 1). Filtrates for *Nitzschia* grown in sea water with no added copper had no complexing capacity [1]. Table 1 shows that *Nitzschia*, at an initial cell density of $2—4 \times 10^4$ cells/ml, produces an exudate which complexes about 20 μg Cu l^{-1}. However, the filtrates from the copper-containing algae

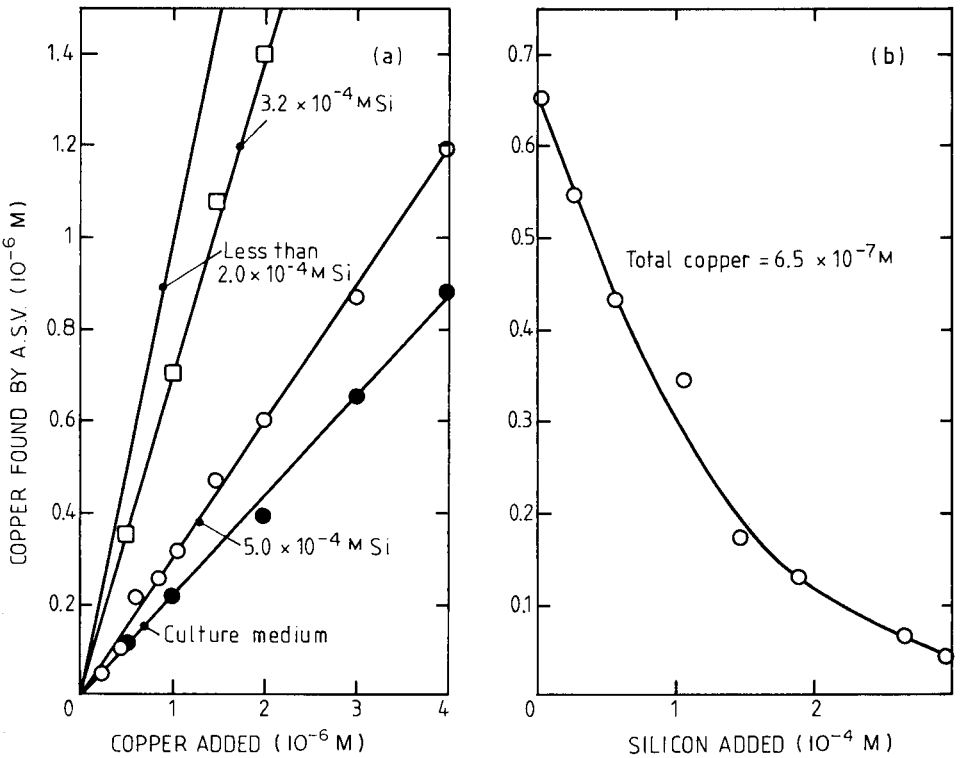

Fig. 1. Reaction between copper(II) and silicon in sea water. (a) The a.s.v. determination of copper in sea water (pH 8.2) and the culture medium in presence of different amounts of silicon: (—) <2.0 × 10^{-4} M Si; (□) 3.2 × 10^{-4} M Si; (○) 5.0 × 10^{-4} M Si; (•) culture medium. (b) The a.s.v. determination of 6.5 × 10^{-7} M copper in sea water (pH 8.2) after the addition of various aliquots of 0.100 M silicon (prepared from spectroscopic-grade silica dissolved in the minimum quantity of Merck Suprapur sodium hydroxide); total copper present is 6.5 × 10^{-7} M.

TABLE 1

Effect of *Nitzschia closterium* on labile copper in sea water
(pH 8.2, initial cell density = 2—4 × 10^4 cells ml^{-1}, measured after 72 h growth)

Copper added ($\mu g\ l^{-1}$)	A.s.v.-labile copper ($\mu g\ l^{-1}$)				Total copper in filtrate ($\mu g\ l^{-1}$)	Copper on algae ($\mu g\ l^{-1}$)
	—0.6 V[a]		—1.3 V[a]			
	Unfiltered	Filtered	Unfiltered	Filtered		
5.0	1.05	1.15	2.3	2.3	4.7	1.0
10.0	2.3	2.3	5.5	5.3	7.9	2.2
17.5	5.7	5.5	9.1	8.6	9.5	8.2
35.0	20.2	9.0	26	16.7	26	8.9
50.0	44	17.6	49	21.2	42	10.1

[a]Deposition potential, V vs. Ag/AgCl.

solutions also had no additional complexing capacity. It appears, therefore, that *Nitzschia* does not produce exudate continuously, but only in response to copper ions, and the amount of exudate increases with the concentration of copper, but is never in excess. This is a reasonable situation, because the unprovoked production of protective compounds would be wasteful of energy.

Table 1 shows that the copper—exudate complex was, to some extent, directly reducible at —1.3 V [30, 31], and that some of the copper adsorbed on the algae was available to the electrode when total added copper was above about 20 $\mu g\ l^{-1}$. Leaching of copper-contaminated *Nitzschia* with fresh sea water removed 40—50% of the adsorbed copper, indicating that this proportion of copper was loosely bound. When *Nitzschia* was killed with 5% formalin, washed, and then suspended overnight in sea water containing 30 μg Cu l^{-1}, it adsorbed only 67% of the copper adsorbed by a live culture of the same final cell density. This result suggests that not all of the copper is simply physically adsorbed on the surface of the cell, but that some is metabolized.

A calibration graph of algal growth rate (expressed as per cent of blank growth rate) versus added copper is shown in Fig. 2. Specific growth rates for blanks were in the range 8—9 $\times$ 10^{-3} h^{-1}, and were not significantly different in sea water and in the culture medium. As found by other workers [6, 19], the data do not give a linear relationship between growth rate and the logarithm of copper concentration. If, however, a.s.v.-labile copper in

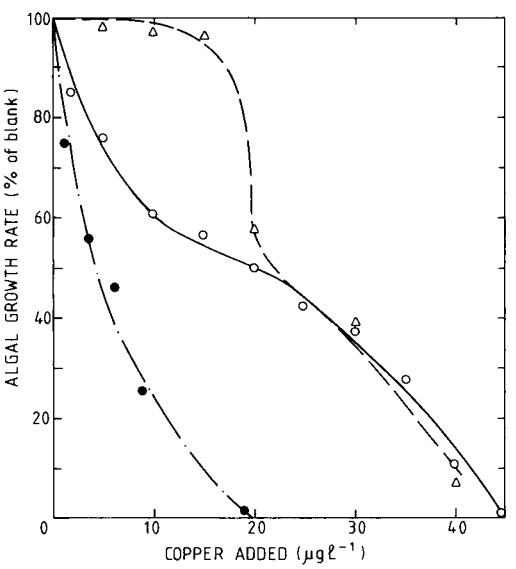

Fig. 2. Growth rate of *Nitzschia closterium* versus added copper(II) in sea water and culture medium. (○) Growth rate in raw sea water; (△) growth rate in culture medium (for composition, see text); (●) growth rate versus a.s.v.-labile copper (—0.6 V) in filtrate from algae in raw sea water.

solution, rather than total copper, is considered (Fig. 2), such a linear relationship is obtained. Growth measurements in the culture medium (Fig. 2) and in Guillard and Ryther media showed a higher tolerance for copper [23].

Results for copper speciation in the original (algae-free) copper—ligand mixtures in sea water are compared in Tables 2 and 3 with the algal assay results. Although full speciation analysis was done on filtrates after each day of algal growth, little additional insight into the relationship between the speciation of copper and its biotoxicity was provided by these measurements. Computer modelling based on the SIAS program for ionic equilibrium [32] was also done in cases for which reliable thermodynamic data in sea water were available [28]. No attempt was made to correct the results for complexing by algal exudate. There was no correlation between growth rate and the calculated concentration of free copper(II) ion.

Each of the complexing agents shown in Table 2 is discussed in more detail below.

Effects of complexing agents

Fulvic acid. The copper—fulvic acid complex shows little a.s.v. lability at −0.6 V and pH 8.2, is almost non-toxic to algae, and almost completely inhibits reaction of copper with the algae. The increased a.s.v.-labile fraction found at a deposition potential of −1.3 V indicates that some direct reduction of the complex takes place. Both Chelex-100 and thiol resins greatly overestimated the toxic fraction of copper. Conditional equilibrium constants (log K') of 9.71, 3.98, and 3.50 were used for the fulvic acid complexes of copper, magnesium, and calcium, respectively [33]. The molecular weight of marine fulvic acid was taken as 1 000 [34]. The ability of fulvic acid to affect a.s.v.-labile copper diminished rapidly with decreasing concentration of the ligand (Table 4); fulvic acid at a concentration of 1 mg l^{-1} caused only a 15% decrease in labile copper. In the oceans, which typically have fulvic acid concentrations of 0.1—0.7 mg l^{-1} [35], complexing with fulvic acid may not be significant.

Tannic acid and the iron—humic acid colloid. These two reagents ameliorate copper toxicity. The best correlations with the bio-assay results were a.s.v. at natural pH for tannic acid, and a.s.v. at either natural pH or pH 4.7 for the iron—humic acid colloid. The complete lability of the copper complexes to Chelex-100 and thiol resins suggests that copper ions can dissociate from the iron—humic acid colloidal particles during passage through the resin column [1]. The small percentage of copper which was extractable by hexane/butanol in the presence of the iron—humic acid colloid may have resulted from particles accumulating at the water/solvent interface.

Desferal. Desferal is the Ciba-Geigy trade name for a trihydroxamate siderophore [31]. Such compounds may be excreted by algae as protective agents against heavy metal toxicity [36]. Desferal increased the growth rate of a copper-free algae solution by 17%, possibly by complexing iron.

TABLE 2

Speciation and toxicity of copper complexes to *Nitzschia closterium*

Ligand[a]	Ligand conc. (10^{-6} M)	Percent of copper added[b]								Copper adsorbed on algae (10^{-13} g Cu/cell)	Depression of algal growth rate by ligand alone (%)
		A.s.v.-labile			Chelex-100 labile	Thiol labile	Solvent extractable[c]	Labile copper from growth curve[d]	Copper on algae		
		pH 8.2		pH 4.7							
		−0.6 V	−1.3 V	−0.6 V							
None	—	100	100	100	100	100	<10	100	42	0.75	—
Fulvic acid	10	1.5	29	41	66	100	<10	7.5	<5	<0.07	<10
Tannic acid	0.59	5.5	10.5	75	100	100	<10	12.5	77	0.66	<10
Iron—humic colloid	—[e]	70	74	65	100	100	13.0	60	53	0.80	<10
Desferal	2.0	100	95	100	95	100	<10	55	60	0.68	<10
Alginic acid	10 mg l^{-1}	100	100	100	95	100	27	155	58	0.90	<10
Lecithin	2.0	32	32	32	95	100	22	15	55	0.73	<10
LAS	0.5 mg l^{-1}	65	100	NQ	95	100	13.0	25	65	1.06	15
NTA	20	100	100	100	100	100	<10	20	40	0.25	23
Acetylacetone	2.0	100	100	100	100	100	25	95	56	0.72	12
Linoleic acid	2.0	77	100	100	100	100	<10	>200	69	0.84	21
Oxine	2.0	64	100	90	98	98	70	—	95	>20	>100
2-Methyloxine	2.0	68	63	91	96	98	61	—	98	>20	>100
Oxine-5-sulphonate	2.0	100	100	100	77	100	<10	35	23	0.37	27
1,10-Phenanthroline	2.0	35	100	59	100	100	<10	120	46	1.64	<10
DMP	2.0	2.5	NQ	52	100	100	<10	—	91	>20	90
α-Benzoinoxime	2.0	35	50	59	100	98	<10	35	20	0.33	32
DDTC	2.0	<0.5	<1.0	<0.5	70	95	85	190	80	2.8	49
APDC	2.0	9.0	8.0	15.5	53	100	100	110	93	3.7	14
Ethyl xanthogenate	2.0	10.5	48	48	63	94	86	>200	80	6.4	22

[a]Abbreviations: LAS, linear alkylbenzene sulphonate; NTA, nitrilotriacetic acid; oxine, 8-quinolinol; DMP, 2,9-dimethyl-1,10-phenanthroline; DDTC, diethyldithiocarbamate; APDC, ammonium pyrrolidinedithiocarbamate. [b]Total of 20 μg Cu l^{-1} (3.15×10^{-7} M) added. An acetate buffer (0.06 M) was used for pH 4.7. [c]n-Hexane/n-butanol (9:1). [d]Corrected for depression by ligand alone. [e]1.0 mg Fe l^{-1} and 5.3 mg humic acid l^{-1}.

TABLE 3

Comparison of computer modelling speciation of copper and toxicity to *Nitzschia closterium*
(Total copper added = 2 $\mu g\ l^{-1}$ or 3.15×10^{-8} M)

Ligand (L)[a]	Ligand conc. (10^{-6} M)	Labile copper from growth curve[b] ($\mu g\ l^{-1}$)	Depression of algal growth by ligand alone (%)	Theor. degree of formation of copper complex (% of total copper)		
				Cu(II)L	$Cu(II)L_2$	$Cu(I)L_2$
Linoleic acid	2.00	3.5	0	—	—	—
Oxine	2.00	27	27(22[c])	10.7	15.6	—
	5.00	>40[d]	45[c]	13.6	47.0	—
2-Methyl-oxine	2.00	24	11	—	—	—
DMP	2.00	20	0	11.7	<0.1	26[e]
	5.00	>40[d]	47[c]	26	<0.1	72[e]

[a]For abbreviations, see Table 2. [b]Corrected for depression of growth rate by ligand alone. [c]Sea water passed through Chelex-100 column before use. [d]Algae thin and transparent. [e]For the separate case where all copper is copper(I).

TABLE 4

Computer modelling of copper—ligand mixtures
(Total added copper = 20 $\mu g\ l^{-1}$ or 3.15×10^{-7} M)

Ligand (L)[a]	Ligand conc. (10^{-6} M)	Free Cu(II) conc. ($-\log_{10}[Cu^{2+}]$)	Percent of total copper			Other species, percent of total ligand
			Cu(II)L	$Cu(II)L_2$	$Cu(I)L_2$	
None	—	8.1	—	—	—	$Cu(OH)_2$,44; $CuCO_3$,42[b]
Fulvic acid	10.00	8.7	74.0	—	—	MgL,91; CaL,6.0
	0.20[c]	9.4	5.4	—	—	MgL,93; CaL,6.1
Acetylacetone	2.00	8.1	3.6	—	—	MgL,93
NTA	2.00	9.1	91.0	<0.1	—	CaL,52; MgL,32
Oxine	2.00	12.2	0.28	99.7	—	MgL,62
Oxine-5-sulphonate	2.00	11.0	3.0	97.0	—	MgL,65
1,10-Phenanthroline	2.00	10.1	40.0	—	98.9[d]	MgL,37
DMP	2.00	9.3	93.0	<0.1	100[d]	MgL,34

[a]For abbreviations, see Table 2. [b]Per cent of total copper. [c]Total copper added = 2.00×10^{-8} M. [d]For the separate case where all copper is copper(I).

Although Desferal apparently does not form sufficiently strong complexes with copper to control its toxicity completely, some protective effect is evident, despite the fact that the copper complex was labile with all techniques used [31].

Lecithin. Phosphatidyl choline (lecithin) constitutes 30–40% of the phosphatides of some algae species [37], and was used in this study as a model for a membrane phospholipid. Lecithin reduced copper toxicity considerably, although a.s.v.-labile copper was about twice the toxic fraction.

Alginic acid. This compound is a product of seaweed, and has been investigated as a heavy metal complexing agent in sea water [38]. The copper complex was highly labile to all techniques used, and 27% of the copper was extractable. Surprisingly, copper showed increased toxicity in the presence of alginic acid. It is possible that this additional toxicity is due to some compound (e.g., an enzyme) extracted from seaweed with the alginic acid [38].

Linear alkylbenzene sulphonate. Linear alkylbenzene sulphonate (LAS) was used as a typical anionic detergent; it can complex heavy metals [39], and it affected the a.s.v. waves of copper. Copper toxicity was reduced in the presence of LAS, although the a.s.v.-labile copper at −0.6 V was more than twice the toxic fraction. The small percentage of extractable copper may have resulted from micelle formation with LAS, and could explain the enhanced uptake of copper by algae in the presence of LAS.

Nitrilotriacetic acid. The copper–nitrilotriacetic acid (NTA) complex was completely a.s.v.-labile, as has been noted previously [30], even though complex formation was almost complete under the conditions used. The adsorption of copper by the algae was reduced in the presence of NTA, and the toxicity diminished by 80%.

Acetylacetone. Computer modelling predicted (Table 4) that little copper will react with acetylacetone under the conditions used. Copper was completely labile with all techniques used, and the ligand had no effect on the toxicity of copper.

Linoleic acid. This compound is an unsaturated fatty acid, and is typical of the fatty acids that are present at high concentrations in algal lipids [37]. Fatty acids are believed to inhibit the growth of some algae, and may act in an auto-inhibition process [40]. Linoleic acid alone inhibited the growth of *Nitzschia* slightly, but its copper complex was much more toxic. The copper complexes of some saturated fatty acids (e.g., butyric acid) are soluble in polar solvents [41], but copper linoleate was not extracted into hexane/butanol. The copper linoleate complex was the only example studied where the complex exhibited greater toxicity than ionic copper, but did not show higher adsorption on the algae. A study of a range of fatty acids is planned in an attempt to explain their unusual toxic action.

8-Quinolinol and its derivatives. Albert, in his authoritative monograph on the selective toxicity of metal ions and metal complexes [15], summarized work on the toxicity of 8-quinolinol (oxine) and its derivatives to bacteria and other micro-organisms. Only the copper and iron 8-quinolinolates were found to have antibacterial and antifungicidal properties, and the 5-sulphonic acid derivative, because of its lipid insolubility, was completely inactive against micro-organisms [15]. The results of the present study are in general agreement with the conclusions reached by Albert. 8-Quinolinol and

2-methyl-8-quinolinol were much more toxic, both as free ligands and as the copper complexes, than the sulphonate derivative, the copper complex of which was not extracted by hexane/butanol. Albert [15] believed that 8-quinolinol has no toxic effect as the free ligand, and must be combined with iron or copper, either deliberately added or present as impurities in the test solution. Passing sea water through Chelex-100 resin decreased, but did not eliminate, the toxicity of 8-quinolinol (Table 3). However, the chelating resin only reduced the total copper content from 0.6 to 0.5 $\mu g\ l^{-1}$, and a thiol resin or oxine-treated porous glass may be more effective [1]. It is interesting to note that, despite the inability of Chelex-100 resin to remove all the copper in sea water, such water treated with Chelex-100 gave blank algal growth rates which were about 15% higher than those measured for untreated water, i.e., equivalent to about 2 μg Cu l^{-1} (Fig. 2). This result implies that Chelex-100 removes toxic substances other than copper from sea water.

None of the speciation techniques yielded results for 8-quinolinol and its derivatives which agreed with the toxic fractions.

1,10-Phenanthroline and its 2,9-dimethyl derivative. 2,9-Dimethyl-1,10-phenanthroline (DMP) is widely used as a selective spectrophotometric reagent for the determination of copper(I) [42]. It forms a copper(I) complex which can be extracted into polar solvents such as the higher alcohols, and so should be lipid-soluble. Steric hindrance by the *o*-methyl groups prevents the formation of iron(II) complexes. The weak copper(II) complex of DMP is not extractable, nor are the copper(I) or (II) complexes of 1,10-phenanthroline [41]. Calculations based on the SIAS equilibrium data (Tables 2—4) show that, for the solution conditions used, the Cu(II)/Cu(I) couple should be 0.14 V more oxidizing when DMP, rather than 1,10-phenanthroline, is the ligand. These considerations explain the results in Tables 2—4. The copper complex of DMP is much more toxic than that of 1,10-phenanthroline, and is accumulated to a far greater extent by the algae. Because copper(II) is more readily reduced in the presence of DMP, the copper(II)—DMP complex may be reduced in a biomembrane (e.g., by protein-bound cysteine groups), and the copper(I) complex, being lipid-soluble, could penetrate the membrane and enter the cell.

A series of phenanthroline derivatives is being studied to establish the relationship between Cu(II)/(I) redox potential, lipid solubility, and toxicity to algae.

α-Benzoinoxime. This compound has been widely used as a gravimetric reagent for copper [43]. It inhibits both the toxic effect and the accumulation of copper on algae. Good agreement was obtained between a.s.v.-labile copper and the toxic fraction.

Diethyldithiocarbamate (DDTC), ammonium pyrrolidine dithiocarbamate (APDC), and ethyl xanthogenate. Dithiocarbamates are extensively used as fungicides, while ethyl and amyl xanthogenates are used in large quantities by the mineral industry as mineral flotation agents. The copper complexes

of these sulphur compounds were all extractable by hexane/butanol, and were strongly accumulated by the algae. The xanthogenate and DDTC copper complexes were also very toxic, although the APDC complex, while having a high lipid solubility, was only moderately toxic. Reliable data for equilibrium constants are not available for the copper complexes of these compounds but, by analogy with similar ligands [28, 44], the compounds would probably be highly stable and formed completely under the conditions used, and would likely have copper in the singly-charged state [1]. Albert [15] showed that copper, but not iron, complexes of dithiocarbamates are toxic to moulds. Poldoski [17] found that DDTC greatly increased the uptake of cadmium by *Daphnia magna*.

Table 2 shows that, with the exception of linoleic and alginic acids, all of the naturally-occurring ligands tested diminished the toxicity of copper and decreased the uptake of copper by the algae. The chelating resins greatly overestimated the toxicity, as did a.s.v. in several cases. Reasonable correlation between copper which was a.s.v.-labile at −0.6 V and the toxic fraction was obtained for the commonly-occurring ligands fulvic acid and iron–humic colloid. The use of a.s.v. with a low deposition potential may therefore give an estimate of the toxic fraction of copper in sea water. With the synthetic ligands, however, no clear pattern emerged between speciation technique and toxicity.

Mechanism of the toxic effect

Albert and his co-workers demonstrated conclusively [15] that the great majority of organic substances which are used as antibacterial and antifungal substances, including 8-quinolinol and the dithiocarbamates, must be combined with a metal to exert their toxic effect. The metal must have a variable valency, and in nature is usually iron or copper.

Some of the copper complexes tested in the present study were extremely toxic; as little as 2 μg Cu l^{-1} in the presence of DMP led to a growth depression greater than that caused by 40 μg Cu l^{-1} alone (Table 3). With the exception of linoleic acid, all the ligands which caused significant toxicity formed copper complexes which were extractable by hexane/butanol and/or increased the uptake of copper by the algae.

The copper complexes which enter the algal cell and exert their toxic effect do so at such remarkably low concentrations that it is difficult to suggest any toxic mechanism other than that the metal complexes catalyze some injurious intercellular reaction. The copper complexes with 8-quinolinol, DMP, and xanthogenate are so stable that they are unlikely to dissociate in the membrane or cytosol. The damaging cellular event may well be catalysis by the metal complex of the formation of hydroxyl radicals (OH·) from molecular oxygen. The hydroxyl free radical is known to be produced by the chelate-catalyzed Fenton reaction [45]:

$O_2 + e^- \rightarrow O_2^-$ (superoxide radical); $O_2^- + 2H^+ + e^- \rightarrow H_2O_2$

$$Cu(chelate)^{2+} + O_2^- \rightarrow Cu(chelate)^+ + O_2$$

$$Cu(chelate)^+ + H_2O_2 \rightarrow Cu(chelate)^{2+} + OH^- + OH\cdot$$

The hydroxyl radical, OH·, reacts at almost diffusion-controlled rates (k = 10^8—10^{10} l mol^{-1} s^{-1}) with most biological substances and, if present at significant concentrations in the cell, could cause devastating damage. Iron chelates are normally used in the Fenton reaction, but copper compounds are also active catalysts [46].

Confirmation that the copper chelate-catalyzed formation of hydroxyl radicals is the cause of the toxic effects observed in the present studies with algae could be obtained by adding specific OH· scavengers (e.g., tryptophan or benzoate) to the growth medium. A more definitive test would be to study the effect of copper complexes on the growth of facultative anaerobic bacteria (i.e., bacteria which can live with or without oxygen) in both aerated and deaerated media. In an oxygen-free environment, copper complexes should have no effect if OH· is the toxic agent. Of the variety of organisms reported by Albert [15] to be susceptible to iron or copper chelates, all were aerobic.

The nature of bound copper in sea water

In an earlier study of the speciation of Cu, Pb, Cd and Zn in coastal sea water [1], it was found that both Chelex-100 and thiol resins removed only a very small fraction of the total dissolved metal. It was concluded that the sea water contained unidentified and powerful ligands, because no model complexing agent tested at a realistic concentration was able to prevent adsorption of metal by these resins. The present study has not resolved this problem; over 90% of copper was removed by the thiol resin with every ligand tested. One of the very few known types of ligand that can bind copper in such an inert complex that it could pass unchanged through a column of thiol resin are the porphyrins, which are known to be present in sea water [47]. Dissolved copper may be inserted into the porphyrin ring via suspended clay particles acting as catalysts [48]. Copper porphyrins have been isolated from deep-sea sediments collected from areas subject to high inputs of organic matter [49], and it is possible that such compounds represent the large inert fraction of dissolved copper in sea water.

This work was sponsored by a grant from the Australian Marine Science and Technologies Advisory Committee. The authors are grateful to Dr. S. W. Jeffrey and Jenny Stauber for advice on culturing algae, and to Kim Miller and Yvonne Farrar for assistance with the experimental work.

REFERENCES

1 T. M. Florence, Anal. Chim. Acta, 141 (1982) 73.
2 C. E. Stephan, U.S. Environmental Protection Agency Rep. No. EPA-660/3-75-009 (April, 1975).

3 J. S. Young, J. M. Gurtisen, C. W. Apts and E. A. Crecelius, Mar. Environ. Res., 2 (1979) 265.
4 R. F. Srna, K. S. Garrett, S. M. Miller and A. B. Thum, Environ. Sci. Technol., 14 (1980) 1482.
5 U. Borgmann, Can. J. Fish. Aquat. Sci., 38 (1981) 999.
6 W. Sunda and R. R. Guillard, J. Mar. Res., 34 (1976) 511.
7 W. Sunda and J. A. Lewis, Limnol. Oceanogr., 23 (1978) 870.
8 G. A. Jackson and J. J. Morgan, Limnol. Oceanogr., 23 (1978) 268.
9 E. E. Dodge and T. L. Theis, Environ. Sci. Technol., 13 (1979) 1287.
10 G. S. Canterford and D. R. Canterford, J. Mar. Biol. Assoc. U.K., 60 (1980) 227.
11 H. E. Allen, R. H. Hall and T. D. Brisbin, Environ. Sci. Technol., 14 (1980) 441.
12 R. Petersen, Environ. Sci. Technol., 16 (1982) 443.
13 V. R. Magnuson, D. K. Harriss, M. S. Sun, D. K. Taylor and G. E. Glass, in E. A. Jenne (Ed.), Chemical Modeling in Aqueous Systems, American Chemical Society, Washington, DC, 1979, p. 635.
14 T. M. Florence, Talanta, 29 (1982) 345.
15 A. Albert, Selective Toxicity, 3rd edn., Methuen, London, 1965.
16 G. W. Bryan, in A. P. Lockwood (Ed.), Effects of Pollutants on Aquatic Organisms, Cambridge University Press, Cambridge, 1976.
17 J. E. Poldoski, Environ. Sci. Technol., 13 (1979) 701.
18 R. D. Guy and A. R. Kean, Water Res., 14 (1980) 891.
19 J. Gavis, R. R. Guillard and B. L. Woodward, J. Mar. Res., 39 (1981) 315.
20 R. R. Guillard and J. H. Ryther, Can. J. Microbiol., 8 (1962) 229.
21 F. M. Morel, J. G. Rueter, D. M. Anderson and R. R. Guillard, J. Phycol., 15 (1979) 135.
22 J. G. Rueter, S. W. Chisholm and F. M. Morel, J. Phycol., 17 (1981) 270.
23 B. G. Lumsden and T. M. Florence, Environ. Technol. Lett., (1983) in press.
24 S. J. Erickson, J. Phycol., 8 (1972) 318.
25 R. J. Phillips and J. S. Fritz, Anal. Chem., 50 (1978) 1504.
26 D. F. Martin, Marine Chemistry, 2nd edn., M. Dekker, New York, 1972.
27 S. Banerjee, S. H. Yalkowsky and S. C. Valvani, Environ. Sci. Technol., 14 (1980) 1227.
28 A. E. Martell and R. M. Smith, Critical Stability Constants, Plenum Press, New York, 1977.
29 R. J. Callaway and D. T. Specht, Estuarine Coastal Shelf Sci., 15 (1982) 561.
30 P. Figura and B. McDuffie, Anal. Chem., 52 (1980) 1433.
31 J. R. Tuschall and P. L. Brezonik, Anal. Chem., 53 (1981) 1986.
32 J. J. Fardy and R. N. Sylva, SIAS, a Computer Program for the Generalised Calculation of Speciation in Mixed Metal—Ligand Aqueous Systems, Aust. Atomic Energy Comm. Rep. AAEC/E445, Australian Atomic Energy Commission, 1978.
33 R. F. Mantoura, A. Dickson and J. P. Riley, Estuarine Coastal Mar. Sci., 6 (1978) 387.
34 S. Hirata, Talanta, 28 (1981) 809.
35 S. R. Piotrowicz, M. Springer-Young, J. A. Puig and M. J. Spencer, Anal. Chem., 54 (1982) 1367.
36 D. M. McKnight and F. M. Morel, Limnol. Oceanogr., 24 (1979) 823; 25 (1980) 62.
37 A. A. Benson and I. Shibuya, in R. A. Lewin (Ed.), Physiology and Biochemistry of Algae, Academic Press, New York, 1962, p. 371.
38 W. Wiessner, in R. A. Lewin (Ed.), Physiology and Biochemistry of Algae, Academic Press, New York, 1962, p. 267.
39 P. Pakalns and G. E. Batley, Anal. Chim. Acta, 99 (1978) 333.
40 G. E. Fogg, Algal Cultures and Phytoplankton Ecology, The Athlone Press, London, 1965, p. 99.
41 G. H. Morrison and H. Freiser, Solvent Extraction in Analytical Chemistry, Wiley, New York, 1957.
42 See, e.g., E. B. Sandell, Colorimetric Determination of Metals, 3rd edn., Interscience, New York, 1959.

43 K. Burger, Organic Reagents in Metal Analysis, Pergamon, Oxford, 1973, p. 90.
44 M. J. Manssen, J. Inorg. Nucl. Chem., 8 (1958) 340.
45 I. Fridovich, Oxygen Free Radicals and Tissue Damage, Ciba Foundation Symp. No. 65, Excerpta Medica, New York, 1979.
46 C. Walling, Acc. Chem. Res., 8 (1975) 125.
47 G. W. Hodgson, Ann. N.Y. Acad. Sci., 206 (1973) 670.
48 J. J. Fripiat and M. I. Cruz-Cumplido, Ann. Rev. Earth Planet Sci., 2 (1974) 239.
49 S. E. Palmer and E. W. Baker, Science, 201 (1978) 49.

Analytica Chimica Acta, 151 (1983) 297—314
Elsevier Science Publishers B.V., Amsterdam — Printed in The Netherlands

THE RAPID DETERMINATION OF ALGAL CHLOROPHYLL AND CAROTENOID PIGMENTS AND THEIR BREAKDOWN PRODUCTS IN NATURAL WATERS BY REVERSE-PHASE HIGH-PERFORMANCE LIQUID CHROMATOGRAPHY

R. F. C. MANTOURA* and C. A. LLEWELLYN

Institute for Marine Environmental Research, Prospect Place, The Hoe, Plymouth PL1 3DH (Gt. Britain)

(Received 1st February 1983)

SUMMARY

A reverse-phase high-performance liquid chromatographic (h.p.l.c.) system is developed for a rapid (≈20 min) separation and quantification of fourteen chlorophylls and their breakdown products and seventeen carotenoids from acetone extracts of algal cultures and natural waters. An ion-pairing reagent is included to achieve good resolution with the acidic chloropigments (chlorophyllides and phaeophorbides). Fluorescence and absorbance detectors are used to quantify chloropigments and carotenoids respectively, with detection limits of 0.01—0.2 ng for these pigments and 200—600 ng for carotenoids. Chlorophyll *a* at concentrations of 0.1 ng l^{-1} may be detected in sea water. Methanol is shown to be unsuitable for extracting pigments because it causes allomerization and transesterification of chlorophylls and chlorophyllides. The spectrophotometric determination of chlorophyll pigments in samples containing breakdown products grossly overestimates the actual concentration of these pigments, as determined by h.p.l.c.

The determination of photosynthetic chlorophyll pigments and their degradation products is one of the most frequently performed analyses in aquatic ecology. Chlorophyll *a* concentrations are routinely used to estimate phytoplankton biomass and productivity, whereas the degradation products (chlorophyllide *a*, phaeophytin *a* and phaeophorbide *a*) are diagnostic indicators of physiological status, detrital content and grazing processes in natural populations of phytoplankton. The commonest methods for the determination of the three chlorophylls, *a*, *b* and *c*, commonly found in alga, are based on spectrophotometric [1, 2] or spectrofluorimetric [3, 4] measurements of acetone extracts of particulate matter. However, as has been pointed out repeatedly [5—8], these methods are often inaccurate because they suffer from several drawbacks: (i) absorption and emission bands of chlorophyll *b* and *c* and even bacteriochlorophyll overlap with those of chlorophyll *a*, giving rise to poor precision and on occasions even "negative" concentrations; (ii) chlorophyll degradation products, which at times constitute a major fraction of green pigments are either not detected or are deter-

0003-2670/83/$03.00

mined along with their parent chlorophylls; (iii) the different spectrophotometric equations reported in the literature [2, 5, 9] often yield different apparent concentrations of individual chlorophylls; (iv) the spectrophotometric method is relatively insensitive, requiring the filtration of large volumes of water; (v) individual carotenoids (carotenes and xanthophylls) are not determined even though these pigments may be better indicators of algal biomass [10] and of different taxonomic groups [11]. The error in prediction of algal biomass by the spectrophotometric procedure may be too high by 75% in water [12] and 400% in sediments [8].

Many of these problems can be overcome if the component pigments are separated chromatographically. Although thin-layer chromatography (t.l.c.) has been widely used in biochemical studies of plant pigments (see reviews by Holden [9] and Davies [13]), its application in the analysis of marine samples [6, 14] has not been widely adopted. This is because sample work-up (rotary evaporation, drying, spotting, etc.), preparation of plates (coating, conditioning, etc.) and mode of detection (scraping, photometry, densitometry) all conspire to render t.l.c. a slow and relatively insensitive technique which is unsuited for shipboard-processing of photolabile samples. The more efficient separation capability and sensitivity of high-performance liquid chromatography (h.p.l.c.) has recently been applied to the separation of chlorophyll *a* and *b* [15], carotenoid standards [16] and petroporphyrins [17]. Abayshi and Riley [5] successfully separated the chlorophyll and carotenoid pigments from algal cultures by normal-phase h.p.l.c., using a Partisil-10 silica column and absorbance detection at 440 nm. Unfortunately, their normal-phase h.p.l.c. is not compatible with aqueous samples and so their method is unsuitable for the direct application to the 90% acetone extracts normally obtained from natural waters and sediments. In addition, the relative insensitivity of absorbance detection for chlorophylls necessitates, as in t.l.c., the preconcentration and drying of samples which runs the risk of breakdown of labile chlorophylls. These and other factors (long elution times, column conditioning stages, reactivity of silica gels) detract from its use with environmental samples. More recently, Brown et al., [7] used reverse-phase h.p.l.c. for rapid ($\approx$12 min) determination of chlorophyll *a* in acetone extracts of muds. However, their chromatographic resolution was so poor that all polar compounds including most of the chlorophyll degradation products, chlorophyll *c* and carotenoids were not separated. For a chromatographic technique to be useful in oceanography, it must separate all the major pigments and degradation products which are found at trace levels (<1 μg l^{-1}) in sea water and it must be rapid and simple to use at sea. This paper describes a sensitive high-resolution reverse-phase h.p.l.c. system for the determination of over thirty algal chlorophyll and carotenoid pigments from estuarine and marine waters.

EXPERIMENTAL

Reagents

Solvents for extraction (acetone, n-hexane) and chromatography (methanol) were Fisons h.p.l.c.-grade and these were filtered and degassed with helium before use. Peroxide-free diethyl ether was prepared by distilling analytical-grade diethyl ether over iron powder and storing dry over anhydrous sodium sulphate in an amber bottle. Double-distilled deionized water (Sybron-Barnstead) was used in all aqueous preparations.

The ion-pairing reagent (solution *P*) was prepared from 1.5 g of tetrabutylammonium acetate (Fluka, 95% purity) and 7.7 g of ammonium acetate (analytical-reagent grade) made up to 100 ml with water. The final pH was 7.1. Mobile phases used in the gradient elution consisted of a primary eluant (*A*) made up of a 10:10:80 mixture, by volume, of solution P:water: methanol, and a secondary eluant (*B*) made up of 20:80 acetone:methanol, by volume.

Standards

The structures and names of various chloropigments, carotenes and xanthophylls investigated are shown in Figs. 1 and 2. Authentic cholorophyll *a* and *b* and β-carotene were obtained from Sigma Chemical Company (Product codes: C-6144 lot 121F-007, C-5878 lot 100-9590 and C-0126 lot 40F-920, respectively). Stock solutions in 100% acetone were found to be stable for at least 6 months when stored at about 0°C in the dark. Fucoxanthin, lutein and zeaxanthin were kindly provided by Prof. G. Brubacher (Hoffman-La Roche); canthaxanthin and echinone were donated by Dr. J. Maxwell of the University of Bristol. All other xanthophylls and chlorophyll *c* were obtained from the following seven species (and classes) of phytoplankton: *Phaeodactylum tricornutum* (Bacillariophyceae), *Isochrysis galbana* (Prymnesiophyceae), *Dunaliella tertiolecta* (Chlorophyceae), *Tetraselmis suecica* (Prasinophyceae), *Oscillatria nigro-verdis* (Cyanophyceae), *Amphidinium carterae* (Dinophyceae), *Gonyaulax tamarensis* (Dinophyceae) and *Gyrodinium aureolum* (Dinophyceae). Most originated from the Cambridge Culture Collection, but some stocks were obtained from the Plymouth (MBA) Collection. These algae were selected not only because they are representative of various classes but also because they all have well-documented carotenoid composition [11, 13].

Phaeophytin *a* and *b* were obtained by acidification (2—3 drops of 1 M HCl) of the respective chlorophyll solutions, extraction into diethyl ether, washing with water and back-extraction into acetone. Acidified samples cannot be used directly on the column because of the irreversible effects of degradation of the silanol groups of the column packing. Chlorophyllide *a* was obtained by enzymatic de-esterification (chlorophyllase) of chlorophyll *a* in 50% acetone suspension of the diatom *Phaeodactylum tricornutum* using the procedures of Barrett and Jeffries [21]. Chlorophyll *a* was then

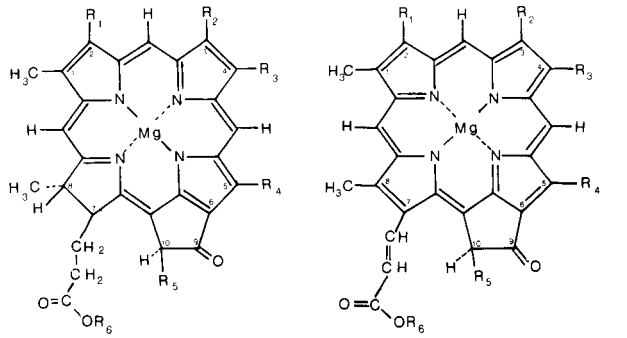

I II

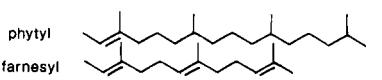

Compound	Porphyrin	Mg present	R_1	R_2	R_3	R_4	R_5	R_6
chlorophyll *a*	I	+	$-CH=CH_2$	$-CH_3$	$-CH_2CH_3$	$-CH_3$	$-COOCH_3$	phytyl
phaeophytin *a*	I	-	$-CH=CH_2$	$-CH_3$	$-CH_2CH_3$	$-CH_3$	$-COOCH_3$	phytyl
chlorophyllide *a*	I	+	$-CH=CH_2$	$-CH_3$	$-CH_2CH_3$	$-CH_3$	$-COOCH_3$	H
phaeophorbide *a*	I	-	$-CH=CH_2$	$-CH_3$	$-CH_2CH_3$	$-CH_3$	$-COOCH_3$	H
chlorophyll *b*	I	+	$-CH=CH_2$	$-CHO$	$-CH_2CH_3$	$-CH_3$	$-COOCH_3$	phytyl
phaeophytin *b*	I	-	$-CH=CH_2$	$-CHO$	$-CH_2CH_3$	$-CH_3$	$-COOCH_3$	phytyl
chlorophyllide *b*	I	+	$-CH=CH_2$	$-CHO$	$-CH_2CH_3$	$-CH_3$	$-COOCH_3$	H
phaeophorbide *b*	I	-	$-CH=CH_2$	$-CHO$	$-CH_2CH_3$	$-CH_3$	$-COOCH_3$	H
chlorophyll c_1	II	+	$-CH=CH_2$	$-CH_3$	$-CH_2CH_3$	$-CH_3$	$-COOCH_3$	H
chlorophyll c_2	II	+	$-CH=CH_2$	$-CH_3$	$-CH=CH_2$	$-CH_3$	$-COOCH_3$	H
phaeophytin c_1	II	-	$-CH=CH_2$	$-CH_3$	$-CH_2CH_3$	$-CH_3$	$-COOCH_3$	H
phaeophytin c_2	II	-	$-CH=CH_2$	$-CH_3$	$-CH=CH_2$	$-CH_3$	$-COOCH_3$	H
bacteriochlophyll	I	+	$-CH_3CHOH$	$-CH_3$	$-CH_2CH_3$	CH_2CH_3	-H	farnesyl

Fig. 1. The structures of the chlorophylls and their degradation products. The phaeophytins and chlorophyllides are Mg-free (replaced by 2 H) and phytyl-free derivatives, respectively, of the parent chlorophylls whereas the phaeophorbides are free of both Mg and phytol. Chlorophyll c_1 and c_2 do not possess an esterified phytol on their propionic side chain at C_7 and in common with the chlorophyllides and phaeophorbides are acidic pigments. The structure of bacteriochlorophyll corresponds to that proposed by Chow et al., [18] for the major component of *Chlorobium lumicola*. Allomerized forms of the chloropigments consist of the more polar keto—enol tautomers centred at the C-9 and C-10 of the cyclopentenone ring [19]. Primed pigments (e.g., chlorophyll *a'*) correspond to the epimeric inversion of R_5 at the C-10 position [20].

separated from other chloropigments either by semi-preparative h.p.l.c., or by the hexane phase-separation procedure of Parsons [22]. Phaeophorbide *a* and *c* were then converted from their respective chlorophyllides by the acidification—ether extraction procedure mentioned above for the phaeophytins.

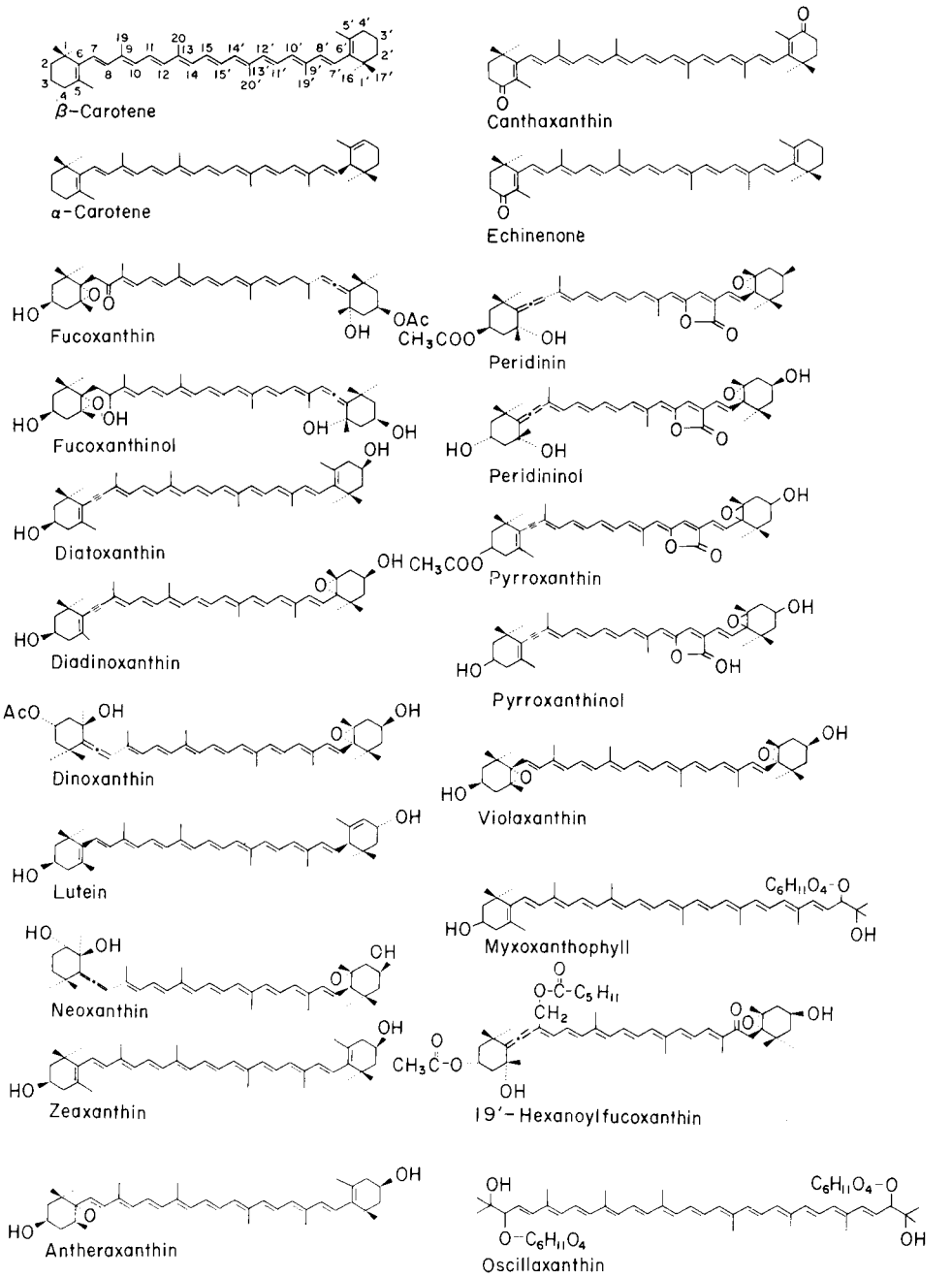

Fig. 2. Structures and common names of the algal carotenes and xanthophylls considered.

The identity and purity of all pigments were confirmed by co-elution with available standards, by stopped-flow absorption spectrophotometry, and by spectrofluorimetry (see Table 1).

Apparatus

The DuPont system used for h.p.l.c. consisted of a model 848 constant pressure pneumatic pump, a model 838 programmable gradient elution system, and a model 836 fluorescence detector (λ_{ex} = 430 ± 40 nm; λ_{em} > 600 nm). In addition, a programmable variable-wavelength stopped-flow absorbance detector (Perkin-Elmer LC-75) was fitted downstream from the fluorimeter and used to obtain the absorbance (440 nm) chromatogram and the spectra (380—600 nm) of the chromatographic peaks. Samples (20—100 µl) were injected via a Rheodyne model 7125 injector valve. Reverse-phase h.p.l.c. was performed at 2000 psi on a 25 × 0.5 cm column packed with octadecyl-silane bonded 5-µm ODS-Hypersil (N = 18 800—20 200 plates; $A_{10\%}$ = 1.05—1.10; Shandon).

Procedure and calibration

Known volumes of sample (10 ml of culture or 100—1000 ml of sea water, prefiltered through a 200-µm mesh) were vacuum-filtered through 47 mm Whatman GF/C; the pigments were extracted from the filters by pulverization and ultrasonication of filters in 10 ml of cold (0—5°C) solvent (usually 90% acetone) under nitrogen and in subdued light. The yellow-green extracts were separated from the particulate residue by centrifugation and if necessary by microfiltration through a 0.5-µm PTFE filter (Millex-SR, Millipore Corporation). To 1000 µl of the clear extract, 300 µl of ion-pairing reagent (solution *P*) was added; after thorough mixing and equilibration for 5 min, 20 µl were injected into the chromatograph. Chromatographic separation of pigments was obtained by linear gradient elution from 100% *A* to 100% *B* in 10 min, followed by an isocratic hold for 12 min at 100% *B*. To avoid any deterioration of silica particles by the ion-pairing reagent [23], the column was always stored in aqueous methanol. Reconditioning of columns between runs was not necessary for reproducible separations.

Quantification

The weights of identified pigments appearing in the absorbance chromatograms were estimated from calibrations based on available standards. When these were not available, the weight (W, g) of pigment was estimated from an extension of Beer's Law based on

$$W = (aA_t f)/(SwE^{1\%}_{440\,nm}\ 100)$$

where a is the peak area (cm^2), A_t is the absorbance setting on the detector (in absorbance), f is the flow rate (cm^3 m^{-1}), S is chart speed (cm m^{-1}), w is the full scale width of chart (cm), and $E^{1\%}_{440\,nm}$ is the specific extinction coefficient of the pigment at 440 nm. Values of $E^{1\%}_{440\,nm}$ used for all pigments

TABLE 1

Source, chromatographic and spectroscopic properties of algal pigments separated by h.p.l.c.

Pigment	Source[a]	Absorption maxima λ_m (nm)	Solvent	Ref.	Observed λ_m (nm)	$E^{1\%}_{440\ nm}$ [b]	k'[c]
Chlorophyll *a*	1, 3—10	410, 430, 663	90% acetone	24	411, 432, 663	687	4.72
Chlorophyll *a'*	2	409, 428, 661	ether	25		687	4.78
Chlorophyllide *a*	2, 3	410, 430, 663	90% acetone	26	418, 432, 664	687	1.74
Phaeophorbide *a*	2	408, 467, 667	ether	19	408 665	713	2.69
Phaeophytin *a*	1, 2	533, 609, 667	ether	19	532, 606, 665	713	6.76
Phaeophytin *a'*	1, 2				532, 606, 664	713	7.00
Chlorophyll *b*	1, 6, 10	595, 642	ether	19	458, 595, 643	853	4.27
Chlorophyllide *b*	2				458, 594, 643	853	0.69
Phaeophytin *b*	2	525, 599, 654	ether	19	523, 597, 652	836	5.51
Chlorophyll c_1	3	444, 583, 634	methanol	27	443, 582, 632	3460	2.09
Chlorophyll c_2	3	452, 586, 634	methanol	27	443, 582, 632	3460	2.09
Phaeophytin c_1	2, 3	530, 574, 648	acetone	28	530, 570, 648	3250	2.80
Phaeophytin c_2	2, 3	532, 574, 651	acetone	28	530, 570, 648	3250	2.80
Fucoxanthin	1, 3, 9	(426), 449, (465)	ethanol	13	446, (465)	1016	2.71
Diadinoxanthin	3, 4, 7	(424), 445, 474	ethanol	13	444, 473	2325	3.21
Neofucoxanthin	3	446	ethanol	29	442	1016	3.24
Diatoxanthin	3, 4, 7	(425), 449, 475	ethanol	13	452, 479	1634	3.57
19'-Hexanoyl-fucoxanthin	4	(427), 445, 474	light petr.	30	452, 470	1369	2.83
Zeaxanthin	5	422, 450, 481	methanol	13	455	2000	3.32
Myxoxanthophyll	5	448, 473, 503	ethanol	13	449, 476	1253	3.79
Canthaxanthin	1, 5	474	ethanol	13	474	2000	4.00
Echinenone	1, 5	461	ethanol	13	455	1881	4.70
Neoxanthin	6, 10	415, 438, 467	ethanol	13	416, 438, 466	2374	2.88
Violaxanthin	6, 10	415, 440, 469	methanol	13	415, 440, 470	2550	2.95
Lutein	6, 10	(418), 444, 474	methanol	13	(419), 442, 471	2393	3.49
Peridinin	7, 8	467	methanol	13	465	1126	2.37
Peridininol	7	466	acetone	31	~460	1084	1.66
β-carotene	1, 3—10	(427), 449, 475	ethanol	13	450	2209	6.27
α-carotene	6	423, 444, 473	ethanol	13	—	—	5.93

[a]Source codes are: (1) authentic standards; (2) conversion from parent chlorophylls; (3) *Phaeodactylum tricornutum*; (4) *Gyrodinium aureolum*; (5) *Oscillatoria nigro-verdis*; (6) *Tetraselmis suecica*; (7) *Amphidinium carterae*; (8) *Gonyaulax tamarensis*; (9) *Isochrysis galbana*; (10) *Dunaliella tertiolecta*. [b]Specific extinction coefficient at 440 nm for 1 cm; when no value is available, an average value of 2000 at 440 nm is assumed [13]. [c]Phase capacity ratio [32].

are included in Table 1 and these were derived from the absorption spectra and $E^{1\%}_{\lambda max}$ reported in the literature [13]. For unidentified carotenoids, a representative value of $E^{1\%}_{440}$ of 2 000, appropriate for alcoholic solvents [13], was used. The chloropigments were quantified from their fluorescence chromatograms after calibration of the fluorescence response (quantum yield) with known quantities of the relevant pigment. However, the fluorescence response factors are specific to the optical conditions (source, filters, photomultiplier response, etc.) of the fluorimeter and separate calibration is essential when other fluorimetric detectors are used.

RESULTS AND DISCUSSION

Figure 3 shows the absorbance and fluorescence chromatograms together with the stopped-flow spectra of the carotenoids and chlorophylls from *Phaeodactylum tricornutum*, separated under optimized conditions. Optimization involved experiments covering various reverse-phase columns, mobile phases, ion-pairing reagents and extraction techniques, on pigments from *Phaeodactylum* sp. and authentic compounds.

Choice of columns

As discussed earlier, reverse-phase chromatography was chosen in preference to the more traditional normal-phase silica packing to circumvent the time-consuming steps of drying the pigment extracts, column conditioning and the problems of pigment breakdown that this may involve.

The effect of alkyl chain length and capping of residual silanol groups was investigated by comparing the retention times and resolution of carotenoids from *Phaeodactylum* sp. on four columns: Zorbax (Du Pont) C_3-TMS; Zorbax C_8-OS; Zorbax C_{18}-ODS and Shandon Hypersil ODS. The polar xanthophylls (fucoxanthin, diadinoxanthin, diatoxanthin) co-eluted with chlorophyll *a* on both the trimethyl (TMS) and octyl (C_8) phases. No β-carotene could be eluted from the Zorbax C_{18} column which contrasts with the Hypersil ODS (Fig. 3), and this may be due to adsorption on residual silanol sites which are vacant in the case of the Zorbax C_{18} and which are capped (with TMS) in Hypersil ODS. Separation efficiencies were consistently in the range 18 000—20 000 plates, and the elution order never changed. Guard pre-columns were not found to be necessary with analytical loadings (20—100 μl, ≈1 μg), and 400—500 samples were separated per column, with no significant deterioration in the chromatography.

Choice of mobile phase and ion pairing

Methanol-based eluants were selected for both primary and secondary mobile phases because of their selectivity and versatility in reverse-phase h.p.l.c. The well known allomerization products of chlorophyll *a* which occur in protolytic solvents [19] including methanol, are apparently not formed in the proposed method (see Fig. 3). Acetone rather than acetonitrile

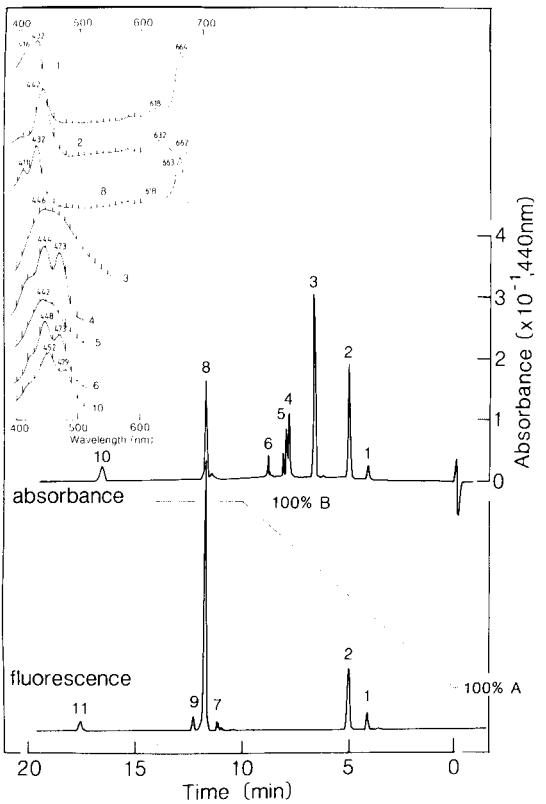

Fig. 3. Ion-pair reverse-phase h.p.l.c. with absorbance (λ_m = 440 nm) and fluorescence (λ_{em} > 600 nm) chromatograms and associated stopped-flow visible spectra (showing λ_{max}) of carotenoids and chlorophyll pigments from a 90% acetone extract of *Phaeodactylum tricornutum*. Spectra above the 600-nm limit of the Perkin-Elmer LC-75 detector were obtained on pooled peaks measured with a Pye-Unicam spectrophotometer SP8-100. H.p.l.c. conditions: gradient (10 min) and isocratic (10 min) elution as in the Procedure; pump pressure 2000 psi; flow rate 1.8 ml min^{-1} (start) to 3.2 ml min^{-1} (end); 20-μl sample of 90% acetone with tetrabutylammonium acetate. Peak identities: (1) chlorophyllide *a*; (2) chlorophylls $c_1 + c_2$; (3) fucoxanthin; (4) diadinoxanthin; (5) neofucoxanthin; (6) diatoxanthin; (7) allomerized chlorophyll *a*; (8) chlorophyll *a*; (9) chlorophyll *a'*; (10) β-carotene; (11) phaeophytin *a*.

was used as modifier to achieve the desired eluotropic strength in the secondary mobile phase, because the spectrophotometric data for carotenoids necessary for quantitative h.p.l.c. are available for acetone but not for acetonitrile solvents [13].

The separation of the acidic (i.e., de-phytolated) pigments chlorophyll $c_1 + c_2$, chlorophyllides *a* and *b* and phaeophorbides *a*, *b* and *c* by conventional reverse-phase h.p.l.c. was poor and not reproducible (see Fig. 4A). This problem, which is encountered in the method of Brown et al. [7] was traced to the anionic character of the propionic carboxylic acid group

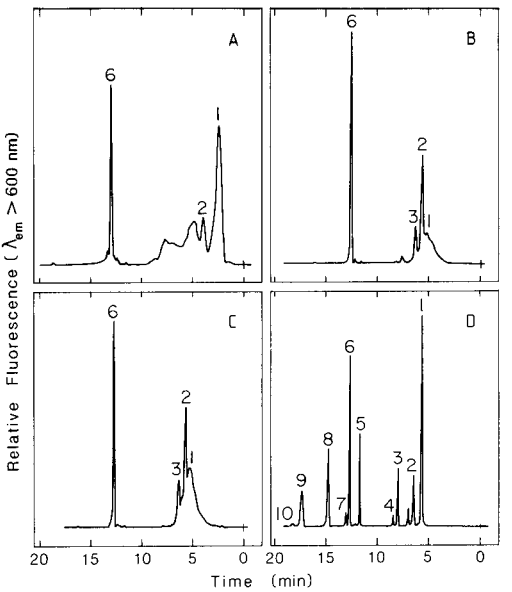

Fig. 4. The effect of ion-pairing with tetrabutylammonium acetate (TBAA) on the chromatographic separation of fluorescent chloropigments extracted from *Phaeodactylum* sp. (A) Reverse-phase separation, 10 min linear gradient from 80:20 methanol—water to 80:20 methanol—acetone; (B) sample and TBAA with chromatographic conditions as in A: (C) TBAA present in 80:20 methanol—water phase; (D) TBAA present in both sample and 80:20 methanol—water phase. The sample for (D) was also spiked with chlorophyll *b*, phaeophytin *b*, phaeophorbide *a* and phaeophorbide *c* to show the complete separation of all possible algal chloropigments. Compound identities: (1) chlorophyllide *a*: (2) chlorophyll $c_1 + c_2$; (3) phaeophorbide *a*; (4) phaeophorbide *c*; (5) chlorophyll *b*; (6) chlorophyll *a*; (7) chlorophyll *a'*; (8) phaeophytin *b*; (9) phaeophytin *a*; (10) phaeophytin *a'*.

($pK_a \approx 2$—4, Fig. 1) which at neutral pH should be dissociated. Dissociation can be suppressed by ion-pairing with a cationic hydrophobic ligand. Of the various ion-pairing reagents tested, buffered (pH 7.1) tetrabutylammonium acetate was found to be superior to the more popular phosphate salt because the acetate has a higher solubility in aqueous methanol and acetone [23] and because the kinetics of its reaction with chloropigments at pH 7.1 to form the hydrophobic ion-pair was faster.

The dramatic effects of this reaction on the separation of chloropigments from *Phaeodactylum* (spiked with phaeophorbide *a* + *c*) are shown in the fluorescence chromatograms of Fig. 4 (B—D). It is apparent from the skew peaks in Fig. 4B and C that when the ion-pair is injected into a mobile phase free of tetrabutylammonium acetate, the ion-pair will dissociate; and that when the pigment is injected into a mobile phase containing tetrabutylammonium acetate, ion-pairing is too slow relative to the elution time. For good separation (Fig, 4D), the ion-pair species must predominate during the chromatography; thus the quaternary ammonium salt must be present in both the sample and mobile phase. The absorptivities, absorbance and

fluorescence spectra of the ion-pairs were found to be essentially similar to those of the unpaired pigments (Table 1), making it possible to use the reported spectral properties of the pigments for their identification and quantification. Ion-pairing reagents do not affect the retention times of the unionized chloropigments (chlorophyll *a*, *b*, phaeophytin *a*, *b*) and carotenoids (Fig. 4).

Pigment extraction

Various solvents have been used for the extraction of chlorophyll [9] and carotenoids [13] from plants, but acetone and/or methanol appear to be most favoured with algae [1–7, 9, 13, 14, 21]. However, the reported merits of these two solvents in terms of extraction efficiency, denaturization, etc., of pigments are not consistent. Figure 5 (A–D) shows the effects of various solvent combinations on the transformation of chlorophylls from *Phaeodactylum* sp. Chlorophyll *c* appears to be unaffected by the choice of solvent. However, when compared to the extraction with 1:9 water–acetone (Fig. 5A), large proportions of chlorophyll *a* are converted to chlorophyllide *a* in 1:1 water–acetone (75% conversion) or 1:1 water–methanol (93% conversion). This arises from the activation of the enzyme chlorophyllase [9] which is abundant in diatoms [21]. Additional breakdown/transformation products of chlorophyll *a* were apparent in methanol-based solvents and these included: (1) trans-esterification by chlorophyllase [21] to form

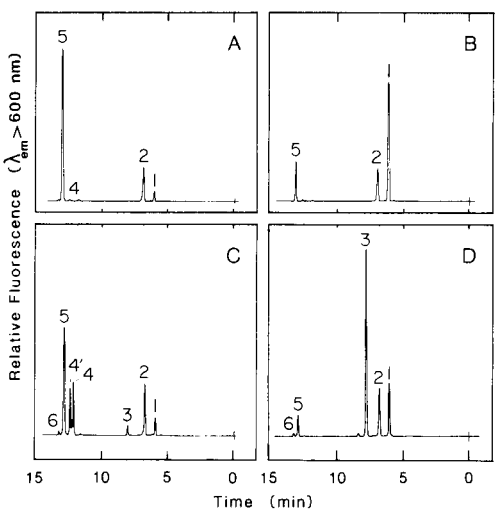

Fig. 5. The effect of solvent on the extraction and transformation of fluorescent chloropigments from *Phaeodactylum tricornutum*. (A) acetone–water, 90:10; (B) 30 min incubation and extraction with 1:1 acetone–water; (C) extraction of large biomass with 100% methanol; (D) 30 min incubation and extraction with 1:1 methanol–water. Compound identities: (1) chlorophyllide *a*; (2) chlorophyll $c_1 + c_2$; (3) methyl chlorophyllide *a* ester; (4') allomerized chlorophyll *a*; (4) chlorophyll *a* dimer; (5) chlorophyll *a*; (6) chlorophyll *a'*.

methyl-chlorophyllide *a* (k' = 2.35) (Fig. 5D); (2) epimerization reactions to form chlorophyll *a'*; and (3) when large amounts of algae are used, the rapid formation (up to 40%) of allomeric [19] and possibly dimeric forms of chlorophyll *a* (Fig. 5C). Methanol should therefore not be used in pigment extraction from algae. Acetone extracts and solutions of authentic chlorophyll *a*, when kept under nitrogen and stored in a dark freezer, were stable for several months. It can be concluded that the popular 1:9 water—acetone [2] is indeed an excellent solvent for extraction of algal pigments.

Quantification

The very high sensitivity and linearity of fluorescence response in the determination of algal chloropigments by h.p.l.c. is shown in Fig. 6. The linearity in fluorescence response of chlorophyll *a* spans five orders of magnitude to approximately 1 μg which is close to the analytical loading limit of the Hypersil ODS column. The different sensitivities of the various pigments arises from differences in the quantum yield [4] and the effects of peak broadening during the isocratic stage (100% *B*, see Fig. 3) of the elution. The detection limits defined as peak heights twice the background noise, are listed in Table 2 for 20-μl injections. They range from 10 pg for chlorophyll *a* to 200 pg for the less fluorescent chlorophyll *b*. Thus for 100-μl injections of the acetone extract (10 ml), as little as 0.1 ng of chlorophyll *a* can be detected in 1 l of sea water by the fluorescence h.p.l.c. method after preconcentration. This compares with 0.1 μg l^{-1} by spectrophotometric methods [2].

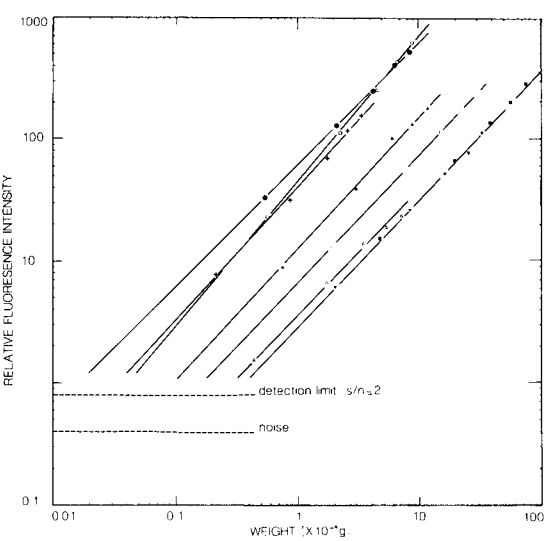

Fig. 6. Quantitative relationship between fluorescence (peak heights) and injected weights of chloropigments (r^2 = 0.95—0.98), relative to the detection limit defined as twice the signal to noise ratio. (●) Chlorophyll *a*; (○) chlorophyllide *a*; (▲) phaeophorbide *a*; (▼) phaeophytin *a*; (■) chlorophyll *b*; (□) phaeophytin *b*; (+) chlorophyll *c*; (△) phaeophorbide *c*.

TABLE 2

Detection limits for algal pigments by h.p.l.c.

Pigment	Detection limit		
	By h.p.l.c. (ng)[a]	In natural waters (ng l^{-1})[b]	
		A	B
Chlorophyll *a*	0.01	5	0.1
Chlorophyllide *a*	0.03	15	0.3
Phaeophorbide *a*	0.1	50	1.0
Phaeophytin *a*	0.2	100	2.0
Chlorophyll *b*	0.05	25	0.5
Phaeophytin *b*	0.06	30	0.6
Chlorophyll $c_1 + c_2$	0.02	10	0.2
Carotenoids[c]	2—6	1000—3000	20—60

[a] $S/N = 2$; 20-μl injections with fluorescence detection except for carotenoids which were detected by absorbance. [b] A for 20-μl injection of 10 ml of 90% acetone extracts from 1 l of sea water. B for 100-μl injection of Sep-pak-preconcentrated extracts from 1 l of sea water. [c] Depending on $E^{1\%}_{440\ nm}$ (see Table 1).

The detection limit for a typical carotenoid (e.g., lutein) under similar conditions is 0.3 μg l^{-1} (see Table 2), because absorbance detection is less sensitive than fluorescence. However, the h.p.l.c. detection and stopped-flow scanning of pigments from dilute (<1 μg l^{-1}) samples may be improved by a modification of the preconcentration technique of Eskins and Dutton [33] used with higher plants. The 10-ml extracts of 90% acetone are diluted to 20 ml with water and passed through a C_{18}-Bondapak Sep-pak cartridge (Waters Associates). The adsorbed pigments may then be recovered with about 1 ml of acetone (>90% recovery) and if 100 μl is injected into the chromatograph, a 50-fold concentration factor over the standard method can be achieved.

The overall reproducibility of the combined operations of filtration, extraction and h.p.l.c. on triplicate samples is 4.8% and that of replicate injection is about 1% ($n = 3$).

Analysis of algae

Shown in Figs. 3 and 7 are examples of the separation and identification of carotenoids and chloropigments from various algal classes. The chromatographic and spectroscopic properties of all the pigments separated by h.p.l.c. are summarized in Table 1 in terms of the phase capacity ratio k' [32], the specific extinction coefficient at 440 nm ($E^{1\%}_{440\ nm}$) and the wavelengths for the absorption maxima (λ_m).

All the carotenoids reported for *Phaeodactylum* sp. were separated by reverse-phase h.p.l.c. (Fig. 3), which contrasts with normal-phase h.p.l.c. [5] in which neither diatoxanthin nor neofucoxanthin are separated. Carotenoid

composition and abundance in *Phaeodactylum* sp. were variable and depended on the polymorphic forms and the growth and light conditions of the culture. *Gyrodinium aureolum* (Fig. 7) is an unusual dinoflagellate in that its principal xanthophyll is 19′-hexanoylfucoxanthin [30] rather than peridinin. Peridinin occurs in *Amphidinium* sp. and *Gonyaulax* sp. (Table 1) and has characteristic chromatographic and spectral properties that allow it to be easily distinguished from 19′-hexanoylfucoxanthin. The two unknown carotenoids (peaks 14, Fig. 7) in *Gyrodinium* sp. correspond in relative polarity and abundance to a cluster of three uncharacterized xanthophylls reported by Tangen and Björnland [30]. The chromatogram of *Oscillatoria* sp. shows myxoxanthophyll to be well separated from other carotenoids. Myxoxanthophyll is the characteristic xanthophyll of the Cyanophyceae (blue-green algae). Echinenone elutes very close to chlorophyll *a*. Lutein, neoxanthin and violaxanthin, which are components of the xanthophyll cycle in higher plants, were completely resolved in the chromatograms of the *Tetraselmis suecica*. *Tetraselmis* sp. also contained minor amounts of α-carotene. *Dunaliella* sp. and *Isochrysis* sp. showed similar carotenoid patterns as in *Tetraselmis* sp. and *Phaeodactylum* sp., respectively. The unidentified peaks in Fig. 7 are most likely to be neo-type or *cis—trans* isomers of the parent xanthophylls.

The co-elution of chlorophyll c_1 with c_2 (Fig. 3) suggests that octadecyl-bonded silica does not possess the same double-bond selectivity of adsorption as polyethylene, which is normally employed to separate chlorophyll c_1 from c_2 [34]. However, when a Hewlett-Packard 1040A diode-array h.p.l.c. spectrophotometer was used, it was possible to show that the wavelength of maximum absorption changes from 444 nm at the frontal edge of the chlorophyll c_1 and c_2 peak to 440 nm at the trailing edge. This indicates [34] that chlorophyll c_2 elutes before c_1 and their separation could be achieved by using more efficient 3-μm ODS columns.

It is clear from Table 2 and Fig. 7 that the h.p.l.c. system described here is capable of separating and quantifying all the key class-specific pigments in algae (fucoxanthin, peridinin, lutein, myxoxanthophyll, chlorophyll *b* and chlorophyll *c*) and their companion xanthophylls. This emphasizes the chemotaxonomic potential of h.p.l.c. for natural water samples.

Natural water samples

In the lower portion of Fig. 7 are shown four fluorescence chromatograms corresponding to the chloropigment content of two marine samples from the Celtic Sea and two brackish samples from the Tamar Estuary. The Celtic Sea samples are dominated by chlorophylls *a* and *c* with some chlorophyllide *a* at 30 m and generally show reasonable correlation with spectrophotometric [2] estimates of chlorophyll *a* ($r^2 = 0.89$, $n = 9$). In contrast, the chromatograms from the Tamar estuary show the additional presence of chlorophyll *b* and are dominated by breakdown products including phaeophytins *a*, *a*′, *b* and *b*′, phaeophorbide *a* and *c*, and chlorophyllide *a*

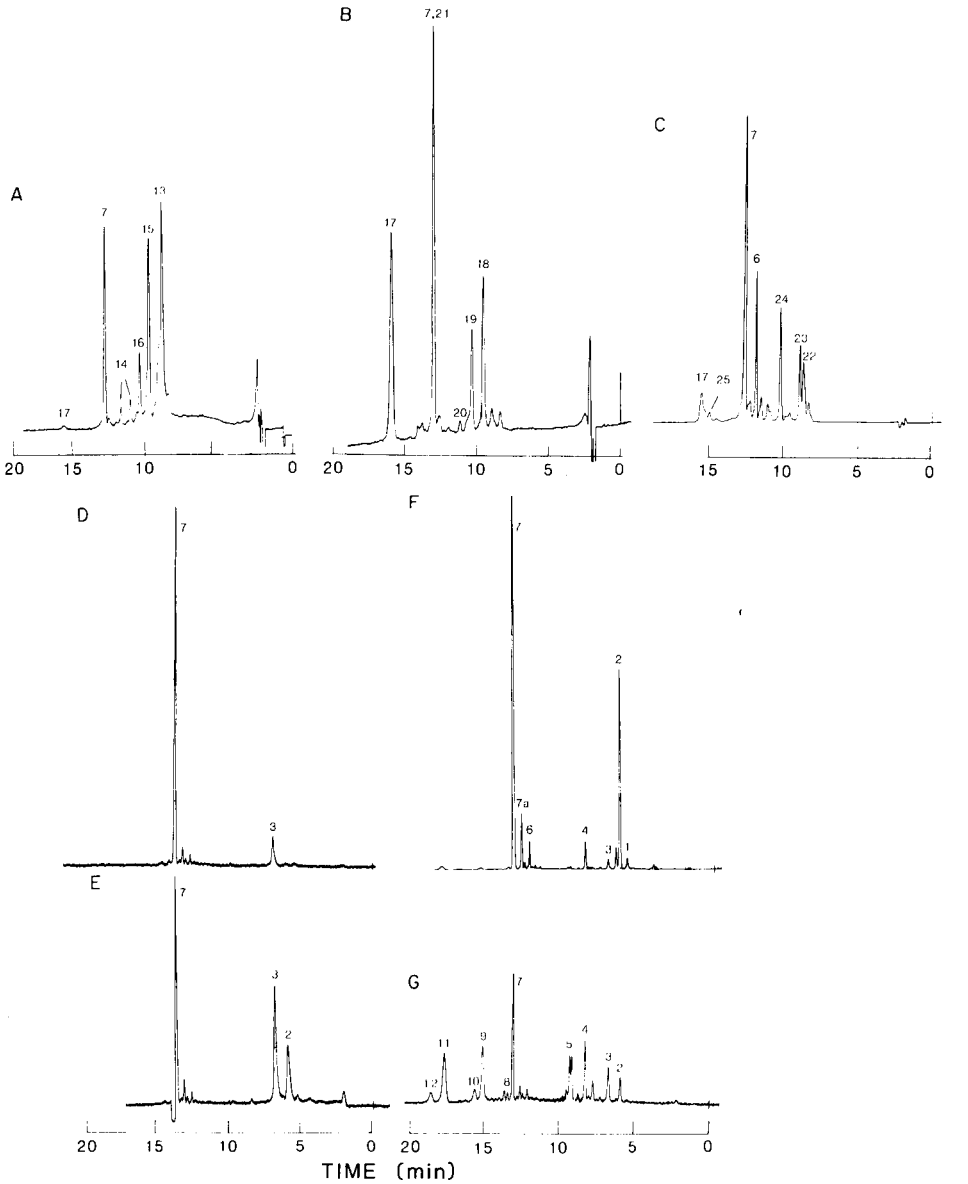

Fig. 7. H.p.l.c. absorbance (440 nm) chromatograms of algal carotenoids and chloropigments extracts from three classes of algae: (A) *Gyrodinium aureolum* (Dinophyceae); (B) *Oscillatoria nigro-verdis* (Cyanophyceae); (C) *Tetraselmis suecica* (Prasinophyceae). Also shown are four fluorescence (λ_{em} > 600 nm) chromatograms of natural water samples (1 l): (D, E) from 5 m and 30 m depths, respectively, in the Celtic Sea (50° 30'N, 07° 00'W, 24/8/82); (F, G) from the Tamar estuary (S.W. England), on August 11 and October 14, 1982, respectively. Compound identities: (1) chlorophyllide *b*; (2) chlorophyllide *a*; (3) chlorophyll c_1 and c_2; (4) phaeophorbide *a*; (5) phaeophorbide *c*; (6) chlorophyll *b*; (7) chlorophyll *a*; (7a) bacteriochlorophyll (?); (8) chlorophyll *a'*; (9) phaeophytin *b*; (10) phaeophytin *b'*; (11) phaeophytin *a*; (12) phaeophytin *a'*; (13) 19'-hexanoylfucoxanthin; (14) unknown; (15) diadinoxanthin; (16) diatoxanthin; (17) β-carotene; (18) myxoxanthophyll; (19) zeaxanthin; (20) canthaxanthin; (21) echinenone; (22) neoxanthin; (23) violaxanthin; (24) lutein; (25) α-carotene.

and *b*. The concentrations of the individual pigments in the October Tamar sample as measured by h.p.l.c. and by the various spectrophotometric equations [2, 34] are shown in Table 3. All three chlorophylls are over-estimated by factors of 3.5—12.6 times the actual concentrations determined by h.p.l.c. This discrepancy arises from the inability of these equations to correct for the swamping presence of chlorophyll breakdown products which account for 74% of the chloropigments. Similar inaccuracies arise in estimates of carotenoids by the Richards equations [2]. These results rule out the use of spectrophotometry for estimation of chlorophyll pigments in many situations, because breakdown products are nearly always found in natural waters [35].

Finally, Fig. 8 shows two absorbance chromatograms of carotenoid and chlorophyll pigments from water samples originating from the river-end (A) and mid-estuarine (B) regions of the Tamar during summer conditions. The pigment distribution is in agreement with that expected from microscopic examination of these samples, which identified the predominance of naked flagellates and dinoflagellates in (A) and dinoflagellates and diatoms in (B). These chromatograms also show sufficient sensitivity to detection of algal carotenoids during summer bloom ($>1\ \mu g\ l^{-1}$) conditions.

We thank Dr. J. Readman, Dr. J. Braven and Dr. P. Donkin for useful discussions, and Dr. I. R. Joint for the provision of Celtic Sea samples. This work forms part of the Estuarine Ecology Programme of the Institute for

TABLE 3

Algal pigments in the Tamar Estuary; $\mu g\ l^{-1}$ (14 October 1982)[a]

Pigment	H.p.l.c.	A	R	PS	SU	JH
Chlorophyll *a*	1.49	9.45	13.39	10.14	9.95	10.33
Chlorophyllide *a*	0.29					
Phaeophytin *a*	3.00					
Phaeophytin *a'*	0.60					
Phaeophorbide *a*	0.83					
Chlorophyll *b*	0.48		4.18	3.63	4.26	3.49
Phaeophytin *b*	1.08					
Phaeophorbide *b'*	0.23					
Chlorophyll $c_1 + c_2$	0.12		1.52	1.55	1.14	0.78
Phaeophytin $c_1 + c_2$	0.06					
Unknowns	1.08					
Total Chloropigments	9.26					
Phaeopigments	6.88	1.20				
Σ carotenoids	1.59		5.98			

[a]Spectrophotometric methods of calculation based on the acid method (A), and the equations of Richards (R), Parsons and Stickland (PS), SCOR-UNESCO (SU) as listed in ref. [2]. JH corresponds to Jeffrey and Humphrey's revised equations [34].

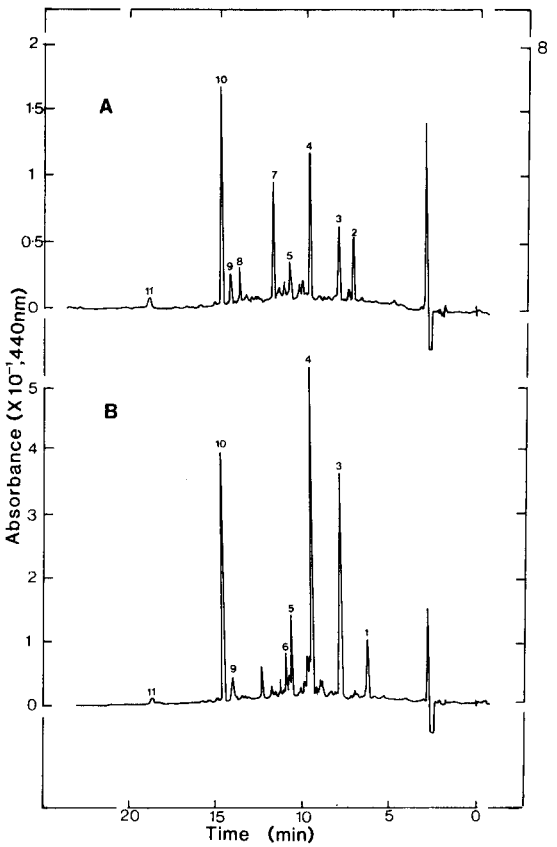

Fig. 8. Absorbance chromatograms of carotenoid and chlorophyll pigments from water samples obtained from the river-end (A) and mid-estuarine region (B) of the Tamar estuary on August 11, 1982. Peak identities: (1) unknown xanthophyll; (2) chlorophyllide *a*; (3) chlorophyll $c_1 + c_2$; (4) fucoxanthin; (5) diadinoxanthin; (6) diatoxanthin; (7) lutein; (8) chlorophyll *b*; (9) allomer of chlorophyll *a*; (10) chlorophyll *a*; (11) β-carotene (20 μl injected).

Marine Environmental Research, a component of the Natural Environment Research Council, and was partly supported by the Department of the Environment under Contract No. DGR 480/48.

REFERENCES

1 F. A. Richards and J. G. Thomson, J. Mar. Res., 11 (1952) 156.
2 J. D. H. Strickland and T. R. Parsons, A Practical Handbook of Seawater Analysis, Fisheries Research Board of Canada Bulletin 167, 2nd edn., 1972.
3 C. S. Yentsh and D. W. Menzel, Deep Sea Res., 10 (1963) 221.
4 M. E. Loftus and J. H. Carpenter, J. Mar. Res., 29 (1971) 319.
5 J. K. Abayshi and J. P. Riley, Anal. Chim. Acta, 107 (1979) 1.
6 L. Garside and J. P. Riley, Anal. Chim. Acta, 46 (1969) 179.

7 L. M. Brown, B. T. Hargrave and M. D. MacKinnon, Can. J. Fish Aquat. Sci., 38 (1981) 205.
8 T. R. Jacobsen, Mar. Sci. Commun., 4 (1978) 33.
9 M. Holden, in T. W. Goodwin (Ed.), Chemistry and Biochemistry of Plant Pigments, Vol. 2, 2nd edn., Academic Press, London, 1976, p. 2.
10 S. Shimura and Y. Fujita, Mar. Biol., 33 (1975) 185.
11 S. Liaaen-Jensen, in D. J. Faulkner and W. H. Fenical (Eds.), Marine Natural Products Chemistry, NATO Conf. Ser. IV, Plenum, New York, 1977, p. 239.
12 A. Jensen and E. Sakshaug, J. Exp. Mar. Biol. Ecol., 11 (1973) 137.
13 B. H. Davies, in T. W. Goodwin (Ed.), Chemistry and Biochemistry of Plant Pigments, Vol. 2, 2nd edn., Academic Press, London, 1976, p. 38.
14 S. W. Jeffrey, Limnol. Oceanogr., 26 (1981) 191.
15 W. T. Shoaf, J. Chromatogr., 152 (1978) 247.
16 A. Fiksdahl, J. T. Mortensen and S. Liaaen-Jensen, J. Chromatogr., 157 (1978) 111.
17 S. K. Hajibrahim, P. J. C. Tibbits, C. D. Watts, J. R. Maxwell, G. Eglinton, H. Colin, and J. Guoichon, Anal. Chem., 50 (1978) 549.
18 H. C. Chow, M. B. Caple and C. E. Strouse, J. Chromatogr., 151 (1978) 357.
19 P. H. Hynninen and N. Elfolk, Acta Chem. Scand., 27 (1973) 1463.
20 J. J. Katz, G. D. Norman, W. A. Svec and H. H. Strain, J. Am. Chem. Soc., 90 (1968) 6841.
21 J. Barrett and S. W. Jeffries, J. Exp. Mar. Biol. Ecol., 7 (1971) 255.
22 T. R. Parsons, J. Mar. Res., 21 (1963) 164.
23 D. W. Fritz and R. D. Strahm, J. High Res. Chromatogr. Chromatogr. Commun., 4 (1981) 584.
24 L. P. Vernon, Anal. Chem., 32 (1960) 1144.
25 P. Hynninen, Acta Chem. Scand., 27 (1973) 1487.
26 J. Barrett and S. W. Jeffrey, Plant Phys., 39 (1964) 44.
27 S. W. Jeffrey, Biochim. Biophys. Acta, 177 (1969) 456.
28 S. W. Jeffrey, Biochim. Biophys. Acta, 279 (1972) 15.
29 S. W. Jeffries, Biochem. J., 80 (1961) 336.
30 K. Tangen and T. Björnland, J. Plankton Res., 3 (1981) 3.
31 J. E. Johansen, W. A. Svec, S. Liaaen-Jensen and F. T. Haxo, Phytochemistry, 13 (1974) 2261.
32 J. H. Knox, High Performance Liquid Chromatography, Edinburgh University Press, 1972, p. 201.
33 K. Eskins and H. J. Dutton, Anal. Chem., 51 (1979) 1885.
34 S. W. Jeffrey and G. F. Humphrey, Biochem. Physiol. Pflanzen, 167 (1975) 191.
35 C. S. Yentsch, in I. Seflick (Ed.), Prediction and Measurement of Photosynthetic Production, Proc. IBP Tech. Meeting, Centre for Agric. Publ. and Documentation, Wageningen, The Netherlands, 1970, p. 489.

Analytica Chimica Acta, 151 (1983) 315–327
Elsevier Science Publishers B.V., Amsterdam — Printed in The Netherlands

DEVELOPMENT OF A NOVEL METHOD FOR MONITORING OILS IN WATER

F. K. KAWAHARA* and R. A. FIUTEM

Environmental Monitoring and Support Laboratory, Environmental Protection Agency, Cincinnati, OH 45268 (U.S.A.)

H. S. SILVUS, F. M. NEWMAN and J. H. FRAZAR

Southwest Research Institute, San Antonio, TX 78284 (U.S.A.)

(Received 10th December 1982)

SUMMARY

A monitor for hydrocarbons in water is described. An unclad optical fiber, inserted through a stainless steel capillary, is coated with an organophilic compound such as octadecyltrichlorosilane. The input radiation is at 632.8 nm from a low-power laser. The normal total internal reflection is degraded by adsorption of hydrocarbons in the organophilic coating, because of the change in refractive index at the surface of the optical fiber, and the variation in output signal can be related to the concentration of hydrocarbon in the water flowing through the capillary. Aromatics, crude oil, and oil products dispersed in water can be measured directly, without solvent extraction. In its present form, the monitor can detect diesel oil in water at 17 mg l^{-1} and crude oil at 3 mg l^{-1}. Moreover, a relationship appears to exist between the solubility of a hydrocarbon and the detection threshold of the monitoring system. With the proper organophilic coating, the use of an optical fiber with a suitable detector will be promising for detection and measurement of such contaminants and, possibly, for specific types.

In recent years, there has been increasing awareness of the potentially harmful effects of world-wide spillage of oils in salt and fresh waters. Sources of waste oils are refineries, shale oil recovery plants, coal conversion operations, chemical plants, ships, offshore drilling platforms, petroleum-handling facilities, and other industries. Oil wastes from these sources may contain toxic and carcinogenic hydrocarbons such as benzenes, polynuclear aromatics, amines, phenols, etc. Methods are needed to detect and quantify oils in water.

Current methods of oil-in-water monitoring are time-consuming and employ extraction and transfer of solvent extract prior to infrared or ultraviolet measurement [1]. Use of an on-line monitor providing direct measurement of oil in water would yield the highly desirable features of simplicity, convenience, and rapid response. Some on-line methods for direct measurement are being developed making use of fluorescence excitation at the 254-nm mercury line [2, 3] but interferences caused by detergents and algae require recalibration before each reading and increase detection limits accordingly. Because of the foregoing difficulties, an entirely different approach for pro-

viding continuous monitoring of oil in wastewaters was sought. One new approach employs an optical fiber that has been precoated with an organophilic grouping, enabling it to adsorb oil from the water matrix. The amount and type of oil adsorbed on the organophilic fiber affects the refractive-index relationship at the fiber surface. A suitable optical sensor then provides the means for measuring oil dispersed in water.

Seventeen pure hydrocarbons, diesel fuel and crude oil were used as contaminants and tested with the new coiled capillary-tube sensor cell. Only well-defined substances were monitored on a batch basis in this preliminary study. Potential real applications of the oil-in-water monitor include the following: monitoring of oil pollutant concentration and providing continuous graphical surveillance, serving as an alarm when an accidental spill occurs, and providing a test method capable of being used for a single sample.

BASIS OF THE TECHNIQUE

Optical fibers are usually composed of two materials arranged coaxially. The inner part of the fiber, the core, can be plastic, glass, fused silica, sapphire, or, in some cases, a liquid. Normally, the fiber core is surrounded by a layer of material, the cladding, which has lower index of refraction than the core. Claddings are typically made of plastic, glass, or silica of low refractive index. A protective jacket of plastic or other material may be applied over the cladding to increase mechanical strength and to facilitate handling of the fiber. Fibers used in this study were not cladded, i.e., only the core of the optical fiber was used in the sensor cell.

Refraction and reflection effects occurring at a refractive interface are important for propagation of light through an optical fiber and are crucial to the operation of the organophilic optical fiber hydrocarbon-in-water monitor described in this paper. Normally, when a light ray is incident on the boundary between two transparent materials of differing refractive index, part of the incident light is reflected, and the remaining energy is refracted or bent through an angle as it enters the second material. In particular, when the refractive index of the material which the light ray is entering is lower than that of the material which it is leaving, the refracted ray is bent toward the material boundary. As the angle of incidence is increased, a critical angle is reached at which the refracted ray is transmitted along the material boundary. As the angle of incidence is increased beyond the critical angle, the ray does not enter the second material, but instead is reflected back into the material from which it came. This phenomenon is known as total internal reflection. Light rays are propagated through the core of an optical fiber by total internal reflection at the core/cladding interface.

The new hydrocarbon-in-water monitor utilizes the core of the optical fiber consisting of fused silica, which was chosen because it had the lowest possible index of refraction and attenuation constant. Detailed research on glass formulations and their properties described by Morey [4] showed that fused silica has the lowest index of refraction of any conventional glass.

However, the index of refraction of fused silica is 1.4585 at 589.3 nm (n_D^{20}), which is relatively high compared to the refractive indices of many organic compounds of interest [5]. Thus, when the medium had a lower index of refraction than the fiber core, light entering the fiber was retained within the fiber by total internal reflection and was transmitted with relatively low attenuation to the opposite end of the fiber.

For the apparatus described here, an unclad optical fiber was chemically treated to render its surface organophilic so that the hydrocarbon material to be measured would adsorb onto the surface. When this fiber, which had greater index of refraction than water, was immersed in water, total internal reflection occurred, and light entering one end of the fiber was propagated to the opposite end with minimum attenuation. This is shown on the left side of Fig. 1. When a small quantity of hydrocarbon material with an index of refraction greater than that of the optical fiber core material was introduced into the water surrounding the fiber, the hydrocarbon contaminant tended to accumulate on the optical fiber because of the organophilic character of the chemically treated surface. Because the hydrocarbon contaminant had greater index of refraction than that of the optical fiber, total internal reflection was degraded in the area contacted by the contaminant. Thus, light propagating through the fiber escaped into the medium, thereby reducing the intensity of light arriving at the output end of the fiber. The degree to which total internal reflection was degraded was related to the quantity of contaminant (i.e., thickness and extent of adsorbed layer) deposited on the fiber surface. This is illustrated on the right side of Fig. 1.

To make this phenomenon useful quantitatively, it is merely necessary to provide a light source of constant intensity at the input end of the fiber and a photosensor at the output end. A flowing sample of the stream to be monitored is then passed over the optical fiber. If the monitored stream contains only water with no hydrocarbon contaminant, then optical transmission through the fiber will be unaffected. In contrast, if hydrocarbons contaminate the water, optical transmission through the fiber will decrease at a rate

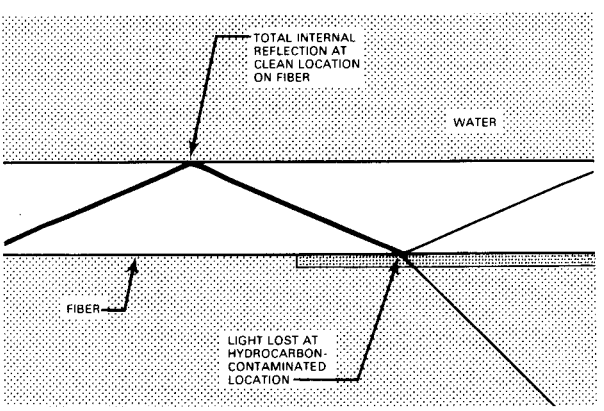

Fig. 1. Unclad optical fiber immersed in water showing light reflection and transmission conditions at clean (left side) and hydrocarbon-contaminated (right side) locations.

related to concentration of the contaminant. Thus, the rate at which optical transmission through the fiber decreases can be interpreted in terms of contaminant concentration.

EXPERIMENTAL

Apparatus

The apparatus used is shown schematically in Fig. 2 [6, 7]. A 1-l reservoir containing the hydrocarbon/aqueous test solution was connected to a stainless steel capillary column via a sample cut-off valve. A reservoir drain valve was also provided for removal of any excess of solution at the end of each test.

The sensor cell was made of stainless steel capillary tubing (0.8 m long, 1.59-mm o.d., 0.58-mm i.d.) formed into a multiturn coil. Inside the capillary tube was a specially treated 0.14-mm diameter fused-silica optical fiber (Amersil). Approximately 5% of the cross-sectional area of the capillary tube was occupied by the optical fiber. The extremes of the optical fiber projecting from the ends of the capillary tube were threaded straight through T-fittings which provided for introduction of test fluids; silicone rubber compression seals were used to retain the test fluid in the sensor cell [7]. The light source for the sensor cell was a 5-mW helium-neon laser (Spectra-Physics Model 120) operating at 632.8 nm. Because of the mounting position of the laser, a 90° prism was used to deflect the beam as shown in Fig. 2. The collimated laser beam was focused by a 10×, 0.33 numerical aperture (N.A.) microscope objective lens to reduce spot size. The objective lens was mounted on a three-axis positioner to facilitate focusing and centering the small spot of light on the input end of the optical fiber. The light beam

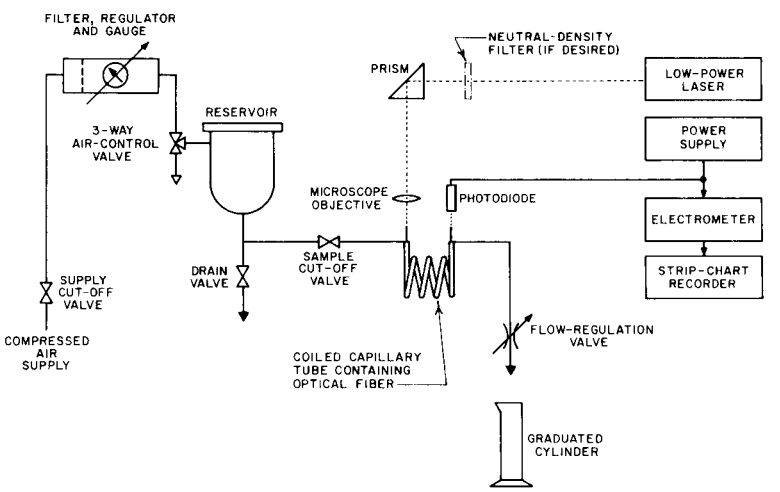

Fig. 2. Schematic diagram of test apparatus including coiled capillary-tube sensor cell.

emerging from the output end of the optical fiber was focused on a silicon photodiode (United Detector Technology, Type PIN-5). The photodiode current, processed by appropriate electronic circuitry, was recorded on a strip-chart recorder.

Two sensor cell designs were evaluated during development of the proposed monitor, but the first design, which was a glass-U-tube, exhibited very low response and was quickly abandoned. The second design involved placing the optical fiber inside a coiled stainless steel capillary as described above. This design exhibited three significant improvements over the U-tube: (1) contact between the test fluid and the organophilic optical fiber was greatly enhanced; (2) the active (i.e., curved) length of the optical fiber was increased; and (3) optical cross-coupling between turns of the coiled optical fiber was eliminated. Effects of these factors were not evaluated individually, but their combined influence on sensor cell sensitivity was determined. The plots in Fig. 3 are of data acquired for the U-tube sensor cell and the coiled capillary-tube sensor cell; the contaminant was 1,2,3,4-tetrahydronaphthalene (tetralin). The capillary-tube sensor cell is obviously better than the U-tube sensor cell: the slope of the capillary-tube plot is greater, providing greater sensitivity, and there is significantly increased response to contaminant concentration. These improvements substantially reduced the effects of system noise.

Reagents

All coating reagents tested are listed in Table 1. Octadecyltrichlorosilane, diphenyldichlorosilane, n-decyltrichlorosilane and tri-n-octylamine were obtained from Aldrich Chemical Co.; octadecyltriethoxysilane (OTES) was obtained from Silar Labs. (Scotia, NY). Methanol, isopropanol, acetone and toluene were all of reagent-grade quality.

Treatment of optical fibers

To minimize handling and possible damage, untreated fibers were placed directly into a straight piece of stainless steel capillary tubing. An apparatus constructed with a four-way cross was used to coat three fibers simultaneously. The drawing compound, a proprietary compound used in optical fiber manufacture, was removed with successive washings of acetone and water. After these cleaning solutions had been drained from the apparatus, the reaction vessel was wrapped with electrical tape and purged with hot, high-purity helium to dry the fibers. Both the incoming helium and reaction-vessel temperatures were held between 150° and 180° C for 8 h. Tubing, fittings, valves, etc. in the fluid flow path were made of 300-series stainless steel. Treating the optical fiber in the same stainless steel capillary tube used for subsequent testing and evaluation not only minimized the possibility of fiber damage, but also provided other benefits, including: (1) use of small quantities of reagents; (2) a constant flow of fresh reagent through the system; and (3) increased contact between the treatment reagent and the optical fiber as a result of small reaction volume.

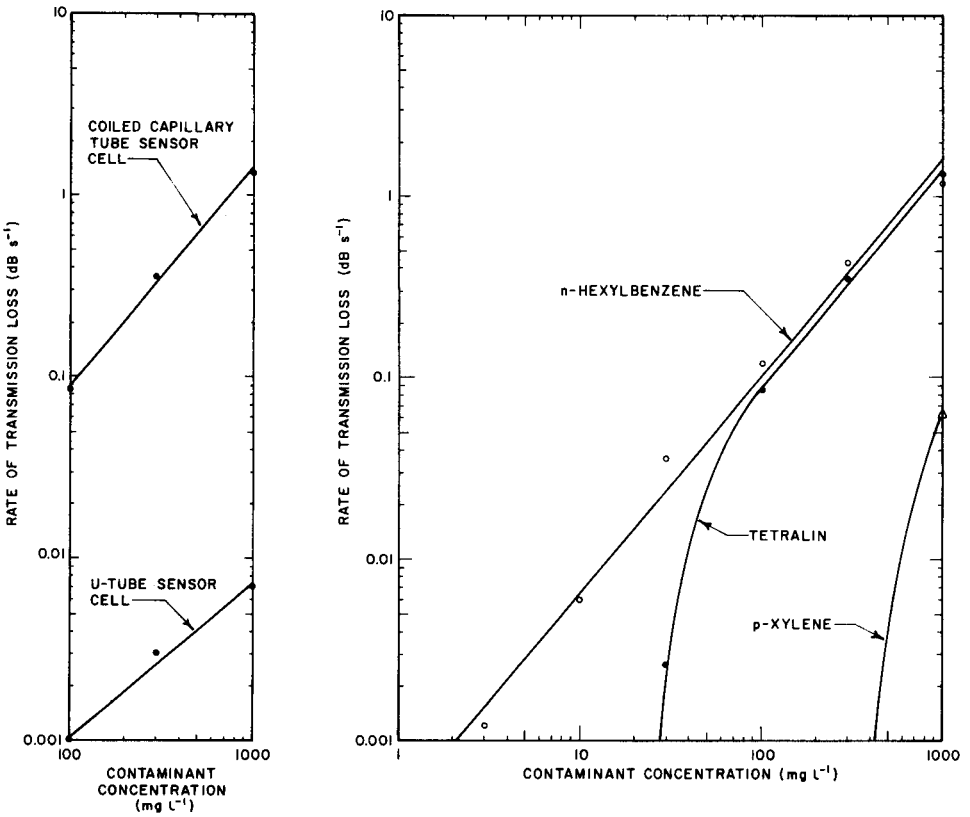

Fig. 3. Comparison of responses of sensor cells of two different designs to tetralin.

Fig. 4. Response of coiled capillary-tube sensor cell to contaminants of varying solubility in water.

TABLE 1

Identification of test fibers

Fiber	Coating reagent composition	Abbreviation
A	Octadecyltrichlorosilane	OTCS
B	Octadecyltriethoxysilane	OTES
C	Octadecyltriethoxysilane 75%	—
	Octadecyltrichlorosilane 25%	—
D	Octadecyltriethoxysilane 95%	—
	Octadecyltrichlorosilane 5%	—
E	Octadecyltriethoxysilane (isopropanol and water as solvent)	—
F	Diphenyldichlorosilane	DDCS
G	n-Decyltrichlorosilane	DTCS

A solution comprising 50 ml of silane treatment reagent in 420 ml of dry solvent (usually toluene) was introduced into the dry apparatus at room temperature. The solution was refluxed for 8 h and then allowed to stand at room temperature for 18 h. Reagents were drained and fibers were washed with dry toluene, followed by 10% tetrahydrofuran/water mixture. The treatment process was then completed by passing dry, high-purity helium over the coated fibers at 150°C for 8 h. Types of organophilic coatings tested are listed in Table 1.

Whenever OTCS was used as a coating agent, tri-n-octylamine was used to neutralize the hydrogen chloride formed as a by-product of the coating reaction. Although this amine has no active hydrogen to react with the organosilane compound, it has a sufficiently long alkyl chain to permit the tri-n-octyl amine—hydrogen chloride salt to be soluble in toluene. The standard hydrogen chloride scavenger, pyridine, was unsuitable because the pyridine—hydrogen chloride salt was insoluble in toluene and would precipitate and clog the capillary.

Test suspension preparation

Test suspensions used to evaluate the chemically treated fibers in the test apparatus were prepared by using an ultrasonic disperser. A 1.0-g quantity of the hydrocarbon contaminant to be used was added to 1 l of deionized water in a glass vessel. Cavitation produced by a sonic horn dispersed the contaminant into very fine particles which remained suspended for several hours. Dilutions were made from the prepared stock to obtain a series of suspensions in half-decade steps of concentration (i.e., 1000, 300, 100,... mg l^{-1}). Because contaminant concentrations greater than 1000 mg l^{-1} were beyond the range of primary interest, concentrations greater than this value were not prepared or used. The lowest concentration was either 10 mg l^{-1} or 1 mg l^{-1} depending on the particular contaminant. The contaminants used during this study included heptadecylbenzene, dodecylbenzene, n-hexylbenzene, tert-butylbenzene, *p*-xylene, ethylbenzene, *m*-xylene, *o*-xylene, chlorobenzene, 2,6-dimethylstyrene, cyclohexylbenzene, tetralin, bromobenzene, 3,3'-dimethylbiphenyl, phenanthrene, 1-methylnaphthalene, 1-phenylnaphthalene, diesel oil, and crude oil. Their refractive indices have been reported [8, 9].

The crude oil used in evaluating the organophilic optical fiber sensor cell was a black, opaque, viscous crude oil from Pearsall, Texas. For characterization purposes, the sample was separated into saturated, aromatic, and polar fractions using a gravimetric liquid chromatographic procedure for oils [10]. Olefins could not be obtained by this method. The composition of the sample by weight was 42% saturated compounds, 25% aromatics and 18% polar compounds; 15% of the sample was lost. Other tests on the crude oil sample indicated a sulfur content of 1.7% by weight and a water content, determined by the Karl Fischer method, of 0.11% by weight. The specific gravity of the sample was 26.0°API at 15.6°C, and the gross heat of

combustion was 43.4 MJ kg^{-1}. Ash content was 0.02% by weight. The pour point was found to be −10°C and the viscosity at 24°C was 97 mm^2 s^{-1} (centistokes).

Evaluation

After a stainless-steel capillary tube containing an organophilic optical fiber had been installed in the apparatus (Fig. 1), 150 ml of reagent-grade acetone was placed in the solvent reservoir and forced through the capillary tube by air pressure (300 kPa or 44 psi). This was followed by a similar amount of methanol. Deionized water (300 ml) was then forced through the sensor cell to ensure that all solvent was flushed from the system. Flow was terminated before all the water had been used so that the flow path remained filled with deionized water.

Test suspensions of a particular hydrocarbon contaminant in water were prepared in various concentrations as previously described and were introduced sequentially into the test apparatus reservoir beginning with the highest concentration. Each test suspension was forced through the sensor cell at a rate of approximately 0.5 ml s^{-1} until the fiber became saturated or all the test solution was used. While the test suspension was flowing through the sensor cell, current through the photodiode was measured on a strip chart recorder. After each suspension had been tested, washings with 150 ml each of acetone and methanol followed by 300 ml of deionized water were repeated as above. In most cases, this cleanup restored optical transmission of the fiber to the value observed prior to the introduction of any hydrocarbon contaminant.

Transmission loss occurring over a specified time interval, given in decibels (dB), was expressed as the rate of change, dB s^{-1}. Slopes obtained with this procedure for a particular hydrocarbon contaminant were plotted on logarithmic graph paper as a function of contaminant concentration (Fig. 4). This format yielded linear plots, in some cases over a range of 2.5 decades. Detection threshold, contaminant concentration at which rate of transmission loss was 0.001 dB s^{-1}, varied from compound to compound and appeared to be related to the solubility of that particular hydrocarbon in water. For crude oil and hexylbenzene, plots were linear from a few mg l^{-1} to 1000 mg l^{-1}; plots were probably linear beyond that point, but no test suspension concentration above 1000 mg l^{-1} was evaluated.

Prototype instrument

The flow diagram of the prototype instrument is illustrated in Fig. 5. The central component of the fluid-handling system is the reservoir which is used for temporary storage of the sample and regeneration solvents. Materials were introduced into the reservoir through either a dip tube which filled the reservoir smoothly from the bottom or a spray nozzle which directed the incoming material against the walls of the reservoir to improve cleaning action. Entry path into the reservoir was determined by the reservoir entry selector,

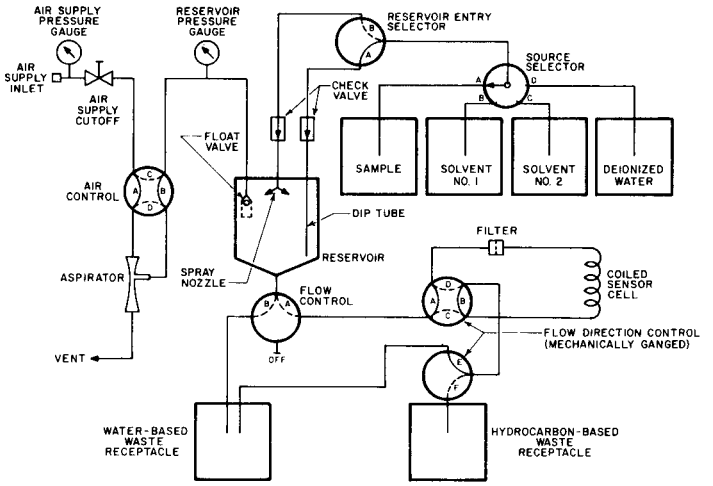

Fig. 5. Flow diagram of prototype instrument.

and the material entering the reservoir (i.e., solvent No. 1, solvent No. 2, sample, or deionized water) was chosen by the source selector. External containers were provided for each of the four materials that could be admitted to the reservoir.

An aspirator operated by compressed air created a partial vacuum in the reservoir, thus providing motive force for transferring fluids from their respective containers to the reservoir. The air control valve provided for directing compressed air into the aspirator during filling of the reservoir and into the reservoir for the purpose of forcing fluids through the sensor cell. An air supply inlet fitting and an air supply cutoff were provided for convenience in handling the compressed air supply, and gauges necessary for monitoring air supply pressure and reservoir pressure were included.

Fluid flow out of the reservoir could be cut off, directed into the sensor cell, or directed into the water-based waste receptacle by the flow control. Direction of flow through the sensor cell was determined by the flow direction control which incorporated two mechanically ganged valves. During the periods of measurement and flushing the sensor cell with deionized water, flow through the sensor cell was in the forward direction, and waste fluid flowed into the water-based waste receptacle.

During the regeneration cycle, when either solvent No. 1 or solvent No. 2 was passed through the system, flow in the sensor cell was in the reverse direction, and waste fluids were delivered to the hydrocarbon-based waste receptacle. A filter in the forward flow inlet side of the sensor cell retained particulate matter which could have clogged the cell; during the regeneration cycle, this filter and the sensor cell were back-flushed with cleaning solutions.

The signal-processing circuit included a logarithmic amplifier which delivered output voltage proportional to the logarithm of the input photodiode

current; the logarithmic signal was then scaled and biased by a linear amplifier. Output voltage from this amplifier was impressed on an analog differentiator which delivered a voltage proportional to the time rate of change of its input voltage. The time constant (i.e., gain factor) of the differentiator was selected by means of a range switch which provided four full scale sensitivity ranges. The output signal of the differentiator was displayed by an analog meter which was calibrated in units of decibels per second (dB s^{-1}) over the range from 0 to 1.0 dB s^{-1}; the range switch provided multipliers of 0.01, 0.1, 1, 10. System noise established a lower limit of 0.001 dB s^{-1} on the operating range.

RESULTS AND DISCUSSION

Seventeen pure hydrocarbons and two hydrocarbon mixtures were used as contaminants during evaluation and test of the new coiled capillary-tube sensor cell. The curves in Fig. 4 illustrate the sensor cell response to three such contaminants: (1) n-hexylbenzene; (2) tetralin (1,2,3,4-tetrahydronaphthalene); and (3) *p*-xylene. The curve for tetralin is typical of the responses observed for many different contaminants; the plot is linear (on logarithmic coordinates) above a particular value of contaminant concentration (100 mg l^{-1} for tetralin) and falls sharply below that value. The value of contaminant concentration at which system response is 0.001 dB s^{-1} is defined, for the present purpose, as the detection threshold. As shown by the curve for *p*-xylene in Fig. 4, the contaminant concentration intercept is about 400 mg l^{-1}. The known solubility of *p*-xylene in water at 25°C is 200 mg l^{-1}. Considering that value, it appears that the detection threshold is slightly greater than the solubility of *p*-xylene. From the plots in Fig. 4, it is evident that the detection threshold for n-hexylbenzene is about 2 mg l^{-1}, for tetralin approximately 30 mg l^{-1}, and for *p*-xylene, slightly greater than 400 mg l^{-1}. Because the greatest contaminant concentration tested was 1000 mg l^{-1}, it is not known how far the linear range extends beyond this value. Data acquired previously [7] indicated that the response for tetralin is linear up to a concentration of at least 7000 mg l^{-1}.

Although most tests of the organophilic optical fiber hydrocarbon-in-water monitor were conducted with pure hydrocarbon compounds, a few tests were done with diesel fuel or crude oil. The system was capable of detecting diesel fuel at a concentration of 17 mg l^{-1}. However, as illustrated in Fig. 6, the system was highly sensitive to crude oil and had a detection threshold of less than 3 mg l^{-1}.

The various organophilic coatings which were applied to the fused-silica fiber are listed in Table 1. Several methods of application were used. Reagent compositions A, F, and G for coating the fibers were dissolved in toluene, but OTES was dissolved in isopropanol because OTES was compatible with alcohol and the chlorosilanes were not. For fiber E, water was tried as a catalyst to aid in fiber coating with OTES in isopropanol. Octadecyltrichlorosilane was also used as a reagent for coating fibers C and D. Assessment of

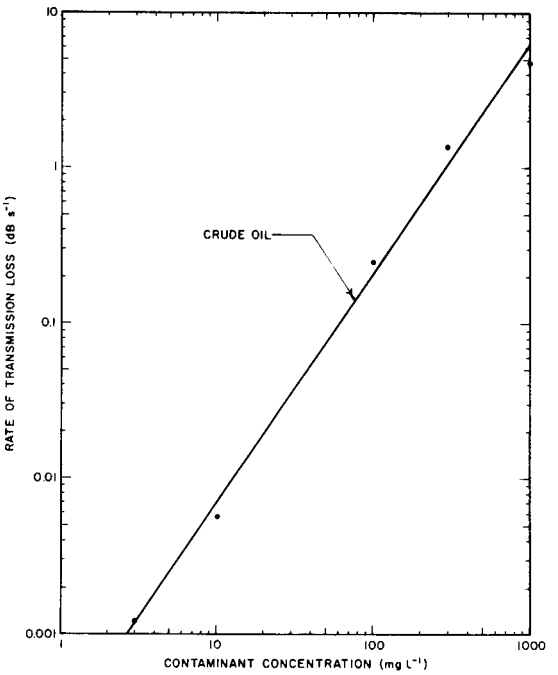

Fig. 6. Response of coiled capillary-tube sensor cell to crude oil in water.

test data indicated that the coating reagent and the method of applying it affected the capability of the optical fiber to adsorb hydrocarbons. Fibers A, B, C, D, and E were prepared to facilitate comparison of OTCS and OTES coating reagents. The hydrocarbon chain chemically bonded on the glass fiber was the same for both of these reagents, but the leaving group was different. With n-hexylbenzene as the test contaminant, better response was obtained with fibers B, C, and E which were treated with OTES; however, the response of fiber D, which was also treated with a triethoxy-based silylating reagent, was about the same as for fiber A which was treated with a trichloro-based silylating reagent. With 1-methylnaphthalene as the test contaminant, fibers B and C exhibited steeper response curves than did fiber A; however, the lower limit of detection of 1-methylnaphthalene was approximately 30 mg l^{-1} for fibers treated with the trichlorosilane reagent and between 30 and 100 mg l^{-1} for fibers treated with the triethoxysilane reagents. Observed sensitivity differences indicate that the chlorosilane reagents generally are superior to the triethoxysilane reagents for treating the fiber surface.

Other reagents which bonded other hydrocarbon groups on the fiber were also tested. A diphenyldichlorosilane reagent was used on fiber F, and n-decyltrichlorosilane was used on fiber G. Test data indicated potentially greater response-curve slope for fibers treated with the diphenyldichlorosilane reagent. The lower limit of detection was approximately the same for

fibers treated with the diphenyl and octadecyl reagents. Fibers treated with the n-decyl reagent were not as sensitive to n-hexylbenzene as fibers treated with the octadecyl or diphenyl reagents, but were more sensitive to crude oil than fibers treated with the octadecyl reagent. The best coating reagent tested for use in the hydrocarbon-in-water monitor instrument was OTCS, which produced the best overall results for a wide variety of hydrocarbon contaminants on a limited number of tests.

Thus, various contaminants with different chemical structures produce different responses in fibers with distinctive coatings. However, it is our expectation that a mixture of OTCS and diphenyldichlorosilane and/or a branched-chain alkyl trichlorosilane and alkylphenyldichlorosilane would provide a more attractive organophilic coating because crude oils are generally mixtures of aromatic, naphthenic, normal branch-chained paraffins, aromatic naphthenic compounds, etc. Thus, with the proper organophilic coating, the use of an optical fiber is promising for detection and measurement of such contaminants.

Detection thresholds (i.e., contaminant concentration for which the rate of transmission loss was 0.001 dB s^{-1}) varied from contaminant to contaminant. From the limited data available, the detection threshold for a particular contaminant seemed related to the solubility of that compound in water. A literature search produced very little specific solubility information because most hydrocarbon compounds which are less than 1% soluble in water are reported as "insoluble". However, specific values of solubility in water at 25°C were found for five of the hydrocarbons tested. For each of these compounds, the detection threshold was slightly greater than the solubility figure illustrated by the curve for *p*-xylene in Fig. 4. Other known aqueous solubilities of tested contaminants at 25°C are 30, 170, 200, and 210 mg l^{-1} for 1-methylnaphthalene, *m*-xylene, *o*-xylene, and ethylbenzene, respectively.

A laser source was selected because it simplified coupling light into the input end of the optical fiber; however, there is no theoretical restriction on the type of light source. Comparison was made of the relative intensity of light emitted from the output end of an optical fiber when the input end was illuminated by four different light sources. The fiber used in these tests was similar to that used in the sensor cell described above. Sources evaluated were a Hewlett-Packard Type 5082-4658 red-light-emitting diode, a Monsanto Type ME 7124 infrared-emitting diode, a General Electric Type 1631X high-intensity incandescent lamp, and a Spectra-Physics Model 120 helium-neon laser.

Each source was tested with the input end of the fiber in several different positions: (1) in contact with the exterior surface of the light source in the region of most intense emission; (2) at the focal point of a 30-mm focal-length, *f*/1.6 plano-convex lens focused to produce minimum spot size; (3) at the focal point of a 12-mm focal-length, *f*/0.676 aspheric condensing lens with focus adjusted for minimum spot size; and (4) at the focal point of a

lens system comprising both of the previously described lenses with the aspheric lens nearest the source. It was found that light intensity emitted from the output end of the fiber was greatest by a factor of 100 when the laser source was used with any of the lenses.

The authors acknowledge the support, interest, and review given by R. L. Booth, J. F. Kopp, and J. J. Lichtenberg. The review made by C. I. Weber is also gratefully acknowledged. This work was supported in part by funds provided by the U.S. Environmental Protection Agency under Grant Number R 805817-01.

REFERENCES

1 M. Gruenfeld, Environ. Sci. Technol., 7 (1975) 636.
2 H. W. Pust, R. E. Kreider and K. W. Gardiner, Proc., 17th Ann. Instrument Soc. Am. Anal. Instrum. Symp., April, 1971, Houston, TX.
3 Sealed Identification Luminescence Monitor. Study of Hazardous Materials, DOT.CG-81-78-1969, Modification 0003, Prepared by Baird Atomic for Coast Guard Academy, New London, CT, December 1980.
4 G. W. Morey, Properties of Glass, 2nd edn., American Chemical Society Monograph Series, Reinhold, New York, 1954.
5 The Aldrich Catalog — Handbook of Organic and Biochemicals, Aldrich Chemical Co., Milwaukee, WI, 1977—78 edn.
6 H. S. Silvus, Jr., F. M. Newman, G. E. Fodor and F. K. Kawahara, in T. F. Yen and D. Walsh (Eds.), Energy and Resource Development of Continental Margins, Pergamon, New York, 1980, pp. 147—162.
7 H. S. Silvus, Jr., F. M. Newman and J. H. Frazar, Technical Report EPA-600/4-80-040, August 1980.
8 P. G. Stecher (Ed.), The Merck Index, 7th edn., Merck and Co., Rahway, NJ, 1960, pp. 1530—1532.
9 R. C. Weast (Ed.), Handbook of Chemistry and Physics, 47th edn., The Chemical Rubber Co., Cleveland, OH, 1966, pp. C75—C601, E150—E151.
10 Annual Book of ASTM Standards, Part 17, Petroleum Products, Designation D1298-67, Standard 2547, 1970, pp. 470—474.

Analytica Chimica Acta, 151 (1983) 329—337
Elsevier Science Publishers B.V., Amsterdam — Printed in The Netherlands

RAPID SEPARATION BY FLOTATION OF SUSPENDED SOLIDS IN FRESH WATERS FOR THE DETERMINATION OF ADSORBED HEAVY METALS

MASATAKA HIRAIDE, JUN MIZUTANI and ATSUSHI MIZUIKE*
Faculty of Engineering, Nagoya University, Chikusa-ku, Nagoya 464 (Japan)
(Received 17th January 1983)

SUMMARY

Microgram or nanogram quantities of heavy metals adsorbed on suspended solids are selectively floated to the solution surface by bubbling for 15 s. Prior to the flotation, negatively charged suspended solids are rendered hydrophobic and coagulated by stirring with a cationic surfactant and sodium chloride. Metal ions, humic acid complexes and colloidal hydrated metal oxides are not floated at all. After the separation of the suspended solids, the trace heavy metals are desorbed by ultrasound in 4 M nitric acid and determined by electrothermal atomic absorption spectrometry. This rapid and convenient flotation technique is successfully applied to the analysis of river, pond and waste waters.

Significant traces of heavy metals are often adsorbed on suspended solids in fresh waters, and their geochemical behavior and biological effects on aquatic organisms can differ greatly from those of dissolved species. Conventionally, suspended solids are defined as the fraction remaining on a 0.45-μm pore size filter, hence filtration is widely used to separate suspended solids from water samples prior to the trace determination. Filtration, however, can become difficult or even impossible because of the clogging of filter pores with the suspended solids. Adsorption of the desired trace heavy metals on filters and contamination from the filter materials can also sometimes cause serious doubts about the results. Centrifugation is not applicable to the separation of suspended solids having densities near unity, and also is inconvenient for large volumes of samples and for operation at sampling locations.

Although flotation of suspended solids has been studied for clarification of turbid waters [1, 2] and for the determination of suspended solids [3], no work has been done on the separation of trace heavy metals adsorbed on suspended solids. In the method described here, suspended solids are rendered hydrophobic and coagulated by stirring with a cationic surfactant and sodium chloride, and the resulting flocs are rapidly floated with the aid of tiny nitrogen bubbles, leaving metal cations and anions, humic acid complexes and colloidal hydrated metal oxides in solution. The flotation technique is faster and more convenient than filtration or centrifugation, and is suitable for operation in the field.

0003-2670/83/$03.00

EXPERIMENTAL

Apparatus

The pyrex glass flotation cell and the polyethylene sampling bottle are shown in Fig. 1. The detachable polyethylene insert prevents adhesion of floated suspended solids on the walls of the flotation cell. Other apparatus used included a Nippon Jarrell-Ash AA-1 Mark II atomic absorption spectrometer with an FLA-10 graphite-furnace atomizer (or with an SA-61 slit burner for iron determination), a Fujitsu well-type NaI(Tl) scintillation counter and a Kaijo Denki TA-4015 ultrasonic generator (29 kHz, 40 W) with a type-4375 transducer (ferrite, 130 × 130 × 110 mm).

Reagents

A surfactant solution (1 mg ml^{-1}) was prepared by dissolving cetyldimethylbenzylammonium chloride (Extra Pure; Tokyo Kasei Kogyo) in 70% ethanol. Kaolin and bentonite (particle size 1—10 μm; Nakarai Chemicals) were used without further purification unless otherwise stated. In some experiments, they were purified as follows: kaolin and bentonite (50 mg each) were dispersed into 25 ml of 7 M nitric acid by ultrasound for 3 min

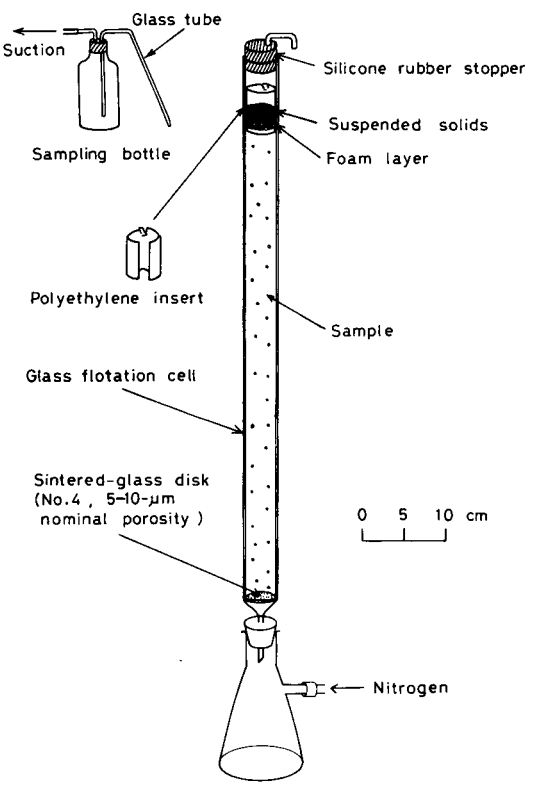

Fig. 1. Flotation apparatus.

and separated by centrifugation at 15 000 rpm for 10 min; this material was washed with 25 ml of water and centrifuged, which was repeated (usually five times) until the pH of the supernatant solution became 5—7. A humic acid solution (0.5 mg ml^{-1}) was prepared by dissolving 25 mg of humic acid powder (Wako Pure Chemical Industries) in 20 ml of 0.1 M potassium hydroxide solution and diluting to 50 ml with water.

The composition of artificial river water was based on analytical results for river waters in Japan [4, 5] (Na 5.9, K 1.1, Mg 2.2, Ca 7.6, Cl 7.4 and SO_4 18.3 mg l^{-1}, pH 7.0). Water was purified by ion-exchange. Reagents used were of reagent grade unless otherwise stated. Radioactive nuclides, ^{51}Cr, ^{54}Mn, ^{65}Zn and ^{115m}Cd, were used as tracers.

Recommended procedure

To a 500-ml sample in a 500-ml beaker, add 2 ml of 5% (w/v) sodium chloride solution and 3 ml of the surfactant solution. Stir the solution magnetically with a 50-mm stirring bar at 500 rpm for 5 min. Transfer the solution quantitatively to a flotation cell, place a polyethylene insert near the solution surface, and close the cell with a silicone rubber stopper (see Fig. 1). Pass nitrogen at a flow rate of 1—1.5 ml cm^{-2} min^{-1} from the lower end of the cell for 15 s. Remove the silicone rubber stopper, and collect the resulting suspended solids/foam layer into a sampling bottle by suction (accompanying solution ca. 2 ml). Suck 2 ml of 7 M nitric acid into the sampling bottle to wash the inner wall of the glass tube. Take out the polyethylene insert using teflon tweezers, and transfer the adhering suspended solids to the sampling bottle with 4 ml of 7 M nitric acid and 2 ml of water. The above operations can easily be done in the field.

Transfer the suspended solids to a 100-ml beaker with 4 ml of 7 M nitric acid and dilute to 4 M in acid with 3 ml of water. Desorb the trace heavy metals from the suspended solids by treating with ultrasound for 3 min. Separate the suspended solids by centrifugation at 15 000 rpm for 10 min, and dilute the supernatant solution to 25 ml with water. If necessary, further dilute the solution with 2.8 M nitric acid. Transfer a 20- or 40-μl aliquot of the solution into a graphite-tube furnace, and determine the heavy metals by graphite-furnace atomic absorption spectrometry (a.a.s.) under the following operating conditions: wavelengths (nm) Cr 357.9, Mn 279.5, Cu 324.8, Cd 228.8 and Pb 283.3; drying at 160°C for 15 s; decomposition at 350°C (Mn, Cd, Pb) or 500°C (Cr, Cu) for 20 s; and atomization at 1 500°C (Cd, Pb), 2 000°C (Mn) or 2 500°C (Cr, Cu) for 10 s.

Other procedures

Filtration. A 500-ml sample was filtered through 0.45-μm pore size filters (47 mm diameter, Millipore HA; previously soaked in 0.1 M hydrochloric acid overnight and washed with water) by replacing filters three times. The separated suspended solids and filters were transferred to a 100-ml beaker with 10 ml of 7 M nitric acid and 7 ml of water. Desorption, centrifugation and determination were then conducted as in the recommended procedure.

Centrifugation. Two 250-ml aliquots were centrifuged by using 300-ml centrifuge tubes at 4000 rpm for 10 min. The separated suspended solids were transferred to a 100-ml beaker with 10 ml of 7 M nitric acid and 7 ml of water. Desorption, centrifugation and determination were conducted as in the recommended procedure.

Tracer experiments. The γ-activity of a 2-ml aliquot of the final 25-ml solution was measured; relative standard deviations were 1—2%.

Turbidimetry. In some experiments, flotation recovery (%) of the suspended solids was estimated from 100 $(A_1 - A_2)/A_1$, where A_1 and A_2 are the absorbances at 400 nm of the solution before and after the flotation.

RESULTS AND DISCUSSION

Flotation of clay particles in water

Clay particles, mainly consisting of kaolin and bentonite, are typical suspended solids in fresh waters and strongly adsorb traces of heavy metals by ion exchange. These particles have negatively charged surfaces [6], which can be rendered hydrophobic with a cationic surfactant. However, direct flotation with the surfactant alone was ineffective. According to a previous study [7], bulky, flocculent precipitates are most suitable for rapid and quantitative flotation. Therefore, prior to the flotation, clay particles (1—10 μm) were coagulated to form flocs of 0.5—2 mm, by stirring with sodium chloride (to increase the ionic strength) and a cationic surfactant. The resulting flocs were rapidly floated by capturing tiny bubbles (0.1—0.5 mm diameter) of nitrogen on the surfaces and in the interstitial spaces. Ethanol, used as a solvent for the surfactant, is essential to obtain a stream of these tiny bubbles, because it prevents coalescence of bubbles which appear from adjacent pores of a sintered-glass disk [8].

Kaolin and bentonite, 30—100 mg each, in 500 ml of water were recovered in greater than 96% yields (estimated by turbidimetry) by the recommended procedure with cetyldimethylbenzylammonium chloride. Flotation with other cationic surfactants, cetylethyldimethylammonium bromide and cetyltrimethylammonium bromide, was also examined, but lower recoveries (81—90%) were obtained.

Flotation behavior of dissolved species

Dissolved species should be left in solution after the flotation. Therefore, various metal cations and anions, iron(III)—humic acid complexes and colloidal hydrated iron(III) oxide passing through a 0.45-μm filter were tested to see if they could be floated. Formation of iron(III)—humic acid complexes in the test solution was confirmed as follows: a large portion of iron(III) was adsorbed on an XAD-2 resin column [9] and the Tyndall effect caused by colloidal hydrated iron(III) oxide was not observed. Table 1 shows that even negatively charged dissolved species, such as iron(III)—humic acid complexes and chromium(VI) ions, are not floated under the recommended

TABLE 1

Flotation of dissolved species in water (500 ml, pH 7)

Metal	Added (μg)	Floated[a] (%)	Metal	Added (μg)	Floated[a] (%)
Zn	2.5	1, 1	Fe(III)	100	0, 0
Cd	5.0	1, 1		400	1, 1
Cr(III)	5.0	0, 1	Fe(III)[b]	100	1, 1
Cr(VI)	10.0	1, 1		400	1, 2
	20.0	1, 2			
	50.0	1			

[a]Determined by atomic absorption spectrometry for Cr(VI) and Fe(III), or γ-activity measurements for Zn, Cd and Cr(III). [b]In the presence of 4 mg of humic acid.

conditions. Chromium(VI) ions could be floated by using higher concentrations (by one order of magnitude) of cetylethyldimethylammonium bromide and longer bubbling times (30 min) [10].

Separation of traces of heavy metals adsorbed on clay particles

The selectivity of flotation was checked with synthetic sample solutions, in which traces of heavy metals were distributed between clay particles and mother liquor. First, the time required for attainment of adsorption equilibria was measured as follows: 500 ml of artificial river water containing a labeled heavy metal and clay particles was stirred continuously, 50-ml aliquots were removed at intervals and centrifuged at 4000 rpm for 10 min, and the γ-activity of the supernatant solution was counted. As shown in Fig. 2, the percentage of heavy metals adsorbed became constant after 1 h. Adsorption of chromium(III) on the clay particles was most significant.

To check the different methods of separation, kaolin and bentonite, 150 mg

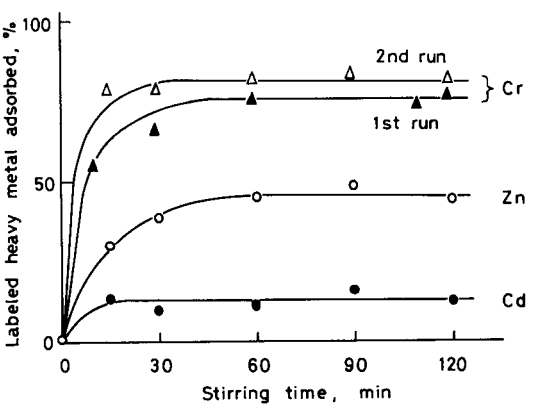

Fig. 2. Adsorption of heavy metals on clay particles (kaolin and bentonite, 50 mg each) in artificial river water (500 ml, pH 7). (△, ▲) Cr(III), 5 μg; (○) Zn, 2.5 μg; (●) Cd, 5 μg.

each, and traces of labeled chromium(III), zinc or cadmium were added to 1 500 ml of artificial river water, and the pH was adjusted to 7 with aqueous 0.1 and 1 M ammonia. The solution was stirred for 2 h and divided into three equal parts. Clay particles in each solution were separated by flotation, filtration or centrifugation. The heavy metals adsorbed on clay particles and remaining in solution were determined separately by γ-activity measurements. As shown in Table 2, the results obtained by the three techniques are in good agreement with each other. Filtration with the Millipore HA filter required ca. 3.5 h because of clogging of filter pores with clay particles; replacing the filter three times reduced the time to ca. 30 min, but the operation was troublesome. Centrifugation with 300-ml centrifuge tubes required ca. 50 min. Flotation is faster (ca. 15 min required) and simpler in operation than filtration and centrifugation.

In further tests designed to check the recovery of adsorbed heavy metals, purified kaolin and bentonite, 150 mg each, and traces of Cr(III), Mn(II), Co, Ni, Cu(II), Zn, Cd and Pb were added to 1 500 ml of water. After pH adjustment and stirring for 2 h, clay particles in a 500-ml aliquot of the solution were separated by flotation, filtration or centrifugation. The heavy metals were then desorbed from the particles and determined by graphite-furnace a.a.s. The spectrometric sensitivity was insufficient for cobalt and nickel, and contamination still occurred for manganese and zinc from purified clay particles. Therefore, the determination was limited to Cr, Cu, Cd and Pb. Calibration graphs were linear up to at least 20 ng ml^{-1} for cadmium, 140 ng ml^{-1} for chromium and copper, and 300 ng ml^{-1} for lead, with maximum

TABLE 2

Separation of heavy metals adsorbed on clay particles (kaolin and bentonite, 50 mg each) and dissolved in artificial river water (500 ml, pH 7)

Labeled heavy metal	Added (μg)		Found, by radioactivity measurements (%)		
			Flotation	Centrifugation	Filtration
Cr(III)	5.0	Adsorbed	78	75	81
		Dissolved	22	21	18
		Total	100	96	99
	5.0	Adsorbed	75	75	79
		Dissolved	20	18	18
		Total	95	93	97
Zn	2.5	Adsorbed	46	45	46
		Dissolved	55	51	52
		Total	101	96	98
	2.5	Adsorbed	46	45	45
		Dissolved	54	52	53
		Total	100	97	98
Cd	5.0	Adsorbed	10	10	11
		Dissolved	88	88	86
		Total	98	98	97

deviations (ng ml^{-1}) of 1 for Cd, 2 for Cr or Cu, and 4 for Pb. The following blank values were obtained by using pure water and purified clays: Cd < 0.03 μg, Pb < 0.1 μg, Cu < 0.05—0.09 μg, Cr < 0.05—0.08 μg (for flotation and centrifugation) and 0.3—0.5 μg (for filtration). The final results corrected for the blank values are shown in Table 3. The values obtained by flotation coincided with those by centrifugation, but filtration often gave higher values for chromium(III) and lead.

Separation of traces of heavy metals adsorbed on suspended solids in pond water

Traces of labeled Cr(III), Mn, Zn or Cd were added to 1 500 ml of pond water. The pH was adjusted to the original value (6—6.5) with aqueous 0.1 or 1 M ammonia, and the solution was stirred for 2 h. Suspended solids in 500-ml aliquots were separated by flotation, filtration or centrifugation, and the γ-activity of the heavy metals adsorbed on the suspended solids was measured. Table 4 shows that the results obtained by the three techniques are in good agreement with each other.

Analysis of fresh and waste waters

Suspended solids in pond, river and waste waters were separated and adsorbed heavy metals were determined by the recommended procedure. The calibration graph for manganese was linear up to at least 40 ng ml^{-1}, with a maximum deviation of 1 ng ml^{-1}. Other calibration graphs were as

TABLE 3

Separation and determination of traces of heavy metals adsorbed on clay particles (purified kaolin and bentonite, 50 mg each) in water (500 ml, pH 7)

Exp.	Heavy metals added		Found, by a.a.s. (μg)		
			Flotation	Centrifugation	Filtration
1	Cr(III), Co, Cd,	Cr(III)	0.5	0.6	1.0
	1.0 μg each;	Cd	0.2	0.2	0.3
	Mn(II), Ni, Cu(II),	Cu(II)	1.1	0.8	1.3
	Zn, Pb, 2.5 μg each	Pb	1.3	1.4	1.4
2	Cr(III), Co, Cd,	Cr(III)	1.4	1.4	1.6
	2.5 μg each;	Cd	0.3	0.3	0.3
	Mn(II), Ni, Cu(II),	Cu(II)	1.9	1.9	1.8
	Zn, Pb, 5.0 μg each	Pb	2.9	2.7	3.4
3	Cr(III), Co, Cd,	Cr(III)	1.6	1.6	2.1
	2.5 μg each;	Cd	0.3	0.3	0.4
	Mn(II), Ni, Cu(II),	Cu(II)	1.7	1.8	1.9
	Zn, Pb, 5.0 μg each	Pb	2.9	3.2	3.0
4	Cr(III), Co, Cd,	Cr(III)	2.8	3.0	3.0
	7.5 μg each;	Cd	0.5	0.5	0.7
	Mn(II), Ni, Cu(II),	Cu(II)	2.0	2.0	2.2
	Zn, Pb, 15.0 μg each	Pb	6.2	6.7	8.5

TABLE 4

Separation of traces of heavy metals adsorbed on suspended solids (SS) in pond water

Sample (500 ml)		Labeled heavy metal added (μg)	Adsorbed (%)		
			Flotation	Centrifugation	Filtration
1[a]		Mn 2.5	2	2	2
(23 mg SS)		Zn 2.5	10	10	11
		Cd 5.0	1	1	3
2[a]	1st	Cr 5.0	64	64	65
(16 mg SS)		Zn 2.5	3	2	2
	2nd	Cr 5.0	65	65	65
		Zn 2.5	2	2	2

[a]Sampled on separate days.

described above. The results are shown in Table 5. For river and waste waters, much higher results for manganese were obtained by filtration. The cause of this is obscure because contamination by manganese from the filtration procedure was less than 0.1 μg. Clogging of filter pores was serious.

TABLE 5

Traces of heavy metals adsorbed on suspended solids (SS) in various water samples

Sample (500 ml)	Metals	Found (μg)		
		Flotation	Centrifugation	Filtration
Pond water[a]	Cr	0.3	0.3	0.2
(12 mg SS)	Mn	40.4	39.3	42.6
	Cu	5.3	5.4	5.1
	Cd	0.1	0.1	0.1
	Pb	3.8	4.0	3.6
Pond water[a]	Cr	0.2	0.2	0.1
	Mn	50.4	50.1	52.9
	Cu	6.1	6.0	5.3
	Cd	0.1	0.1	0.1
	Pb	3.3	3.2	3.4
River water	Cr	0.8	0.7	1.0
(21 mg SS)	Mn	10.0	9.2	15.8
	Cu	0.2	0.3	0.3
	Cd	0.0	0.0	0.0
	Pb	3.9	3.9	6.8
Industrial	Cr	0.1	0.1	0.3
waste water	Mn	11.2	12.9	21.3
(27 mg SS)	Cu	0.3	0.3	0.3
	Cd	0.0	0.0	0.0
	Pb	4.3	3.9	5.5

[a]Sampled on separate days.

Although three sheets of filter were renewed during filtration, ca. 1 and 3 h were required for waste and river waters, respectively.

The experimental results for synthetic and natural water samples confirm that flotation offers a rapid and convenient separation technique for the determination of traces of heavy metals adsorbed on suspended solids.

REFERENCES

1 R. B. Grieves and C. J. Crandall, Water Sewage Works, 113 (1966) 432.
2 R. B. Grieves and W. L. Conger, Chem. Eng. Progr. Symp. Ser., 65 (1969) 200.
3 M. Hiraide, J. Mizutani and A. Mizuike, Bunseki Kagaku, 31 (1982) E 269.
4 J. Kobayashi, Nogaku Kenkyu, 48 (1961) 63.
5 K. K. Turekian, in K. H. Wedepohl (Ed.), Handbook of Geochemistry, Vol. I, Springer, Berlin, 1969, p. 320.
6 H. van Olphen, An Introduction to Clay Colloid Chemistry, Wiley-Interscience, New York, 1963, p. 89.
7 A. Mizuike and M. Hiraide, Pure Appl. Chem., 54 (1982) 1555.
8 M. Hiraide and A. Mizuike, Bunseki Kagaku, 26 (1977) 47.
9 Y. Sugimura, Y. Suzuki and Y. Miyake, Deep-Sea Res., 25 (1978) 309.
10 M. Aoyama, T. Hobo and S. Suzuki, Bunseki Kagaku, 30 (1981) 224.

Analytica Chimica Acta, 151 (1983) 339—347
Elsevier Science Publishers B.V., Amsterdam — Printed in The Netherlands

PREPARATION AND CHARACTERIZATION OF IMINODIACETIC ACID—CELLULOSE FILTERS FOR CONCENTRATION OF TRACE METAL CATIONS

MARIA CARLA GENNARO*, CLAUDIO BAIOCCHI, ENNIO CAMPI, EDOARDO MENTASTI and ROBERTO ARUGA

Istituto di Chimica Analitica, Università di Torino, Via P. Giuria 5, 10125 Torino (Italy)

(Received 13th October 1982)

SUMMARY

The chelating material described has iminodiacetate functional groups chemically bonded to commercial cellulose filters in order to preconcentrate trace metals in aqueous samples. The ions investigated were Cd(II), Co(II), Cu(II), Hg(II), Ni(II), Pb(II) and Zn(II). The influence of pH on the uptake efficiency was studied. While mercury(II) ion was very poorly retained, the capacity values for the other investigated cations were between 171 and 218 μmol g^{-1} of filter. Preconcentration factors of about 100 are easily achieved from solutions containing 100 μg of each metal in one liter. Recovery factors for a single ion were within 96 ± 5% and better than 90% for multicomponent mixtures, when measured by d.c. plasma emission spectrometry.

In trace analysis, a preconcentration procedure is not simply an alternative to the use of sophisticated instrumentation, but is often an integral stage in the sample treatment before the final measurement. When the species of interest have to be determined at or below the detection limit of the instrumental method, preconcentration is essential to raise the analyte concentrations to measurable levels; it may also serve to improve accuracy and precision when separation from interferences is needed. Sometimes, the preconcentration enables simpler instruments to be used in the final measurements, which can simplify automation.

The environmental importance of heavy metals at trace concentrations needs no emphasis here. Most of the toxic metals act through their soluble forms and are not biodegradable in the biogeochemical cycle. Water must be regarded as the most important medium for distribution of these metals along the food chain. Many preconcentration techniques have been proposed. Methods based on direct electrodeposition from waters on mercury cathodes [1], precipitation [2], and liquid—liquid extraction [3] (particularly with chelating agents) are well established.

Recently, various methods have been proposed that involve ion-exchange and complex formation with suitable chelating agents which are adsorbed, absorbed, impregnated or chemically bonded on solid substrates. Activated

0003-2670/83/$03.00

carbon, silica gel with bound aliphatic C-18 chains, polyurethane foams, cellulose, porous glass beads, and polyacrylamide and polystyrene resins have been utilized as substrates. Among the chelating agents tested are 8-quinolinol and its derivatives [4—10], dithiocarbamate [11], polyamines [12], iminodiacetate (Chelex-100 resin) groups [13, 14], thiols [15] and amino acids [16, 17]. The aim of these binding methods is to fix trace metals quantitatively from large volumes of water, by either column or batch procedures. Sometimes, the stationary phase can be used directly for measurements but more often the concentrated metals must be eluted.

In the system described below, iminodiacetate groups are chemically bonded to ordinary cellulose filter discs. Preconcentration of Cd(II), Co(II), Cu(II), Hg(II), Ni(II), Pb(II) and Zn(II) ions on the treated filters is described. The metals are eluted with hydrochloric acid and measured by d.c. plasma emission spectrometry.

EXPERIMENTAL

Preparation of the filters

The iminodiacetate groups were attached to the paper by adapting the method of Smits and Van Grieken [18] for treatment with diethylenetriamine. Disodium iminodiacetate was prepared by slowly adding sodium hydroxide pellets (about 10% excess) to 200 g of iminodiacetic acid in 500 ml of water; the mixture was stirred and cooled until the reaction was complete. The salt solution was then passed through activated carbon. After evaporation and four recrystallizations from water and ethanol, the salt purity was checked by potentiometric titration with standard acid.

The absence of contaminating inorganic impurities in the filters was checked by passing 1.0 M HCl through the filters and examining the solution by d.c. plasma emission spectrometry.

For the preparation, about twenty Whatman 41 cellulose filter discs (47-mm diameter) were conditioned for 60 min in about 400 ml of dry dimethylformamide (DMF), freshly distilled in presence of 10% of benzene (to maximize the chlorination yield, solvents must be anhydrous). The DMF was then removed from the filters and mixed with 12 ml of phosphorus oxychloride. The brown-red mixture was heated on a water bath to 90°C, and the cellulose filters were added. Heating was continued for about 30 min; during this time, the filters were carefully separated from each other with a glass rod. The brown filters produced in this chlorination reaction were washed with DMF, twice-distilled water, 5% sodium hydroxide solution, twice-distilled water, 5% acetic acid solution, twice-distilled water and DMF, in that order. The filters, again white, were then treated at 105—110°C for about 150 min, in a saturated solution of disodium iminodiacetate in DMF (about 600 ml) and water (250 ml); water was replaced as it evaporated. In this reaction, the iminodiacetate (IDA) group replaced the chlorine group attached to the cellulose:

$$\text{Cell.}{-}\text{OH} \xrightarrow[\text{DMF}]{\text{POCl}_3} \text{Cell.}{-}\text{Cl} \xrightarrow{\text{Na}_2\text{IDA}} \text{Cell.}{-}\text{N}(\text{CH}_2\text{COONa})_2$$

The filters were washed repeatedly with twice-distilled water and left to dry on a glass plate. They were then ready for use; they appeared similar to untreated filters, apart from some surface roughness.

Reagents and equipment

Metal stock standard solutions (1000 mg l^{-1}; C. Erba for atomic absorption) were diluted as required. All other chemicals were analytical-grade reagents, and were checked by plasma emission spectrometry for the absence of contaminating metals at relevant levels. Water was twice-distilled from quartz.

All laboratory glassware, and polyethylene and polypropylene equipment, was thoroughly cleaned by soaking it in 6 M nitric acid and repeatedly rinsing with twice-distilled water.

For the emission measurements, a d.c. plasma emission spectrometer Spectraspan IV (SMI, Andover, MA, U.S.A.) was used. Two-point calibration (high and low standards) was done. The standard solutions contained the same amount of hydrochloric acid as the samples. At least two independent measurements were made for each sample. In order to check the reliability of the measurements of the metal concentrations in mixtures, and to choose the most suitable wavelength, multicomponent mixtures were prepared in 1 M hydrochloric acid. Table 1 shows the wavelength, accuracy and reproducibility for each cation in a mixture.

The pH was measured with a Metrohm 605 pH meter and glass and calomel electrodes. Adjustable Eppendorf pipets were used for solution preparation. A Millipore filtration system was used to ensure reproducible placement of the prepared filters.

RESULTS AND DISCUSSION

As is very well known, iminodiacetic acid in aqueous solution forms moderately stable complex species, hydroxylated and not, containing ligand-to-metal ratios of 1 and 2 with many metal ions [19]. Nevertheless, information about the affinity shown by an immobilized ligand towards metal cations, predicted from equilibrium data in homogeneous aqueous solutions, implies disregard of the fact that the equilibria leading to the metal ion fixation actually take place in a heterogeneous phase. Furthermore, the distribution of the chelating sites on the filter surface might affect the possible stoichiometry of the complex species formed, so that the stoichiometry might be different from that obtained from aqueous solutions. Moreover, ionic-exchange equilibria also probably contribute to the uptake of the metal by the filter.

On the basis of these arguments, it was necessary to conduct a systematic preconcentration study for each investigated metal ion, as a function of pH.

TABLE 1

Spectral and statistical data for the spectrometric measurements

Cation	λ (nm)	Mean recovery and r.s.d. (%)	No. of measurements
Cd(II)	214.4	98.5 ± 1.4	11
Co(II)	345.3	100.5 ± 1.2	8
Cu(II)	324.7	99.5 ± 0.3	10
Hg(II)	253.6	98.5 ± 1.8	8
Ni(II)	352.5	96.5 ± 2.1	10
Pb(II)	405.8	97.2 ± 2.0	12
Zn(II)	213.8	100.3 ± 1.5	10

Preliminary measurements at the pH values corresponding to the maximum recovery made it possible to choose the best working conditions. The treated filter was fitted in a Millipore filtration system; solutions of 1000.00 ml containing 0.100 $\mu g\ ml^{-1}$ of the investigated cation were prepared. The release was done with 10.00 ml of 1.0 M hydrochloric acid. The filtration of the 1 l of the solution required a mean time of 60--75 min: no appreciable increase in the recovery efficiency was obtained by passing the solution a second time. In these conditions, a preconcentration factor of 100 is gained; therefore emission measurements were made on solutions with concentrations of about 10 mg l^{-1}, well above the detection limits of the measurements. After elution with hydrochloric acid and repeated washings with water (negative test for chloride) the chelating filters were ready to be utilized for another measurement. No filter efficiency loss was noticed after several re-uses; anyway, the filter was prudently changed after about ten filtrations.

When solutions having pH values greater than 6 were passed through the filters, a sharp decrease in the pH value could be observed. Such a decrease is due not only to complex formation but also to proton--metal exchange equilibria, as was proved when a similar decrease was observed when solutions containing only sodium ions were filtered. In order to evaluate the effect of pH on the recovery yield, measurements were made on solutions containing the investigated cations at different pH values, using filters previously conditioned at the same pH values. The percentage recoveries (with relative standard deviation estimates) as a function of pH, obtained for nickel(II) ion, are listed

TABLE 2

Recovery (%) for nickel(II) ion uptake (100 $\mu g\ l^{-1}$ of solution) on IDA—cellulose filter as a function of pH

pH	2.3	3.0	4.1	5.2
Ni found (μg)[a]	88.5 ± 1.0	98.5 ± 1.6	96.3 ± 2.3	95.0 ± 2.1
pH	6.2	7.5	8.8	9.9
Ni found (μg)[a]	94.5 ± 3.5	90.8 ± 4.1	82.5 ± 2.5	73.0 ± 3.0

[a]Mean and relative standard deviations for 4—6 measurements.

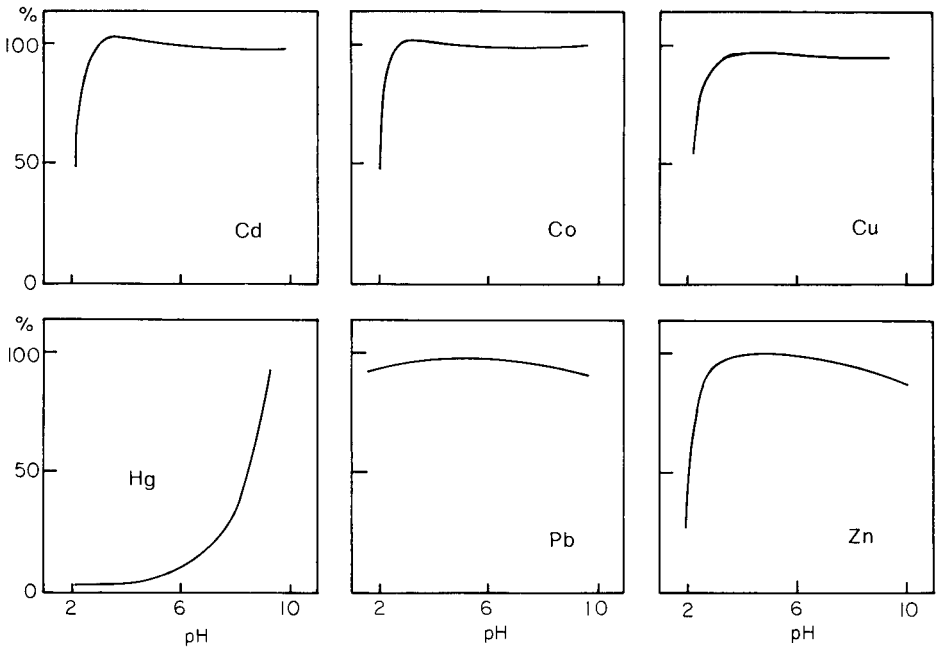

Fig. 1. Variation with pH of recovery (%) for Cd(II), Co(II), Cu(II), Hg(II), Pb(II) and Zn(II) ions on IDA—cellulose filters.

in Table 2. Figure 1 shows the recoveries as a function of pH for the other investigated ions. It may be observed that for all the ions studied the mean recovery is 96 ± 5% in the pH range 3—7, with the exception of mercury(II), for which the maximum recovery reaches only 20% at a pH value about 7 in this pH range.

TABLE 3

Capacity values and related quantities for the uptake of Cd, Co, Cu, Hg, Ni, Pb and Zn ions on IDA—cellulose filters

Ion	pH	Ion found (mg)[a]		Error (%)	Amount retained	
		Unretained	Retained		μmol/ filter	μmol g^{-1}
Cd(II)	3.0	7.09	3.07	+1.6	27.3	171
Co(II)	3.0	8.40	1.61	+0.1	27.3	171
Cu(II)	3.0	7.51	2.06	—4.3	32.4	202
Hg(II)	9.0	8.02	2.80	+8.0	14.0	88
Ni(II)	3.0	8.35	1.73	+0.8	29.5	184
Pb(II)	5.0	2.80	7.23	+0.3	34.9	218
Zn(II)	3.0	8.26	1.64	—0.1	25.1	157

[a]10 mg of the ion was taken.

For each cation studied, the filter capacity (maximum amount of a metal cation fixed by a filter) was evaluated. A portion (100 ml) of solution containing 10 mg of one metal ion was passed through the filter. The filtrate was put aside and the metal fixed on the filter was released with hydrochloric acid. The metal concentration in this solution, evaluated by titration with EDTA [20], represents the capacity value; the titration of the unretained metal in the filtrate confirmed the data and gave also the error of the measurement. The values obtained are listed in Table 3, as mg or μmol fixed by a single filter; in order to compare the data obtained with literature data, the capacity was also expressed as μmol g^{-1}, by evaluation of the mean weight of a single filter (0.16 g).

The correlation between the affinity shown by the metal for the filter and its complex formation constants [19] with iminodiacetic acid is clear: this is most obvious in the case of mercury(II) ion, which shows the lowest affinity among the studied ions and which has the lowest formation constants [19].

Some mixtures were prepared with different cations (100 μg of each metal in 1 l, at pH about 3). Typical results (preconcentration factor $\approx$100) are

TABLE 4

Uptake evaluation in multicomponent mixtures (100 μg of each metal in 1 l was used in each case, at pH 3) and mean uptake recovery for the investigated ions in multicomponent mixtures

Mixture	Recovery (%)	Mixture	Recovery (%)	Mixture	Recovery (%)
Cd(II)	98.0	Cd(II)	95.0	Cu(II)	92.0
Ni(II)	101.5	Pb(II)	103.5	Pb(II)	106.2
Pb(II)	103.0	Zn(II)	100.5	Zn(II)	98.2
Cd(II)	92.8	Cd(II)	97.4	Cd(II)	88.0
Co(II)	91.8	Co(II)	96.4	Co(II)	81.5
Ni(II)	89.5	Ni(II)	95.6	Cu(II)	90.8
Pb(II)	103.5	Pb(II)	99.5	Ni(II)	81.5
Zn(II)	98.0	Zn(II)	101.4	Pb(II)	96.9
Hg(II)	~4.4			Zn(II)	90.5
	~93.8 (unretained)				

Ion	Mean recovery (%)	No. of measurements
Cd(II)	94.7 ± 4.0	12
Co(II)	91.4 ± 6.7	8
Cu(II)	91.4 ± 0.9	4
Ni(II)	92.8 ± 7.7	10
Pb(II)	102.0 ± 4.6	15
Zn(II)	97.9 ± 4.3	12

listed in Table 4. It can be noted that an increase in the number of components decreases the recovery. Moreover, mercury(II) ion in mixtures, is very poorly retained, so that a separation of mercury(II) from the other cations studied appears feasible. In Table 4, the average collection efficiency (%) is also listed together with the standard deviations for each cation in a multicomponent mixture; these values are always greater than 90%.

With the described procedures, it is possible to preconcentrate a natural water sample directly on site, without preliminary pH adjustment. The transfer of large water sample volumes to the laboratory can thus advantageously be replaced by transport of the filtration system, with elution in the laboratory. Contamination during storage is thus also avoided.

As regards the capacity of the filter towards metals, a comparison with other fixing materials is of interest (Table 5). Most data are not directly comparable, as they were evaluated by batch or immersion methods, which probably gave greater capacity values than the filtration method. If comparison is made on the strictly analogous Chelex 100 (Dowex A1) chelating resin, comparable capacity values are observed (see Table 5). An advantage of the treated cellulose filters is that they are prepared from preformed filters under mild conditions so that the iminodiacetate units are inserted on surface positions, thus ensuring no retardation in metal uptake or release (during the subsequent acid desorption) because of migration into the inner substrate

TABLE 5

Capacity values (at the optimum pH) of various chelating materials (mmol g^{-1})

	Cd(II)	Co(II)	Cu(II)	Ni(II)	Zn(II)	Pb(II)	Hg(II)
IDA—cellulose filters[a]	0.171	0.171	0.202	0.184	0.157	0.218	0.088
Chelex 100 [21][b]		0.50			0.50		
Chelex 100 membranes [13]					0.36[c]		
Chelex 100 on Makrolon (batch eq. 20 h) [14]	1.765						
Silica immobilized oxine (batch eq.) [8]			0.061				
Porasil—oxine (batch eq. 30 min) [9]			0.052				
Aminopropyl—silica gel oxine [10]			0.070				
Resorcinol—oxine—formaldehyde (H^+ cat.; batch eq. 48 h) [7]		0.01	>0.05	0.005	0.01		
Resorcinol—oxine—formaldehyde (OH^- cat.; batch eq. 48 h) [7]		0.02	0.05	0.02	0.05		
Polystyrene—azo—oxine (batch eq. 48 h) [7]		0.25	0.048	0.10	0.33		
Azo—oxine from 4-nitrosoresorcinol—CH_2O polycondensate (batch eq. 48 h) [7]		1.48	1.51	1.45			
3:1 Nitrosoresorcinol—phenol—CH_2O polycondensate (batch eq. 48 h) [7]		1.32	1.82	1.38			
Polyacrylamide thiol resins : PX_n—SH (eq. time 5—120 min) [15]							
n = 10					2.1		
n = 30					1.7		
Polystyrene—oxime—diethylamino resin (batch exp.) [4]			2.0				

[a]This paper. [b]Chelex 100 is stated by the manufacturer (Bio-Rad) to have a capacity of 0.40 meq ml^{-1} for all the metal ions listed above. [c]Recomputed value.

TABLE 6

Uptake evaluation in a multicomponent mixture containing sodium ions (pH 3)

Cation	Amount of metal (μg)		Recovery (%)
	Taken	Collected	
Cd(II)	100.0	96.2	96.2
Pb(II)	100.0	91.0	91.0
Zn(II)	100.0	93.2	93.2
Na(I)	292.0	97.5	33.4

structure; such retardation is expected for polymeric substrates like Chelex 100. Batch uptakes may also be easier with the proposed IDA-cellulose, cut in the desired form. X-ray fluorescence detection may be applied directly to the filter, thus avoiding manipulations like pelletization of the resin [21, 22]. The availability of high-purity analytical cellulose papers ensures low levels of impurities as well as low cost for the proposed filters.

In order to use IDA-cellulose filters for preconcentrating metal ions in natural aqueous samples, it is necessary to consider possible competitive complexation equilibria from other chelating agents (e.g., humic acids) and interferences, during the immobilization and measurement steps, from cations present in the samples in high amounts (Na^+, Ca^{2+}, Mg^{2+}, etc.). Tests on the retention of lead and zinc ions in the presence of comparable amounts of sodium ions (10 mg in 100 ml) showed that the capacity values for Pb^{2+} and Zn^{2+} (166 and 188 μmol g^{-1}, respectively) were not significantly different from those evaluated in absence of sodium.

The collection efficiencies obtained for a mixture containing in 1 l of solution Cd^{2+}, Pb^{2+}, Zn^{2+} (100 μg each) and Na^+ (in about three-fold amount, 292 μg) showed (Table 6) that only 33% of sodium is fixed and that its presence does not appreciably affect the recoveries of the other cations. However, when natural waters are examined, as in the case of industrial [23] or sea waters [24], recoveries are not quantitative with Chelex 100, presumably because of the formation of non-labile coordinated forms of the metals and adsorption of ions on colloidal particles; the present filters would suffer from the same problem because the same coordinating unit is present. Acid digestion or ultraviolet irradiation to decompose organic substances may make the uptake quantitative [25].

REFERENCES

1 P. Figura and B. McDuffie, Anal. Chem., 52 (1980) 1433.
2 H. Watanabe, S. S. Berman and D. S. Russell, Talanta, 19 (1972) 1363.
3 W. D. Silvey and R. Brennan, Anal. Chem., 34 (1962) 784.
4 A. Sugii, N. Ogawa and H. Hashizume, Talanta, 26 (1979) 189.
5 S. P. Bag and H. Freiser, Anal. Chim. Acta, 134 (1982) 333.

6 M. B. Colella, S. Siggia and R. M. Barnes, Anal. Chem., 52 (1980) 967, 2347.
7 F. Vernon and H. Eccles, Anal. Chim. Acta, 63 (1973) 403.
8 R. E. Sturgeon, S. S. Berman, S. N. Willie and J. A. H. Desaulniers, Anal. Chem., 53 (1981) 2337.
9 J. R. Jezorek and H. Freiser, Anal. Chem., 51 (1979) 366.
10 J. M. Hill, J. Chromatogr., 76 (1973) 455.
11 A. Miyazaki and R. M. Barnes, Anal. Chem., 53 (1981) 299.
12 J. A. Smits and R. E. Van Grieken, Anal. Chem., 52 (1980) 1479.
13 R. E. Van Grieken, C. M. Bresseleers and B. M. Vanderborght, Anal. Chem., 49 (1977) 1326.
14 F. Clanet, R. Deloncle and G. Popoff, Water Res., 15 (1981) 591.
15 A. Deratani and B. Sebille, Makromol. Chem., 182 (1981) 1875.
16 C. Y. Liu and P. J. Sun, Anal. Chim. Acta, 132 (1981) 187.
17 A. Sugii, N. Ogawa and I. Katayama, Talanta, 29 (1982) 263.
18 J. Smits and R. Van Grieken, Angew. Makromol. Chem., 72 (1978) 105.
19 L. G. Sillèn and A. E. Martell, Stability Constants of Metal-Ion Complexes, The Chemical Society, Spec. Publ. 17 and 25, London, 1964 and 1971; A. E. Martell and R. M. Smith, Critical Stability Constants, Vol. 1, Plenum Press, New York, 1974.
20 G. Schwarzenbach and H. Flaschka, Complexometric Titrations, Methuen, London, 1969.
21 J. Smits, J. Nelissen and R. Van Grieken, Anal. Chim. Acta, 111 (1979) 215.
22 R. Van Grieken, Anal. Chim. Acta, 143 (1982) 3.
23 J. Minczewski, J. Chwastowska and R. Dybczynski, Separation and Preconcentration Methods in Inorganic Trace Analysis, Horwood, Chichester, 1982.
24 T. M. Florence and G. E. Batley, Talanta, 23 (1976) 179.
25 T. M. Florence and G. E. Batley, CRC Crit. Rev. Anal. Chem., 9 (1980) 219; T. M. Florence, Anal. Chim. Acta, 141 (1982) 73.

Analytica Chimica Acta, 151 (1983) 349—358
Elsevier Science Publishers B.V., Amsterdam — Printed in The Netherlands

DETERMINATION OF HYDROXYBENZENES IN FOSSIL FUEL-DERIVED LIQUIDS AND IN ASSOCIATED PROCESS WATERS[a]

LEROY B. YEATTS, Jr., GREGORY B. HURST and JOHN E. CATON*

Analytical Chemistry Division, Oak Ridge National Laboratory, Oak Ridge, TN 37830 (U.S.A.)

(Received 22nd November 1982)

SUMMARY

Elution of a nonpolar stationary (reversed)-phase C_{18} column with 40% (v/v) acetonitrile in water, buffered with sodium acetate—acetic acid at pH 4.6, produced good resolution of several low-molecular-weight hydroxybenzenes including phenol, *o*-cresol, *m* + *p*-cresol, resorcinol, catechol, and hydroquinone. The unique fluorescent characteristics of hydroxybenzenes enhanced both selectivity and detection limits and facilitated the quantitative estimation of these compounds in a complex mixture after a simple extraction followed by isocratic elution. The determinations can be made within a 24-h period and require small amounts of sample-handling and personnel time. Applications of this scheme to the quantitation of hydroxybenzenes in fossil fuel-derived liquids and associated process waters are described.

With the increased production of liquid and gaseous fuels from coal and oil shale, the need for convenient and reliable procedures for the determination of hydroxybenzenes in synthetic fuels and the associated environmental samples becomes quite important. Several of these compounds are considered to be toxic [1]. Phenol is reported to be a tumor-promoter [2, 3] and catechol a cocarcinogen [4]. Although these materials may be present in crude petroleum, they are present in much greater quantities in materials derived from oil shale or coal. Consequently, during the processing and refining of such materials, losses to the environment by volatilization to the atmosphere and by extraction into aqueous waste streams and process water discharges may occur.

Hydroxybenzenes in environmental samples have been quantified by gas—liquid chromatography utilizing wall-coated open tubular glass (w.c.o.t.) columns [5—12], packed columns [13—18], and porous layer open tubular (p.l.o.t.) columns [19]. In many cases, the w.c.o.t. columns are interfaced with a mass spectrometer [6—10] to produce less ambiguous identification of each compound. Ultraviolet (u.v.) spectra have also been used for identification [8]. In addition, derivatization techniques have been used as part of the determination of hydroxybenzenes by gas—liquid chromatographic methods [5, 6, 8, 15].

In recent years, several investigators have examined the possibilities of utilizing high-performance liquid chromatography (h.p.l.c.) for the determination of hydroxybenzenes in water. In most cases, a u.v. detector was used [20—25]. Generally, some labor-intensive sample clean-up steps, such as solvent extraction and sample preconcentration, were required before utilization of the relatively inselective u.v. detector. Ogan and Katz [26] exploited the u.v. fluorescence of hydroxybenzenes to develop a reversed-phase h.p.l.c. method for the determination of phenol in aqueous samples, using isocratic elution with 20% acetonitrile in water. More recently Ogan and Katz [27] reported a h.p.l.c. method for the detection of 19 alkylphenols by gradient elution with acetonitrile/water followed by fluorimetric detection.

The object of this present work was to extend the work of Ogan and Katz so that those hydroxybenzenes most commonly found in fossil fuel-derived liquids and in associated process waters could be accurately quantified after minimal sample preparation. The hydroxybenzenes of general interest in such samples were monohydroxybenzene, *o*-, *m*-, and *p*-cresols, resorcinol, and catechol.

EXPERIMENTAL

Reagents and samples

Chemical compounds of the best grade available were used as received from the following sources: resorcinol, Fisher Scientific Co.; 4-methylcatechol, Pfaltz and Bauer; β-naphthol, Matheson Co.; 4-allyl-2-methoxyphenol (eugenol), Eastman Organic Chemicals; hydroquinone, catechol, phenol, *o*-, *m*-, *p*-cresols, 2-methylresorcinol, 4-ethylresorcinol, 3-methylcatechol, *o*-methoxyphenol (guaiacol), *m*-methoxyphenol, 3-ethylphenol, 2,3-dimethylphenol, 4-ethylphenol, 3,4-dimethylphenol, 2-ethylphenol, 2,3,5-trimethylphenol, and 2,4,6-trimethylphenol, Aldrich Chemical Co.; ^{14}C-phenol, Amersham/Searle Corp. High-purity acetonitrile (Burdick and Jackson Laboratories) served as the solvent for all the standard solutions and as a component in the buffered 40% (v/v) acetonitrile/water eluent. The buffer solution was prepared from analytical reagent-grade glacial acetic acid (Mallinckrodt) and analyzed reagent-grade sodium acetate (J. T. Baker Chemical Co.).

The water samples were procured at various stages in an operating coal liquefaction pilot plant. They are, therefore, realistic mixtures for testing the system.

The oil samples were supplied by the USEPA/USDOE Fossil Fuels Research Materials Facility [28] at Oak Ridge National Laboratory, Oak Ridge, TN.

Apparatus

A Perkin-Elmer Model 3920 gas chromatograph with a flame ionization detector (FID) was used to separate and quantify the hydroxybenzenes

present in water samples. The system and method, with minor modifications, were as described by Ho et al. [29]. Resolution was accomplished with a 15 ft × 1/8 in. o.d. glass column packed with 60/80 mesh Tenax-GC.

The liquid chromatographic system was assembled in this laboratory. The ion-modified eluent was filtered through a Hasteloy steel, 2-μm pore-size cylindrical frit (Upchurch Scientific) to protect the check valves on the high-pressure, continuously-adjustable flow pump (Laboratory Data Control). A reversed-phase (C_{18}) guard column (Brownlee Labs) was used to protect the reversed-phase (C_{18}) analytical column (Alltech Associates). A Rheodyne Model 7020 injection valve with a 20-μl loop was used to introduce the sample solution to the system. The RSIL-C18-HL analytical column (25 cm × 4.6 mm i.d. × 6.3 mm o.d.) was packed with 10-μm particles coated with 18% bonded organic material. In addition to the high amount of organic phase, this packing material is end-capped. Such a packing is ideal for reversed-phase chromatography of polar compounds eluted with pH-modified solvents. This column was monitored by a Perkin-Elmer Model 203 fluorescence spectrophotometer followed by a Beckman Model 153 u.v. monitor. The flow cell for the fluorescence spectrophotometer was purchased from NSG Precision Cell.

Liquid scintillation counting of ^{14}C-phenol spiked solutions was done with a Packard C-2425 Tri-Carb Spectrometer. Aquasol-2 (New England Nuclear) was used as scintillation cocktail for all such samples.

Sample preparation

Process water samples of approximately 5-ml volume were filtered through a 13-mm diameter nylon-66 filter (Rainin Instrument Co.) mounted in a stainless steel filter holder with Luer connections (Millipore Corp.) for syringe-driven filtration. In many instances, the samples were so concentrated in hydroxybenzenes that they were diluted with distilled water. A 20-μl aliquot was then injected directly onto the reversed-phase h.p.l.c. column.

Duplicate oil samples of about 25 mg each were weighed into scintillation vials; subsequently, 100 μl of ^{14}C-phenol in benzene ($\sim 4.5 \times 10^4$ dpm ml^{-1}, 5 mCi mmol^{-1}), and 3 ml of dichloromethane were added. The hydroxybenzenes were extracted from the oils by adding 3.0 ml of 0.1 M sodium hydroxide and vigorously stirring the phases with a small magnetic bar overnight or about 16 h. The alkaline layer (acid fraction) was separated with a Pasteur pipette, placed in a 5-ml volumetric flask, made slightly acidic with 20 μl of glacial acetic acid, and diluted with the buffered 40% acetonitrile eluent to the 5.0-ml mark. Portions of this solution were injected onto the h.p.l.c. column. The recovery of the ^{14}C-phenol spike was established by counting radioactive decays of 100 μl of the neutralized, buffered solutions. Although this recovery evaluation was subsequently considered to be the proportion of the sample recovered, it applies only to phenol in the strictest sense. Other hydroxybenzene compounds with similar acidity and molecular weight are likely to be recovered in about the same proportion as phenol. However,

the recovery of highly alkylated hydroxybenzenes could be substantially lower than the recovery estimated from the phenol tracer. Nevertheless, such an estimation of recovery facilitates the procedures for low-molecular-weight phenols because the aqueous extract does not have to be quantitatively removed.

Procedure

Hydroxybenzenes in process water samples and standard solutions were quantified by gas chromatography (g.c.) [29] by direct injection of 5-μl portions onto the Tenax column. The column temperature was initially held at 150°C for 4 min and then programmed at 2°C min^{-1} to a final temperature of 230°C; the inlet and detector temperature was 300°C in both cases. The helium carrier gas inlet pressure was regulated at 80 psig. The hydroxybenzenes were identified on the basis of their retention times and quantified by comparing peak heights with those of standard solutions.

A sample was introduced into the h.p.l.c. system with a 20-μl sample loop on the injection valve. The degassed eluent, 40% v/v acetonitrile in distilled water buffered at pH 4.6 with sodium acetate (5×10^{-4} M)—acetic acid (10^{-3} M), was pumped at a rate of 1.0 ml min^{-1}. The fluorescence detector was operated at an excitation wavelength of 266 nm and an emission wavelength of 300 nm. Tentative identifications of hydroxybenzenes were based on retention volumes while quantitations were based on peak heights and carbon-14 recovery corrections. As a quality control measure, standard solutions were processed at the beginning and end of each day. The column was cleaned after every 20 runs by eluting it with 90% (v/v) acetonitrile in distilled water. With such care, this h.p.l.c. column has shown insignificant deterioration even after more than 250 runs over a period exceeding one year.

RESULTS AND DISCUSSION

The ion-modified isocratic eluent provided good resolution for these hydroxybenzenes. In this system, isocratic elution with 20—60% (v/v) acetonitrile in water mixtures without ion modification yielded less satisfactory resolution for the hydroxybenzenes of interest than did the same system with ion modification. The chromatogram in Fig. 1 of a standard solution of eight hydroxybenzenes (~10 μg ml^{-1} each), which are of greatest interest in most samples associated with synfuels, shows quite acceptable resolution of the isomers 1,3- and 1,2-dihydroxybenzene (resorcinol and catechol, respectively) and of *o*-cresol from its isomers. However, *m*- and *p*-cresols were not resolved at these operating conditions. The precision of fluorescence response following the h.p.l.c. separation of several low-molecular-weight hydroxybenzenes was assessed by injecting five replicates of a standard solution (~10 μg ml^{-1}). The chromatographic peak height for phenol, *m* + *p*-cresols, and *o*-cresol had relative standard deviations (RSD) of

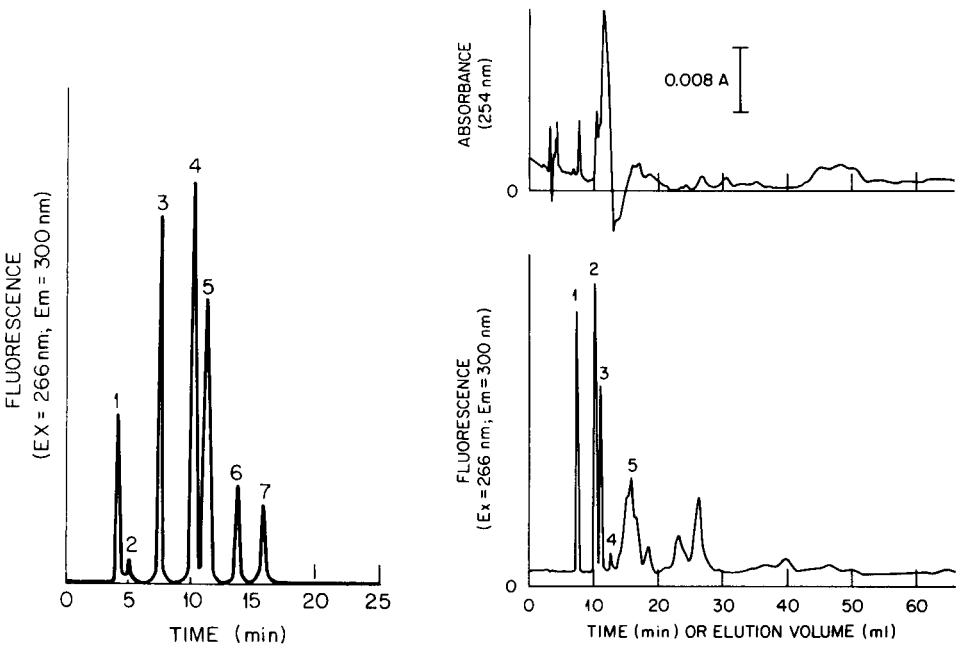

Fig. 1. Chromatogram of several hydroxybenzenes in a standard solution. Peaks: (1) resorcinol; (2) catechol; (3) phenol; (4) *m* + *p*-cresols; (5) *o*-cresol; (6) 3,4-dimethylphenol; (7) 4-ethylphenol.

Fig. 2. Comparison of u.v. absorbance and fluorescence response of several hydroxybenzenes in the weak acid fraction of a synthetic fuel. Peaks: (1) phenol; (2) *m* + *p*-cresols; (3) *o*-cresol; (4) 3,4-dimethylphenol; (5) 4-ethylphenol.

±1.5% while the RSD for 3,4-dimethylphenol was ±2.5% and for 4-ethylphenol, ±2.9%.

Inspection of the elution volumes and relative retentions listed in Table 1 indicates that elution volume increases with the extent of alkyl substitution. Although not surprising, this increased retention is fortuitous because coal-derived synfuels contain numerous alkyl phenols [21] which could not be completely resolved by this isocratic separation. The hydroxy- and dihydroxy-benzenes with either no alkyl substitution or a single methyl substitution are eluted with a retention of 1.5 (Table 1) or less relative to phenol. Beyond a relative retention of 1.5, it is evident from the chromatogram of the synthetic fuel sample extract illustrated in Fig. 2 that resolution may be less than adequate with Peak 5 (relative retention 2.1) showing several unresolved species. However, the portion of this chromatogram occurring at retentions of up to 1.8 relative to phenol showed sharp symmetrical chromatographic peaks for all synthetic fuel samples or associated water samples which were studied. This region of lower retention contains the hydroxybenzenes of major interest (phenol, and *o*-, *m*-, and *p*-cresol as

TABLE 1

Relative retention of hydroxybenzenes on a C_{18} reversed-phase h.p.l.c. column

Compound	Elution volume (ml)	Relative retention volume[a]	Compound	Elution volume (ml)	Relative retention volume[a]
Hydroquinone	3.8	0.48	3,4-Dimethylphenol	14.4	1.8
Resorcinol	4.4	0.55	3-Ethylphenol	16.4	2.1
2-Methylresorcinol	5.0	0.63	4-Ethylphenol	16.6	2.1
Catechol	5.2	0.65	2,3-Dimethylphenol	17.0	2.1
4-Methylcatechol	6.4	0.80	β-Naphthol	18.2	2.3
4-Ethylresorcinol	7.0	0.88	2-Ethylphenol	19.2	2.4
3-Methylcatechol	7.2	0.90	4-Allyl-2-methoxyphenol	21.6	2.7
Phenol	8.0	1.0	2,3,5-Trimethylphenol	25.6	3.2
m-Methoxyphenol	8.0	1.0	2,4,6-Trimethylphenol	28.1	3.5
o-Methoxyphenol	8.4	1.1			
p-Cresol	10.7	1.3			
m-Cresol	10.8	1.4			
o-Cresol	11.8	1.5			

[a]Elution volume for compound/elution volume for phenol; column was eluted with 40% acetonitrile in water buffered at pH = 4.6.

well as the dihydroxy compounds, resorcinol, catechol, and hydroquinone) in any screening evaluation for hydroxybenzenes. Because the phenols and cresols tend to be major hydroxybenzene constituents and because the ultraviolet fluorescence of these compounds greatly enhances the selectivity of detection, this chromatographic method facilitates the quantitation of these compounds. However, samples associated with synfuels processes contain a complex mixture of hydroxybenzenes and there is always a possibility of interference by co-elution.

The fluorescence responses of phenol, catechol, resorcinol, *o*-cresol, *p*-cresol, and 3,4-dimethylphenol were measured and found to be linear with injected amounts, as the results in Table 2 indicate. With the exception of catechol, no significant stability problems were noted, and calibrations remained linear with essentially zero intercepts even after extended storage. Catechol solutions were observed to degrade significantly during routine storage (0°C, dark), so that it was necessary to prepare standard solutions weekly. In fact, standard solutions of catechol stored at room temperature on the laboratory bench (no protection from light) failed to show a catechol peak in the chromatogram after 2—3 days of storage. Such degradation can provide an explanation for the significant negative intercept and the relatively greater uncertainty in the slope shown for catechol in Table 2. If a larger proportion of the catechol had degraded in the more dilute standards, then the relationship between fluorescence and concentration would depart from linearity by showing some concave curvature with fluorescence response values lower than expected for a given concentration. This behavior

TABLE 2

The linear relationship between fluorescence response and amount of hydroxybenzene injected

Compound	Range of amount[a] (ng)	Slope (Fl g^{-1})[b]	Intercept (F)[b]	Standard error (F)	Correlation coefficient
Phenol	20—200	23.5 ± 0.2[c]	0.0010 ± 0.0026[c]	0.002	0.9998
Catechol	30—225	4.30 ± 0.16	—0.104 ± 0.018	0.015	0.9913
Resorcinol	50—400	9.86 ± 0.10	—0.0050 ± 0.0047	0.004	0.9996
o-Cresol	80—920	14.7 ± 0.1	0.0008 ± 0.0025	0.002	0.9998
p-Cresol	200—2200	6.94 ± 0.03	0.0015 ± 0.0024	0.002	0.9999
3,4-Dimethylphenol	200—2300	5.16 ± 0.02	—0.0028 ± 0.0013	0.001	0.9999

[a]Five data points in each case.
[b]F is the peak height determined as fraction of full scale; therefore, slope units are fraction-liter/gram.
[c]Standard deviation.

was observed for the calibration curve for catechol even with careful protection (0°C, dark) of the catechol standard. Because of this apparent instability of catechol, it might be considered of little relevance in synfuel studies. However, catechol is considered to be bioactive [4] and may be able to exist in the synfuel product because of the protection against radiation afforded by the intense color of the crude oil.

In Table 3, levels of hydroxybenzenes in several typical synfuel process waters determined by this method are compared to levels determined by a g.c. method [29]. In general, the results by h.p.l.c. are somewhat higher than those from g.c. measurements. However, the agreement between results from two diverse methods applied to a complex mixture is satisfactory for quanti-

TABLE 3

Comparison of g.c. and h.p.l.c. results for the hydroxybenzene content of several process waters from a synfuels plant

Sample No.	Concentration (g l^{-1})					
	G.c. method			H.p.l.c. method		
	Phenol	*o*-Cresol	*m* + *p*-Cresols	Phenol	*o*-Cresol	*m* + *p*-Cresols
1	1.4	0.3	0.8	1.9	0.36	1.0
2	2.4	0.4	1.0	1.9	0.34	1.0
3	1.8	0.3	0.8	2.2	0.43	1.2
4	2.7	0.4	1.3	3.3	0.66	1.9
5	2.2	<0.1	0.6	2.9	0.03	1.0
6	3.8	0.1	1.8	3.9	0.13	2.7
7	3.1	<0.1	0.9	3.0	0.01	2.2
8	2.8	<0.1	1.1	3.4	0.02	1.9

tative estimates; especially when one considers that the g.c. method is less sensitive and shows lower reproducibility for water samples. A single g.c. determination may estimate *m*- + *p*-cresol best because the flame ionization detector response to *m*- and *p*-cresols might be expected to be the same for all practical purposes whereas the fluorescence detector response to these two isomers is quite different, the fluorescence measurements being about 1.8 times more sensitive to *m*-cresol than to *p*-cresol. Because the proportions of these isomers would almost certainly vary from the 50/50 mixture used in the calibration standards, the estimation of the total amount of *m*- plus *p*-cresol in a real sample may be less reliable when an average response factor is applied to the response for one sample concentration measured at one set of fluorescence excitation and emission parameters. Although beyond the scope of this present work, good estimates for both *m*- and *p*-cresol could be obtained by measurements at two different sets of fluorescence conditions.

Although a shale-derived crude synfuel product may have a chemical composition that is different from a coal-derived synfuel, NBS Standard Refer-

TABLE 4

Determination of several hydroxybenzenes in typical fossil fuel-derived liquids

Sample[a]	Concentration, mg g^{-1} of sample			
	Phenol	*o*-Cresol	*m* + *p*-Cresols	3,4-Dimethyl-phenol
Coal-derived				
H-Coal ASOH (Syn) No. 1308	29	12	56	2.2
H-Coal ASB (Syn) No. 1309	0.65	0.6	2.3	<1
H-Coal VSOH (Syn) No. 1310	0.4	<0.6	1.2	<1
H-Coal VSB (Syn) No. 1311	<0.4	<0.6	<1	<1
H-Coal ASOH (FO) No. 1312	24	14	41	1.3
H-Coal ASB (FO) No. 1313	2.8	2.2	7.7	<1
H-Coal VSOH (FO) No. 1314	1.0	0.8	3.0	<1
H-Coal VSB (FO) No. 1315	<0.4	<0.6	<1	<1
H-Coal Distillate No. 1601	8.2	11	47	1.9
H-Coal "Dist" HDT-L No. 1602	2.9	6.6	15	<1
H-Coal "Dist" HDT-M No. 1603	0.7	3.8	3.3	<1
H-Coal "Dist" HDT-H No. 1604	<0.4	<0.6	<1	<1
SRC II FO Blend No. 1701	41	20	126	4.5
$ZnCl_2$ Dist No. 1801	<0.4	<0.6	1.9	<1
Shale-derived				
Paraho No. 4601	0.4	<0.6	<1	<1
Petroleum crude oils				
Wilmington No. 5301	<0.4	<0.6	<1	<1
Recluse No. 5305	<0.4	<0.6	<1	<1

[a]These materials are described in detail elsewhere [30].

ence Material 1580, a shale oil, is the only standard reference material available for crude synfuel products. Therefore, the precision and accuracy of the proposed method was tested with six replicates of this reference shale oil. The recovery of the ^{14}C-phenol spike added to each oil sample was found to be 79.6% ± 1% (RSD); blank determinations of spike added to dichloromethane indicated that the oil matrix had no effect upon the recovery. The concentration of phenol in NBS 1580 is listed by NBS as 407 ± 50 $\mu g\ g^{-1}$ of oil compared to our determination of 444 ± 26 $\mu g\ g^{-1}$. This agreement is quite acceptable and supports the overall validity of the method for the determination of phenol in synfuels. Nevertheless, it should be remembered that this validity check was done on a shale-derived synfuel which, like most shale-derived products, has a much lower phenolic content than comparable coal-derived materials.

In Table 4 are listed the average concentrations of several hydroxybenzenes in duplicate samples of typical fossil fuel-derived liquids. Phenol and the cresol isomers are the hydroxybenzenes most commonly found in these liquids and their concentrations are seen to vary widely from one liquid to another. None of the three dihydroxybenzene isomers (catechol, resorcinol, and hydroquinone) nor their simple alkyl derivatives were detected even though the measurement system was sensitive to their presence (see Table 1). It is possible that the basic extraction conditions enhance the decomposition of dihydroxybenzenes in oil samples. Future studies will deal with this possible decomposition and with the application of this simplified procedure to other complex organic mixtures.

This research was sponsored by the U.S. Environmental Protection Agency under Interagency Agreement DOE No. 40-601-76, EPA No. 79-D-X0319-1 under Union Carbide Corporation contract W-7405-eng-26 with the U.S. Department of Energy.

REFERENCES

1 W. B. Deichmann and M. L. Keplinger, in G. D. Clayton and F. E. Clayton (Eds.), Patty's Industrial Hygiene and Toxicology, 3rd revis. edn., Vol. 2A, Wiley, New York, 1981, Ch. 36.
2 M. H. Salaman and O. M. Glendenning, Br. J. Cancer, 11 (1957) 434.
3 R. K. Boutwell and D. K. Bosch, Cancer Res., 19 (1959) 413.
4 B. L. Van Duuven, C. Katz and B. M. Goldschmidt, J. Nat. Cancer Inst., 51 (1973) 703.
5 V. Fell and C. R. Lee, J. Chromatogr., 121 (1976) 41.
6 M. P. Maskarinec, G. Alexander and M. Novotny, J. Chromatogr., 126 (1976) 559.
7 H. S. Hertz, J. M. Brown, S. N. Chesler, F. R. Guenther, L. R. Hilpert, W. E. May, R. M. Parris and S. A. Wise, Anal. Chem., 52 (1980) 1650.
8 M. E. Snook, P. J. Fortson and O. T. Chortyk, Tobacco Sci., 24 (1980) 78.
9 F. R. Guenther, R. M. Parris, S. N. Chesler and L. R. Hilpert, J. Chromatogr., 207 (1981) 256.
10 V. Raverdino and P. Sassetti, J. Chromatogr., 153 (1978) 181.

11 J. Hrivnak and J. Macak, Anal. Chem., 43 (1971) 1039.
12 L. Renberg and K. Lindstrom, J. Chromatogr., 214 (1981) 327.
13 C. D. Criswell, R. C. Chang and J. S. Fritz, Anal. Chem., 47 (1975) 1325.
14 K. Callmer, L.-E. Edholm and B. E. F. Smith, J. Chromatogr., 136 (1977) 45.
15 L. Tullberg, I.-B. Peetre and B. E. F. Smith, J. Chromatogr., 120 (1976) 103.
16 P. A. Mulawa and S. H. Cadle, Anal. Lett., 14 (1981) 671.
17 R. A. Baker, Am. Water Works Assoc., 58 (1966) 751.
18 D. A. J. Murray, J. Fish. Res. Board Can., 32(2) (1975) 292.
19 P. C. Uden, P. Carpenter, Jr., H. M. Hackett, D. E. Henderson and S. Siggia, Anal. Chem., 51 (1979) 39.
20 K. Bhatia, Anal. Chem., 45 (1973) 1344.
21 J. F. Schabron, R. J. Hurtubise and H. F. Silver, Anal. Chem., 51 (1979) 1428.
22 N. V. Raghavan, J. Chromatogr., 168 (1979) 523.
23 P. Roumeliotis, W. Liebold and K. K. Unger, Int. J. Environ. Anal. Chem., 9 (1981) 27.
24 P. A. Realini, J. Chromatogr. Sci., 19 (1981) 124.
25 K. A. Pinberton, J. High Resolut. Chromatogr. Chromatogr. Commun., 4 (1981) 33.
26 K. Ogan and E. Katz, Chromatogr. Newsl., 7 (1979) 15.
27 K. Ogan and E. Katz, Pittsburgh Conf. Anal. Chem. Appl. Spectrosc., Atlantic City, NJ, March, 1980 (Paper No. 225).
28 W. H. Griest, D. L. Coffin and M. R. Guerin, Fossil Fuels Research Matrix Program, ORNL/TM-7346, Oak Ridge National Laboratory, Oak Ridge, TN (June 1980).
29 C.-H. Ho, B. R. Clark and M. R. Guerin, J. Environ. Sci. Health, A11(7) (1976) 481.
30 M. R. Guerin, I. B. Rubin, T. K. Rao, B. R. Clark and J. L. Epler, Fuel, 60 (1981) 282.

Analytica Chimica Acta, 151 (1983) 359—369
Elsevier Science Publishers B.V., Amsterdam — Printed in The Netherlands

MEMBRANE SEPARATION IN FLOW INJECTION ANALYSIS
Gas Diffusion

W. E. VAN DER LINDEN

Laboratory for Chemical Analysis, Department of Chemical Technology, Twente University of Technology, P.O. Box 217, 7500 AE Enschede (The Netherlands)

(Received 20th January 1983)

SUMMARY

A general expression is derived for the membrane transport process in a flow-through unit as commonly used in flow injection systems. The validity of the formulae was tested for gas-diffusion membranes by using compounds with different volatilities such as ammonia, carbon dioxide and acetic acid. Several microporous hydrophobic membranes were tested. A new module design is proposed.

Membranes can be used in flow analysis systems in order to transfer certain compounds from a donor (sample) stream to an acceptor (detector) stream. This principle has been used for many years in continuous flow systems, with gas-diffusion and dialysis membranes. Baadenhuijsen and Seuren-Jacobs [1] seem to be the first who have exploited this concept in flow injection analysis (f.i.a.) in a procedure for the determination of carbon dioxide in plasma using a gas-permeable membrane. Růžička and Hansen [2] refer to a similar procedure for the determination of ammonia, but details have not been published. As no quantitative description seems to have been presented of the membrane transport process in a flow-through unit and its dependence on the characteristic membrane parameters, it was decided to investigate this problem both from the theoretical and the practical point of view. The general equation derived was tested for some volatile compounds such as carbon dioxide, ammonia and acetic acid, with different types of gas-diffusion membranes.

THEORY

A mathematical relationship of the concentrations on both sides of the membrane as a function of time in dependence on the transfer coefficient and the flow rate can be derived starting from a tank-in-series model. In this model, the membrane separation unit (Fig. 1) is supposed to consist of a series of hypothetical units in each of which the solutions are homogeneous, i.e., ideally mixed (Fig. 2). If ΔV is taken as the volume on one side of the

0003-2670/83/$03.00

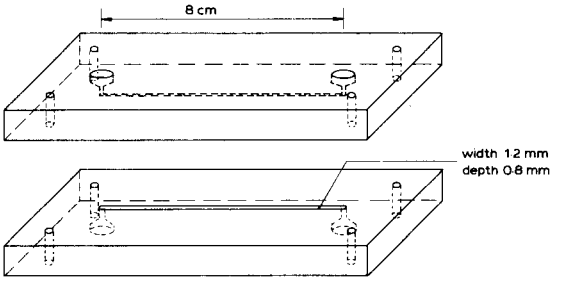

Fig. 1. Membrane separation module.

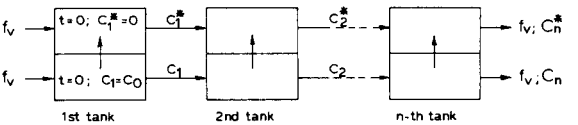

Fig. 2. Tanks-in-series model of membrane separation module.

membrane of such a hypothetical unit and it is assumed that the degree of transfer of the relevant compound is proportional to the concentration difference across the membrane, the following mass balances hold:

$$\Delta V \, dC_n/dt = -f_v C_n + f_v C_{n-1} - k(C_n - C_n^*) \quad (1)$$

$$\Delta V \, dC_n^*/dt = -f_v C_n^* + f_v C_{n-1}^* + k(C_n - C_n^*) \quad (2)$$

where the flow rate, f_v, is equal for both the donor and acceptor streams for simplicity reasons; C_n is the concentration on the donor side, and C_n^* is the concentration on the acceptor side, both for the nth separation unit (tank). Apart from the compound to be transferred, both streams are assumed to have basically the same composition. The transfer coefficient, k, is not specified here but will contain the parameters governing the different steps leading to the overall transfer: i.e., diffusion of the compound from the bulk to the solution/membrane interface, partition between donor solution and membrane phase, diffusion inside the membrane, partition between membrane and acceptor solution, and diffusion from the surface into the bulk of the acceptor phase.

Starting with the pulse-wise introduction of an amount of the relevant component corresponding to a concentration of C_0 in the first tank in the donor stream at $t = 0$, Eqns. (1) and (2) can be solved (see Appendix A) leading to the general expressions:

$$C_n = 1/2 \frac{1}{(n-1)!} (f_v t/\Delta V)^{n-1} \exp[-f_v t/\Delta V] \{1 + \exp[-2kt/\Delta V]\} C_0 \quad (3)$$

$$C_n^* = 1/2 \frac{1}{(n-1)!} (f_v t/\Delta V)^{n-1} \exp[-f_v t/\Delta V] \{1 - \exp[-2kt/\Delta V]\} C_0 \quad (4)$$

Already for $n > 10$, the terms before the braces lead to approximately Gaussian peaks with a maximum at

$$t_{max} = (n-1)\,\Delta V/f_v \tag{5}$$

and a variance of

$$\sigma_t^2 = (n-1)\,(\Delta V/f_v)^2 = t_{max}^2/(n-1) \tag{6}$$

For larger values of t, the term within braces in Eqns. (3) and (4) will reach the value 1 and the compound will ultimately become equally distributed between the two streams.

In many practical applications, the component that permeates through the membrane will be chemically converted to a product, P (e.g., $CO_2 + H_2O \rightleftharpoons HCO_3^- + H_3O^+$ or $NH_3 + H_2O \rightleftharpoons NH_4^+ + OH^-$). If the conditions in the acceptor stream are chosen in such a way that the conversion is complete and the stoichiometry of the reaction is 1:1, then the mass balance equations reduce to

$$\Delta V\, dC_n/dt = -f_v C_n + f_v C_{n-1} - kC_n \tag{7}$$

$$\Delta V\, dC_{p,n}^*/dt = -f_v C_{p,n}^* + f_v C_{p,n-1}^* + kC_n \tag{8}$$

where $C_{p,n}^*$ stands for the concentration of P in the nth tank in the acceptor stream. According to the development presented in Appendix B, these equations lead to the general expressions:

$$C_n = \frac{1}{(n-1)!}\,(f_v t/\Delta V)^{n-1}\,\exp[-f_v t/\Delta V]\exp[-kt/\Delta V]\,C_0 \tag{9}$$

$$C_{p,n}^* = \frac{1}{(n-1)!}\,(f_v t/\Delta V)^{n-1}\,\exp[-f_v t/\Delta V]\,\{1-\exp[-kt/\Delta V]\}C_0 \tag{10}$$

Starting from the same mass balances, Eqns. (3), (4), (9) and (10) can also be derived in an elegant way by means of Laplace transformation as shown by Reijn et al. [3] in a treatment of kinetics in f.i.a. In general, only the concentration C^* leaving the membrane separation unit and transported to the detector, or detecting system, is of importance. Depending on the magnitude of the term $kt/\Delta V$, two extremes will be considered.

Extreme cases

Small kt/ΔV. In the case of gas diffusion, this situation will occur, for instance, if the permeability is low or if the vapor pressure of the relevant component is relatively low, i.e., the compound is very readily soluble in the donor stream. Expansion of the exponential term within braces in Eqn. (10) leads to

$$C_{p,n}^* = \frac{1}{(n-1)!}\,(f_v t/\Delta V)^{n-1}\,\exp[-f_v t/\Delta V]\,\{kt/\Delta V - 1/2(kt/\Delta V)^2 + \ldots\}C_0$$

which approaches

$$C^*_{p,n} \simeq \frac{1}{(n-1)!} (f_v t/\Delta V)^{n-1} \exp[-f_v t/\Delta V] \{kt/\Delta V\} C_0 \quad (11)$$

In an experimental set-up of constant geometry, the peak maximum is found at $t_{max} = (n-1)\,\Delta V/f_v$, so $f_v t_{max}/\Delta V$ is constant as long as the number of tanks can be considered to be constant. This situation is approximately warranted, e.g., in a single bead string reactor (SBSR) [4]. In that case

$$(C^*_{p,n})_{t_{max}} = \text{constant} \times (kt/\Delta V) C_0 \quad (12)$$

which means that the peak height is directly proportional to the residence time in the separation unit and inversely proportional to the flow rate.

Large kt/ΔV. In this case, the exponential term within braces in Eqn. (10) approaches zero:

$$C^*_{p,n} = \frac{1}{(n-1)!} (f_v t/\Delta V)^{n-1} \exp[-f_v t/\Delta V] C_0 = \text{constant} \times C_0 \quad (13)$$

and, again at a constant value of n, the peak height will become independent of the flow rate.

EXPERIMENTAL

Chemicals and solutions

All chemicals used were of analytical-reagent grade.

Indicator stock solutions. For the cresol red solution, 1 g of cresol red was dissolved in 20 ml of 0.1 M NaOH and diluted to 1 l with water. This indicator was used in combination with the carbonate buffer. For the phenolphthalein solution, 1 g of phenolphthalein was dissolved in 100 ml of ethanol (96%) and diluted to 1 l with water. This indicator was used in combination with the ammonia buffer. For the bromocresol green solution, 2 g of bromocresol green was dissolved in 125 ml of 0.1 M NaOH and diluted to 1 l with water. This indicator was used in combination with the acetate buffer.

Buffer solutions. The $NaHCO_3/Na_2CO_3$, NH_4Cl/NH_3 and acetic acid/sodium acetate buffers of the desired pH were prepared from 10^{-3} M solutions of sodium carbonate, ammonium chloride or acetic acid, respectively, by adding hydrochloric acid or sodium hydroxide as appropriate.

Reagent solutions. Acceptor solutions were prepared by adding 10 ml of the indicator stock solution to 1 l of the buffer solution. The donor stream for the determination of ammonia was 0.1 M sodium hydroxide, for carbon dioxide 0.1 M sulphuric acid, and for acetic acid 1 M sulphuric acid.

In the case of ammonia, Nessler's reagent was also used. This reagent was obtained from Merck, but a solution prepared by the procedure of Krug et al. [5] was also tested. Because the addition of Nessler's reagent to the acceptor stream caused clogging of the membrane pores, 0.1 M sodium

hydroxide was used as the primary acceptor solution, which was then mixed with the reagent in a mixing coil after the stream had passed the membrane unit, as shown schematically in Fig. 3. In this set-up, it was easy to interchange the outlets of the membrane unit so that the ammonia concentration in both the acceptor and the donor stream could be measured (C and C^*), thus allowing the calculation of an absolute value of the overall transfer of ammonia across the membrane.

Equipment

Membrane separation module. Three types were examined. The first was a laboratory-made module manufactured in perspex (see Fig. 1) with a groove of 8-cm length, 1.2-mm width and 0.8-mm depth; the groove was filled with polystyrene beads of approximately 0.6-mm diameter. This module was used in all tests unless explicitly stated otherwise. The second was a laboratory-made module with a groove (10-cm long, 3.0-mm wide and 0.2-mm deep) with right-angled bends as shown in Fig. 4. The third was a commercial module (Tecator) with a groove 10 cm long, 2 mm wide and 0.2 mm deep.

The membranes tested are listed in Table 1.

Flow injection components. Absorbances were measured with a Metrohm E1009 spectrophotometer. The peristaltic pump was a Gilson Minipuls II. Polyethylene tubing (i.d. 0.8 mm) was used. Because small pressure differences between the two channels in the separation module lead to deformation and possible perforation of the membranes, the tubes (transport lines and/or reaction/mixing coils) were not filled with beads, but coiled as tightly as possible in order to minimize dispersion. Injections were done with a Rheodyne teflon rotary valve type 50 provided with a pneumatic actuator. The injection volume was about 100 μl.

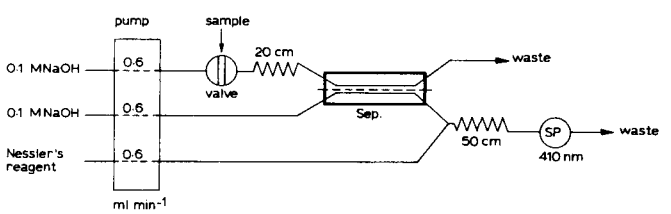

Fig. 3. Experimental set-up for the determination of ammonia with Nessler's reagent.

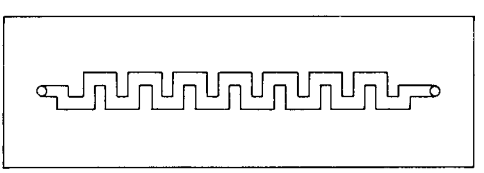

Fig. 4. Shape of the groove in the right-angled bends module.

TABLE 1

Membranes examined

	Pore diameter (μm)	Thickness (mm)
PTFE (TBA)[a]	≤ 0.5	ca. 5×10^{-2}
PTFE (Tecator)[a]	< 0.5	ca. 3×10^{-2}
Celgard[b] 2400	0.02	2.5×10^{-2}
Celgard[b] 2402	0.02	5.0×10^{-2}
Celgard[b] 2500	0.04	2.5×10^{-2}
Celgard[b] 3501	0.04	2.5×10^{-2}

[a]Both PTFE membranes are available as tape. Pore diameters are estimated from observations with an electron microscope. [b]Celgard is a microporous polypropylene film (Celanese Corporation, Charlotte, NC); 2400, 2402 and 2500 are hydrophobic films, whereas 3501 has a hydrophilic character [6].

RESULTS AND DISCUSSION

To obtain absolute values of the permeability of the membranes, the first experiments were done with ammonia and Nessler's reagent. Each experiment was duplicated, first with the outlet of the acceptor stream of the membrane module connected to the reagent stream, and then with the donor stream connected to the reagent stream (Fig. 3). The percentage transference across the membrane, expressed as $\{C^*/(C + C^*)\} \times 100$, was calculated for the injection of five different solutions containing 10^{-4}—5×10^{-4} mol l^{-1} ammonia. When the membranes are rather impermeable, the value of C^* is so low that no reliable absorbance values could be obtained; in those cases, the concentration of the injected solution was increased five-fold. The standard deviation obtained from ten successive injections was found to be about 2%. The results are summarized in Table 2.

A good qualitative agreement can be observed between the permeability

TABLE 2

Percentage transference of ammonia across membranes in the concentration range 10^{-4}—10^{-3} mol l^{-1} at 20°C
(Flow rate in both donor and acceptor streams was ca. 0.5 ml min^{-1})

	PTFE (TBA)	PTFE (Tecator)	Celgard[a]			
			2400	2402	2500	3501
Home-made module[b]	9.2	—	2.40	1.03	7.2	1.38
			2.36	0.95	9.6	0.92
Tecator module	20.2	24.6	—	—	—	—

[a]Each value is the result of a complete set of measurements of at least five different concentrations. [b]As shown in Fig. 1.

and the characteristic membrane parameters such as pore size and thickness. Between Celgard 2400 and 2402 a two-fold decrease in transference is to be expected. The slightly larger decrease might be due to the fact that the 2402 film is not homogeneous but consists of two 2400 films on top of each other introducing extra boundary effects. The three- to four-fold increase in transference for the 2500 film compared to the 2400 film is in good agreement with the four-fold increase expected from doubling the pore diameter. The PTFE (TBA) tape has about the same permeability for ammonia as the 2500 Celgard film although it seems to have larger pores. Electron microscopy revealed, however, that the membrane is rather inhomogeneous and that the number of these larger pores is limited. The PTFE tape supplied by Tecator seems to be a little better in this respect. Both PTFE tapes are easily stretched, which might cause a change of pore shape and even the number of pores. This may explain why each new membrane of the same tape yields slightly different results. The difference between the laboratory-made and the Tecator module corresponds approximately to the 2.5—3 times increase in the contact surface of solutions and membrane. Celgard 3501 tended to swell on contact with water, which led to an undefined effective film thickness. Therefore, and because its permeability was not favourable compared to the other membranes, this film was not used in further experiments.

The relatively low permeability for ammonia suggests that $2kt/\Delta V$ is small. Equation (4) can then be reduced to an expression similar to Eqn. (12) and the absorbance at t_{max} plotted as a function of the inverse flow rate must yield a straight line through the origin. This was actually found, as can be seen in Fig. 5. At the same time, C_n should remain constant according to Eqn. (4). It has to be kept in mind, however, that in using Eqns. (3) and (4) it is assumed that no extra band broadening occurs in the tubes to the membrane module and from this module to the detector. This might be the reason why C_n is not exactly constant for the various inverse flow rates.

Because in practice it is much easier to work with an acid—base indicating system instead of Nessler's reagent, the experiments were also done with a phenolphthalein—ammonium buffer system as the acceptor solution. The best choice of pH depends on the pK_a value of the buffer substance, the pK_a value of the indicator and the concentration range to be measured. Theoretical considerations about such a choice will be presented in a separate paper. At this stage, it was found experimentally that for pH 9.0 good linear calibration curves were obtained (Fig. 6). Although measured with a completely new set of membranes, the same order of permeability is again observed: the PTFE membranes show the best permeability, the Celgard 2500 is almost as good, whereas the Celgard films 2400 and 2402 are permeable only to a limited extent.

For microporous PTFE and polypropylene membranes, the degree of transfer depends mainly on the volatility of the compound, as has been noted by Kobos et al. [7]. Accordingly, it is to be expected that carbon dioxide will show a much greater permeability than will ammonia; the solu-

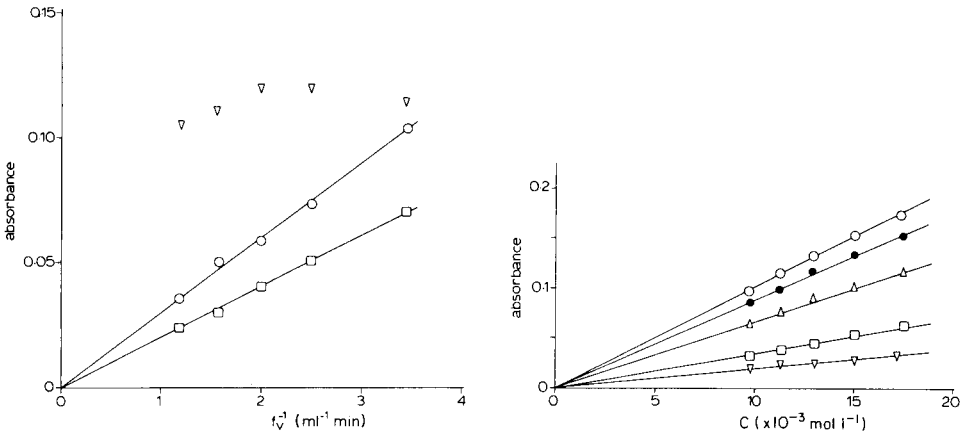

Fig. 5. Absorbance at peak maximum versus the inverse flow rate of the acceptor/donor stream, for the Celgard 2500 membrane at 20°C. Concentration injected: (○) 1.5 × 10^{-3} mol l^{-1}; (□) 1.2 × 10^{-3} mol l^{-1}; (▽) 2.4 × 10^{-4} mol l^{-1}. (○, □) Absorbance measured in the acceptor stream; (▽) absorbance measured in the donor stream.

Fig. 6. Absorbance at peak maximum vs. injected concentration of ammonia (as ammonium chloride). Volume injected, ca. 100 µl; flow rate, 0.5 ml min^{-1}; buffer solution, 10^{-3} M (NH_4Cl + NH_3) + phenolphthalein, pH 9.0. Membrane: (○) PTFE (TBA); (●) PTFE (Tecator); (□) Celgard 2400; (▽) Celgard 2402; (△) Celgard 2500.

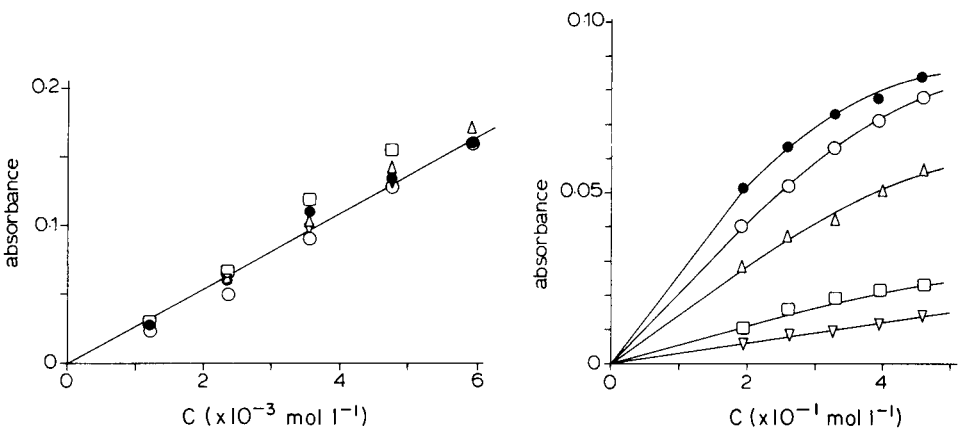

Fig. 7. Absorbance at peak maximum vs. injected concentration of carbon dioxide (as sodium hydrogencarbonate). Buffer solution, 10^{-3} M (Na_2CO_3 + $NaHCO_3$) + cresol red, pH 8.8; flow rate 0.6 ml min^{-1}; other details as for Fig. 6.

Fig. 8. Absorbance at peak maximum vs. injected concentration of acetate. Buffer solution, 10^{-3} M (NaAc + HAc) + bromocresol green, pH 5.5; flow rate, 0.6 ml min^{-1}; other details as for Fig. 6.

bility of ammonia at 20°C is 0.515 g g^{-1} of water [8] whereas the solubility of carbon dioxide at 20°C is 0.00172 g g^{-1} of water [9]. In the case of carbon dioxide, $kt/\Delta V$ will become large for all the membranes under investigation and Eqn. (13) will apply, which means that the calibration curves for all membranes must coincide. This was found experimentally, as depicted in Fig. 7.

Acetic acid was used as another example. As acetic acid is infinitely soluble in water, it was expected that transference across the membranes would be even more limited than for ammonia. This was actually observed; much larger concentrations had to be injected in order to achieve any response. Probably because of the use of such high concentrations, the calibration curves are not exactly linear. As for ammonia, the slopes of the calibration curves for the various membranes were different (Fig. 8).

Especially for ammonia and acetic acid the volatility, and hence the transference across the membrane, can be increased by raising the temperature. For both ammonia and acetic acid, a markedly enhanced signal was observed by raising the temperature from 20°C to 60°C. For ammonia, this increase was found to be approximately inversely proportional to the solubility as shown in Fig. 9. For carbon dioxide the temperature-dependence was less pronounced. It must be stated, however, that the results of these temperature experiments must be considered with great caution because changing the temperature can shift not only the value of the molar absorptivity but also all the equilibria.

In conclusion, it has been proven that the general equations derived are essentially correct. To obtain maximum sensitivity in the case of less volatile compounds, it is advisable to use microporous PTFE membranes or the microporous polypropylene film commercially available as Celgard 2500. Because the latter is less prone to electrostatic charging, it is easier to handle, and it is available as sheets from which membranes of any shape or size can be cut.

For less volatile compounds it is advisable to increase the proportionality factor (k) for the mass transfer across the membrane by increasing the active surface area. In order to accomplish this and to maintain the condition of

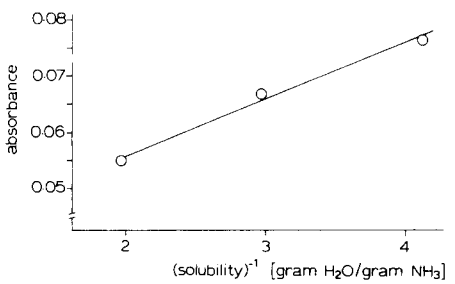

Fig. 9. Absorbance at peak maximum vs. inverse solubility of ammonia in water at different temperatures.

ideal mixing, a membrane module with right-angle bends was constructed (Fig. 4). Preliminary experiments showed that the two- to three-fold increase in membrane surface area leads indeed to a corresponding increase in signal, whereas the peak width hardly changes. With a flow rate of 1 ml min^{-1}, a sample rate of 70 samples h^{-1} is feasible without any carryover.

Although reproducible measurements can be made in a fixed set-up with one membrane, it must be kept in mind that regular calibration is necessary and certainly is a prerequisite when the membrane is changed, even when it is taken from the same tape or film.

The author expresses his gratitude to R. Wasser and M. Scheltinga for their experimental help, to Dr. Ir. M. Bos for his critical comments on the manuscript, to Mrs. B. Verbeeten-van Hettema for preparing the manuscript and to R. H. Arends for making the drawings. The Celgard films were kindly provided by Celanese Corporation (USA), and a membrane module and tape by Tecator (Sweden).

APPENDIX A

Mass balances for the first tank are

$$dC_1/dt = -C_1 f_v/\Delta V - (C_1 - C_1^*)k/\Delta V \quad \text{(A1)}$$

$$dC_1^*/dt = -C_1^* f_v/\Delta V + (C_1 - C_1^*)k/\Delta V \quad \text{(A2)}$$

Combination of (A1) and (A2) yields $d(C_1 + C_1^*)/dt = (C_1 + C_1^*)f_v/\Delta V$, and integration leads to $C_1 + C_1^* = \text{const.} \exp[-f_v t/\Delta V]$. For the starting conditions $t = 0$, $C_1 = C_0$, $C_1^* = 0$, the result obtained is $C_1 + C_1^* = C_0 \exp[-f_v t\Delta V]$. Introduction of this equation in Eqns. (A1) and (A2) leads to

$$dC_1/dt = -C_1 f_v/\Delta V - (C_1 - C_0 \exp[-f_v t/\Delta V] + C_1)k/\Delta V \rightarrow dC_1/dt + C_1(f_v + 2k)/\Delta V = C_0 \exp[-f_v t/\Delta V] \quad \text{(A3)}$$

This Leibniz-type linear differential equation has the general solution

$$C_1 = 1/2C_0 \exp[-f_v t/\Delta V] + a \exp[-(f_v + 2k)t/\Delta V] + b \quad \text{(A4)}$$

where a and b are constants.

For $t \rightarrow \infty$, $C_1 \rightarrow 0$ so $b = 0$; for $t = 0$, $C_1 = 1/2C_0 + a = C_0$ so $a = 1/2C_0$. This leads to the expression

$$C_1 = 1/2C_0 \exp[-f_v t/\Delta V]\{1 + \exp[-2kt/\Delta V]\} \quad \text{(A5)}$$

Similarly,

$$C_1^* = 1/2C_0 \exp[-f_v t/\Delta V]\{1 - \exp[-2kt/\Delta V]\} \quad \text{(A6)}$$

For the second tank the mass balances yield

$$dC_2/dt = +C_1 f_v/\Delta V - C_2 f_v/\Delta V - (C_2 - C_2^*)k/\Delta V \quad \text{(A7)}$$

$$dC_2^*/dt = +C_1^* f_v/\Delta V - C_2^* f_v/\Delta V + (C_2 - C_2^*)k/\Delta V$$

Thus

$$d(C_2 + C_2^*)/dt = (C_1 + C_1^*) f_v/\Delta V - (C_2 + C_2^*)f_v/\Delta V \quad \text{(A8)}$$

which again is a linear differential equation of the Leibniz-type. With the boundary condition $t = 0 \rightarrow C_2 + C_2^* = 0$, this leads to

$$C_2 + C_2^* = -C_0 t f_v / \Delta V \exp[-f_v t / \Delta V] \quad \text{(A9)}$$

and after substitution in Eqns. (A7) and (A9)

$$C_2 = -C_1 t f_v / \Delta V = 1/2 C_0 (f_v t / \Delta V) \exp[-f_v t / \Delta V] \{1 + \exp[-2kt / \Delta V]\} \quad \text{(A10)}$$

$$C_2^* = 1/2 C_0 (f_v t / \Delta V) \exp[-f_v t / \Delta V] \{1 - \exp[-2kt / \Delta V]\} \quad \text{(A11)}$$

Continuation through the subsequent tanks leads eventually for the nth tank to Eqns. (3) and (4) in the main text.

APPENDIX B

Mass balances for the first tank are

$$dC_1/dt = -(f_v / \Delta V) C_1 - kC_1 \quad \text{(B1)}$$

$$dC_{p,1}^*/dt = -(f_v / \Delta V) C_{p,1}^* + kC_1 \quad \text{(B2)}$$

where $C_{p,1}^*$ is the concentration of the product, P, resulting from a 1:1 stoichiometric reaction. Equation (B2) only holds for a 1:1 stoichiometry of the reaction. Equation (B1) leads in a straightforward way to

$$C_1 = C_0 \exp[-t(f_v + k) / \Delta V] \quad \text{(B3)}$$

Substitution in Eqn. (B2) yields

$$C_{p,1}^* = C_0 \exp[-f_v t / \Delta V] \{1 - \exp[-kt / \Delta V]\} \quad \text{(B4)}$$

For the nth tank, continuation of the derivation leads to Eqns. (9) and (10) in the main text.

REFERENCES

1 H. Baadenhuijsen and H. E. H. Seuren-Jacobs, Clin. Chem., 25 (1979) 443.
2 J. Růžička and E. H. Hansen, Flow Injection Analysis, Wiley, New York, 1981.
3 J. M. Reijn, W. E. van der Linden and H. Poppe, submitted for publication.
4 J. M. Reijn, W. E. van der Linden and H. Poppe, Anal. Chim. Acta, 126 (1981) 1.
5 F. J. Krug, J. Růžička and E. H. Hansen, Analyst, 104 (1979) 47.
6 H. S. Bierenbaum, R. B. Isaacson, M. L. Druin and S. G. Plovan, Ind. Eng. Chem., Prod. Res. Develop., 13 (1974) 2.
7 R. K. Kobos, S. J. Parks and M. E. Meyerhoff, Anal. Chem., 54 (1982) 1976.
8 W. Braker, Matheson Gas Data Book, Matheson Gas Prod., Milwaukee, 1971.
9 L. Medard (Ed.), L'Air Liquide, Gas Encyclopedia, Elsevier, 1976.

Analytica Chimica Acta, 151 (1983) 371—376
Elsevier Science Publishers B.V., Amsterdam — Printed in The Netherlands

AMPEROMETRIC DETERMINATION OF CREATININE WITH A BIOSENSOR BASED ON IMMOBILIZED CREATININASE AND NITRIFYING BACTERIA

IZUMI KUBO[a], ISAO KARUBE* and SHUICHI SUZUKI

Research Laboratory of Resources Utilization, Tokyo Institute of Technology, Nagatsuta-cho, Midori-ku, Yokohama 227 (Japan)

(Received 18th November 1982)

SUMMARY

A selective biosensor consisting of immobilized creatininase (E.C.3.5.4.21) and immobilized nitrifying bacteria is applied to the amperometric determination of creatinine. The response time for creatinine is < 3 min. The relationship between the current decrease and creatinine concentration is linear below 100 mg dl^{-1}. The minimum detectable concentration is 5 mg dl^{-1}. The current decrease was reproducible within 6.7% (within-day) or 8.8% (day-to-day). The current output of the sensor was almost constant for more than 3 weeks and 300 assays.

The determination of creatinine in serum and urine is a diagnostically important test [1]. External dialysis (artificial kidney) has become so widely practiced that a precise, rapid and simple method for creatinine determination is very desirable. Spectrophotometric methods, based on the Jaffé reaction [2], have conventionally been used for measuring serum creatinine. However, these methods are time-consuming, complicated and other substances in serum interfere seriously. Rechnitz and co-workers [3, 4] showed the possible application of an enzyme sensor based on creatinine deaminase (E.C.3.5.4.21) with a gas-sensing ammonia electrode to measure ammonia produced by the enzymatic reaction. However, this potentiometric determination does not seem to be practical because of the sensitivity limitation of the gas-sensing ammonia electrode.

This paper describes a new sensor for the amperometric determination of creatinine. It is based on amalgamation of an enzyme reaction and bacterial metabolism. Creatininase (E.C.3.5.4.21) hydrolyzes creatinine to *N*-methylhydantoin and ammonium ion, and the ammonia produced is successively oxidized to nitrite and nitrate by nitrifying bacteria, which have already been used in an ammonia sensor [5]. The bacteria have not been completely characterized, but are known to be a mixed culture of *Nitrosomonas* sp.

[a]Present address: Fuji Electric Corporate Research and Development Ltd., Nagasaka, Yokosuka, 240-01, Japan.

0003-2670/83/$03.00

and *Nitrobacter* sp. The sequence of reactions is

$$\text{creatinine} + H_2O \xrightarrow{\text{creatininase}} NH_4^+ + N\text{-methylhydantoin}$$

$$NH_4^+ \xrightarrow{\textit{Nitrosomonas sp.}} NO_2^- \xrightarrow{\textit{Nitrobacter sp.}} NO_3^-$$

The reacting bacteria consume oxygen, so that the oxygen decrease may be detected by an oxygen electrode. The hybrid creatinine sensor thus consists of a cellulose dialysis membrane, immobilized creatininase, immobilized nitrifying bacteria, and an oxygen electrode. The sensor is applied to the determination of serum creatinine.

EXPERIMENTAL

Materials

Creatininase (Creatinine deiminase, E.C.3.5.4.21; 2.3U mg^{-1}) was donated by Kyowa Hakko Kogyo Co. Creatinine was purchased from Tokyo Kasei Kogyo Co.

Culture of bacteria. Nitrifying bacteria were obtained from a fermentation factory (Ajinomoto Central Research Laboratory, Kawasaki). The bacteria had already been isolated by Hikuma et al. [5], and were cultivated under aerobic conditions at 20°C.

Immobilization of enzyme and bacteria. The bacteria were immobilized as reported previously [5]. Thus 6 ml of the culture broth containing nitrifying bacteria was filtered through a porous acetylcellulose membrane (Toyo Roshi; 0.45-μm pore size, 25 mm diameter) under slight suction. After the bacteria were retained on the membrane, it was rinsed with 6 ml of pH 8.5 buffer solution (0.01 M borate with hydrochloric acid).

A triamine membrane was used to immobilize creatininase. It is a triacetylcellulose membrane containing 1,8-diamino-4-aminomethyloctane [6]. After being cut to the proper size, the membrane was immersed in 1% glutaraldehyde solution for 1 h, rinsed in distilled water and immersed in a solution containing creatininase (1 mg ml^{-1} in 0.01 M pH 7.0 phosphate buffer) for more than 15 h at 4°C.

Apparatus

Assembly of the hybrid sensor. A schematic diagram of the sensor is shown in Fig. 1. The oxygen electrode (Ishikawa Seisakusho, DG-5) consisted of a teflon membrane, a platinum cathode, a lead anode and 30% sodium hydroxide as electrolyte. The acetylcellulose membrane retaining nitrifying bacteria was carefully attached to the teflon membrane of the oxygen electrode so that the bacteria were between the two membranes. The immobilized enzyme membrane was attached over the acetylcellulose membrane. These membranes were covered with a dialysis membrane (Visking Co. seamless cellulose tubing) and fastened with a rubber O-ring.

Figure 2 shows a schematic diagram of the sensor system. It consists of

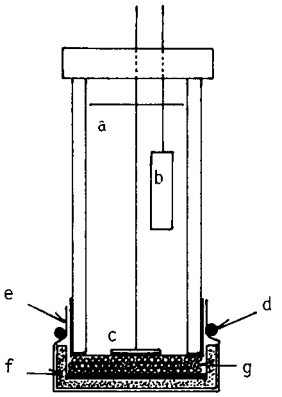

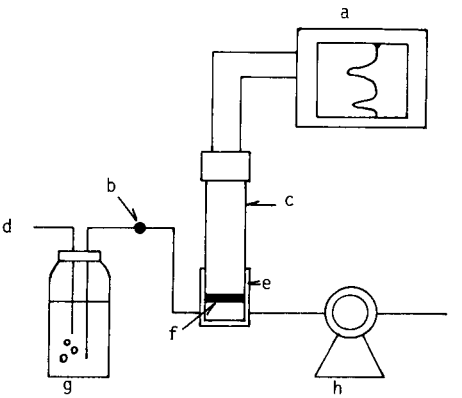

Fig. 1. Schematic diagram of creatinine sensor: (a) electrolyte; (b) Pb anode; (c) Pt cathode; (d) rubber O-ring; (e) dialysis membrane; (f) immobilized enzyme; (g) immobilized bacteria.

Fig. 2. Schematic diagram of creatinine sensor system: (a) recorder; (b) injection port; (c) oxygen electrode; (d) air; (e) flow cell; (f) enzyme—bacteria membrane; (g) carrier solution; (h) peristaltic pump.

the sensor inserted in a flow cell, a carrier solution, a peristaltic pump (Mitsumi Scientific Industry, Model SJ-1211), an injection port and a recorder (TOA Electronic Polyrecorder, Model EPR 20A).

Procedures

Enzyme assay. The assay of creatinine deiminase activity [7] was based on the determination of the amount of ammonia released from creatinine according to the method of Berthelot [8]. The assay was done at 37°C for 10 min at pH 8.0 with shaking. One unit of enzyme activity was defined as the amount of the enzyme which catalyzes the formation of 1 μmol min^{-1} of ammonia under the assay conditions.

Use of the electrode. The temperature of the carrier solution and the flow cell was maintained at 30 ± 1°C. Carrier solution containing the borate buffer (pH 8.5, containing 1 mg l^{-1} chloramphenicol) was saturated with dissolved oxygen and transferred to the flow cell by the peristaltic pump. When the current reached a steady state, 0.1 ml of sample solution was injected into the system, after which the current gradually decreased, and reached a minimum value. The flow cell was then washed with buffer solution and the current gradually returned to the initial level. The maximum current decrease was used as a measure of the creatinine concentration.

RESULTS AND DISCUSSION

Response curve of the sensor

Figure 3 shows typical response curves, obtained by the procedure described above. The initial steady current indicates the endogenous respiration

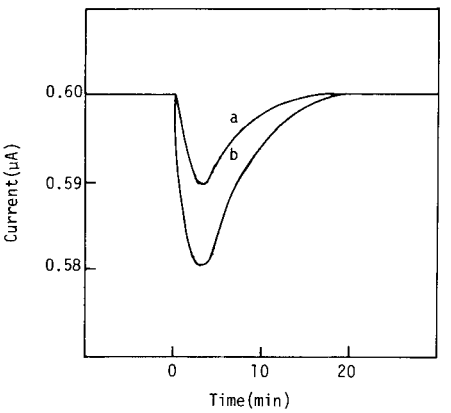

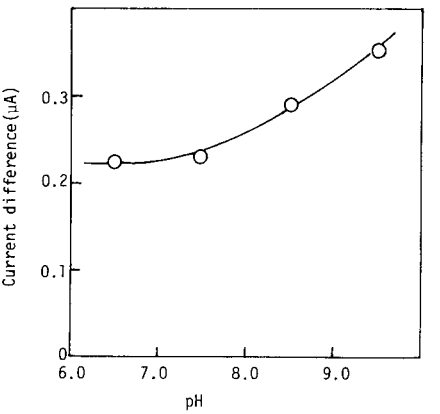

Fig. 3. Responses to creatinine: (a) 5 mg dl^{-1}; (b) 10 mg dl^{-1}. Conditions: 30°C, pH 8.5, flow rate 1 ml min^{-1}.

Fig. 4. Effect of pH for 50 mg dl^{-1} creatinine (30°C, 1 ml min^{-1}).

level of the immobilized nitrifying bacteria. When a sample solution containing creatinine was applied to the sensor system, creatinine permeated through the dialysis membrane and was decomposed to ammonia and *N*-methylhydantoin. The ammonia was assimilated by the immobilized bacteria. At the same time, the bacteria consumed dissolved oxygen from round the membrane, so that the current from the oxygen electrode decreased markedly and reached a minimum value within 3 min. Carrier solution was continuously transferred to the system. Therefore, the current gradually returned to an initial value within 15 min. When the bacteria and the enzyme are sufficiently active, the current difference between the initial and minimum values depends on the creatinine concentration.

Influence of pH and flow rate

In general, the activities of the enzyme and bacteria are affected by pH. Therefore, the influence of pH on the current output of the creatinine sensor was examined. The carrier solutions tested were 0.01 M phosphate (pH 6.5), 0.01 M borate–hydrochloric acid (pH 7.5, pH 8.5) and 0.01 M borate–sodium hydroxide (pH 9.5) buffers; and a standard creatinine solution (50 mg dl^{-1}) was employed. Figure 4 shows the pH–current difference profile of the sensor system. The current difference increased with increasing pH up to at least pH 9.5. However, at this pH, the re-usability of the sensor was poor. Therefore, 0.01 M borate–hydrochloric acid buffer (pH 8.5) was used as a carrier solution. In order to prevent the growth of contaminating microorganisms around the immobilized nitrifying bacteria, the antibiotic chloramphenicol (1 mg l^{-1}), was added to the carrier solution [5].

In the system, the flow rate affects the response time, the working range and the sensitivity of the sensor. Figure 5 shows the influence of flow rate

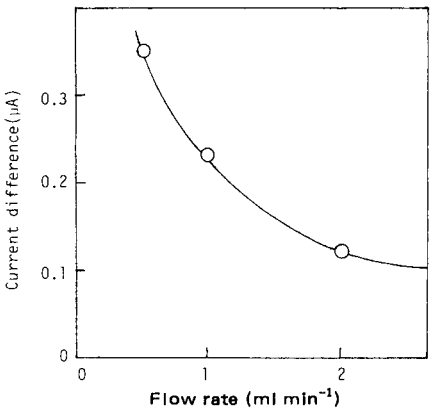

Fig. 5. Effect of flow rate for 50 mg dl^{-1} creatinine (pH 8.5, 30°C).

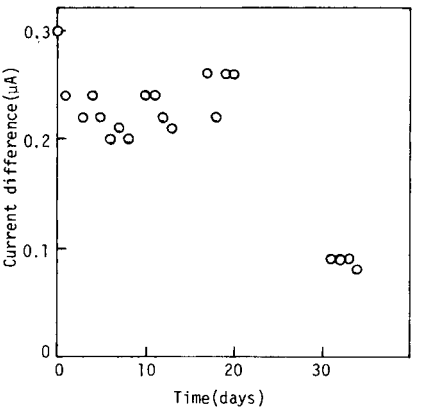

Fig. 6. Stability of creatinine sensor (pH 8.5, 30°C, 1 ml min^{-1}, 50 mg dl^{-1} creatinine).

on the current difference. When the flow rate was 2 ml min^{-1}, the response time was satisfactorily short, but the maximum current difference was small. The current difference was large when the flow rate was 0.5 ml min^{-1}, but it was difficult to keep the pH in the flow cell constant. Thus the optimum flow rate was considered to be 1.0 ml min^{-1}.

Calibration graph, selectivity and stability

There was a linear relationship between the current difference and the concentration of creatinine below 100 mg dl^{-1}, with a maximum current difference of ca. 0.23 μA at 50 mg dl^{-1}. The minimum detectable concentration of creatinine with this sensor was 5 mg dl^{-1}.

The reproducibility of the sensor was examined with a 50 mg dl^{-1} solution. The determination was done about 20 times a day. The current difference was reproducible to within 6.7% (within-day) and 8.8% (day-to-day).

The selectivity of the hybrid biosensor for creatinine was examined with solutions containing other organic compounds. The sensor did not respond (current = 0.00 μA) to urea (5 mg l^{-1}), uric acid (10 mg dl^{-1}), citrate (50 mg dl^{-1}), pyruvate (5 mg dl^{-1}), glucose (100 mg dl^{-1}), arginine (2 mg dl^{-1}), glutamine (10 mg dl^{-1}) or EDTA (80 mg dl^{-1}). Therefore, the selectivity of the hybrid biosensor was satisfactory.

The re-usability of the creatinine sensor was examined with a sample solution containing 50 mg dl^{-1} creatinine. The results are shown in Fig. 6. The current output of the sensor eventually decreased but it could be used for more than 3 weeks and 300 assays. Thus, the hybrid biosensor appears to be promising and attractive for the routine determination of creatinine in biological fluids.

REFERENCES

1 N. Ishii, Med. Technol., 8 (1980) 309.
2 M. Jaffé, Z. Physiol. Chem., 10 (1886) 391.
3 T. Huvin and G. A. Rechnitz, Anal. Chem., 46 (1974) 246.
4 M. Meyerhoff and G. A. Rechnitz, Anal. Chim. Acta, 84 (1976) 2771.
5 M. Hikuma, T. Kubo, T. Yasuda, I. Karube and S. Suzuki, Anal. Chem., 52 (1980) 1020.
6 M. Aizawa, A. Morioka and S. Suzuki, Anal. Chim. Acta, 115 (1980) 61.
7 T. Uwazima and O. Terada, Agric. Biol. Chem., 40 (1976) 1055.
8 J. Berthelot, Rerit. Chem. Appl., 1 (1859) 284.

Analytica Chimica Acta, 151 (1983) 377—382
Elsevier Science Publishers B.V., Amsterdam — Printed in The Netherlands

DETERMINATION OF UREA IN BLOOD SERUM WITH USE OF IMMOBILIZED UREASE AND A MICROWAVE CAVITY AMMONIA MONITOR

SACHIO HIROSE, MITSUHIRO HAYASHI, NORIYOSHI TAMURA and TAMIO KAMIDATE

Central Research Laboratory, Mitsubishi Petrochemical Co. Ltd., Wakaguri, Ami-cho, Inashiki-gun, Ibaraki 300-03 (Japan)

ISAO KARUBE* and SHUICHI SUZUKI

Research Laboratory of Resources Utilization, Tokyo Institute of Technology, Nagatsuta-cho, Midori-ku, Yokohama 227 (Japan)

(Received 30th November 1982)

SUMMARY

The system for urea determination consists of urease immobilized on porous PVC coated on the inside of a test tube, and a dissolved ammonia monitor comprising a dialyzer and a Stark microwave cavity resonator. The total time required for the determination of urea in serum is 18 min (the enzymatic reaction requires 10 min) and the calibration graph for urea—nitrogen is linear from 10 to 750 mg l^{-1}. The relative standard deviation is 5%; there are very few interferences.

The determination of urea in serum and other biological fluids is an important diagnostic routine test in clinical laboratories [1]. Almost all methods for urea determination are based on the measurement of ammonia produced after urease catalyzed hydrolysis. The most popular method for the determination of ammonia is the indophenol spectrophotometric method [2]. However, the calibration graph is not linear at high ammonia concentrations. The glutamate dehydrogenase method is sometimes used for blood urea determinations [3], but this method requires enzyme, NADH and α-ketoglutarate. Various enzyme and microbial electrodes consisting of immobilized biocatalysts and electrodes have also been used [4—7], but volatile amines and various ions in biological fluids may interfere.

A dissolved ammonia monitor consisting of a Stark microwave cavity resonator and a dialyzer for vaporizing ammonia from a strong alkaline solution has been developed for control and supervision of process waters in a petrochemical complex by the present authors [8]. This new system also seemed to be applicable to clinical analysis, e.g., for blood ammonia nitrogen, blood urea nitrogen and creatinine based on a similar measurement of ammonia. It was expected that this system would provide continuous and reproducible ammonia determination in biological fluids without interference.

0003-2670/83/$03.00

Furthermore, for urea determination, immobilization of urease should prolong the useful lifetime of the enzyme. Therefore, the use of immobilized urease and the dissolved ammonia monitor would appear to provide an excellent approach for the determination of urea in serum; a method is described in this paper. Urease is immobilized on wet poly(vinyl chloride) [9, 10] coated on the inside of a test tube. Optimum conditions for urea determination in serum are investigated.

EXPERIMENTAL

Apparatus and materials

The system used for serum urea determination was the same as described previously for dissolved ammonia [8]. The urease-coated test tubes were placed in the turntable. The output corresponding to ammonia concentration was measured with a recorder (Type 3066, Yokogawa Electric Works). Plastic test tubes were obtained from Eiken Kizai Co. (Tokyo).

Urease (E.C. 3.5.1.5) from jack bean (type IV: Sigma Chemical Co.) was used without further purification. Other materials were poly(vinyl chloride) (PVC; m.w. 48,400; Kanegafuchi Chemical Co.), dimethylformamide (DMF) and methanol (Wako Pure Chemicals). The control serum (grade Hyland II; Japan Travenol Co.) contained 500 mg l^{-1} urea—nitrogen. Various urea concentrations were prepared by diluting the control serum with deionized water. Other reagents were commercially available analytical-grade or laboratory-grade materials. Ammonium sulfate was used for making calibration solutions.

Preliminary procedures

Preparation of immobilized urease coated on a test tube. A 6% (w/w) solution of PVC in DMF was poured into a test tube (diameter 8 mm, length 70 mm). The inside of the tube became coated with poly(vinyl chloride) on soaking in methanol at room temperature for 4 h. The inside of the tube was washed with distilled water.

Phosphate buffer (0.1 M, pH 7.0, 2.5 ml) containing urease (1.0 mg ml^{-1}) was added to the PVC-coated tube and allowed to stand for 24 h at 25° C. The tube was washed with a large volume of the phosphate buffer, and stored containing phosphate buffer at 4° C. No leakage of urease was observed from the coating.

Enzyme assay. Urease solution (1 ml) in 0.02 M phosphate buffer, pH 7.0, was placed in a stoppered tube and allowed to stand at 25° C; 1 ml of 3% urea solution (in 0.75 M phosphate buffer, pH 7.0) was added and the mixture was allowed to stand for 5 min at 25° C. The ammonia produced was determined by the indophenol method at 630 nm [2]. The formation of 1 μmol of ammonia per minute at 25° C was defined as one unit [11]. The activity of the immobilized urease in the tube was determined by using 0.5 ml of the 3% urea solution.

Procedure for urea determination

For the enzymatic reaction, 50 μl of serum and 0.45 ml of 0.1 M phosphate buffer (pH 7.0) were added to the urease-coated test tube (3.0 units) and the reaction mixture was incubated for 10 min at 37°C. After this time, the solution was diluted with 2.0 ml of deionized water.

A 6 M sodium hydroxide solution was transferred to the dialyzer [8] at a flow rate of 0.16 ml min^{-1} together with air at 0.42 ml min^{-1}. When the output of the system reached a steady state, the diluted sample solution was transferred to the 6 M sodium hydroxide at 0.32 ml min^{-1} for 6 min by the proportioning pump. The concentration of ammonia produced was measured by the dissolved ammonia monitor and the signal obtained was displayed on the recorder. The peak height was related to the concentration of urea. A calibration graph was prepared by using ammonium sulfate solution as the standard [8]. In this paper, the concentrations of sample given are those in original serum.

RESULTS AND DISCUSSION

Immobilization and reaction conditions for urease

Preliminary experiments showed that the optimal concentration of PVC required for coating the inside of the test tube was 6% (w/w). The lifetime of the urease immobilized by the method of adsorption as described previously [9, 10] was 4 weeks, while that of native urease was 1 week. Figure 1 shows the effect of the reaction volume on the immobilized urease activity. Urea solutions (3%, in 0.75 M phosphate buffer, pH 7.0) were allowed to stand in the urease-coated tubes for 5 min at 25°C, 0.5 ml of sample gave the highest activity. No leakage of urease from the walls was observed during the experiments. It is thought that urease is adsorbed by hydrophobic interaction and remains in an appropriate pore size which is controlled by the

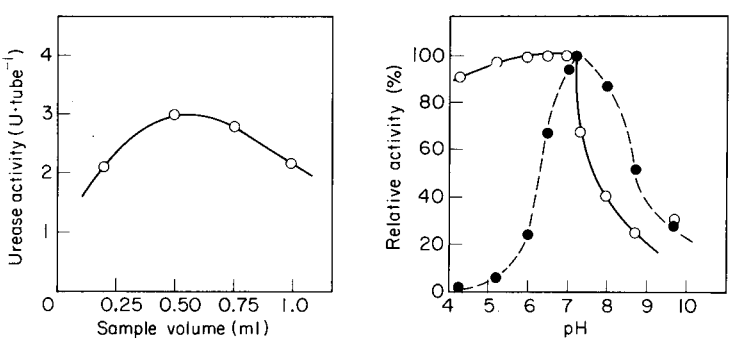

Fig. 1. Effect of sample volume on urease activity (standard conditions described in experimental section except for the sample volume).

Fig. 2. pH—activity profiles of: (○) urease test tube; (●) native enzyme (other conditions as in recommended procedure).

PVC concentration in the coating solution [12]. Therefore, the wet PVC layer inside the test tube plays an important role in urease immobilization. Further reactions were carried out by a 0.5-ml sample.

Effect of pH

The effect of the pH of the buffer solution on the enzymatic reaction was examined. The results obtained are shown in Fig. 2. A broad pH optimum from 4 to 7.0 was observed, although the pH optimum for native urease was 7.3. Shift of the optimum pH and broadening of the optimal pH range of an enzyme after immobilization are common, and have been explained by Goldstein et al. [13]. Figure 3 shows the pH—stability profile obtained for the urease test tube and the native enzyme. The bound urease was stable between pH 6.0 and 7.0. All subsequent studies were done at pH 7.0.

Response of the system

Figure 4 shows the effect of the sodium hydroxide concentration on the response of the system. The response increased with increasing sodium hydroxide concentration. However, 6 M sodium hydroxide solution was used in the recommended procedure because a stronger solution might hydrolyze amino acids present in blood. When the flow rate of 6 M sodium hydroxide was 0.08 ml min^{-1}, the highest signal was obtained. However, the time required for the determination of serum urea was more than 25 min in this case; thus 0.16 ml min^{-1} is recommended. The output rose with increasing sample flow rate, and became constant above 0.32 ml min^{-1}. Therefore, this sample solution flow rate was used in further studies. The ammonia determination could then be done within 6 min and the output returned to the initial level within 2 min. The total time required for the measurement of serum urea was 18 min including the enzymatic reaction time of 10 min. The measurements were done continuously at 10-min intervals.

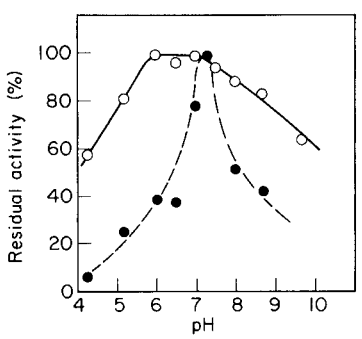

Fig. 3. pH—stability profiles of: (○) urease test tube; (●) native enzyme (experiments done at 37°C for 4 h; recommended assay conditions).

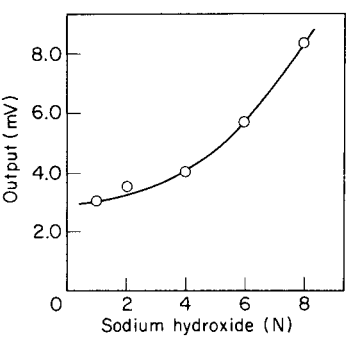

Fig. 4. Effect of concentration of sodium hydroxide on the response from 50 μl of control serum (otherwise recommended conditions, except that the sample was finally diluted with buffer solution).

TABLE 1

Effect of other substances

Other substances[a]	Ammoniacal nitrogen concentration (mg l^{-1})	
	Proposed method	Indophenol method
Control[b]	10.0	10.0
Alanine	9.9	—
Ascorbic acid	9.9	—
Glutamine	10.7	10.5
Glutathione	9.9	—
Creatine	9.8	—
Creatinine	10.4	10.6
Hemoglobin	9.8	—
Bilirubin	10.2	—

[a] 100 mg l^{-1} in the sample solution (0.5 ml) in the test tube. Reaction at 37° C. [b] 50 μl of control serum (500 mg l^{-1} urea—nitrogen).

The total sample volume required for the determination of urea by this procedure was more than 2 ml. Consequently, the minimum concentration for serum urea determined by this system was 10 mg l^{-1} urea—nitrogen.

Effect of various interfering substances

In strongly alkaline conditions, ammonia may be liberated from amino acids, amides and proteins. Therefore the effect of alanine, glutamine, glutathione, creatine, creatinine, hemoglobin and bilirubin, as well as ascorbic acid, on the response of the system was examined. As shown in Table 1, only glutamine and creatinine significantly affected the response, giving slightly high results. Thus, the selectivity of this procedure for urea—ammonia was satisfactory. If ammonium ions are present in serum, these can be measured by repeating the procedure without recourse to the enzymatic reaction.

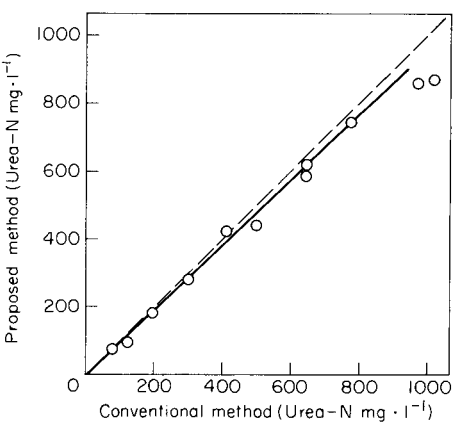

Fig. 5. Correlation between urea—nitrogen concentrations determined both by the proposed (3 U enzyme) and conventional indophenol (5 U enzyme) methods.

Reproducibility, accuracy and stability of the assay system

The reproducibility of the recommended procedure was examined using the control serum containing 500 mg l^{-1} urea—nitrogen. The relative standard deviation was 5% (20 experiments). The immobilized enzyme retained its activity for 4 months at 4°C, after which the activity gradually decreased.

Ten sera containing different concentrations of urea were processed by the new method and the conventional method. The results obtained are compared in Fig. 5. The correlation coefficient is 0.995. Thus the system based on the urease test tube and the dissolved ammonia monitor is suitable for the routine determination of urea in serum.

The authors are grateful to Mr. M. Sennari and Dr. M. Uchiyama of the Mitsubishi Petrochemical Co. Ltd. for their helpful advice and encouragement during this study.

REFERENCES

1 CRC Handbook of Clinical Laboratory Data, CRC press, Cleveland, OH, 1968, p. 356.
2 H. McCullough, Clin. Chim. Acta, 19 (1968) 101.
3 C. J. Hallett and J. G. H. Cook, Clin. Chim. Acta, 35 (1971) 31.
4 I. Karube and S. Suzuki, Biochem. Biophys. Res. Commun., 47 (1972) 51.
5 I. Karube, T. Matsunaga, S. Mitsuda and S. Suzuki, Biotechnol. Bioeng., 19 (1979) 1535.
6 M. Hikuma, J. Kubo, T. Yasuda, I. Karube and S. Suzuki, Anal. Chem., 52 (1980) 1020.
7 R. A. Llenado and G. A. Rechnitz, Anal. Chem., 46 (1974) 1109.
8 S. Hirose, M. Hayashi, N. Tamura, T. Kamidate, I. Karube and S. Suzuki, Anal. Chem., 54 (1982) 1690.
9 S. Hirose, M. Hayashi, N. Tamura, S. Suzuki and I. Karube, J. Mol. Cat., 6 (1979) 251.
10 S. Hirose, E. Yasukawa, M. Hayashi, N. Tamura, A. Kanai, I. Karube and S. Suzuki, J. Appl. Biochem., 2 (1980) 45.
11 J. B. Sumner, in N. O. Kaplan and S. P. Colowick (Eds.), Methods in Enzymology, Vol. 2, Academic Press, New York, 1955, p. 378.
12 S. Hirose, E. Yasukawa, M. Hayashi and W. R. Vieth, J. Membrane Sci., 11 (1982) 177.
13 L. Goldstein, Y. Levin and E. Katchalski, Biochemistry, 3 (1964) 1913.

Analytica Chimica Acta, 151 (1983) 383—389
Elsevier Science Publishers B.V., Amsterdam — Printed in The Netherlands

GRAVIMETRIC STANDARD ADDITIONS IN ION-SELECTIVE ELECTRODE POTENTIOMETRY WITH APPLICATION TO FLUORIDE MEASUREMENTS

T. DENIS RICE

New South Wales Department of Mineral Resources, Chemical Laboratory Branch, P.O. Box 76, Lidcombe, N.S.W. 2141 (Australia)

(Received 9th November 1982)

SUMMARY

Gravimetric single standard addition and double standard addition ion-selective electrode measurements are described and used for the determination of fluoride in dilute sodium hydroxide solutions. Fluoride concentrations below 5 $\mu g\ g^{-1}$ were determined accurately when the electrode was regularly conditioned with 0.06 M lanthanum nitrate solution at pH 2.0—2.3. The only significant errors in the technique described arise from the millivolt and response slope measurements; the latter require careful measurement of blanks. It is shown that the relative error in concentration measurement by single standard addition will not exceed ±0.8% if the error in the response slope of the electrode does not exceed ±0.1 mV/decade, and if the potential difference after standard addition is at least 20 mV with an error not exceeding ±0.1 mV. Single standard addition is as satisfactory as double standard addition for accurate measurements of fluoride in simple solutions.

The use of polyethylene dispensing bottles and top-loading balances, for solution-handling by mass rather than volume in various analytical procedures, has previously been described [1, 2]. The present paper describes the application of gravimetric solution-handling to ion-selective electrode (i.s.e.) measurements with standard additions. To illustrate the technique, the determination of fluoride in aqueous solution by both single standard addition (with separate measurement of electrode slope) and double standard addition (with simultaneous measurement of electrode slope) is discussed. If electrode slope is affected by the chemical background of the sample, double standard addition is more accurate than single standard addition [3].

PRINCIPLE OF THE MEASUREMENTS

The potential, E_1 (mV), of an unspiked solution of concentration C_x of analyte ($\mu g\ g^{-1}$) can be described by the simplified Nernst equation

$$E_1 = E_c \pm S \log C_x \qquad (1)$$

0003-2670/83/$03.00

where E_c is a constant incorporating terms for the activity coefficient and the degree of complexation of the analyte; and S is the slope, which for a monovalent ion at 25°C is 59.16 mV/decade. Equation (1) does not apply when C_x is below the linear portion of the calibration graph. In such a case, the solution is initially spiked with M_1 g of a standard solution containing C_1 μg g^{-1} analyte so that E_1 is brought onto the low-concentration region of this linear portion. If the unspiked solution weighs M_x g, E_1 is given by

$$E_1 = E_c \pm S \log (C_x M_x + C_1 M_1)/(M_x + M_1) \quad (2)$$

Single standard addition

The solution mentioned above is then spiked with M_2 g of standard solution containing C_2 μg g^{-1} analyte so that the potential, E_2, differs from E_1 by about 30 mV [4]. Then E_2 is given by

$$E_2 = E_c \pm S \log (C_x M_x + C_1 M_1 + C_2 M_2)/(M_x + M_1 + M_2) \quad (3)$$

In practice, if $M_x \approx 50$ g, C_1 and C_2 are chosen so that M_1 and M_2 are 1—2 g. The solution temperature is recorded to the nearest 0.2°C for any necessary temperature correction. Potentials must not drift by more than 0.1 mV min^{-1} when read. For the fluoride-selective electrode used here, this was the case after equilibration for 5 min.

Provided that the electrode slope, S, is known for the anion considered, Eqns. (2) and (3) can be solved for C_x:

$$C_x = \left(\frac{C_2 M_2/(M_x + M_1 + M_2)}{\text{antilog}\,[(E_1 - E_2)\,298/ST_x] - [(M_x + M_1)/(M_x + M_1 + M_2)]} - \frac{C_1 M_1}{M_x + M_1} \right) \frac{(M_x + M_1)}{M_x} \quad (4)$$

where S is the observed electrode slope at 298 K, and T_x is the solution temperature in Kelvin. The above procedure is termed single standard addition with initial spiking or, if $M_1 = 0$, single standard addition.

Measurement of slope

In general, for any number, $(j + 1)$, of standard additions to a blank solution, the (anion) electrode slope at 25.0°C, S_j, can be shown to be:

$$S_j = [(E_j - E_{j+1})\,298/T_s]/\log\,[(C_b M_b + \sum_{i=1}^{j+1} C_i M_i)\,(M_b + \sum_{i=1}^{j} M_i)/(C_b M_b + \sum_{i=1}^{j} C_i M_i)\,(M_b + \sum_{i=1}^{j+1} M_i)] \quad (5)$$

where E_j is the potential after the jth addition, E_{j+1} is the potential after the $(j + 1)$th addition, T_s is the temperature (K) of the solution, C_b is the blank concentration in the initial solution (μg g^{-1}), M_b is the mass of the initial

solution (g), and M_i is the mass (g) of standard of concentration C_i (μg g^{-1}) used in the ith addition.

If C_{j+1} and M_{j+1} are such that the difference, $E_j - E_{j+1}$, is not less than 30 mV, three (j = 2) or four (j = 3) standard additions suffice. Initially C_b, the blank level of analyte, is taken as zero when S_j is calculated. An appreciable blank is indicated by S_1 being less than S_2. C_b is calculated by single addition with initial spiking (Eqn. 4) taking $T_x = T_s$ and $S = S_2$ if j = 2, or $S = 1/2(S_2 + S_3)$ if j = 3 (step 1). This value of C_b is then used in Eqn. (5) (step 2). Repetition of steps 1 and 2 until C_b converges provides blank-corrected slope values. The arithmetic mean blank-corrected slope is subsequently used.

In general, the potential E_j corresponds to an analyte concentration (μg g^{-1}) of $(C_bM_b + \Sigma_{i=1}^{j} C_iM_i)/(M_b + \Sigma_{i=1}^{j} M_i)$. A calibration graph drawn from these data can be used to give the approximate concentration of a sample solution after E_1 has been measured, during slope determination.

Double standard addition

After the single standard addition has been made as described previously, a mass M_3 of a standard solution with C_3 μg g^{-1} analyte is added, so that the potential measured, E_3, differs from E_2 by at least 30 mV and M_3 is 1—2 g. The analyte concentration, C_x, is then calculated as follows. In step A, Eqn. (4) is used with a nominal value of S based on previous experience with the particular electrode, to calculate a preliminary value of C_x. The term $298/T_x$ is omitted. In step B, S is calculated by Eqn. (5), with the preliminary concentration value calculated in step A regarded as C_b, $M_b = M_x$, and j = 2; the term $298/T_s$ is omitted. In step C, step A is repeated with the value of S obtained in step B, and the C_x value so obtained is used in step B to calculate another value of S. This iterative calculation is repeated (with the aid of a programmed calculator or computer) until C_x and S become constant.

In contrast to single standard addition, double standard addition does not require measurement of solution temperature.

Equations (2—5) can obviously be modified for measurements by volume instead of mass.

EXPERIMENTAL

Apparatus and reagents

Solutions were prepared and measured in 60-ml clear polystyrene vials with polyethylene screw caps. Small PTFE-coated magnetic bars were used to stir solutions during measurement. Standard and buffer solutions were stored in 250-ml polyethylene dispensing bottles [1].

A Sartorius Model 1205 MP electronic top-loading balance, readable to 1 mg and with a capacity of 220 g, was used for measuring solutions. An Orion Model 94-09 fluoride electrode, an Orion Model 90-02 double-junction reference electrode and an Orion Model 811 pH/millivolt meter with an Orion Model 917002 glass temperature probe were used. Calculations were

done with a Texas Instruments TI-59 card-programmed calculator with printer. Programs for slope determination, and single and double standard additions (Eqns. 4 and 5) are available from the author on request.

The buffer solution was 0.05 M in *trans*-1,2-diaminocyclohexanetetraacetic acid, 3 M in ammonium acetate and 0.2 M in potassium nitrate, adjusted to pH 5.5 with acetic acid. The filling solution in the outer chamber of the reference electrode was a mixture of 10 parts of buffer and 6 parts of water by mass. Standard fluoride solutions containing C_1 = 20.00 μg $F^- g^{-1}$ and C_2 = 200.0 μg $F^- g^{-1}$ were prepared by appropriate dilution of a standard fluoride solution containing C_3 = 2000 μg $F^- g^{-1}$. All standard and measurement solutions contained 11.8% buffer solution by mass.

Procedure

To assess the accuracy of the proposed measurement of fluoride, and to simulate absorption solutions from pyrohydrolytic procedures, test solutions were prepared by measuring 25 ml of 0.05 M sodium hydroxide solution and appropriate amounts of standard fluoride solution into 60-ml polystyrene vials, diluting with deionised water to about 45 g (= m g), and then adding 0.1333m g of buffer solution.

The fluoride and reference electrodes were used essentially as recommended by the manufacturer. It was found useful to dip the fluoride electrode daily in stirred (1 + 1) hydrochloric acid for 20 s and then rinse with water; this treatment prevents response times from becoming unacceptably long and ensures potential equilibration within 5 min for concentrations >0.3 μg $F^- g^{-1}$. Both electrodes were stored in an aqueous sodium fluoride solution containing 4 μg $F^- g^{-1}$, as suggested by Jagner and Pavlova [5]. After the electrodes had been removed from the storage solution or after a series of measurements, they were rinsed with water, placed for >30 s in a stirred 0.06 M lanthanum nitrate solution at pH 2.0—2.3 (nitric acid), rinsed well with water and gently shaken to remove surplus water before the next measurement; tissues were not used.

After the 5-min potential reading had been noted, standard solution was added from a 250-ml dispensing bottle into the stirred solution. The bottle, without its dispensing-tube closure, was weighed to the nearest mg immediately before and after the standard addition.

RESULTS AND DISCUSSION

Slope determination

Slope was determined on 24 occasions during a 10-month period for the same fluoride electrode. The solution temperature on a given occasion was constant to within 0.2°C but ranged between 19.5 and 23.5°C over 10 months. The means of the 24 blank-corrected slopes (calculated at 25°C by Eqn. 5) and 24 blank determinations, with their 99% confidence limits, were 59.01 ± 0.08 mV/decade and 0.003 ± 0.004 μg $F^- g^{-1}$. The ranges of

individual slope and blank values were 58.82—59.36 mV/decade, and —0.008—0.018 μg $F^- g^{-1}$. The mean blank corresponds to a fluoride concentration of about 2×10^{-7} M which agrees well with the residual fluoride concentration (probably from dissolution of the lanthanum fluoride crystal) of about 3×10^{-7} M reported by Rix et al. [6].

Measurement of fluoride concentration

Table 1 gives the results for recovery of fluoride from the alkaline test solutions. The fluoride concentrations studied cover the range encountered in most solid geological materials when 30—300-mg subsamples are pyrohydrolysed. Measurements were also made without any conditioning of the electrode between samples other than rinsing with water (Table 1); such measurements had a systematic error of about 2% relative for fluoride concentrations between 0.5 and 1.0 μg g^{-1}. This error seems to be due to a memory effect of the electrode after immersion in the more concentrated solutions involved in the standard additions. As can be seen, conditioning the electrode with lanthanum solution gave accurate results. The precision of ±0.3% relative shown in Table 1 for the standard-addition measurement of fluoride concentrations in the range 5—10 μg g^{-1} would be unattainable by direct measurements at constant temperature. Table 1 also shows that accuracy and precision were not improved by double rather than single standard addition.

Sources of error in standard addition measurements with ion-selective electrodes

Errors in standard concentrations and solution masses in Eqn. (4) can be considered negligible, i.e. not exceeding 0.1% relative, when the recommended

TABLE 1

Recovery of fluoride from spiked sodium hydroxide solutions with single and double standard additions

Fluoride range (μg g^{-1})	Recovery of fluoride (%)[a]			
	Electrode only rinsed with H_2O between samples		Electrode conditioned with 0.06 M La^{3+} for ⩾ 30 s	
	Single addition	Double addition	Single addition	Double addition
0.05—0.10[b]	108 ± 6	107 ± 10	100 ± 9	100 ± 9
0.5—1.0[c]	102.9 ± 1.3	103.0 ± 1.4	100.5 ± 0.8	100.4 ± 1.1
5—10[c]	100.1 ± 0.3	—	100.2 ± 0.3	—

[a]Mean of 6 determinations with the 99% confidence limit of mean. [b]Initially spiked so that the fluoride concentration before standard addition was between 0.5 and 1.0 μg $F^- g^{-1}$. [c]These solutions were not initially spiked.

technique is used. The increased relative error in the calculated net concentration after initial spiking reflects the error in the measured concentration of the initially spiked solution. For example, in Table 1, the relative error of ±9% at the lowest concentration measured implies that the relative error in measuring the initially spiked solution (containing 0.5—1.0 μg F^- g^{-1}) is about ±1%.

The terms in Eqn. (4) which contribute most to the error in C_x are the slope, S, and the difference in potential, $E_1 - E_2$. For simplicity in discussing Eqn. (4), M_1 is taken as zero, and $M_x/(M_x + M_2)$ is taken as unity, because M_2 is much less than M_x; T_x is taken as 25°C and S as 59 mV/decade. It can then be seen that the relative error in C_x equals the relative error in antilog$[(E_1 - E_2)/S] - 1$. Figure 1 plots the % relative error in C_x as a function of $E_1 - E_2$ for four different situations. The factor by which the % error in C_x exceeds the % error in $(E_1 - E_2)/S$ varies with $E_1 - E_2$; Fig. 1 gives these factors at 10-mV intervals, in parentheses.

As an example of the insight provided by Fig. 1, the measurements of 5—10 μg $F^- g^{-1}$ in Table 1 are worth noting: $E_1 - E_2$ in these measurements was typically about 40 mV; if the error in $E_1 - E_2$ were ±0.1 mV and S were 59.0 ± 0.1 mV decade^{-1}, then the relative error in $(E_1 - E_2)/S$ would be ±0.30%, giving a relative error in C_x of ±0.60% (0.30 × 1.98; cf. Fig. 1). The actual error in measuring 5—10 μg $F^- g^{-1}$ was less (Table 1).

Figure 1 shows that in order to obtain (by single standard addition) a relative error in C_x not exceeding ±0.8%, $E_1 - E_2$ should be at least 20 mV,

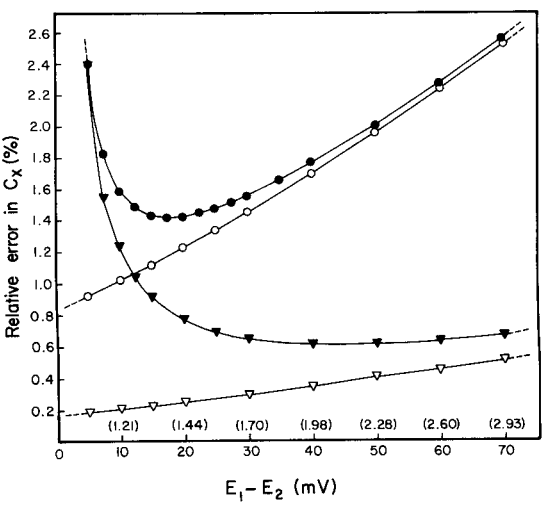

Fig. 1. Percentage relative error in C_x as a function of $E_1 - E_2$ (Eqn. 4). (▽) Error in $E_1 - E_2 = 0$ mV; error in $S = \pm 0.1$ mV/decade; (▼) error in $E_1 - E_2 = \pm 0.1$ mV; error in $S = \pm 0.1$ mV/decade; (○) error in $E_1 - E_2 = 0$ mV; error in $S = \pm 0.5$ mV/decade; (●) error in $E_1 - E_2 = \pm 0.1$ mV; error in $S = \pm 0.5$ mV decade^{-1}. (The factor by which the % error in C_x exceeds the % error in $(E_1 - E_2)/S$ is given at 10-mV intervals in parentheses.)

the error in $E_1 - E_2$ should not exceed ±0.1 mV, and the error in S should not exceed ±0.1 mV/decade. Further, if S has a relatively large error (e.g., ±0.5 mV/decade) the error in C_x is minimised when $E_1 - E_2$ is ca. 20 mV.

It can be concluded that gravimetric single standard addition, with separate slope measurement accurate to ±0.1 mV/decade, is suitable for precise and accurate determinations of fluoride in simple solutions. Because of the excellent agreement observed between concentrations measured by single and double standard addition, occasional use of the latter technique serves to verify the electrode slope. However, when fluoride is measured in more complicated aqueous samples (e.g., wastewaters), double standard addition would be required in order to test whether the sample matrix affects the slope.

Permission to publish this paper was given by the Secretary, New South Wales Department of Mineral Resources. The author thanks J. A. McGlynn for helpful discussion and J. N. Wilson for help with the experimental work.

REFERENCES

1 T. D. Rice, Anal. Chim. Acta, 97 (1978) 213.
2 T. D. Rice, Analyst, 107 (1982) 47.
3 C. E. Efstathiou and T. P. Hadjiioannou, Anal. Chem., 54 (1982) 1525.
4 G. Troll, A. Farzaneh and K. Cammann, Chem. Geol., 20 (1977) 299.
5 D. Jagner and V. Pavlova, Anal. Chim. Acta, 60 (1972) 153.
6 C. J. Rix, A. M. Bond and J. D. Smith, Anal. Chem., 48 (1976) 1236.

Analytica Chimica Acta, 151 (1983) 391—400
Elsevier Science Publishers B.V., Amsterdam — Printed in The Netherlands

DETERMINATION OF BISMUTH AND LEAD IN STEEL AND CAST IRON BY HYDRIDE GENERATION AND ZEEMAN ATOMIC ABSORPTION SPECTROMETRY

B. VANLOO, R. DAMS and J. HOSTE*

Institute of Nuclear Sciences, Rijksuniversiteit Gent, Proeftuinstraat 86, 9000 Gent (Belgium)

(Received 4th January 1983)

SUMMARY

Procedures are described for the determination of lead and bismuth in steel and cast iron by atomic absorption spectrometry (a.a.s.). Two alternative decomposition procedures are applied, namely, sodium peroxide fusion in zirconium crucibles and digestion with a nitric—perchloric acid mixture in a Bethge digestion apparatus. The latter technique is preferred. Lead is measured by electrothermal a.a.s. with Zeeman background correction. Bismuth is determined after hydride generation with sodium tetrahydroborate. Calibration is done by standard addition. The sensitivities obtained are 1 $\mu g\ g^{-1}$ for lead in steel and cast iron and 5 $\mu g\ g^{-1}$ for bismuth in white and grey cast iron. The r.s.d. is generally better than 10% for $>10\ \mu g\ g^{-1}$. The method is applied to standard reference steel samples and several specimen cast irons.

The favourable mechanical properties of cast iron are strongly influenced by the morphological structure of the graphite nodules. These nodules are only present in grey cast iron where the carbon is precipitated as nodules, so-called nodular graphite, or as lamels, called lamellar graphite. In white cast iron, all the carbon is present as iron carbide. Because nodular cast iron has mechanical properties that are comparable to those of steel, it is desirable to favour the formation of nodular graphite. This is achieved by adding elements such as Ce, La, Mg, Ca and Sr, but the effect is counteracted by elements such as Pb, Bi, Sb, S and O. Some of these (Pb, Bi) are deleterious even at the $\mu g\ g^{-1}$ level. To investigate this effect, the determination of lead and bismuth in cast iron is an obvious requirement.

Several papers [1—5] have dealt with similar analyses. Two of them describe the determination of lead in steel and cast iron by atomic absorption spectrometry (a.a.s.) [1, 2], while two others describe the determination of lead, bismuth and other elements in iron, copper and zinc alloys [3, 4]. Also, a.a.s., after volatilization as hydrides, has been applied for the determination of Bi, As and Sb in steel [5].

Owing to the possible interference of a large variety of metals present in great excess, electrothermal a.a.s. with background correction based on the

0003-2670/83/$03.00

Zeeman effect seemed an attractive approach for the determination of lead. The low concentrations of bismuth (10—100 $\mu g\ g^{-1}$) to be determined imply that <1 ng will be injected. Generation of bismuth hydride (BiH_3) allows a larger amount of bismuth to be introduced into the atomization tube, resulting in better sensitivity, and also a nearly interference-free measurement. This paper describes the accurate determination of lead in grey and white cast iron and in steel. Bismuth is determined in grey and white cast iron and in ferrosilicon alloys used for the addition of bismuth before the solidification of the molten iron. For dissolution of the samples, wet digestion with nitric—perchloric acid is compared to an oxidizing fusion with sodium peroxide. The uptake of bismuth during the solidification is discussed.

EXPERIMENTAL

Apparatus

Lead. Absorbances were measured with a Hitachi model 180-70 polarized Zeeman atomic absorption spectrometer equipped with a graphite cup cuvette (Hitachi model 180-7402), a Hitachi lead hollow-cathode lamp and a Hitachi model 056 double-pen strip-chart recorder. Solutions (10 μl) were injected into the graphite cup by an automatic sample changer (Hitachi model 170-0125). The operating parameters and the temperature settings of the graphite cup are summarized in Table 1. In order to increase the sensitivity, the internal gas stream was interrupted (gas stop) during atomization. Correction for unspecific background absorption was applied by means of the Zeeman effect. The principle of Zeeman atomic absorption spectrometry has recently been discussed in several papers [6—8]. Absorbance values were obtained after integration of the peak area by a data processor (Hitachi model 180-0205).

TABLE 1

Operating parameters and temperature settings for the electrothermal a.a.s. determination of lead and bismuth

Element	Lamp current (mA)	Wavelength (nm)	Slit width (nm)	Temperature program	
				Temp. (°C)	
Pb	7.5	283.3	1.3	25—120 (25 s)	Drying
				120—600 (35 s)	Drying
				600 (20 s)	Ashing
				2050 (7 s)	Atomizing
				2400 (5 s)	Cleaning
				Atomization tube temp. (°C)	
Bi	10	223.0	0.2	900	

Bismuth. A Perkin-Elmer model 503 double-beam atomic absorption spectrometer, equipped with a bismuth Intensitron hollow-cathode lamp and a Hitachi—Perkin-Elmer model 56 strip-chart recorder, was used to measure the absorbance of bismuth. For the generation of the bismuth hydride, an automatic mercury/hydride system (Perkin-Elmer model MHS-1) was used. The operating parameters of the spectrometer are also summarized in Table 1. The absorbance was measured by peak height.

Reagents and standards

All solutions were prepared with doubly-distilled water. For the wet digestion, Suprapur nitric acid, Suprapur hydrochloric acid and reagent-grade perchloric acid (Merck) were used. The oxidizing fusions were done with reagent-grade sodium peroxide (UCB) in zirconium crucibles (55 ml; Willamette Valley Rehabilitation Center). The hydride generation was done with Suprapur sulfuric acid (Merck), reagent-grade sodium tetrahydroborate (Aldrich) and sodium hydroxide (Carlo Erba). The reducing solution was prepared by dissolving sodium tetrahydroborate in water to obtain a 5% (w/v) solution to which sodium hydroxide was added up to 2% (w/v) as a stabilizer. Standards were prepared by diluting 1000 mg l^{-1} standard solutions of lead (Merck) and bismuth (Fluka).

Sample decomposition

Fine drillings of the cast iron and steel samples were taken. In order to be able to oxidize not only the iron and the other alloying metals but also the free graphite, a powerful oxidizing attack is required. Two alternative procedures were successfully applied.

Sodium peroxide fusion. The sample (ca. 0.25 g) is weighed carefully into a zirconium crucible and 2.5 g of sodium peroxide is added. The sample is thoroughly mixed with the flux with a glass rod and subsequently heated over a bunsen burner, slowly and carefully at the outset to avoid losses by sputtering. The production of a clear homogeneous melt signals completion of the decomposition. The mass is allowed to cool and just before solidification the crucible is rotated to distribute the solid around the walls in a thin layer. The melt is readily dissolved in doubly distilled water and then carefully neutralized with 20 ml of concentrated nitric acid. The clear solution is evaporated, any residue is dissolved in doubly distilled water and the solution is diluted to the mark in a 50- or 100-ml volumetric flask. Blanks are prepared with the same amounts of reagents in the same crucibles.

The use of nickel crucibles should be avoided because attack by the flux results in unreproducible blank values, especially for lead. In addition, the dissolved nickel is reduced during the hydride generation and interferes strongly with the determination of bismuth.

Dissolution in nitric—perchloric acid. The sample (0.1—1 g) is weighed into a 150-ml digestion flask, and 25 ml of 6 M nitric acid is added. After the evolution of nitrous gases, 10 ml of concentrated perchloric acid is added. If

the digestion were done in an open vessel, the nitric acid would be volatilized and the oxidation continued only by the perchloric acid, which also volatilizes at 203° C. Large amounts of reagents, therefore, would be required, increasing the blank values. Accordingly, a Bethge digestion apparatus [9] provided with a reflux condenser was used. This permits heating to ca. 220° C. When the undissolved residue turns white (silica), the condensate is returned to the reaction flask by readjusting the stopcock of the Bethge apparatus. The contents of the flask are finally transferred to a beaker. The salts adhering to the walls of the flask are dissolved in 10 ml of 1 M hydrochloric acid and also transferred to the beaker, and the solution is evaporated to dryness. If much silicon is present, it can be evolved as the tetrafluoride, by addition of hydrofluoric acid. This was generally not needed in the present work. The residue is taken up in doubly distilled water and the solution is diluted to the mark in a 100-ml volumetric flask. Blanks are made from the same amounts of acid, in the same digestion equipment.

Decomposition of ferrosilicon alloys. To ca. 0.1 g of sample in a platinum crucible is added 20 ml of (1 + 1) nitric acid. In small portions, 10 ml of 50% hydrofluoric acid is carefully added, each time waiting until gas evolution has ceased. Finally the mixture is heated and the volatile fluorides are evaporated. The clear solution is transferred to a 100-ml volumetric flask, diluted to the mark with doubly distilled water and treated as described immediately below.

Absorbance measurements

Lead. Four 10-ml aliquots of the sample solution are diluted 5—10 times, at the same time adding 0, 0.5, 1.0 and 1.5 μg of lead, respectively. After mixing, 10 μl of each solution is injected into the graphite cup and the absorbance is measured. After subtraction of the absorbance of the blank, a calibration graph is calculated by the method of least squares and the concentrations of lead in the samples are determined.

Bismuth. A 100—250-μl aliquot of sample solution is injected into a reaction flask which already contains 10 ml of 1.5% sulfuric acid solution. After this solution has been purged with argon to remove air from the system, 2.5 ml of 5% sodium tetrahydroborate is injected. Simultaneously, the magnetic stirrer in the reaction flask is started, to improve the generation of bismuth hydride, which is swept into a preheated quartz cell by the argon. These steps are programmed as described in the manufacturer's manual. Standard addition is applied by injecting together with the unknown solution 20—100 μl of a 1 mg l^{-1} bismuth solution and running the above program. From peak height measurements, a calibration graph is drawn and the concentration of bismuth in the sample is calculated.

RESULTS AND DISCUSSION

Determination of lead in steel

To test the precision, accuracy and sensitivity of the procedures, three B.C.S. standard reference steel samples with lead concentrations from 30 to 140 $\mu g\ g^{-1}$ were decomposed by sodium peroxide fusion and by a nitric–perchloric acid mixture. Table 2 lists the results obtained by these methods. The relative standard deviation varies from 2% for the highest concentrations to 8% for the lowest. There is no significant difference between the methods of decomposition. The results are also in excellent agreement with the certified values.

The sensitivity obtained is 20 pg (for 0.0044 absorbance) as compared to 15 pg specified by the manufacturer. This corresponds to a concentration of 4 $\mu g\ g^{-1}$ in the steel sample, and could be decreased to 1 $\mu g\ g^{-1}$ by dissolving 1 g of sample. In practice, however, the sensitivity is limited by the blank. When the decomposition is done by sodium peroxide fusion, the blank value corresponds to 30—70 pg of lead, which stems largely from the sodium peroxide and is difficult to monitor within 10 pg. Increasing the sample size implies increasing the amount of flux, so that the sensitivity is limited primarily by this blank value. When the sample is dissolved in Suprapur acids, blank values of less than 30 pg were obtained when a 0.25-g sample was used. This can further be reduced if needed by increasing the sample size, without increasing the amount of acid.

The application of the sodium peroxide flux should be avoided for additional reasons. During atomization, double peaks are produced after fusion with sodium peroxide, while single peaks are obtained after wet digestion, as can be seen in Fig. 1. As a consequence, the absorbance from double peaks must be calculated by integration of the peak areas for accurate results. After wet digestion, the peak height and peak area modes give nearly identical results. The use of fusion also implies the danger of losses by sputtering, and requires in the present case the use of expensive zirconium crucibles. An additional argument against the use of sodium peroxide is the recent worldwide cessation of its production.

TABLE 2

Determination of lead in BCS standard reference mild steel samples

	Lead content ($\mu g\ g^{-1}$)		
	BCS 326	BCS 327	BCS 459
Certified value	141 ± 8	105 ± 5	25.6 ± 2.3
Na_2O_2 fusion[a]	143 ± 3	103 ± 6	29.0 ± 2.1
$HNO_3 + HClO_4$[a]	141 ± 4	108 ± 4	27.4 ± 1.8

[a]Mean ±2 standard deviations of the mean ($n = 5$).

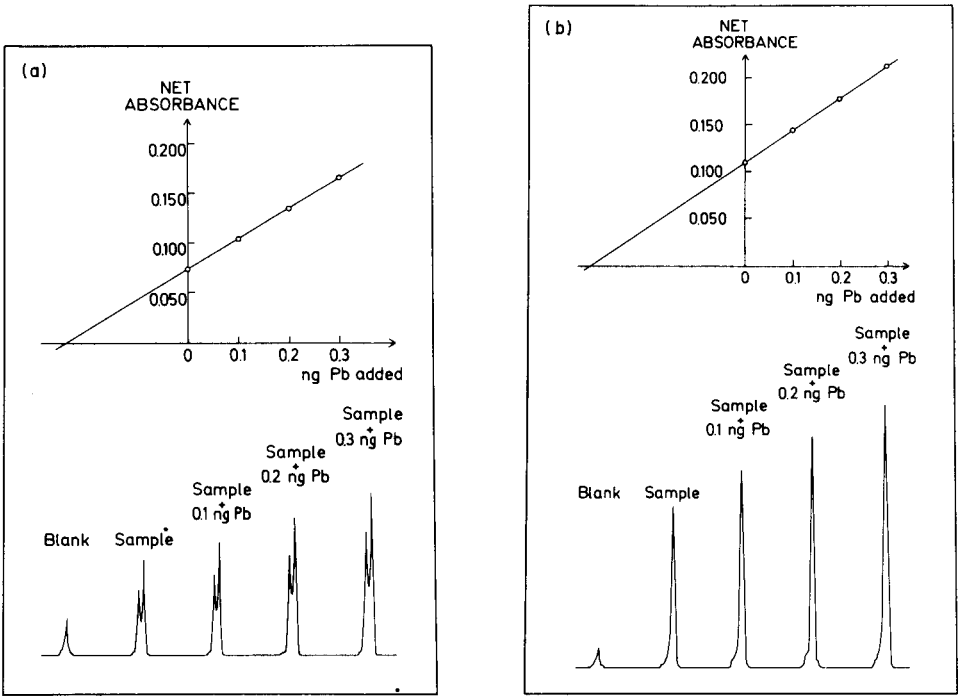

Fig. 1. Absorbance signals for lead, with standard addition calibration graph, after: (a) Na_2O_2 fusion; (b) HNO_3 + $HClO_4$ digestion.

Determination of lead in cast iron

The same procedure was applied for the analysis of two specimen cast iron samples, produced by the CRIF (Center for Scientific and Technical Research of the Metalworking Industry in Belgium). A white and a grey sample, with silicon and carbon contents of 2.4% and 3.6%, respectively, were analyzed, both decomposition procedures being applied. As shown in Table 3, there is again no significant difference in the results obtained by the two procedures, except that for the 20 $\mu g\ g^{-1}$ sample, the relative standard deviation exceeds 10% after the sodium peroxide fusion because of the blank, which accounts for ca. 30% of the signal.

TABLE 3

Determination of lead in cast iron

Decomposition method	Lead content ($\mu g\ g^{-1}$)[a]	
	B 108 white	B 108 grey[a]
Na_2O_2 flux	59.5 ± 2.7	19.5 ± 2.9
HNO_3 + $HClO_4$	61.5 ± 2.4	19.5 ± 1.8

[a]See footnote to Table 1, but n = 3.

Determination of bismuth in cast iron

A large number of white and grey cast irons produced by the CRIF were analyzed for bismuth by the procedure described above, mostly with sodium peroxide fusion on 0.25-g samples. The bismuth concentrations were all determined by the method of standard additions in order to avoid all matrix effects as much as possible. Owing to the lack of certified standards for bismuth, the accuracy of the method was evaluated by analyzing a cast iron to which a known amount of bismuth had been added before the sodium peroxide fusion. The average bismuth recovery was 97 (±5%, n = 3). In order to check the precision and sensitivity, two cast irons were produced by adding to the molten iron 29 or 100 $\mu g\ g^{-1}$ bismuth. Because it was known [10] that only a fraction of the bismuth is taken up by the cast iron itself, a much lower content was expected. In an effort to cast the white and grey modification under identical circumstances, a specially designed casting mould was used [11]. The results are summarized in Table 4. The precision, calculated as the relative standard deviation, does not exceed 15% even at the low concentration of 10 $\mu g\ g^{-1}$. The sensitivity was found to be 1 ng (for 0.0044 absorbance). This corresponds to 0.8 $\mu g\ g^{-1}$ for a 0.25-g sample dissolved in 50 ml of which 250 μl is injected. The blank did not give a significant signal, indicating a concentration of less than 2 ng in 10 ml of reducing solution. This is equivalent to an apparent concentration of less than 1.6 $\mu g\ g^{-1}$ in the sample. For the presently applied conditions, the practical sensitivity can be estimated at 5 $\mu g\ g^{-1}$, which can be further reduced if necessary, by using more concentrated sample solutions or injecting larger volumes.

The wet digestion method was also used for the dissolution of these cast irons. As can be seen from Table 4 there is no significant difference between the decomposition methods. The bismuth uptake by the cast irons was ca. 36%, but the most important result was the excellent agreement between the bismuth contents of the grey and white modifications.

In another experiment, the segregation during solidification of a thick casting piece was investigated. A round nodular iron bar with a diameter of

TABLE 4

Determination of bismuth ($\mu g\ g^{-1}$) in white and grey cast irons

Sample	H_1 white	H_1 grey	H_2 white	H_2 grey
Bi added	29	29	100	100
Bi found				
Na_2O_2 fusion[a]	11.4 ± 0.5	10.4 ± 1.4	33.6 ± 2.9	33.2 ± 2.7
$HNO_3 + HClO_4$[b]	12	11	33	30
Bi uptake (%)	39	36	34	33

[a]Mean ±2 standard deviations (n = 5). [b]Mean (n = 2).

14 cm was cast in a horizontal position. An amount of bismuth was added so as to give 72 $\mu g\ g^{-1}$ for 100% uptake. Because the slag was expected to contain large amounts of bismuth, a sample of it was also analyzed. During cooling, the sequence of solidification was as follows: the bottom, the top and finally the centre of the bar. Drillings were taken from these sections and samples of the surface were also taken. This surface was strongly contaminated with sand particles and consisted of coarse and fine material. The results are summarized in Table 5. The precision is similar to that in the previous experiment (r.s.d., 7—15%); this is sufficient to conclude that no significant segregation occurred during solidification. The lower values found in the surface material, especially in the fine material, can be explained by the significant dilution with sand particles in this material. It is also important that the bismuth concentration in the slag is about ten times higher than that in the iron. This enrichment in the slag explains the uptake of only 42%.

Some information about the mechanism of the solidification of the cast can be obtained by varying the time between the addition of bismuth and the casting. The results obtained for grey cast iron (Table 6) indicate that immediate casting results in unreproducible, high values, which are probably due to contamination by the slag. If this is allowed to rise in the melt after a few minutes the uptake stabilizes to 50—55%. This confirms that bismuth is not lost by volatilization during standing in the ladle. The incomplete uptake must thus be explained by enrichment in the slag.

Determination of bismuth in ferrosilicon alloys

Bismuth was added to the melt as a ferrosilicon alloy which contained 72% silicon, 25% iron and a number of minor elements including ca. 1% bismuth; 1% was added to the liquid mixture just before the casting. In order to calculate the percentage uptake accurately, an exact knowledge of the bismuth content of this alloy was required. Dissolution of this alloy presented a problem because fusion with sodium peroxide produced an explosive mixture and the high silicon content precluded attack with nitric and perchloric acids. Therefore the silicon was volatilized as its tetrafluoride by adding hydrofluoric acid as outlined under Experimental. The blank value was found to be insignificant.

In Table 7, the results are compared with the concentrations specified by the producer. Alloy 2A consisted of coarse and fine particles. These

TABLE 5

Investigation of the homogeneity of a thick bar of nodular cast iron with respect to bismuth

Sample	H_3 (1) bottom	H_3 (2) centre	H_3 (3) top	H_3 surface		Slag
				Coarse	Fine	
Bi found ($\mu g\ g^{-1}$)[a]	32.4 ± 3.1	30.0 ± 3.0	30.2 ± 1.8	28.4 ± 3.9	20.2 ± 1.5	280[b]

[a]Mean ±2 standard deviations (n = 5). [b]Mean of 2 results.

TABLE 6

Investigation of bismuth uptake by grey cast iron as a function of the residence time in the pouring ladle

Sample number	Time after Bi addition (min)	Bi found[a] ($\mu g\ g^{-1}$)	Uptake (%)
B70-1	0	56, 56, 78, 108	>100
B70-2	1	10 ± 1	20
B70-3	3	27.5 ± 1	55
B70-4	5	25 ± 1	50
B70-5	8	26 ± 2	52
B70-6	11	28 ± 1	56

[a]50 $\mu g\ g^{-1}$ bismuth added.

fractions were roughly separated and both were analysed. The agreement between the stated concentration and the value found is good. The relative standard deviation of the measurements is 6—9%, which may partly be due to inhomogeneity of the material.

Conclusions

The experiments have shown that lead can be determined accurately in steel and cast iron samples, after wet digestion, by electrothermal atomic absorption spectrometry. The interferences of other elements are efficiently compensated by Zeeman background correction. Bismuth concentrations at $\mu g\ g^{-1}$ levels can be determined by atomic absorption spectrometry after the same decomposition procedure or after a sodium peroxide fusion. Hydride generation increases the sensitivity and avoids possible interference of alloying elements in steel or cast iron. The relative standard deviation is better than 10% for concentrations above 10 $\mu g\ g^{-1}$ bismuth. The analysis of a number of grey and white specimen cast irons showed that the results are not affected by the solidification mode of the iron. Fluid slag entrapment in the samples, however, may falsify the results because the slag is strongly en-

TABLE 7

Determination of bismuth in ferrosilicon alloys

Sample	H	2A	
		Fine fraction	Coarse fraction
Bi present (%)[a]	0.50	1.45	1.45
Bi found (%)[b]	0.51 ± 0.03 (8)	1.31 ± 0.11 (5)	1.49 ± 0.08 (5)

[a]As stated by the producer. [b]Mean ±2 standard deviations with number of determinations in parentheses.

riched with bismuth. The analysis of samples taken from a cross-section of a thick grey cast iron bar demonstrates that segregation of bismuth is insignificant.

The authors are indebted to Ir. Lietaert and Ir. Defrancq of the CRIF for preparing the specimen cast iron samples and for fruitful discussions. Thanks are also due to Miss M. Coene for technical assistance. The investigation is part of a research program sponsored by IWONL (Instituut voor Wetenschappelijk Onderzoek in Nijverheid en Landbouw).

REFERENCES

1 W. Frech, Anal. Chim. Acta, 77 (1974) 43.
2 F. Shaw and J. M. Ottaway, Analyst, 99 (1974) 184.
3 F. Shaw and J. M. Ottaway, Analyst, 100 (1975) 217.
4 W. B. Barnett and E. A. McLaughlin, Jr., Anal. Chim. Acta, 80 (1975) 285.
5 H. D. Fleming and G. R. Ide, Anal. Chim. Acta, 83 (1976) 67.
6 F. J. Fernandez, S. A. Myers and W. Slavin, Anal. Chem., 52 (1980) 741.
7 M. T. C. De Loos-Vollebregt and L. de Galan, Spectrochim. Acta, Part B, 35 (1980) 495.
8 J. A. C. Broekaert, Spectrochim. Acta, Part B, 37 (1982) 65.
9 G. F. Smith, The Wet Chemical Oxidation of Organic Compositions Employing Perchloric Acid, G. F. Smith Chemical Co., OH, 1965, p. 20.
10 H. Kowalke, Giesserei, 59 (1972) 498.
11 F. Lietaert, CRIF, personal communication, 1982.

Analytica Chimica Acta, 151 (1983) 401—407
Elsevier Science Publishers B.V., Amsterdam — Printed in The Netherlands

ATOM FORMATION PROCESSES IN THE PRESENCE OF THIOUREA IN ELECTROTHERMAL ATOMIC ABSORPTION SPECTROMETRY WITH A MOLYBDENUM MICROTUBE ATOMIZER

MASAMI SUZUKI* and KIYOHISA OHTA

Department of Chemistry, Faculty of Engineering, Mie University, Kamihama-cho, Tsu, Mie-ken 514 (Japan)

(Received 20th December 1982)

SUMMARY

The processes of atom formation of antimony, bismuth, cadmium, copper and silver atomized in the presence of thiourea in a molybdenum microtube atomizer are discussed. These elements form complexes with thiourea and are converted to their sulfides during the charring stage. Atomization in argon—hydrogen occurs by reduction of the metal sulfide by hydrogen followed by vaporization of the free metal, or by thermal dissociation of the metal sulfide. Atom formation processes in pure argon are somewhat different. The activation energies for bismuth, cadmium and copper atomization are unaltered in a chloride matrix, provided that thiourea is present.

The effects of thiourea on the atomization of bismuth [1], antimony [2], copper [3] and cadmium [4] have been previously described. Thiourea improves the atomization profiles of these elements to give a higher absorption peak and removes the effects of different chemical species. Interferences from diverse elements are also suppressed by the addition of thiourea. However, there has been no reasonable explanation of the process of atom formation in the presence of thiourea. This work was undertaken in an attempt to obtain better understanding of the atomization of antimony, bismuth, cadmium, copper and silver in the presence of thiourea.

EXPERIMENTAL

Apparatus

The monochromator, photomultiplier and fast-response amplifier were the same as used previously [5]. The output signal from the amplifier was fed to a microcomputer (SORD M223) through an AD converter (DATEL ADC-HX 12BGC) and multiplexer (DATEL MX-808) [5]. The atomizer was a molybdenum microtube (20 mm long, 1.5 mm i.d.) machined from molybdenum sheet (0.05 mm thick; Rembar Co.). The atomizer was mounted in the absorption chamber (300 ml) which was purged with argon (480 ml min^{-1}) and hydrogen (20 ml min^{-1}). The atomizer temperature was measured with a

0003-2670/83/$03.00

photodiode (Hamamatsu TV Co. S641). Corrections were made for non-black body emissivity. The signal from the photodiode was calibrated with an optical pyrometer (Chino Works) and was recorded simultaneously with the absorbance signal.

Hollow-cathode lamps (Hamamatsu TV Co.) were used as radiation sources. The spectral lines used were 217.59, 233.06, 228.80, 324.75 and 328.07 nm for antimony, bismuth, cadmium, copper and silver, respectively. Samples were injected into the microtube from a 1-μl glass micropipet. A Rigaku x-ray diffractometer was used for identification of the residues formed on heating metal solutions with thiourea at 573 K before atomization.

Reagents

All reagents used were of analytical reagent grade. The stock solutions were prepared from pure metals with the exception of antimony, which was prepared from antimony(III) potassium tartrate. All solutions except silver contained hydrochloric acid, and all working solutions were prepared just before use by dilution with deionized water. The concentration of acid in the working solutions was 10^{-4} M.

Programming and procedures

Programs were written for data manipulation and presentation. For activation energies a logarithmic plot of the measured absorbance vs. the reciprocal absolute temperature and the evaluation of the energies from the slope of this plot by a least-squares analysis [6] were programmed. The precision of the measurements was <15%. The appearance temperatures were also indicated together with the activation energies.

Atomization was done by heating a sample (1 μl) to give a final temperature of 2073—2473 K after drying at 373 K for 10 s and charring at 573 K for 10 s.

For the identification of the chemical species of elements formed on the surface of the atomizer by heating the sample with thiourea before atomization, aliquots of sample solutions containing thiourea were injected into the atomizer and dried at 373 K for 10 s. The residue was heated at 573 K for 10 s before cooling to room temperature. After cooling, the x-ray diffraction pattern of each residue was recorded. Irradiation by Cu $K\alpha$ at 0.154184 nm was used at 35 kV and 15 mA.

RESULTS AND DISCUSSION

Antimony, bismuth, cadmium, copper and silver form complexes with thiourea. X-ray diffraction was used to identify the products which were formed by heating these complexes at 573 K in the molybdenum microtube. Diffraction lines for sulfide were present in each of the recorded patterns. Elemental antimony was also identified together with sulfide. This shows that thiourea complexes decompose to give metal sulfides. Therefore, atomization from the sulfide can be considered to be the most likely process.

The atomization profiles of antimony, bismuth, cadmium, copper and silver in argon and argon—hydrogen atmospheres are shown in Figs. 1 and 2. Similar appearance temperatures were shown in the two atmospheres for silver, cadmium and copper, while those for bismuth and antimony were shifted to lower temperatures in argon—hydrogen. The appearance temperature is defined as the temperature of the atomizer at the time when a 1% absorption signal of the analyte can first be perceived above the baseline noise by the microcomputer.

The combined thermodynamic—kinetic approach described by Sturgeon et al. [6] was used for elucidation of the atomization processes for antimony, bismuth, cadmium, copper and silver in the presence of thiourea. This assumes that an analyte surface—gas phase equilibrium exists within the tube, and the production of observable atoms is characterized by a unimolecular rate constant. The difference between the temperature of the gas phase in the microtube and that of the tube temperature is negligible at the heating rate used [7]. Therefore, it seems reasonable to expect that the physical and chemical processes in the microtube attain equilibrium before the atoms are

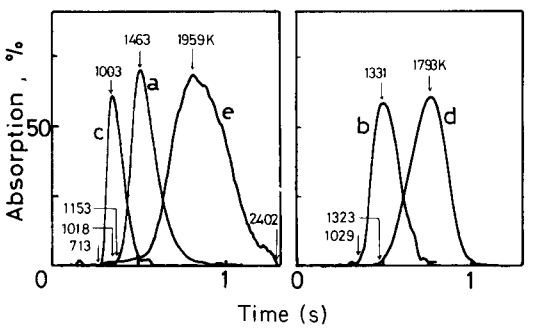

Fig. 1. Atomization profiles in the presence of thiourea with an argon atmosphere for: (a) Ag; (b) Bi; (c) Cd; (d) Cu; (e) Sb.

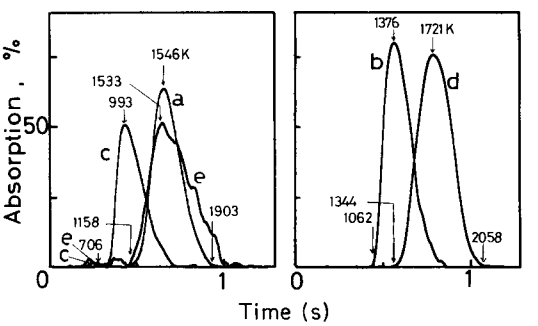

Fig. 2. Atomization profiles in the presence of thiourea with an argon—hydrogen atmosphere; (a)—(e) as Fig. 1.

lost. The activation energies were also determined by Smet's method [8], and were in agreement with the values obtained by the above procedure.

Tables 1 and 2 present the activation energies, E_a, obtained by atomizing 5—500 pg of the elements in the presence of thiourea, together with the appearance temperatures, T_{app}.

Atomization processes for the different elements

Antimony. The E_a values were 163 and 255 kJ mol^{-1} in argon and argon–hydrogen, respectively. The E_a value in the argon—hydrogen atmosphere may be rationalized as the heat of atomization of Sb(l), 264 kJ mol^{-1}. Antimony sulfide is reduced by hydrogen to antimony at temperatures near the melting point of the metal [9]. According to a mass spectrometric study at 670—793 K, the vaporization of antimony sulfide is primarily due to the reaction $Sb_2S_3(s) = 2SbS(g) + 0.5S_2(g)$, and various other antimony species are also detected as very minor mass spectrometric peaks [10]. The chief atomization process for antimony in the argon atmosphere may be the reaction $SbS(g) = Sb(g) + S(g)$. However, no reasonable experimental energy value was obtained. The atomization process, therefore, may not be simple.

Bismuth. Two E_a values were obtained in the argon atmosphere: 314 kJ mol^{-1} in the low temperature portion of the E_a plot (1037—1095 K), corresponding to the Bi—S bond energy (315 kJ mol^{-1}), and 209 kJ mol^{-1} above 1095 K, corresponding to the heat of vaporization of the metal (210 kJ mol^{-1}). Sublimation of bismuth sulfide occurs at 673—873 K [9]. The following thermal dissociation reactions for bismuth trisulfide may be responsible for the two experimental energy values. At lower temperatures:

$Bi_2S_3(s) \rightarrow 2BiS(g) + 0.5S_2(g)$; $BiS(g) \rightarrow Bi(g) + S(g)$

At higher temperatures:

$Bi_2S_3(s) \rightarrow 2Bi(l) + 1.5S_2(g)$; $Bi(l) \rightarrow Bi(g)$

TABLE 1

Appearance temperatures and activation energies with an argon atmosphere[a]

Element	T_{app} (K)	E_a (kJ mol^{-1})	Temperature range (K)	Possible atomization process
Ag	1158	209	1227—1518	$Ag_2S(s) \rightarrow 2Ag(g)$
Bi	1062	314	1062—1095	$BiS(g) \rightarrow Bi(g)$
		209	1095—1187	$Bi(l) \rightarrow Bi(g)$
Cd	707	185	707—840	$CdS(g) \rightarrow Cd(g)$
Cu	1344	410	1368—1563	$Cu_2S(s) \rightarrow 2Cu(s) \rightarrow 2Cu(g)$
		176	1563—1734	$Cu_2(g) \rightarrow 2Cu(g)$
Sb	1217	163	1217—1473	not established

[a]500 ml Ar min^{-1}; 5 μg thiourea. Heating rates: 3.00, 2.03, 1.85, 1.95 and 2.04 K ms^{-1} for Ag, Bi, Cd, Cu and Sb, respectively.

TABLE 2

Appearance temperatures and activation energies with an argon—hydrogen atmosphere[a]

Element	T_{app} (K)	E_a (kJ mol^{-1})	Temperature range (K)	Possible atomization process
Ag	1153	285	1176—1432	Ag(s) → Ag(g)
Bi	950	209	1018—1205	Bi(l) → Bi(g)
Cd	713	184	762—893	CdS(g) → Cd(g)
Cu	1323	326	1302—1389	Cu(s) → Cu(g)
		163	1398—1773	Cu_2(g) → 2Cu(g)
Sb	1018	255	1757—1980	Sb(l) → Sb(g)

[a]480 ml Ar min^{-1}, 20 ml H_2 min^{-1}; thiourea and heating rates as Table 1.

The E_a value of 209 kJ mol^{-1} obtained for bismuth in the argon—hydrogen atmosphere is in agreement with the heat of vaporization of the element, 210 kJ mol^{-1}. Bismuth sulfide can be reduced by hydrogen to give bismuth [9]. The free-energy change for the reaction shows that reduction of bismuth sulfide by hydrogen is feasible.

Cadmium. An E_a value of 185 kJ mol^{-1} was obtained for cadmium in both atmospheres. This energy correlates with the CdS bond energy (201 kJ mol^{-1}). The appearance temperatures of cadmium in both atmospheres are also similar. Therefore, the same atomization process is proposed for both cases. Cadmium sulfide sublimes in an inert atmosphere [11]. Cadmium atoms may thus be formed by dissociation of the sulfide in the gas phase after sublimation. Thermodynamically, hydrogen reduction of cadmium sulfide at the appearance temperature is not favored.

Copper. Two E_a values were obtained for copper in an argon atmosphere, 410 and 176 kJ mol^{-1}, correlating with the sum of the negative heat of formation of Cu_2S(s) from the elements at 1300 K and the heat of vaporization of Cu(s), 382 kJ mol^{-1}, and the Cu—Cu bond energy, 195 kJ mol^{-1}, respectively. Copper(II) sulfide on moderate heating forms copper(I) sulfide by the loss of sulfur [11]. Therefore, atomization from copper(I) sulfide seems reasonable. The existence of Cu_2(g) at higher temperature has been proposed [6].

In the argon—hydrogen atmosphere, two values, 326 and 163 kJ mol^{-1}, were also obtained corresponding to the heat of vaporization of Cu(s), 337 kJ mol^{-1}, and the Cu—Cu bond energy, respectively. Copper(I) sulfide is reduced by hydrogen to copper.

Silver. Two E_a values, 209 and 285 kJ mol^{-1}, were obtained for silver in argon and argon—hydrogen, respectively. The energy in the argon—hydrogen atmosphere correlates with the heat of vaporization of Ag(s), 284 kJ mol^{-1}. Silver sulfide is reduced to silver by hydrogen above 473 K [11]. Silver sulfide decomposes at higher temperatures (>1223 K). Therefore, dissociation of the sulfide may be proposed as the atomization process for silver in

an argon atmosphere, although the lack of a literature thermodynamic energy value precludes a more definite statement.

Conclusions

The experimental energy values provide information only about the major processes of atom formation during the initial stages of signal production. However, a broad picture of the atomization processes in the presence of thiourea can be obtained.

A linear relationship between the appearance temperature and the atomization energy of the analyte was observed for antimony, bismuth, copper and silver in argon—hydrogen. This is in agreement with the findings of Johnson et al. [12] who used a carbon filament atomizer. Sturgeon et al. [6] have also shown a linear correlation between atomization energy and appearance temperature for a carbon tube atomizer. The slope of the plot was 0.25 kJ mol^{-1}. This is in agreement with the published data [6, 12]. The data for sulfides in an argon atmosphere also gave a linear plot.

Thiourea is known to suppress matrix interferences, especially from alkali metal chlorides [3, 4]. To obtain information concerning the suppression of interferences for bismuth, cadmium and copper, the atomization processes for these elements in a sodium chloride matrix were studied. The activation energies obtained are given in Table 3. Similar values are obtained for bismuth and cadmium in the absence and presence of sodium chloride. A value for copper was obtained only in the higher temperature range. These values show that the chloride matrix has no effect on the atomization processes of bismuth, cadmium and copper, provided that thiourea is used. No reproducible values for E_a were obtained in the presence of chloride when thiourea was absent, because of the complex atomization profiles obtained under these conditions. Although the determination of activation energies confirms the suppression of chloride interference when thiourea is present, further experimental work is required to substantiate the similar suppression of interferences from various other elements.

TABLE 3

Appearance temperatures and activation energies in the presence of sodium chloride[a]

Element	T_{app} (K)	E_a (kJ mol^{-1})	Temperature range (K)
Bi	904	197	916—1327
Cd	785	222	835—915
Cu	1341	201	1526—1601

[a]480 ml Ar min^{-1}, 20 ml H_2 min^{-1}; 125 ng NaCl; thiourea and heating rates as in Table 1.

REFERENCES

1 K. Ohta and M. Suzuki, Anal. Chim. Acta, 96 (1978) 77.
2 K. Ohta and M. Suzuki, Talanta, 26 (1979) 207.
3 M. Suzuki, K. Ohta and T. Yamakita, Anal. Chem., 53 (1981) 9.
4 M. Suzuki and K. Ohta, Anal. Chem., 54 (1982) 1686.
5 M. Suzuki, K. Ohta and T. Yamakita, Anal. Chim. Acta, 133 (1981) 209.
6 R. E. Sturgeon, C. L. Chakrabarti and C. H. Langford, Anal. Chem., 48 (1976) 1792.
7 M. Suzuki, K. Ohta, T. Yamakita and T. Katsuno, Spectrochim. Acta, Part B, 36 (1981) 679.
8 B. Smets, Spectrochim. Acta, Part B, 35 (1980) 33.
9 J. W. Mellor, Comprehensive Treatise on Inorganic and Theoretical Chemistry, Vol. IX, Longmans, Green and Co., London, 1930, pp. 520, 686.
10 F. M. Faure, M. J. Mitchell and R. W. Bartlett, High Temp. Sci., (1972) 181; Chem. Abstr., 77 (1972) 282.
11 F. W. Abel, in J. C. Bailar, H. J. Emeleus, R. Nyholm and A. F. Trotman-Dickenson (Eds.), Comprehensive Inorganic Chemistry, Vol. 3, Pergamon, Oxford, 1973, pp. 268, 29, 79.
12 D. J. Johnson, B. L. Sharp, T. S. West and R. M. Dagnall, Anal. Chem., 47 (1975) 1234.

Analytica Chimica Acta, 151 (1983) 409—417
Elsevier Science Publishers B.V., Amsterdam — Printed in The Netherlands

DETERMINATION OF MAJOR, MINOR AND TRACE ELEMENTS IN BONE BY INDUCTIVELY-COUPLED PLASMA EMISSION SPECTROMETRY

HIMANSU S. MAHANTI[a] and RAMON M. BARNES*

Department of Chemistry, University of Massachusetts, GRC Towers, Amherst, MA 01003-0035 (U.S.A.)

(Received 20th October 1982)

SUMMARY

Inductively-coupled plasma emission spectrometry (i.c.p.e.s.) is applied to the measurement of the concentrations of twenty elements in human and animal bone (IAEA H-5) samples. Hydride and elemental generation i.c.p.e.s. are employed for the determination of arsenic, selenium and mercury, and electrothermal vaporization—i.c.p.e.s. is used for the verification of copper. For low concentration levels of eight elements (Cd, Cu, Co, Mo, Ni, Pb, Ti, V), a poly(dithiocarbamate) chelating resin provides a 30-fold preconcentration factor and separation from the matrix prior to the spectrometric measurement.

The concentrations of metals in bone, especially trace elements, can serve as useful indicators of dietary habits, nutrition, and disease [1], and common techniques used to quantify trace elements in bone include neutron activation, d.c. arc emission, and x-ray fluorescence spectrometry. Although inductively-coupled plasma atomic emission spectroscopy (i.c.p.e.s.) is becoming popular for biological materials [2—10], few reports include determinations in bone. The determination of trace elements in teeth and milk with i.c.p.e.s. was described by Kluckner et al. [11, 12], and Lee determined 11 elements in standard reference bone by i.c.p.e.s. [13]. Brätter et al. [14] included animal bone in a study of reference materials as i.c.p.e.s. calibration standards. Stedt [15] reported the i.c.p.e.s. results for bone from two prehistoric populations, and Price and Kavanagh [16] related i.c.p.e.s. bone compositional results to diet. Despite the excellent powers of detection obtained with i.c.p.e.s., limits exist in the determination of many trace elements in bone either because their concentrations lie below the lowest quantitatively determinable level or because the limits of detection for some elements are degraded by background shifts and stray light effects arising from major bone constituents. Matrix-matching standard solutions for bone require high-purity reagents, and the maximum concentration of samples and

[a]Present address: National Institute of Foundry and Forge Technology, Hatia, Ranchi-834003, India.

0003-2670/83/$03.00

solutions can be limited by the intolerance of some nebulizers for high levels of dissolved solids.

The poly(dithiocarbamate) resin [17] is an effective means for separation and concentration of numerous trace elements from complex matrices prior to quantitation by i.c.p.e.s. [9, 10, 18, 19]. Because the resin does not complex alkali and alkaline earth elements, the stray light and background effects observed in i.c.p.e.s. resulting from the presence of these elements at elevated concentrations are eliminated. Furthermore, solutions prepared from digested poly(dithiocarbamate) resin contain substantially lower total dissolved solids than the original matrix and are less susceptible to salt deposition in the nebulizer and torch.

The present report describes a procedure for the direct determination of major, minor, and trace element concentrations in bone by means of i.c.p.e.s., and of ultratrace element levels after preconcentration by the poly(dithiocarbamate) resin prior to introduction into the i.c.p. discharge.

EXPERIMENTAL

Apparatus and reagents

The i.c.p.e.s. instrumental facilities and operating conditions used are summarized in Table 1. Simplex optimization [20] was used to establish optimum operating conditions for each determination. The graphite rod used for electrothermal vaporization was coated first with pyrolytic graphite and then with tantalum [21].

Stock solutions were prepared from high-purity and reagent-grade metals or salts with distilled, deionized water and high-purity acids. The poly(dithiocarbamate) resin was synthesized as described earlier [9, 17]. Calcium solution and other reagents were purified by treatment with poly(dithiocarbamate) resin to minimize reagent blanks. Standard solutions were prepared by serial dilution of 1000 μg ml^{-1} stock solutions with distilled water, and the concentration of calcium in each reference solution was held constant.

Procedures

Sample preparation. Human bone samples were supplied by the Anthropology Department, University of Massachusetts, and the animal bone sample (International Atomic Energy Agency. IAEA H-5) was undergoing certification [22]. Powdered bone samples were first dried in an oven at 100° C for 2 h. Portions (1—3 g) of dried powdered bone sample were weighed into polytetrafluoroethylene (PTFE) beakers (100 ml), and 15 ml of concentrated nitric acid was added. The mixture was heated slowly on a hot plate. Hydrogen peroxide (30%) was added dropwise until all organic material was destroyed. Approximately 15—30 min was required for complete dissolution. After cooling, the solution was transferred to a 50-ml volumetric flask and diluted to volume with distilled water.

For As, Se, and Hg determinations in bone, hydride and elemental generation techniques [18] were used. For the arsenic and mercury determinations,

TABLE 1

Instrumentation and operating conditions

A. Instrumentation	
Generator	Plasma-Therm Model HFS-5000D, 40.68 MHz with 3-turn (1/8 in. copper) load coil
Nebulizer	Modified Babington [27] with double-barrel glass spray chamber and sample uptake of 1.2 ml min^{-1}
Plasma torch	Conventional 18 mm i.d. quartz with 1.5 mm i.d. injector orifice
Detection	Minuteman monochromator Model 310-SMP, 1-m Czerny-Turner with 1200 groove mm^{-1} grating. Slit widths 40—60 μm, slit heights 5 mm. 1:1 image formed by quartz lens (Oriel A-11-661-37). RCA 1P28 photomultiplier (—700 V), Keithley 411 picoammeter, Heath EU-201V log/linear recorder
Electrothermal vaporizer	Varian carbon rod atomizer (CRA-90) with laboratory fabricated graphite rod electrode and enclosed quartz chamber [21]
B. I.c.p.e.s. operating conditions	
Power, kW	0.70[a]
Outer gas flow, l min^{-1}	16
Intermediate gas flow, l min^{-1}	0
Aerosol flow rates, l min^{-1}	0.8[b]
Nebulizer back pressures, psig	23—26
Observation zone	5 mm × 50 μm from 13.5 to 18.5 mm above the induction coil[c]
C. Electrothermal vaporization—i.c.p.e.s. operating conditions	
Power, kW	0.55
Outer gas flow, l min^{-1}	16
Intermediate gas flow, l min^{-1}	1
Chamber flow rates, l min^{-1}	Inner 1.6, outer 4.6
Observation zone	As above
Monochromator slit widths, μm	50
Temperature	Drying 100°C for 10 s; ashing 200°C for 10 s; Vaporization 2100°C for 3 s after a heating rate of 800°C s^{-1}

[a]Except for Cu and Fe (0.8 kW), Na (0.6 kW), Ni (0.5 kW), P (0.9 kW), and Se (0.75 kW). [b]Except for Ca, P, and Zn at 0.9 l min^{-1} and As, Se, and Hg carrier gas flow of 0.5 l min^{-1} and auxiliary gas flow of 1 l min^{-1}. [c]Except for Ba, Co, Ni, and Sr (11.5—16.5 mm above the induction coil).

2 g of bone sample was dissolved slowly at 70°C by heating with concentrated nitric acid and hydrogen peroxide as described. The final solution volume was 5 ml. To a 1-ml aliquot of sample solution for each determination, 0.5 ml of concentrated hydrochloric acid and 0.5 ml of freshly prepared 2% sodium tetrahydroborate were added. For the arsenic determination, 0.1 ml of 10% potassium iodide solution was used. For the selenium determination, 2 ml of

concentrated hydrochloric acid were added, and the solution was slowly heated on a hot plate at 70°C. The final volume was 5 ml. A 1-ml aliquot of sample solution was used for the selenium determination, and 0.5 ml of concentrated hydrochloric acid and 0.5 ml of 2% sodium tetrahydroborate were added.

Poly(dithiocarbamate) resin treatment. Many of the trace elements in bone can be quantitatively separated and concentrated at a pH of about 5 by using the poly(dithiocarbamate) resin [9, 10, 18, 19, 23]. A 3-g bone sample was dissolved as described, 120 ml of 0.2 M EDTA, purified earlier with the resin, was added, and the pH was adjusted to 5 with ammonia solution. The solution was passed through a column containing 80 mg of 70—80 mesh resin at 1 ml min^{-1}. After washing, the resin was digested with hydrogen peroxide (30%) and 2 ml of concentrated nitric acid by heating slowly on a hot plate. Dilute (3 + 1) nitric acid was added to obtain a final volume of 5 ml. The concentrations of trace elements were quantified by using acid-matched calibration standards. A concentration factor of 30 was obtained beginning with a 150-ml sample solution.

Copper determination. Copper was determined in both the sample solution and resin digested solution by using an electrothermal vaporization i.c.p. arrangement [21]. A 5-μl aliquot of sample solution was placed into the graphite electrode, and the copper emission from the plasma was measured. Intensities of standard copper solutions containing matched calcium or acid concentrations were also measured.

Spectral line selection. Wavelengths for quantitation (Table 2) were selected from the available lists of prominent i.c.p.e.s. lines [24, 25]. Background equivalent concentrations (BEC) and spectral interferences, expressed as the interference equivalent concentration values (IEC) and corresponding to the analyte concentration equivalent to an interference, were established experimentally from intensity values of 1 mg ml^{-1} of a test solution and 0.2 mg ml^{-1} sodium and magnesium and 5.4 mg ml^{-1} calcium corresponding to the approximate concentrations of these matrix elements in bone. Because reagent-grade calcium salts contain appreciable concentrations of Ba, Mg, Na, and Sr, evaluation and correction for the reagent blank level was necessary.

RESULTS AND DISCUSSION

Quantitative performance

The i.c.p.e.s. limits of detection and background equivalent concentrations (BEC) were determined with reference solutions containing calcium (Table 2). Although these values are comparable to other reported i.c.p.e.s. detection limits [24, 26], they were insufficient for the determination of all trace metals in bone. Preconcentration with the poly(dithiocarbamate) resin provided 30-fold improvement in detection limit, and the 30-fold improvement in the lowest quantitatively determinable concentration (LQD = 5 times the limit of detection or 15 times the standard deviation of the background)

TABLE 2

Wavelengths and figures of merit[a]

Wavelength (nm)	Detection limit (ng ml^{-1})	IEC (mg l^{-1})	BEC (mg l^{-1})	LQD bone ($\mu g\ g^{-1}$)
Al 236.705	50	0.02	1.6	12.5
Ba 455.40	0.6	0.014	0.02	0.15
Ca 422.67	7	—	0.20	1.75
Cd 228.80	2	0.12	0.10	0.5 (0.0165)[b]
Cu 324.75	6	0.06	0.26	1.5 (0.05)
Co 345.35	10	0.06	0.35	2.5 (0.083)
Fe 259.94	6	0.12	0.26	1.5
Mg 279.55	0.5	0.10	0.12	0.125
Mn 257.61	2.8	0.04	0.13	0.7
Mo 202.03	10	0.08	0.40	2.5 (0.083)
Na 588.995	11		0.46	2.75
Ni 341.45	12	0.06	0.44	3 (0.10)
P 214.91	150	3.0	5.0	37.5
Pb 220.35	100	3.0	4.0	2.5 (0.833)
Sr 407.77	0.8	0.014	0.03	0.2
Ti 334.94	4		0.22	1.0 (0.033)
V 292.4	10	0.03	0.4	2.5 (0.083)
Zn 213.86	9	0.12	0.42	2.25
As 193.69[c]	1		0.04	0.0125
Se 196.02[c]	1		0.04	0.0125
Hg 253.65[d]	0.5		0.02	0.006

[a]Detection limit in a calcium solution equivalent to a 2% bone solution is defined as the concentration giving a signal equal to three times the standard deviation of the background. The interference equivalent concentration (IEC) is the equivalent concentration at each element wavelength corresponding to the spectral interference from a 5400 mg l^{-1} Ca solution. The background equivalent concentration (BEC) is the analyte concentration equivalent of the background level at the analyte wavelength. LQD is the lowest quantitatively determinable concentration calculated from five times the limit of detection with a 1-g sample dissolved in 50 ml. Values in parentheses are the LQD values for a 3-g bone sample in a final volume of 5 ml after resin preconcentration. For As and Se by hydride generation and Hg by elemental Hg generation, LQD is calculated for a 2-g sample in 5 ml of solution. [b]With poly(dithiocarbamate) resin preconcentration. [c]With hydride generation. [d]With elemental Hg generation.

values is indicated in Table 2. The major spectral IEC values (Table 2) resulted from calcium, and the IEC values for sodium and magnesium at 0.2 mg ml^{-1} were negligible. Because calcium was the major source of spectral interference, purified calcium was added to reference solutions to match the sample calcium concentrations. The purification procedure is described elsewhere [28].

Analysis of bone

Results for the direct determination of 15 elements and the determination of 8 elements after resin preconcentration in animal and human bone are

summarized in Tables 3 and 4. The values are means for three determinations, and the relative standard deviations range from one to several percent. The preliminary mean values reported for the International Atomic Energy Agency (IAEA H-5) bone sample are also included for comparison.

For these determinations, the digestion procedure is rapid and provides complete dissolution. Preparation of 1 g of bone sample in a final volume of 50 ml results in 4.7—5.4 mg Ca ml^{-1}, which causes a change in spectral background. Based on the spectral IEC values (Table 2), the most sensitive lines can be used for all elements except aluminum. The aluminum line at 396.15 nm is affected strongly by the nearby calcium emission, and an alternative wavelength (236.705 nm) was substituted. Matrix matching for the determination of barium and strontium could not be applied owing to the high blank levels in the calcium reagent available. A background-correction procedure was applied instead. Calibration data were generally linear over the concentration range 0.1—400 mg ml^{-1}.

The poly(dithiocarbamate) resin does not complex Ca, Mg, Na, and K whereas it strongly complexes Cd, Cu, Mo, Ni, Pb, Ti, and V at pH 5. The concentrations of these elements determined by the resin preconcentration treatment in animal and human bone samples are given in Table 4. Recoveries from human bone samples spiked with the above elements were quantitative at the 5—27 μg level (Table 5).

The concentrations of arsenic, selenium and mercury in bone samples could not be measured directly by using pneumatic nebulization, but the generation of arsenic and selenium hydrides and elemental mercury directly

TABLE 3

Quantitative results for bone, given as $\mu g\ g^{-1}$ except where specified

Element	Animal bone (IAEA H-5)		Human bone
	Standard	Found[a]	Found[a]
Ca	21.17 ± 2.4	23.7 ± 0.3%[b]	27.1 ± 0.3%[b]
P	9.578 ± 4.43	11.0 ± 0.2%[b]	13.8 ± 0.2%[b]
Mg	0.353 ± 0.0025	0.312 ± 0.004%[b]	0.226 ± 0.004%[b]
Na	0.477 ± 0.097	0.455 ± 0.005%[b]	1.066 ± 0.02%[b]
Sr	104.85 ± 17.61	91 ± 1	149 ± 2
Fe	80.65 ± 11.00	66.1 ± 0.7	29.4 ± 0.6
Zn	89.91 ± 15.39	76.7 ± 0.9	102.0 ± 1
Ba	71.63 ± 28.09	68.6 ± 0.8	21.0 ± 0.4
Al	101.12 ± 63.56	30.1 ± 0.4	42.9 ± 0.8
Mn	0.76 ± 0.24	0.99 ± 0.03	1.56 ± 0.08
Pb	2.97 ± 1.08	—[c]	25.0 ± 2
As	0.0135 ± 0.0021	0.015 ± 0.0005	0.011 ± 0.0005
Se	0.0537 ± 0.0127	0.068 ± 0.001	0.101 ± 0.002
Hg	0.0080 ± 0.0055	0.011 ± 0.0003	0.012 ± 0.0003

[a]Standard deviation for triplicate samples. [b]With 0.1% bone. [c]Present below the limit of detection.

TABLE 4

Quantitative results for bone after preconcentration on poly(dithiocarbamate) resin ($\mu g\ g^{-1}$)

Element	Animal bone (IAEA H-5)		Human bone
	Standard	Found	Found
Cu	0.64 ± 0.33	0.30 ± 0.01	1.0 ± 0.03
Pb	2.97 ± 1.08	3.0 ± 0.05	22.4 ± 0.4
Ni	1.51 ± 0.76	0.60 ± 0.01	2.1 ± 0.02
Co	0.25 ± 0.14	0.47 ± 0.01	0.4 ± 0.01
Ti	no mean	0.20 ± 0.01	0.5 ± 0.01
V	1.19 ± 1.02	0.22 ± 0.01	1.1 ± 0.03
Mo	0.45 ± 0.39	1.0 ± 0.03	—[a]
Cd	0.0229 ± 0.0160	0.054 ± 0.002	—[a]

[a]Not determined.

TABLE 5

Recovery of elements from human bone with poly(dithiocarbamate) resin[a]

Element	Amount added (μg)	Final amount (μg)		Recovery (%)
		Expected	Measured	
Cu	5	6.0	6.1 ± 0.1	101.6
Ni	5	7.1	6.8 ± 0.1	95.8
Pb	5	27.4	26.5 ± 0.5	96.7
V	5	6.1	6.0 ± 0.1	98.4
Co	5	5.4	5.2 ± 0.1	96.3
Ti	5	5.5	5.3 ± 0.1	96.4

[a]Mean of three replicates.

into the i.c.p. extended the LQD values in bone samples. No losses during sample preparation occurred, and no interferences from other elements in the bone were observed (Table 5) as indicated by the similarity of the present and reported values for the IAEA H-5 sample. Quantitative recovery was obtained on addition of standard amounts of these elements to bone samples prior to dissolution.

The i.c.p.e.s. determination of major, minor, and trace elements in human bone and animal bone (IAEA H-5) reference material gave satisfactory results (Table 3). The calcium concentration in human bone was also established by conventional EDTA titration (26.9 ± 0.05%) and compared well with the 27.1% measured by i.c.p.e.s. Preconcentration of Cd, Cu, Co, Mo, Ni, Pb, Ti and V by means of the poly(dithiocarbamate) resin before i.c.p.e.s. determinations provided concentration values (Table 4) within the range of preliminary data reported as a part of the ongoing certification program [22]. Lead was determined by both methods in human bone, and the reproducibility

was improved as a result of the 30-fold preconcentration provided by the resin technique. Within experimental error, the values are the same. The Fe, Al, and Se concentrations reported in Table 3 and the Cd, Co, Mo, and Ni concentrations in Table 4 fell within the range of preliminary certification data provided by the IAEA but outside the standard deviation of the means given. Extension of these procedures to other trace elements complexed by the poly(dithiocarbamate) resin is underway.

Copper by electrothermal vaporization

Copper was quantified by the electrothermal vaporization—i.c.p. method directly in bone solution as well as after preconcentration with the resin. The presence of high calcium concentrations in the bone solution increased the copper intensity, and matrix matching was required. The detection limit was 5 pg for single-element standard solution [21] and 20 pg in the presence of calcium. By direct electrothermal vaporization—i.c.p.e.s. of the bone solution, 1.2 ± 0.2 μg Cu g^{-1} was observed in human bone, whereas 1.1 ± 0.2 μg Cu g^{-1} was measured by the same technique after separation and preconcentration with the poly(dithiocarbamate) resin. These values compare well with the copper result in Table 4. The extension of this technique for quantifying elements in autopsy bone samples is underway.

This research was supported by Department of Energy contract DE-AC02-77EV-0432 and by Grant No. 5 R01 OH 01085-2, awarded by the National Institute for Occupational Safety and Health.

REFERENCES

1 E. A. Eads and M. J. Nicar, Trace Metals in Bone, 8th Int. Symp. Trace Anal., Geneva, Switzerland, 1978.
2 R. L. Dahlquist and J. W. Knoll, Appl. Spectrosc., 32 (1978) 1.
3 R. C. Munter, R. A. Grande and P. C. Ahn, ICP Inform. Newsl., 5 (1979) 368.
4 J. B. Jones, Comm. Soil Sci. Plant Anal., 8 (1977) 349.
5 J. W. Jones, S. G. Capar and T. C. O'Haver, Analyst, 107 (1982) 353.
6 J. B. Jones, Jr., in R. Barnes (Ed.), Developments in Atomic Plasma Spectrochemical Analysis, Heyden, London, 1981, p. 644.
7 R. C. Munter and R. A. Grande, in R. Barnes (Ed.), Developments in Atomic Plasma Spectrochemical Analysis, Heyden, London, 1981, p. 653.
8 N. R. McQuaker, D. F. Brown and P. D. Kluckner, Anal. Chem., 51 (1979) 1082.
9 R. M. Barnes and J. S. Genna, Anal. Chem., 51 (1979) 1065.
10 R. M. Barnes, P. Fodor, K. Inagaki and M. Fodor, Spectrochim. Acta, Part B, 38 (1983) 245.
11 P. D. Kluckner and D. F. Brown, in R. Barnes (Ed.), Developments in Atomic Plasma Spectrochemical Analysis, Heyden, London, 1981, p. 713.
12 P. D. Kluckner, D. F. Brown and R. Sylvester, in R. Barnes (Ed.), Developments in Atomic Plasma Spectrochemical Analysis, Heyden, London, 1981, p. 681.
13 J. Lee, ICP Inform. Newsl., 8 (1983) 553.
14 P. Brätter, K. P. Berthold and P. E. Gardiner, Spectrochim. Acta, Part B, 38 (1983) 221.
15 P. G. Stedt, Trace Element Analysis of Two Prehistoric Populations, The Fremont and the Anasazi, Ph.D. Dissertation, San Diego State University, San Diego, CA, 1979.

16 T. D. Price and M. Kavanagh, Mid-Continent J. Archaeol., 7 (1982) 61.
17 D. S. Hackett and S. Siggia, in G. W. Ewing (Ed.), Environmental Analysis, Academic Press, New York, 1977, p. 253.
18 P. Fodor and R. M. Barnes, Spectrochim. Acta, Part B, 38 (1983) 229.
19 Zhuang Mianzhi and R. M. Barnes, Spectrochim. Acta, Part B, 38 (1983) 259.
20 M. Cave, R. M. Barnes and P. Denzer, 1982 Winter Conf. Plasma Spectrochem., Orlando, FL; ICP Inform. Newsl., Amherst, MA, 1982, Abstr. 23.
21 R. M. Barnes and P. Fodor, Spectrochim. Acta, Part B, 38 (1983) in press.
22 Progress Rep. No. 1, Intercomparison of Minor and Trace Elements in IAEA Animal Bone (H-5), International Atomic Energy Agency, Vienna, 1982.
23 A. Miyazaki and R. M. Barnes, Anal. Chem., 53 (1981) 299, 364.
24 R. K. Winge, V. J. Peterson and V. A. Fassel, Appl. Spectrosc., 33 (1979) 206.
25 P. W. J. M. Boumans, Line Coincidence Tables for Inductively Coupled Plasma Atomic Emission Spectrometry, Vols. 1 and 2, Pergamon Press, Oxford, 1980.
26 P. W. J. M. Boumans and R. M. Barnes, ICP Inform. Newsl., 3 (1978) 445.
27 L. Ebdon and M. R. Cave, Analyst, 107 (1982) 172.
28 H. S. Mahanti and R. M. Barnes, Appl. Spectrosc., 37 (1983) in press.

Analytica Chimica Acta, 151 (1983) 419—431
Elsevier Science Publishers B.V., Amsterdam — Printed in The Netherlands

THE USE OF FAST FOURIER TRANSFORMATION IN INFORMATION SYSTEMS BASED ON INFRARED SPECTROSCOPY[a]

M. NOVIČ* and J. ZUPAN
Boris Kidrič Institute of Chemistry, Ljubljana (Yugoslavia)
(Received 20th October 1982)

SUMMARY

The fast Fourier transform algorithm is applied to a collection of infrared spectra and the advantages of transformed spectra are discussed in detail. The truncation of the transformed spectra permits a reduction of the computer space needed for the storage of the data collection, and greatly accelerates the computer manipulation of full curve spectra. The latter aspect is particularly important in analysis of mixtures where the identification of components from the spectrum of the unknown mixture is based on "distance" or similarity calculations between the original spectrum of the mixture and any of the possible combination of components. Special emphasis in this calculation was given to the quantitative estimation of the ratio of components in the mixture. Some examples of the procedure for the analysis of mixtures from a collection of 104 infrared spectra of surfactants are discussed in detail.

Infrared spectroscopy is a very powerful tool for identification of compounds in analytical chemistry. The best identification results are obtained when the full spectral curves are compared, so that a very large number of reference spectra must be available at any time. In the past thirty years, infrared spectra have been collected extensively and different data bases have been formed; these vary from general large and bulky libraries [1—3] to very specialized small ones (see, e.g., [4—7]). Some twenty years ago, computers began to replace the manual searching procedure. The main problem then, which has still not been solved satisfactorily, was how to encode the infrared spectra. Initially, only the band positions were coded in the form of large bit strings [8, 9]. For positive identification of compounds, this is inadequate, because too much information about the structure is lost by omitting the intensities and band shapes. Later, the peak intensities were added to peak positions [10] and some systems try to simulate the complete spectrum curve from more parameters per peak [11]. Unfortunately, the determination of the additional parameters is quite complicated and uncertain, which makes the methods convenient only for small collections of data. Today, as most

[a]This paper was presented in part at the International Conference on Biochemical and Instrumental Analysis, Munich, 1982.

0003-2670/83/$03.00

instruments have digital outputs and can easily be linked to computers, the main problem is not the input of data to the computer but the storage and handling procedure for the thousands of spectra needed as reference data.

The present paper describes an attempt to solve both problems (storage requirement and fast handling) simultaneously through representation of the spectra by truncated sets of Fourier coefficients. Not only does the truncated set of Fourier coefficients reduce the amount of the computer space necessary for storing each spectrum, it also guarantees a very acceptable reproduction of the original curve which is essential for the final visual comparison of the retrieved spectrum with the input spectrum. An additional goal, besides those mentioned, was to establish a quantitative procedure for determination of the component ratio in the spectrum of an unknown mixture.

METHODS

Fourier transformation as a means of condensing spectra

In the present work, the digitized spectra of two origins were used: first, a manually digitized collection of more than 700 infrared spectra [12] and second, a small dedicated collection of 104 surfactant compounds, 28 of which were recorded on a Perkin-Elmer 180 spectrophotometer linked to a PDP 11/34 computer, while the rest was carefully selected from the larger collection [12] mentioned above. The first collection was used to test the general performance of the contracted spectra, while the second was applied in the program for mixture analysis. Both types of spectra could be transformed to be internally equivalent, so that the program for mixture analysis finds zero difference between the spectra of the same compound from different sources.

Little need be said about the generation of the first collection of infrared spectra. The method used for the digitization and the accompanying software has been explained and discussed in detail [11, 12]. Each spectrum recorded on the Perkin-Elmer spectrophotometer in the range 4000—200 cm^{-1} consists of 3800 intensity values at 1 cm^{-1} intervals, requiring more than 7000 bytes for storage of the entire curve. This adds up to 2.5 Mbytes (one disk cartridge) for just over 300 spectra. This is certainly not acceptable, especially for a minicomputer system that is supposed to be in the laboratory and connected to at least one instrument while offering as much as possible of the supporting applicative software, including data collection.

In the present approach, the spectra were reduced to 512 points. On the 512 points the FFT (fast Fourier transform) algorithm [13] was applied and as a result 512 complex Fourier coefficients (FCs) were obtained for each spectrum. A trial-and-error procedure was used to establish the best trade-off between the storage requirement and the reproduction ability. It was decided to use only the first 80 FCs to represent the whole spectrum. This decision was based on the results shown in Fig. 1. The differences (dis-

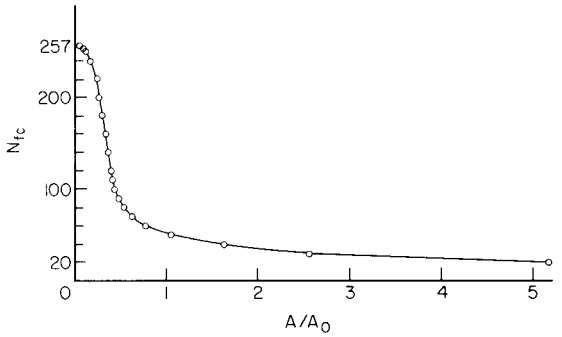

Fig. 1. The effect of the number of Fourier coefficients (N_{fc}) on the quality of the reproduced spectra. The quality is represented as A/A_0, where A is the sum of absolute differences between the original and reproduced spectrum while A_0 is the sum of the intensity values of the original one.

tances) between the original and reproduced spectra increase more quickly if less than 80 FCs are used for the reproduction, while more than 100 FCs does not improve the reproduced spectrum very significantly.

In order to show the influence of the number of FCs used for reproduction of the infrared spectra, three spectra are reproduced in Fig. 2, using three different sets of FCs. The reproduction based on only the first 80 complex FCs was good enough (Fig. 2c), while the necessary computer storage space was reduced by more than two thirds (512/160). A simple linear reduction of the entire spectral region from 1800 to 80 or any other number of digitized points would also linearly reduce the content of information, e.g., by providing shifted and reduced maximal intensities or even loss of single peaks. By using the reduction of FCs where most of the information about the shape of the entire curve (number and intensity of peaks) is mainly stored in the first coefficients, the reduction is not linear (see Fig. 1).

The omission of 432 high-order FCs from the original 512 FCs, (Fig. 2c) influences the quality of the spectra in two ways: first, small waves are superimposed over the "flat" regions with no absorption bands; secondly, the resolution is diminished. The first problem (small waves) could be eliminated if the FCs were truncated by a wedge-shaped function, but the second problem (resolution) would then be even worse. Additionally, the second problem is more serious than the first, because narrow bands are broadened: two narrow bands separated by less than 9 cm^{-1} merge into one if the spectrum is reproduced by 80 FCs. Fortunately, in the entire test collection of 740 spectra only 10 spectra had peaks so close together and none were found in the small collection of surfactants.

Although the application of the FFT to a large collection is still a time-consuming operation, it is necessary only once for each spectrum, thus the investment of time for such preprocessing of spectra is more than repaid by the computer storage gain and the good performance of the system.

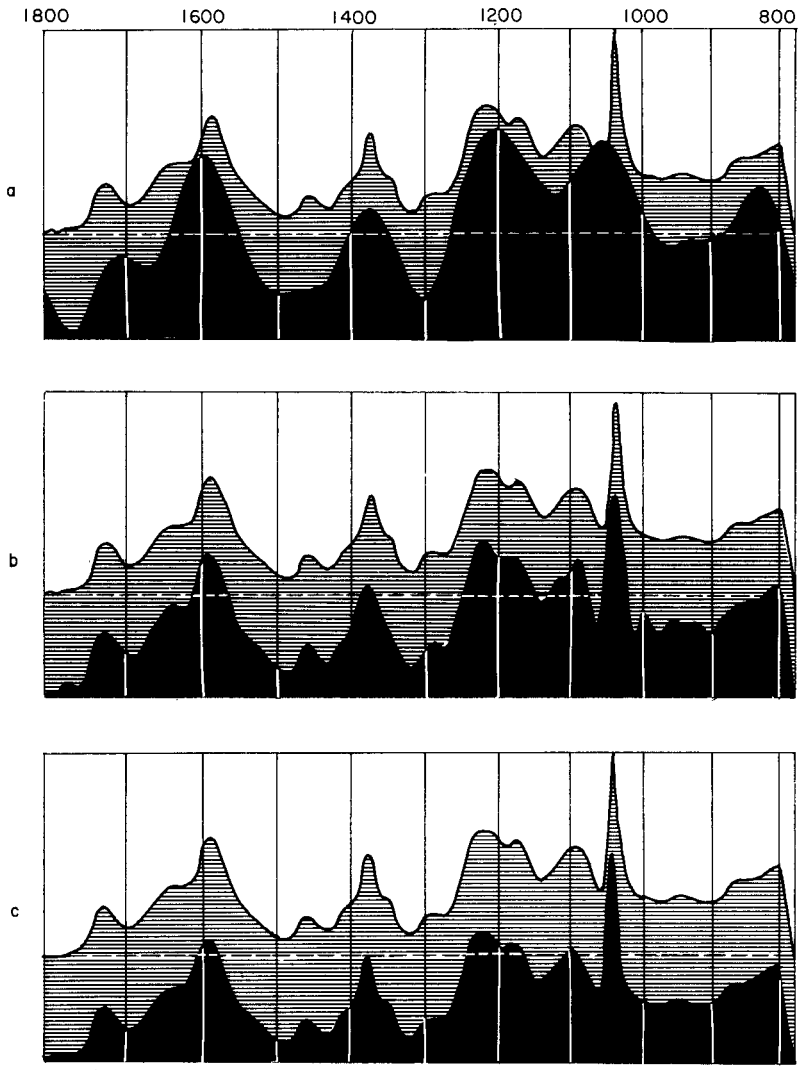

Fig. 2. Comparison of the digitized spectrum (upper curves) with the spectra reproduced by using (a) 10, (b) 30, (c) 80 complex Fourier coefficients. With increasing number of FCs used for the reproduction, the resolution is improved and the peaks superimposed on the "flat" spectral regions tend to disappear.

Library search

A very important reason for contraction of the original spectral curves was the intention to build up a retrieval system based on full-curve comparisons. Library searches are mainly designed to use inverted files [14], which makes them much faster than sequential searches. There are two main problems with point-by-point calculations of distances between the query and all reference spectra. First, the storage space needed for even modest

data collection is much larger than for an inverted file containing only peak positions and the identification numbers of spectra. Secondly, access to each spectrum (the collection cannot reside in direct memory) together with the computational effort needed to evaluate the distances between the query and reference spectra are prohibitively time-consuming for on-line computer handling.

In order to avoid, or at least minimize, both effects, a new method for hierarchical clustering of infrared spectra was recently discussed in detail [15]. The most outstanding property of a binary hierarchical tree is that the object (the spectrum) at the end of any branch of the tree can be reached in approximately $\log_2 N$ steps if the tree is nearly balanced. To utilize this property, a hierarchical tree was generated from the 500 spectra (each represented by 80 complex FCs) from the described collection. All spectra were initially recorded from 4000 to 200 cm^{-1}.

Besides the 100% retrieval ability of the tree, the average path was only 12 vertices long which means that only 12 comparisons (on average) are needed to retrieve any of the 500 spectra. The minimal and maximal paths in the tree (the best and worst cases for retrieval) are 3 and 20 vertices long, respectively. The calculation of only 12 distances between two "spectra" represented in 160-dimensional space is clearly a considerable improvement over the standard sequential point-by-point comparison.

Where retrieval from the tree is concerned, the compression of the spectral curve is not essential because the number of comparisons is proportional to the logarithm of the number of spectra in the tree. However, the generation of the tree is much more time-consuming and would not be economical with spectra represented by, say, a few thousand points. The problems in the generation of the hierarchical tree of 500 spectra have been discussed recently [16].

Analysis of mixtures

For the analysis of mixtures, a special collection of i.r. spectra was selected, simply because of the frequent need in this laboratory for quantitative interpretation of surface-active mixtures like soaps, shampoos, and other detergents. However, for quantitative analysis, only those spectra from the collection recorded in this laboratory are used; spectra selected from other collections do not give correct quantitative results because they cannot be satisfactorily normalized. Difficulties concerning the transmittance measurements in aqueous solution, including the measurement of liquid cell length, were circumvented by using the attenuated total reflection (a.t.r.) method [17].

The most important chemical classes of substances that belong to different types of surfactants from the collection in the study are listed in Table 1. The spectra used for the analysis of mixtures were digitized at 2 cm^{-1} intervals in the region 1800—776 cm^{-1}, i.e., the fingerprint region of the spectrum which contains most of the structural information.

TABLE 1

Chemical classes of four types of surface-active substances

Type and number of compounds	Chemical class
Anionic 55	Carboxylic acids, salts Sulfonic acids, salts Sulfuric acid esters, salts Phosphate esters, salts
Nonionic 15	Polyoxyethylene adducts ethoxylated alkylphenols, ethoxylated aliphatic alcohols, ethoxylated glycerol esters, ethoxylated polyol (sorbitol, pentaerythritol, etc.) esters, ethoxylated fatty acids Fatty acid amides Alkylene oxide block copolymers
Cationic 25	Aliphatic mono-, di-, and polyamines Amine oxides and substituted amines Quaternary ammonium salts
Amphoteric 9	Amino and carboxyl groups on the same molecule Amino and sulfuric ester groups Amino and alkane sulfonic acid Amino and aromatic sulfonic acid

In a general procedure, several steps are needed to unify the spectral curves. The consecutive steps can be defined as follows:
(a) recording the spectrum and transferring it to the computer;
(b) transformation from transmittance to absorbance if necessary;
(c) subtraction of the baseline which is normally the spectrum of the empty cell, though for aqueous solutions the spectrum of pure water is treated as the baseline;
(d) smoothing;
(e) storing the spectrum into the predefined random-accessible file (this step is normally used only in building up the collection and not for a single entry input, e.g., in the case of an unknown sample).

All these steps are implemented in the system as separate, interactive programs monitored by a command file under the operating system RSX 11M. The use of the command file is shown in Fig. 3. Linking of several independent programs, as shown in Fig. 3, by means of the command file, gives the user great flexibility in handling the spectra as well as the opportunity of adding and modifying the existing programs. Additionally, this concept utilizes the small storage (112K words) and timesharing environment of a minicomputer more efficiently than large programs which cause many unpleasant delays, especially to other users. The above reasoning led to the implementation of the entire procedure in the manner of a command file rather than to merge all programs in one big package. Any of the implemented procedures

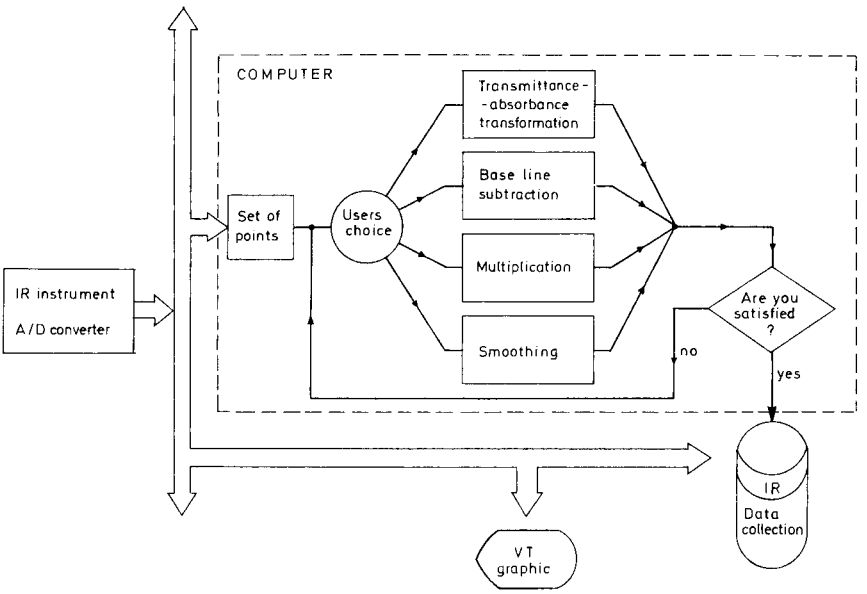

Fig. 3. Various possibilities for handling the i.r. spectra are enabled by use of the command file that connects different programs. When the spectrum is recorded and transferred to the computer, it can be treated by any of the programs shown before storage in the main data collection.

may be skipped or repeated on the old (or the new) file if the result of the previous processing is not satisfactory.

It is worthwhile noting that the concept of the search system, particularly for the analysis of mixtures [18—23], is strongly dependent on the method of encoding the data collection. Once the format of spectra for storage, reproduction and manipulation has been established, the program for analysis of mixtures can be designed. The flow chart for the analysis of mixtures implemented in the program is shown in Figs. 4 and 5.

The first part of the procedure (Fig. 4) selects all possible components from the main data collection. This is done by sequential comparison of the spectrum of the mixture with a very compressed "mask-file". In this abbreviated file, each spectrum from the main collection is represented by a 660-bit string (42 words) where only the strongest peaks (relative intensities 80—100% in the absorbance scale) are coded as ones. Because rather broad tolerance should be taken into account at both ends of each no-band region, even shorter bit strings could be used to represent each spectrum. If one bit is used to represent a 10 cm^{-1} interval, which is considered as the upper limit for such a fast screen, the entire fingerprint region could be covered by 132 bits or 9 words. The spectra in the mask-file are sequentially matched to the no-band regions of the spectrum of the mixture (represented in the same way): the spectra that do not have any strong peak in these no-band regions are put on the "good list" as possible components. From the entire collec-

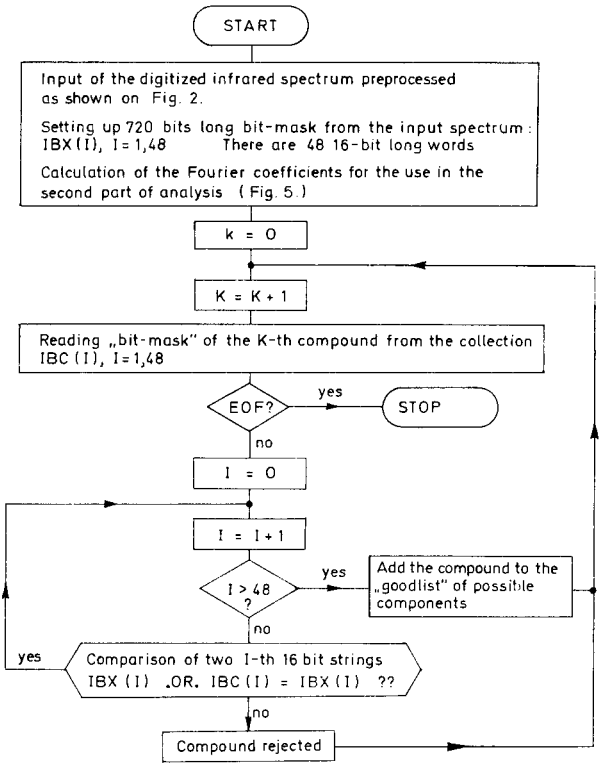

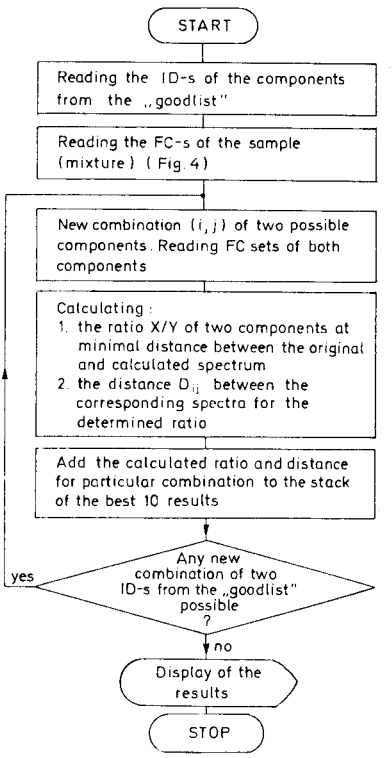

Fig. 4. The flow chart of the first part of the program for mixture analysis: determination of the possible components by comparison of the mask-files and their transference to the "good list".

Fig. 5. The flow chart of the second part of the program for mixture analysis: determination of the best combinations of two components based on the determination of the smallest distance between the original mixture spectrum and the calculated possible combination.

tion, all potential components of the unknown mixture can be selected very quickly by applying logical operations between the corresponding bits in the mask-file and in the spectrum of the mixture. No component on the "good list" has any strong absorption band in the regions where the mixture does not absorb. As a rule, the mask-file is generated or updated simultaneously with the main data collection. The only purpose of this file is to speed up the selection of all possible components; selection can become time-consuming as a collection is built up.

The second part of the program for mixture analysis (Fig. 5) looks for the combination of two spectra from the "good list" that best resembles the original spectrum. The criterion for the resemblance of two spectra i and j is the Euclidian distance D_{MC} between the vectors representing these two spectra by the truncated set of complex FCs:

$$D_{MC} = [\sum_k (M_k - C_{ijk})\,(M_k^* - C_{ijk}^*)]^{1/2} \quad (1)$$

where M_k and C_{ijk} are kth FCs of the mixture and of the combination of two spectra S_i and S_j, respectively:

$$C_{ijk} = x\,S_{ik} + y\,S_{jk} \quad (2)$$

The summation in Eqn. (1) runs from 1 to N, where N is the number of stored FCs. In Eqn. (2) both parameters x and y (determining the mixture ratio) must be adjusted for D_{MC} to be minimal. In fact, the distance should be zero at the minimum, if the Beer–Lambert law (which is introduced by Eqn. (2)) is valid over the whole spectral region and if there are no experimental errors and interactions between the components. In practice, however, the distance is always slightly larger than zero. In order to find the minimal value of D_{MC}, the first partial derivatives have to be calculated for each combination:

$$x \sum_k S_{ik}S_{ik}^* - 1/2 \sum_k (M_k S_{ik}^* + M_k^* S_{ik}) + 1/2\,y \sum_k (S_{ik}S_{jk}^* + S_{ik}^* S_{jk}) = 0 \quad (3)$$

$$y \sum_k S_{jk}S_{jk}^* - 1/2 \sum_k (M_k S_{jk}^* + M_k^* S_{jk}) + 1/2\,x \sum_k (S_{ik}S_{jk}^* + S_{ik}^* S_{jk}) = 0 \quad (4)$$

The smallest D_{MC} found in the calculations for all possible combinations of two components from the "good list" indicates the best resemblance between the spectrum of the original mixture and the spectrum calculated from two components that can be found in the "good list". The first partial derivatives also yield the proportion x/y in which the two components are mixed.

RESULTS AND DISCUSSION

In order to discuss the advantages, limitations and problems of the described method, three examples of "unknown" mixtures treated by the program will be discussed in detail. The results obtained by the computer, as well as the actual data for the "unknown" mixtures (prepared in the laboratory), are given in Table 2. As can be seen, the system found proper combinations of both components in all three cases. However, the quantitative estimate of the ratio in which both components are mixed is still far from being good, particularly for test 3 (Fig. 6c). The problem is that the distance values calculated between different components (i.e., different mixtures) are not easily comparable. The cause is that the components are aqueous solutions of surfactants. Different concentrations of the same component in water yield different intensities of the same absorption bands. The order to make the distance D_{ix}^{calc} between the original mixture spectrum x and the calculated spectra i comparable, the following normalization was used:

$$D_{ix}^{norm} = D_{ix}^{calc}/(\max_i - \min_i)$$

TABLE 2

Three examples of the analysis of mixtures. The distances D were calculated from Eqn. (1)

Test No.	Mixture[a]		All possible components	First 3 from the top list		
	IDs	Ratio		IDs	Ratio	Distance D
1	10, 9	60:40	6, 9, 10, 13, 23, 25, 27	10, 9	61:39	2.63
				25, 1	56:44	4.08
				27, 10	61:39	4.67
2	16, 28	70:30	6, 9, 13, 16, 17, 18, 19, 20, 21, 23, 28, 37	16, 28	63:37	10.32
				13, 28	56:44	10.43
				13, 18	56:44	11.18
3	2, 24	80:20	2, 7, 8, 9, 13, 16, 23, 24, 43, 55, 75	2, 24	66:34	6.87
				2, 9	59:41	7.60
				9, 24	60:40	7.85

[a]These mixtures correspond to the spectra shown in Fig. 6(a—c).

where $\max_i$ and $\min_i$ are the maximal and minimal intensity values, respectively, in the entire region of the calculated spectrum. The normalization eliminates the effect of the different maximal intensities appearing in the different spectra of the components used for calculation of the predicted mixture.

Table 3 shows that the normalized distance D_{ix}^{norm} between the spectrum of the real mixture and the calculated best-hit spectrum is much more in line with the reliability of the quantitative ratio of components than the distance D. Unfortunately, this normalization of the calculated distances give only a measure of the reliability of the calculated results; it does not improve the results themselves. The main source of error had already been introduced in the preprocessing step, after all the spectra of possible components (the entire collection) had been "standardized" by subtracting the spectrum of pure water. Although this preprocessing is necessary in order to achieve reasonable quantitative work, it still leaves the "standardized" spectra with baselines of quite different shape (curvature). The effect of different baselines is necessarily reflected in the calculated spectrum of the mixture (unless it is compensated by two component spectra having complementary baselines); this is clearly seen in the sequence of Fig. 6(a—c). In the first case (Fig. 6a) where the two spectra (original and calculated) are almost parallel, the calculated and true ratios (Table 3) agree very well, whereas in the third case (Fig. 6c), where the divergence of baselines in the region 1200—800 cm^{-1} is evident, the quantitative estimation of the ratio is considerably worse.

CONCLUSION

The representation of full-curve infrared spectra by 80 complex FCs not only provides large storage savings but also enables inter-spectra comparisons

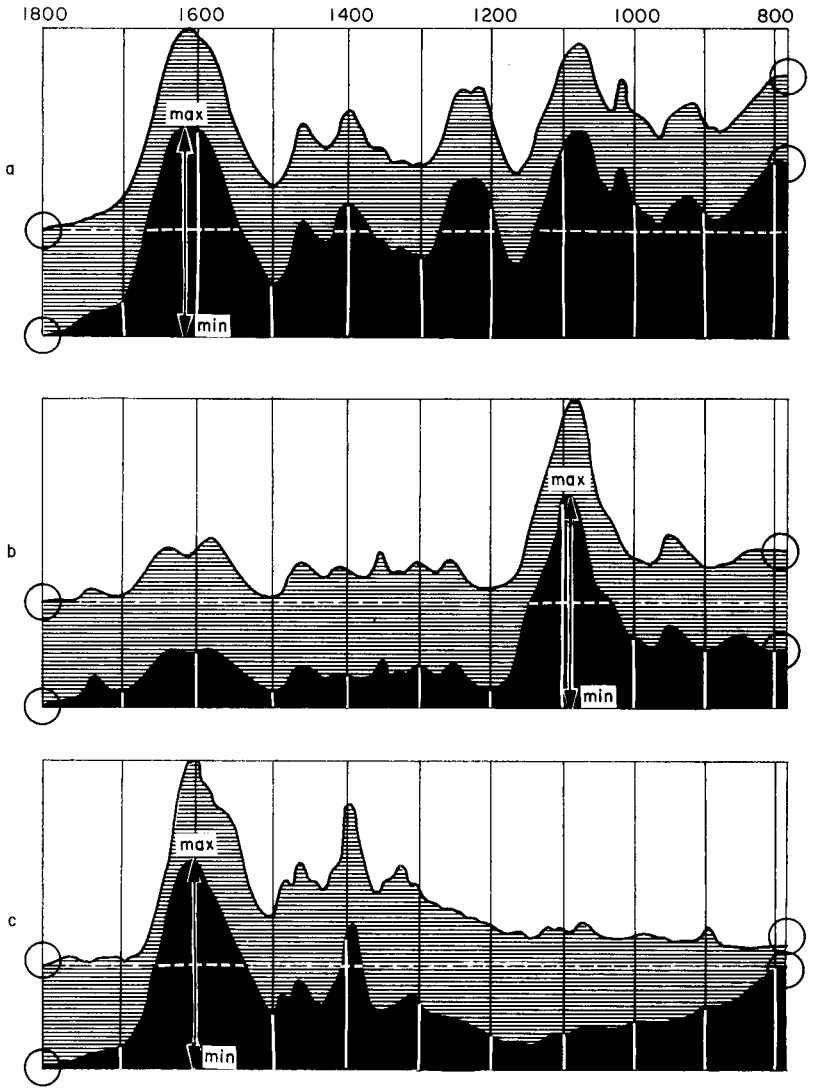

Fig. 6. Spectra (a—c) of three real mixtures. The upper curves are the real spectra; the lower curves are the calculated best hits obtained by the program for mixture analysis. The difference D between the minimal and maximal absorption is used to normalize the distance between the particular spectrum and the spectrum of the real mixture.

to be done much better and more economically than in previous attempts [18—23].

The interactive procedure for qualitative and quantitative analysis of mixtures based on the use of whole infrared spectra, was developed with the intention of solving real-world problems for mixtures of surfactants in aqueous solutions. The results obtained with known mixtures show that the

TABLE 3

Comparison of the distances with the determined ratios for the three mixtures

Mixture No.	IDs	Actual ratio	Distance D	Normalized distance	Calculated ratio	Error at the larger comp. (%)
1	10, 9	60:40	2.63	1.65	61:39	2
2	16, 28	70:30	10.32	2.79	63:37	10
3	2, 24	80:20	6.87	4.41	66:34	18

system is very reliable in the qualitative sense but that the error in quantitative estimation of the ratio of two components in one example was as high as 18%. As has been pointed out above, the main source of the quantitative error is not the method of calculation itself but the experimental errors in the input spectra, changes of the baseline, and an increase in the error during the subtraction of two similar spectra.

The entire system from the building of the collection up to the analysis of mixtures, is designed in such a way that the collection can easily be expanded and even a multicomponent analysis may become possible later.

All programming was done in PDP Fortran IV and implemented on the PDP 11/34 presently extended to 112K words of memory. The entire mixture analysis for 104 spectra requires on average only 40 seconds despite the very slow RKO5j disk-cartridges.

The authors thank Prof. Dušan Hadži for his suggestions and helpful comments during the work. Financial support by the Research Community of Slovenia is gratefully acknowledged.

REFERENCES

1 C. J. Pouchert, The Aldrich Library of Infrared Spectra (10000 spectra), Aldrich Chemical Company, Milwaukee, WI, U.S.A.
2 WYANDOTTE-ASTM Collection (103000 spectra), Am. Soc. Test. Mat., Philadelphia, PA, U.S.A.
3 Sadtler Collection of Infrared Spectra (63000 spectra) Sadtler Research Laboratories, Philadelphia, PA 19104, U.S.A.
4 Sadtler Collection of Infrared Spectra Monomers and Polymers (700 spectra), Sadtler Research Laboratories, Philadelphia, PA 19104, U.S.A.
5 Infrared Spectroscopy, Its Use in the Coating Industry (740 spectra), Fed. Soc. Paint Technol., 1969.
6 D. O. Hummel, F. Scholl, Atlas der Kunststoff-Analyse, Zusatzstoffe und Verarbeitungshilfmittel (1100 spectra), Carl Hauser, Munich, 1968.
7 D. O. Hummel, F. Scholl, Atlas der Kunststoff-Analyse, Hochpolymere und Harze (1800 spectra), Carl Hauser, Munich, 1968.
8 D. S. Erley, Anal. Chem., 40 (1968) 894.
9 J. Zupan, M. Penca, D. Hadži and J. Marsel, Anal. Chem., 49 (1977) 2141.
10 E. C. Penski, D. A. Padovski and J. B. Bonek, Anal. Chem., 46 (1974) 955.

11 M. Razinger, J. Zupan, M. Penca and B. Barlič, J. Chem. Inf. Comput. Sci., 20 (1980) 158.
12 M. Razinger, M. Penca and J. Zupan, Anal. Chem., 53 (1981) 1107.
13 E. O. Brigham, The Fast Fourier Transform, Prentice-Hall, Englewood Cliffs, NJ, 1973.
14 J. Zupan, Fresenius Z. Anal. Chem., 313 (1982) 466.
15 J. Zupan, Clustering of Large Data Sets, Research Studies Press, Wiley, Chichester, 1982.
16 J. Zupan, Anal. Chim. Acta, 139 (1982) 143.
17 W. N. Hansen, Spectrochim. Acta, 21 (1965) 815.
18 R. W. Sebasta and G. G. Johnson, Anal. Chem., 44 (1972) 260.
19 J. Zupan, J. T. Clerc and D. Hadži, Vestn. Slov. Kem. Drus., 23 (1976) 73.
20 T. Hirschfeld, Anal. Chem., 48 (1976) 721.
21 J. L. Koening, L. D'Esposito and M. K. Antoon, Appl. Spectrosc., 33 (1977) 292.
22 Chi-Hsiung Lin and Shi-Chung Liu, J. Chinese Chem. Soc., 25 (1978) 167.
23 J. L. Koenig and D. Kormos, Appl. Spectrosc., 33 (1979) 349.

Analytica Chimica Acta, 151 (1983) 433—439
Elsevier Science Publishers B.V., Amsterdam — Printed in The Netherlands

REDUCTION OF ANALYTICAL VARIANCE BY USING A DISCRETE-TIME DATA-WEIGHTING FILTER TO ESTIMATE ABRUPT CHANGES IN BATCH-TYPE PROCESSES
Part 1. Theory

HENNIE N. J. POULISSE

Delft Hydraulics Laboratory, Department of Mathematics, P.O. Box 152, 8300 AD Emmeloord (The Netherlands)

ROB T. P. JANSEN*

Laboratory for Clinical Chemistry, St. Anna Hospital, Bogardeind 2, 5664 EH Geldrop (The Netherlands)

(Received 4th October 1982)

SUMMARY

A discrete-time state-space model is proposed for describing the behaviour of analytical methods in which the samples are processed in batches. A characteristic of such methods is that the quantity describing the behaviour of such processes may undergo an abrupt change between different batches. A modified data-weighting Kalman filter is formulated which estimates the state of the batch-type analysis model and takes advantage of the batch-type situation. This leads to a procedure which is claimed to reduce the analytical variance in the measurements of the unknown samples in the batches.

In many routine analyses, particularly in clinical chemistry, samples are investigated in batches. Like all measurements, these batch analyses are subject to disturbances. The disturbances eventually appear as a deviation in the quantity to be evaluated, usually the concentration. However, in many batch analyses the deviations in the quantities found cannot be explained by the uncertainties introduced by the measurement noise alone [1]. Limonard [2] has suggested a model which would explain the behaviour of analytical processes in the clinical laboratory. It is argued in the present paper that an important disadvantage of Limonard's method is that it ignores the characteristic batch situation; in particular, it is impossible to explain the presence of the typical and often significant between-batch variance [1]. Therefore, an alternative model is proposed which is believed to give an adequate description of batch analysis. Specifically, the quantity characterizing the behaviour of such analyses, called the state [3], may undergo abrupt changes when a new batch of samples is started. This state is estimated by a Kalman filter [3] which processes measured quantities of the control samples in each batch. It is known that the standard Kalman filter cannot be used in such a situation. Therefore, a modified Kalman filter is proposed. The main feature

0003-2670/83/$03.00

of this modified Kalman filter is that it forgets any past information which is no longer relevant. These state estimates are used here in a procedure suggested by Jansen and Bonants [4] to reduce the variance in the measurements of unknown samples in each run. The performance of the proposed methods when applied to practical situations is described in a companion paper [5].

EARLIER MODELS

To explain the deviations in the measured quantities which have been observed in practice for batch analysis [1], Limonard [2] suggested that the measurements cannot be regarded as independent random variables [6], but that the measurement process should be treated as a time series. He assumed that such a process can be described as a first-order, stationary autoregressive time series [7]:

$$y(j) = ay(j-1) + b(j) \tag{1}$$

where j is the measurement or sample number, $y(j)$ the measured value of the jth control sample relative to its known reference value $z_{ref}(j)$ (see Eqn. 6 below), and $b(j)$ is discrete-time white noise [3] with constant variance, affecting the signal caused by the jth sample. The coefficient a is unknown but constant.

Limonard estimated the parameter a by first calculating the quantity

$$\psi(k) = \phi(k)/\phi(0) \tag{2}$$

$$\text{where } \phi(k) = [1/(n_t - k - 1)] \sum_{i=1}^{n_t-k} \{[y(i+k) - \bar{y}][y(i) - \bar{y}]\} \tag{3}$$

for $k = 0, 1, 2, \ldots$ and

$$\bar{y} = (1/n_t) \sum_{i=1}^{n_t} y(i) \tag{4}$$

and n_t is the total number of measurements. He then fitted an exponential curve of the form $\exp(-\alpha k)$ through the pairs $[\psi(k), k]$; from the quantity α an estimate of a can be obtained. This procedure is based on the fact that the normalized autocorrelation function $\psi^*(k)$ of a stationary first-order autoregressive process is given [7] by

$$\psi(k) = a^{|k|} = \exp[|k| \ln a] \quad (k = 0, \pm 1, \pm 2, \ldots) \tag{5}$$

while the quantity given by Eqn. (2) is an estimate of the normalized autocorrelation function, assuming that the process $[y(j)]$ is ergodic rather than stationary [6]. Having estimated the parameter a from control sample measurements, Limonard [2] proposed a correction procedure for the measurements of the unknown samples. When this procedure is applied, however, the

batch character of the processes is ignored. It is well known that these batch methods exhibit a significant between-run variance [1, 4]. This leads to the conclusion that the quantity which controls the behaviour of the batch processes may undergo sudden changes when a new batch is processed.

If the coefficient of variation of measured values of samples having varying concentration levels is constant, the relative measurement $y(j)$, defined by

$$y(j) = (z(j) - z_{\text{ref}}(j))/z_{\text{ref}}(j) \tag{6}$$

where $z(j)$ is the measured value of the jth control sample and $z_{\text{ref}}(j)$ is its reference value, may be used as a measurement of the quantity which controls the behaviour of the process. The above verbal description of the batch process can be translated mathematically in the following way:

$$x(j) = x(j-1) + u(j)\delta(j, rm+1) + w(j) \tag{7}$$

$$y(j) = x(j) + v(j) \tag{8}$$

where $j = 1, 2, \ldots, n \cdot m$; $r = 0, 1, 2, \ldots (n-1)$; $\delta(i, k) = 1$ if $i = k$ or $\delta(i, k) = 0$ if $i \neq k$. In Eqns. (7) and (8) $x(j)$ represents the quantity which controls the behaviour of the process; $u(j)$ is an unknown deterministic, impulse-like disturbance. The integer j is again the sample number; n is the number of runs (batches) and m is the number of control samples per run; $w(j)$ is discrete-time white noise and accounts for uncertainties in the description of the process. Indeed, in many cases $w(j)$ should be regarded as "fictitious noise" [3]. The quantity $v(j)$ represents discrete-time measurement noise. The following assumptions are made with respect to the noise sequences $w(j)$ and $v(j)$:

$$E[v(j)] = E[w(j)] = 0 \text{ for all } j \tag{9}$$

$$E[v(j)v(k)] = \sigma_v^2\, \delta(j, k) \tag{10}$$

$$E[w(j)w(k)] = \sigma_w^2\, \delta(j, k) \tag{11}$$

$$E[v(j)w(k)] = 0 \text{ for all } j, k \tag{12}$$

The quantity $x(j)$ is called the state and Eqns. (7) and (8) represent a discrete-time state space model [3]. In this terminology Eqn. (7) is called the dynamic state equation, Eqn. (8) the measurement equation, and $w(j)$ the system noise.

Returning the Limonard's method, it is of course possible to calculate a quantity as defined in Eqn. (2), based on the relative measurements $y(j)$ defined in Eqn. (6), and subsequently fit an exponential curve through the pairs $[\psi(k), k]$, but if the process is described by the state space model (Eqns. 7 and 8), the results will be meaningless. Instead an estimator is sought for the state $x(j)$. An outstanding method for estimating the state $x(j)$ based on the relative measurements $[y(j)]$ is the Kalman filter [3]. However, the performance of the Kalman filter will generally be unaccept-

able if the impulse-like disturbances $u(j)$ are ignored. To clarify this statement, the Kalman filter equation will be given, the unknown disturbances $u(j)$ being ignored in the first instance [3]:

$$\hat{x}(j/j) = \hat{x}(j-1/j-1) + K(j)v(j) \tag{13}$$

$$v(j) = y(j) - \hat{x}(j-1/j-1) \tag{14}$$

$$K(j) = P(j/j-1)/[P(j/j-1) + \sigma_v^2] \tag{15}$$

$$P(j/j-1) = P(j-1/j-1) + \sigma_w^2 \tag{16}$$

$$P(j/j) = [1 - K(j)]P(j/j-1) \tag{17}$$

initial estimates: $\hat{x}(0/0)$ and $P(0/0)$ (18)

and $j = 1, 2, \ldots, n \cdot m$; $\hat{x}(\cdot/\cdot)$ is an estimate of the state $x(\cdot)$ and $P(\cdot/\cdot)$ may be regarded as an estimate of the variance in the state estimate. In the notation (i, k), i refers to the sample number, and k to the number of measurements on which the estimate is based; e.g., $\hat{x}(j/j)$ is the estimate of $x(j)$ at sample number j and based on the measurements $[y(1), \ldots y(j)]$. $K(j)$ is the Kalman gain. An heuristic explanation of the quantities in the Kalman filter is available [8]. From Eqns. (15—17) it follows that

$$P(j/j-1) = \sigma_v^2 P(j-1/j-2)/[P(j-1/j-2) + \sigma_v^2] + \sigma_w^2 \tag{19}$$

It is well known that the quantity $P(j/j-1)$ in the Kalman filter (Eqns. 13—18), which is based upon the scalar state space model (Eqns. 7, 8) with constant system and statistical parameters and without disturbances $u(j)$, converges to a limit $\bar{P}$ [3]. This limit readily follows from Eqn. (19):

$$\bar{P} = 1/2\{\sigma_w^2 + [\sigma_w^4 + 4\sigma_w^2\sigma_v^2]^{1/2}\} \tag{20}$$

From Eqns. (19) and (15), it follows that the limit of the Kalman gain is $\bar{K} = \bar{P}[\bar{P} + \sigma_v^2]^{-1}$. Thus $\bar{L} = (1 - \bar{K}) = \sigma_v^2[\bar{P} + \sigma_v^2]^{-1}$. It must be noted that $0 < \bar{K} < 1$ and $0 < \bar{L} < 1$. If the true estimation error is defined as $\tilde{x}(j/j) = x(j) - \hat{x}(j/j)$, it follows from Eqns. (7, 8, 13, 14) that

$$\tilde{x}(j/j) = [1 - K(j)][\tilde{x}(j-1/j-1) + \delta(j, rm+1)u(j) + w(j)] - K(j)v(j) \tag{21}$$

Hence

$$\tilde{x}(j/j) = \bar{L}[\tilde{x}(j-1/j-1) + \delta(j, rm+1)u(j) + w(j)] - \bar{K}v(j) \tag{22}$$

if j is sufficiently large. From Eqn. (22) it follows that

$$|\tilde{x}(j/j)| < \bar{L}[|\tilde{x}(j-1/j-1)| + \delta(j, rm+1)|u(j)| + |w(j)|] + \bar{K}|v(j)| \tag{23}$$

It will be assumed that in practice the noise processes $w(j)$ and $v(j)$ as well as the impulse-like disturbances $u(j)$ are bounded, i.e., for all j, $|w(j)| < W$, $|v(j)| < V$, and $|u(j)| < U$.

So the true estimation errors $\tilde{x}(j/j)$ are maximized by a solution of the difference equation [9]:

$$s(j) = \bar{L}s(j-1) + \bar{L}[\delta(j, rm+1)U + W] + \bar{K}V \tag{24}$$

Alternatively

$$s(j+k) = \bar{L}^k s(j) + \sum_{i=1}^{k} \{\bar{L}^i[\delta(j+k-i+1, rm+1)U + W] + \bar{L}^{i-1}\bar{K}V\} \tag{25}$$

for $k = 1, 2, \ldots$. Every time the processing of a new batch of samples is started, the Kronecker delta function $\delta(j, rm+1)$ equals 1, and the maximized estimation error is subject to an impulse-like change. It follows from Eqn. (25) that the estimation errors will always have bounds, but that if $\bar{L} = 1 - \epsilon$, where ϵ is a very small real number and U is relatively large, the bounds in the estimation error can be very large. The relative measurements contain information about the disturbances $[u(j)]$ but the Kalman filter, which is used to process these measurements, does not. Thus there is a discrepancy between the true model and the model on which the Kalman filter is based. Generally this will lead to divergence of the Kalman filter.

Divergence is said to occur when the actual errors in the measurements become totally inconsistent with the covariance given by the Kalman filter equations, the quantity $P(j/j)$. Many modifications of the standard Kalman filter equations have been suggested [9—17] to cope with the divergence problem. In general, the proposed modifications try to prevent, in a more or less sophisticated way, the Kalman gain $K(j)$ from becoming too small too soon. In these modifications, the information content of the previous measurements is forgotten at a quicker rate than in the standard Kalman filter. Kalman filters in which the past is forgotten at an exponential rate have particularly proved to be useful [11, 13]. This is intuitively appealing: as there is a discrepancy between the true model and the model assumed in the Kalman filter design, the past no longer represents the behaviour of the system and hence should be forgotten as quickly as possible. A disadvantage of most of the proposed schemes is that the modification is ad hoc, or at least not dictated by the data. Exceptions are the adaptive measurement schemes, where the error variance, and so $K(j)$, is increased by increasing the variance of the system noise (see Eqn. 16) by letting the innovation sequence $[\nu(j)]$ dictate its magnitude. An admirable scheme in this connection is Jazwinski's adaptive filter [18]. However, the adaptive feature generally increases the complexity of the filter considerably.

THE PROPOSED MODEL

The modified Kalman filter proposed below takes full advantage of the batch-type situation. The increase in the error variance $P(j/j)$ is dictated by the data. Nevertheless, the modified filter has the same degree of complexity as the standard Kalman filter:

$$\hat{x}(j/j) = \hat{x}(j-1/j-1) + K(j)\nu(j) \tag{26}$$

$$\nu(j) = y(j) - \hat{x}(j-1/j-1) \tag{27}$$

$$P(j/a_r - 1) = \{(1/m)\left[\sum_{i=1}^{m} [y(j-1+i) - \hat{x}(j-1/j-1)]^2\right] + \sigma_w^2\}\delta(j, rm+1) \tag{28a}$$

$$(r = 0, 1, \ldots, (n-1); a_r = 1, \ldots, m)$$

$$P(j/a_r - 1) = [P(j-1/a_r - 1) + \sigma_w^2]\ \delta(j, rm+i) \tag{28b}$$

$$(i = 2, \ldots, m; a_r = 2, \ldots, m)$$

$$K(j) = P(j/a_r - 1)/[P(j/a_r - 1) + \sigma_v^2] \tag{29}$$

$$P(j/a_r) = [1 - K(j)]P(j/a_r - 1) \tag{30}$$

where $j = 1, 2, \ldots, n \cdot m$. It follows from Eqn. (28a) that each time a new batch of data is processed, the calculation of the error variance is restarted. As the data in each batch have to be collected first, regarding Eqn. (28a), the algorithm represented by Eqns. (26—30) is strictly speaking, not a filter, but actually a batch processor. The symbol a_r in Eqns. (28a—30) indicates that the calculation of the variances, and hence also of the Kalman gain, is always based on the current information; the past is abruptly forgotten, as it no longer represents the behaviour of the process, because of the impulse-like disturbances $u(j)$. This periodic restarting of the Kalman gain calculations is certainly not new and dates at least back to Battin and Levine [19].

There is still another possible approach to the problem of impulse-like disturbances. An important contribution in this area has been made by Willsky and Jones [20] and Willsky [21]. In this approach, the impulses $u(j)$ are estimated and the state estimate and error covariance matrix are adapted [21]. In the practical situation investigated in this work [5] Willsky's approach was used initially, but it turned out to be unsatisfactory, probably because Willsky's procedure is more suited for situations where impulses occur very infrequently [21].

Once the state $x(j)$ in run r has been estimated using control samples, the measurements of unknown samples in this run may be corrected for it [4, 5]:

$$z_c(i) = z(i) - z(i)\ \hat{x}\ (j/j) \tag{31}$$

$$i = 1, 2, \ldots s; j = r \cdot m; r \in (1, 2, \ldots, n)$$

where $z_c(i)$ is the corrected measurement of the ith unknown sample in the rth run and $z(i)$ is the uncorrected measurement; s is the number of unknown samples in the rth batch; $\hat{x}(j/j)$ is the final estimate of the state $x(j)$, given in Eqn. (7), in the rth run, produced by the data weighting algorithm (Eqns. 26—30) using m control samples. By placing additional control samples, which are not processed by this algorithm, in the runs, the variance reduction achieved may be estimated from

$$VR = [1 - \sigma_c^2/\sigma_n^2] \times 100\% \quad (32)$$

where σ_c^2 is the estimated variance in the corrected measurements z_c of an additional control sample, and σ_n^2 is the estimated variance in the uncorrected measurements of this sample. The successful application of the proposed procedure to a practical situation is described in the subsequent paper [5], where the choice of the statistical parameters σ_v^2 and σ_w^2, and the initial condition $\hat{x}(0/0)$ are discussed.

Finally, the proposed algorithm can be readily extended to more general situations, in particular when the measurements in each run are, apart from noise, also affected by drift. Such an extension, however, will probably be made at the expense of placing additional control sera in the batches.

REFERENCES

1 J. Büttner, R. Borth, P. G. M. Broughton and R. C. Bowyer, Clin. Chim. Acta, 106 (1980) 109F.
2 C. B. G. Limonard, Clin. Chim. Acta, 94 (1979) 137.
3 B. D. O. Anderson and J. B. Moore, Optimal Filtering, Prentice-Hall, Englewood Cliffs, NJ, 1979.
4 R. T. P. Jansen and P. J. M. Bonants, Ann. Clin. Biochem., accepted.
5 R. T. P. Jansen and H. N. J. Poulisse, Anal. Chim. Acta, 151 (1983) 441.
6 A. Papoulis, Probability, Random Variables and Stochastic Processes, McGraw-Hill, New York, 1965.
7 G. M. Jenkins and G. Watts, Spectral Analysis and Its Applications, Holden-Day, San Francisco, CA, 1968.
8 H. N. J. Poulisse and P. L. M. Engelen, Anal. Chim. Acta, submitted.
9 F. H. Schlee, C. J. Standish and N. F. Toda, AIAA Journal, 5 (1967) 1114.
10 A. H. Jazwinski, IEEE Trans. Autom. Control, AC-13 (1968) 558.
11 H. W. Sorenson and J. E. Sacks, Inf. Sci. (N.Y.), 3 (1971) 101.
12 H. Sriyananda, Int. J. Control, 16 (1972) 1101.
13 B. D. O. Anderson, Inf. Sci. (N.Y.), 5 (1973) 217.
14 A. L. C. Quigley, Int. J. Control, 17 (1973) 741.
15 F. M. Boland and H. Nicholson, Electron Lett., 12 (1978) 367.
16 A. E. Bryson, J. Guidance and Control, 1 (1978) 71.
17 A. H. Jazwinski, Stochastic Processes and Filtering Theory, Academic Press, New York, 1970.
18 A. H. Jazwinski, Automatica, 5 (1969) 475.
19 R. H. Battin and G. M. Levine, Applications of Kalman Filtering Techniques in the Apollo Program, NATO AGARD-ograph 139, (1970).
20 A. S. Willsky and H. L. Jones, IEEE Trans. Autom. Control, AC-21 (1976) 108.
21 A. S. Willsky, Automatica, 12 (1976) 601.

Analytica Chimica Acta, 151 (1983) 441—446
Elsevier Science Publishers B.V., Amsterdam — Printed in The Netherlands

REDUCTION OF ANALYTICAL VARIANCE BY USING A DISCRETE-TIME DATA-WEIGHTING FILTER TO ESTIMATE ABRUPT CHANGES IN BATCH-TYPE PROCESSES
Part 2. Applications

ROB T. P. JANSEN*

Laboratory for Clinical Chemistry, St. Anna Hospital, Bogardeind 2, 5664 EH Geldrop (The Netherlands)

HENNIE N. J. POULISSE

Delft Hydraulics Laboratory, Department of Mathematics, P.O. Box 152, 8300 AD Emmeloord (The Netherlands)

(Received 4th October 1982)

SUMMARY

A well known characteristic of analytical methods in clinical laboratories is the presence of a significant between-batch variance component. This is confirmed by an analysis of variance of data obtained for the determination of inorganic phosphate in blood serum with a continuous flow system. Based on a model describing the process fluctuations, the proposed discrete-time digital filter algorithm estimates abrupt changes in the process values between two runs of samples. Subsequent correction of the control sera data for these estimates leads to a reduction of about 50% in the variance. Similar results were obtained for other analytical methods including a centrifugal fast analyzer, an automatic discrete system and a semi-automatic coulometric titration.

Efforts to reduce the variance of analytical procedures in the clinical laboratory are mainly concentrated on the introduction of procedures that yield more precise measurements than current techniques. Relatively little attention has been given to mathematical techniques like digital filtering procedures [1]. Such filter algorithms are based on models describing the system dynamics of the analytical procedures. The filter produces estimates of quantities such as the concentration of a constituent and aims to improve the signal/noise ratio of the process.

A well known feature of most analytical methods in clinical laboratories is the presence of a significant between-batch variance in addition to a within-batch variance component. In this paper, the model presented in the preceding paper [2] is used to describe some practical situations. A discrete-time recursive data-weighting filter algorithm based on this model is used to estimate the process fluctuations. The theoretical details of this filter have been given [2]. In order to reduce the variance, measurements are corrected for the estimated deviations. As an example, results obtained for the deter-

0003-2670/83/$03.00

mination of inorganic phosphate in blood serum with a continuous flow analyzer in 250 runs, each composed of standards, patient sera and control sera, are presented.

EXPERIMENTAL

Data sets

The results of 250 batches of samples assayed with a continuous flow system for the determination of inorganic phosphate in blood serum [3] were used to investigate whether the variance can be reduced by digital filtering. During a period of 25 days, 10 batches a day were assayed. The batches were composed of 5 aqueous standards, 6 control sera and 9 randomly chosen fresh patient sera. The standards were positioned at the start of each run. The control sera were placed at fixed positions randomly between the patient sera. The six control sera were lyophilized sera of varying origin (human, bovine, equine) and cover the concentration range of medical interest (Table 1).

Though not discussed extensively here, the filtering procedure was also applied to four other analytical methods used in daily routine: a centrifugal fast analyzer method for the determination of cholesterol; an automatic discrete system for the determination of lactate dehydrogenase; a continuous flow system for the determination of creatinine; a semi-automatic amperometric titration of chloride. Because these methods were used routinely, only three control sera could be included in the runs, to avoid excessive additional work load.

Statistical methods

In the concentration range covered by the six control sera, no differences could be demonstrated between the coefficients of variation in F-tests at $\alpha = 0.01$ (Table 1). Therefore the results of the control sera relative to their mean values (Eqn. 1) may be compared and used in an analysis of variance:

TABLE 1

Mean values, standard deviations and coefficients of variation of the six control sera

Control serum	$\bar{x}$[a]	S.d.	C.v. (%)
1	1.136	0.019	1.67
2	1.491	0.024	1.61
3	2.404	0.036	1.50
4	1.137	0.019	1.67
5	1.496	0.025	1.67
6	2.420	0.037	1.53

[a] $N = 250$.

$$y(j) = [z(j) - z_{ref}(j)]/z_{ref}(j) \quad (1)$$

in which $z(j)$ is the measured value of control serum j in mmol l^{-1} and $z_{ref}(j)$ is its reference value for which the mean value of 250 results was used. The relative measurements $y(j)$ are used in the model describing the process fluctuations [2]:

$$x(j) = x(j-1) + u(j)\,\delta(j, rm+1) + w(j) \quad (2)$$

(where $\delta(j, rm+1) = 1$ if $j = rm+1$ and $\delta(j, rm+1) = 0$ if $j \neq rm+1$)

$$y(j) = x(j) + v(j) \quad (3)$$

where y_j is the relative value of control sample j for $j = 1, 2, \ldots n \cdot m$; n is the number of batches, m is the number of control sera per batch; $r = 0, 1, 2, \ldots (n-1)$; u_j is an impulse-like disturbance in batch r acting upon the term x_{j-1}. The quantity x_j, called the state [2], is assumed to be constant if no such disturbance occurs. The measurement noise $v(j)$, the system noise, w_j, which accounts for the uncertainty of the model [2], and the features $E[v(j)v(k)]$, $E[w(j)w(k)]$ and $E[v(j)w(k)]$ were as given in Eqns. (9—12) in Part 1 [2]. Equation (2) is called the state equation; Eqn. (3) is called the measurement equation. Equations (2) and (3) constitute a so-called state-space description of a system in which abrupt changes occur at known times [2].

A one-way analysis of variance was done for the values of the six control sera transformed by using Eqn. (1). If between-batch variance is significantly larger than within-batch variance, support is obtained for the model expressed by Eqns. (2) and (3).

The algorithm used to estimate the terms x_j which represent the between-batch lack of stationarity was presented in Eqns. (26)—(30) [2]. In Eqn. (28a) of Part 1, $r = 0, \ldots (n-1)$ because $P(1/0)$ is estimated from the deviation of the measurements in run 1 from $\hat{x}(0/0)$; therefore an initial estimate is needed for $\hat{x}(0/0)$ but not for $P(0/0)$.

In each batch of samples, three control sera (sera 1, 2 and 3, see Table 1) were used to compute $\hat{x}(j/j)$; hence $m = 3$. The value obtained after the third control sample in each run is used to correct the measurements of the remaining three samples in the run. Thus the measurements $z(i)$ of these remaining samples in each run are not processed with the algorithm (Eqns. (26)—(30) [2]); instead they are corrected according to the following equation:

$$z_c(i) = z(i) - z(i)\hat{x}(j/j) \text{ (for } i = 1, 2, \ldots, 5; j = r \cdot m; r = 1, 2, \ldots, n) \quad (4)$$

where $z(i)$ is the measured value of a control serum i in batch r which has not been processed by the discrete-time filter algorithm. For each of the three additional control sera, the variance reductions obtained by correcting the measured values are computed from the equation

$$VR = [1 - \sigma_c^2/\sigma_n^2] \times 100\% \quad (5)$$

where σ_c^2 is the variance in the corrected results $z_c(i)$, and σ_n^2 is the variance in the uncorrected results $z(i)$.

RESULTS AND DISCUSSION

Analysis of variance of the relative values for inorganic phosphate in the six control sera measured in 250 runs, showed a highly significant between-runs variance component (Table 2). In the model describing the process fluctuations (Eqns. 7—12 [2]), σ_v^2 accounts for the within-batch variance and u_j for the between-batch lack of stationarity. The algorithm for the detection of these variances is of a recursive nature, so that initial estimates are needed. The initial values chosen are $\hat{x}(0/0) = 0$ and, if in Eqn. (28a) [2] $r = 1,\ldots (n-1)$, $P(0/0) = \sigma_v^2$; in the example, however, r may take the values $0,\ldots (n-1)$ because the initial estimate for $\hat{x}(0/0)$ is rather a good one, namely, the expected value for $x(j/j)$ (= 0); therefore no initial estimate is needed for $P(0/0)$. The within-run variance $\sigma_v^2 = 1 \times 10^{-4}$ (Table 2). Values for σ_w^2 are varied to investigate its influence on the variance reductions obtained. In Table 3, the reductions in variance achieved for the three control sera not processed by the filter algorithm are presented for various σ_w^2 values. The maximal obtainable reduction in variance may be estimated from the results of Table 2:

$$VR_{\max} = [1 - \sigma_{wr}^2/\sigma_t^2] \times 100\% \qquad (6)$$

in which σ_{wr}^2 denotes the within-batch variance and σ_t^2 the total variance; $VR_{\max}$ is 60% for the inorganic phosphate determination in this example. The average reduction in variance obtained for the three control sera at a σ_w^2 value of 1×10^{-6} is 49%. The large reduction achieved indicates that the filter estimates follow the process fluctuations quite well. A typical example of the values and the process variations in relative units is given in Fig. 1.

Exactly the same filtering procedure was applied to results obtained from the determination of four other serum components using various instruments (see Experimental). For these routine analytical methods, two control sera were used in the filter algorithm and one additional serum was used to estimate the reduction in variance obtained. Maximal obtainable reductions in variance computed from Eqn. (6) amounted to 27% for the determination of

TABLE 2

Analysis of variance of the relative values of the six control sera

Source of error	Sum of squares	Degrees of freedom	Mean squares	F	$p(F)$
Between-batch	0.265	249	0.001063	10.3	<0.001
Within-batch	0.129	1250	0.000103		
Total	0.393	1499	0.000262		

TABLE 3

Reductions (%) in variance obtained for sera 4, 5 and 6 at various σ_w^2 values

Control serum	% reductions for σ_w^2 values of							
	1×10^{-1}	1×10^{-2}	1×10^{-3}	1×10^{-4}	1×10^{-5}	1×10^{-6}	1×10^{-7}	1×10^{-9}
4	13.7	14.3	18.8	34.5	43.8	44.8	44.9	44.9
5	36.2	36.7	40.6	53.3	59.2	59.4	59.4	59.4
6	22.8	23.3	27.3	39.5	43.4	43.0	42.9	42.9

cholesterol, 74% for lactate dehydrogenase, 42% for creatinine and 20% for chloride. Estimated reductions in variance achieved by applying the proposed filter algorithm (Eqns. (26)–(30)[2]) amounted to 27%, 72%, 29% and 12% for the determination of cholesterol, lactate dehydrogenase, creatinine and chloride, respectively.

CONCLUSIONS

A well known feature of analytical methods in clinical laboratories is the presence of a significant between-batch variance component. The method for the determination of inorganic phosphate used above exhibits this behaviour, as is shown by the analysis of variance listed in Table 2.

A model describing such a process forms the basis of a discrete-time recursive filter algorithm [2] which estimates the between-batch variances. The estimates made by the filter appears to follow the process fluctuations quite well. Application of the filter algorithm leads to a reduction in variance of about 50% of the original value for this determination. In the algorithm, values of the control sera were used relative to their respective reference values. If, for instance, the standard deviation does not vary with concentrations, absolute values should be used in the computations. To apply the algorithm, initial values are needed. A good estimation of σ_v^2 may be obtained from the within-batch variance of the method of determination as computed in an analysis of variance. The value of σ_w^2 must be found experimentally. For the example investigated here, a value of $0.01 \times \sigma_v^2$ or less appeared to be satisfactory (Table 3). The proposed filter algorithm is applicable to systems

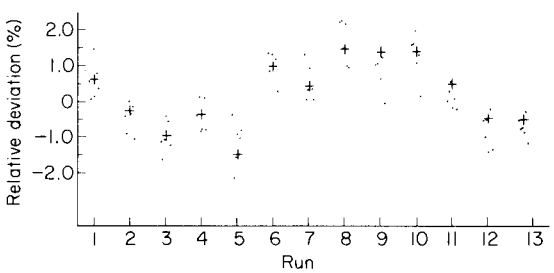

Fig. 1. Relative values (•) of the six control sera in 13 runs and the estimates $\hat{x}(3/3)$ produced by the filter algorithm (+).

characterized by the presence of a significant between-batch variance component. The larger the contribution of this variance to the total variance, compared with the within-run variance, the larger the reductions in variance will be. In the example, a reduction of 50% is achieved. Though not presented here in detail, similar results were obtained for determinations of other serum components by various analytical methods and instruments.

An additional advantage of the algorithm is the possibility of extending it to estimate possible within-batch drift parameters [2]. However, such an extension would involve decreased numbers of patient sera per batch, because additional control sera would be needed.

The authors thank Miss Madeleine Jansen for doing many computations.

REFERENCES

1 R. T. P. Jansen and P. J. M. Bonants, Ann. Clin. Biochem., accepted for publication.
2 H. N. J. Poulisse and R. T. P. Jansen, Anal. Chim. Acta, 151 (1983) 433.
3 H. Baadenhuysen, H. E. M. Seuren-Jacobs and A. P. Jansen, Clin. Chem., 23 (1977) 1275.

Analytica Chimica Acta, 151 (1983) 447—455
Elsevier Science Publishers B.V., Amsterdam — Printed in The Netherlands

LIQUID—LIQUID EXTRACTION OF METAL IONS BY THE THIACROWN COMPOUND 1,4,8,11-TETRATHIACYCLOTETRADECANE

KEIITSU SAITO, YOSHITAKA MASUDA and EIICHI SEKIDO*

Department of Chemistry, Faculty of Science, Kobe University, Nadu-ku, Kobe 657 (Japan)

(Received 24th December 1982)

SUMMARY

The possibilities of thiacrown compounds in liquid—liquid extraction were tested by using 1,4,8,11-tetrathiacyclotetradecane (TTCT). Class *a* metals were not extracted at all; of the class *ab* metals, only copper(II) was extracted. Class *b* metals were extracted but their extractabilities varied considerably. The relationship between the distribution ratio of the *b* metal and its softness is discussed. The extraction behavior of copper(I) with TTCT was studied in detail. The copper(I)—TTCT cation was completely extracted at pH > 4.0 as an ion-pair with perchlorate, picrate or tetraphenylborate. The extraction of copper(I) with TTCT and picrate into different solvents decreased in the order nitrobenzene >1,2-dichloroethane > chloroform > carbon tetrachloride. A study of the extraction equilibria for copper(I) with TTCT in the presence of the picrate (Pic^-) showed that copper(I) and TTCT form a 1:1 cation complex $[Cu(TTCT)]^+$, which reacts with picrate to form the 1:1 ion-pair $[Cu(TTCT)]^+Pic^-$. The extraction constants are log K_{ex} = 7.3 ± 0.3 and 9.0 ± 0.2 for chloroform and 1,2-dichloroethane, respectively, as the organic solvent.

Studies of crown ethers and related compounds have developed extensively since the first paper on crown ethers was published by Pedersen [1]. Generally, crown ethers have an affinity for alkali metal ions, tending to form cationic complexes that can react with an appropriate anion to form an ion-pair. As such ion-pairs can be extracted into suitable organic solvents, crown ethers have become known as selective ligands for alkali metals [2—5]. In contrast, thiacrown ethers, in which sulfur atoms replace the oxygen atoms in crown ethers, are soft Lewis bases. Accordingly, thiacrown ethers would be expected to have an affinity for soft Lewis acids, i.e., for the class *b* metals as classified by Ahrland et al. [6]. In general, organic reagents in which the ligand sulfur atom is present as a mercapto group ($R—S^-$) will react with class *ab* metals as well as with class *b* metals. Thiacrown ethers, however, contain the sulfur atoms in thioether groups (R—S—R′), so that they will act as softer Lewis bases. It was considered of interest to find out whether thiacrown compounds will react with class *ab* metals or not, and also how they react with class *b* metals. Moreover, from the consideration that the metal ion should fit into the cavity of the molecule, the selectivity

0003-2670/83/$03.00

for metal ions should increase further. And, from the viewpoint of analytical separations, selectivity for class *b* and *ab* metals might be achieved by an appropriate choice of the anion for formation of the ion-pair and the extraction solvent.

Although some metal complexes of thiacrown ethers have been isolated and characterized in recent years [7—9], there are few studies concerning the extraction of metal thiacrown ethers. Liquid—liquid extractions of mercury [10] and silver [11, 12] seem to be the only known analytical applications. In the present study, the liquid—liquid extraction of various metal ions with 1,4,8,11-tetrathiacyclotetradecane (TTCT), a typical thiacrown ether, was examined in order to obtain general information for the extraction of metals with thiacrown compounds. The extraction equilibria of copper(I) with TTCT was also investigated.

EXPERIMENTAL

Reagents and apparatus

The method described by Rosen and Bush [7] was used to prepare TTCT, which was recrystallized twice from ethanol. A 5×10^{-3} M TTCT solution was prepared by dissolving in chloroform, carbon tetrachloride, 1,2-dichloroethane or nitrobenzene just prior to use. Except for thallium(I) nitrate and methylmercury(II) chloride, the metal sulfates (guaranteed-reagent grade) were used to prepare 1×10^{-2} M solutions of metal ions, which were standardized by compleximetric titrations. The thallium(I) solution was standardized by compleximetric titration after oxidation to thallium(III). The concentration of silver(I) was determined by potentiometric titration, and that of methylmercury(II) was determined by atomic absorption spectrometry, by using for calibration a mercury(II) sulfate solution which had been standardized compleximetrically. Sodium perchlorate was recrystallized twice from distilled water, and dried under vacuum. Chloroform was shaken three times with 2 M hydrochloric acid, 2 M sodium hydroxide and then distilled water, then dried with anhydrous sodium sulfate and distilled. 1,2-Dichloroethane was shaken three times with 2 M potassium hydroxide and distilled water, dried with calcium chloride, and distilled. Other reagents were of guaranteed-reagent grade.

Extraction was done in a Taiyo M incubator at 25 ± 0.1°C. A Seiko SAS-725 atomic absorption spectrometer was used for the determination of most metal ion concentrations. Absorption spectra were measured with a Hitachi 124 double-beam spectrophotometer and the pH of aqueous phases was measured with a Hitachi-Horiba H-5 pH meter.

Extraction of metals

An aliquot (10 ml) of aqueous solution containing the metal ion (5×10^{-5} M), the anion for the formation of the ion-pair (0.1 M perchlorate, 1×10^{-3} M or 5×10^{-4} M picrate, 1×10^{-3} M tetraphenylborate) and the

buffer solution (1×10^{-2} M), was taken in a 50-ml glass cylindrical tube with a glass stopper. The buffer solution was made with sulfuric acid or perchloric acid (below pH 3.0), or acetic acid and sodium acetate (pH 3—6). The ionic strength was kept at 0.1 with sodium sulfate. For the copper(I) solution, hydroxylammonium sulfate was added to copper(II) sulfate solution in addition to the above reagents to give a 0.1 M solution. After the addition of 10 ml of 5×10^{-3} M TTCT solution, the mixture was shaken for 30 min at 200 strokes/min at 25 ± 0.1°C. After the mixture had been centrifuged for 5 min, the pH of the aqueous phase was measured and the concentration of metal was measured by atomic absorption spectrometry at the resonance line for each metal. Copper concentrations in organic phases were determined as follows: 5 ml of the chloroform phase was allowed to evaporate; the residue was dissolved in concentrated nitric acid and diluted to 25 ml with water, and the metal in this solution was determined by atomic absorption spectrometry. The concentration of the picrate ion in the aqueous phase was determined spectrophotometrically at 354 nm.

RESULTS AND DISCUSSION

Liquid—liquid extraction of various metals with TTCT

The following metals were examined: Na(I) and Mg(II) as class *a* metals, Mn(II), Co(II), Ni(II), Cu(II), Zn(II) and Tl(I) as class *ab* metals; and Cu(I), Ag(I), Pd(II), Cd(II) and Hg(II) as class *b* metals. The results of the extraction of these metals in the presence of picrate ions with TTCT in 1,2-dichloroethane solution are shown in Table 1. All conditions of the extraction, such as ionic strength (0.1), pH (5.4 and 3.9), concentrations of metal ions, TTCT and picrate ions (5×10^{-5} M, 5×10^{-3} M and 1×10^{-3} M, respectively), volume of aqueous and organic phase (10 ml), were kept the same, so that the data for percent extraction (*%E*) and logarithmic distribution ratio (log *D*) for each metal could be mutually compared. As can be seen in Table 1, the values of *%E* for each metal are very similar for different pH values (3.9 and 5.4), indicating that the extraction of each metal is little affected by pH in this range.

It is well known that sulfur atoms do not react with class *a* metals; this is confirmed in Table 1. Thiacrown ethers would be expected to bond more strongly with class *b* metal ions than with class *ab* metals. The *%E* values for the latter half of first transition metal group, Mn(II), Co(II) and Ni(II) except for Cu(II), and for the post-transition metals, Zn(II) and Cd(II), are below 1, i.e., log $D < -2.0$; this implies that these metals were practically not extracted. The value of *%E* for copper(II) is 6—7, which is only slightly more in terms of extractability. The *%E* value for thallium(I), which belongs to class *ab* but is classified as a soft acid by Pearson [13], is 1.0—2.2. Copper(I), Ag(I), Hg(II) and $CH_3Hg(II)$, which are class *b* ions, are extracted well, but Cd(II), also a class *b* metal, is extracted hardly at all.

TABLE 1

Data for the extraction of various metals in the presence of picrate ion with TTCT in 1,2-dichloroethane solution

Metal ion	Classification of metal (by Ahrland et al.)	pH	Extraction (%)	log D
Na(I)	*a*	5.4	0	—
Mg(II)	*a*	5.4	0	—
Mn(II)	*ab*	3.9	0.5	−2.3
		5.4	0.8	−2.1
Co(II)	*ab*	3.9	0.8	−2.1
		5.4	0.8	−2.1
Ni(II)	*ab*	3.9	0.8	−2.1
		5.4	0.7	−2.2
Cu(II)	*ab*	3.9	7.5	−1.1
		5.4	5.9	−1.2
Zn(II)	*ab*	3.9	0.4	−2.4
		5.4	0.5	−2.3
Cd(II)	*b*	3.9	0.6	−2.2
		5.4	0.8	−2.1
Tl(I)	*ab*	3.9	2.2	−1.7
		5.4	1.0	−2.0
Hg(II)	*b*	3.6	88.7	0.9
		5.1	89.5	0.9
Cu(I)	*b*	4.0	99.4	2.2
		5.4	99.4	2.2
Ag(I)	*b*	3.9	99.9	3.0
		5.4	99.9	3.0
Pd(II)	*b*	3.9	12.7	−0.8
		5.4	14.3	−0.8
$CH_3Hg(II)$	*b*	3.9	84.4	0.7

In order to examine the relationship between the extractability of class *b* metals and the quantity representing the softness of these metals, log D vs. α values of these metals were plotted. The parameter α obtained from Edwards' equation [14], as modified by Yamada and Tanaka [15], represents the softness of the metals. The results are shown in Fig. 1. If the extractability of metals depends primarily on the stability of the metal—TTCT complex (i.e., on the strength of covalent bonding between sulfur and metal), log D for class *b* metals should be proportional to their α values, but Fig. 1 shows no such relationship. However, class *b* metals seem to cluster in two groups, one with metals having α values less than 2, [Tl(I), Cd(II) and Cu(II)] and the other with metals having α values more than 3 [Ag(I), Cu(I), Hg(II), $CH_3Hg(II)$ and Pd(II)]. There is no obvious relationship between the metals in each group. The extractabilities of metals depend on many other factors, such as the fit of the metal ion in the TTCT cavity, the anion selected to form the ion pair, and the extraction solvent, and probably other factors

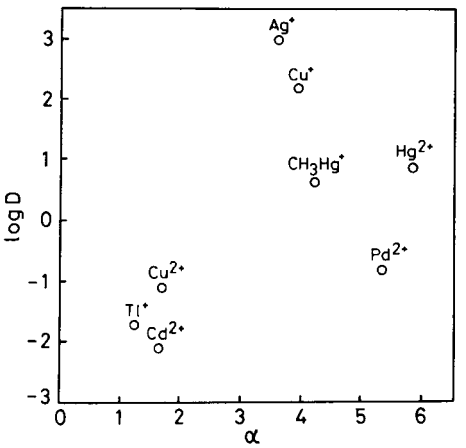

Fig. 1. Plot of distribution ratio of class *b* metals against α values.

also. It is necessary to confirm the composition of the extraction species by other experiments.

Extraction behavior of copper(I) with TTCT and various anions

Extraction of copper(I) with TTCT from aqueous solutions containing perchlorate, picrate or tetraphenylborate into chloroform was examined in the pH range 1—6. Plots of the logarithmic distribution ratio of copper(I) against the pH of the aqueous solution are shown in Fig. 2. The extraction of copper(I) from aqueous solutions containing 0.1 M perchlorate depends on the pH of the aqueous phase, contrary to what one would expect, and increases rapidly in the pH range 2—4, reaching a constant value of 95% ($\log D > 1.3$) at pH > 4. The pattern was similar for picrate, whereas extraction from the tetraphenylborate solution was greater and almost independent of pH in the range 3—5. Protonation of TTCT could be a cause of the pH dependence. However, a study of the distribution ratio for TTCT between chloroform and aqueous solution at various pH values showed no pH dependence in the pH range 1.5—6 (Fig. 3). Another cause of the pH dependence in the case of copper ions could be the decreased reducing power of hydroxylammonium sulfate at pH < 4. This was confirmed by examining the extraction of copper(II) as well as copper(I); Fig. 3 shows that extraction of copper(II) from aqueous solutions containing perchlorate or picrate was poor and independent of pH, and that at pH < 2.2 the plots for Cu(II) and Cu(I) (cf. Fig. 2) agree well. In contrast, copper(II) was almost completely extracted with tetraphenylborate though again there was little pH dependence.

As copper(I) is extracted satisfactorily into chloroform in the presence of perchlorate, picrate or tetraphenylborate, and copper(II) is significantly extracted only in the presence of tetraphenylborate, it should be possible to separate copper(I) from copper(II) by extraction from perchlorate or picrate solutions at suitable pH.

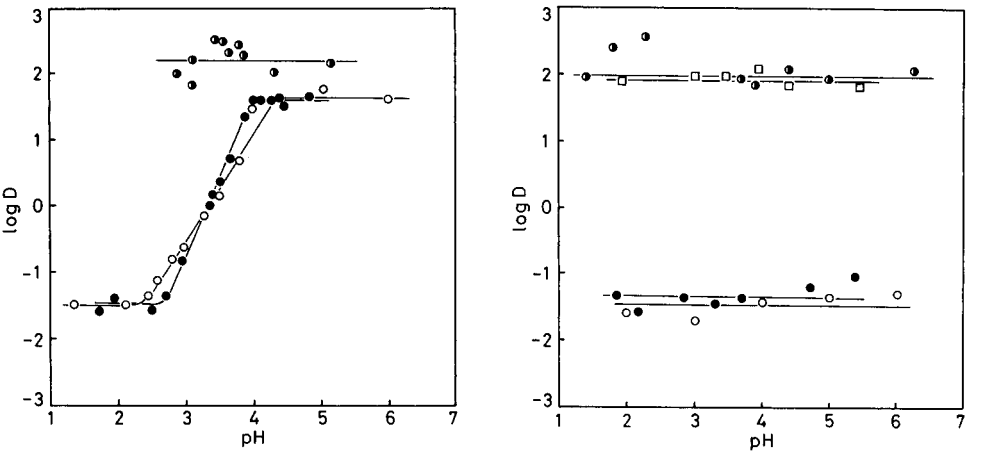

Fig. 2. Plots of distribution ratio of copper(I) vs. pH. Initial concentrations: 5×10^{-5} M copper(I), 5×10^{-3} M TTCT. (○) 0.1 M perchlorate; (●) 5×10^{-4} M picrate; (◑) 1×10^{-3} M tetraphenylborate.

Fig. 3. Plots of distribution ratio of copper(II) and TTCT vs. pH. Initial concentrations: 5×10^{-5} M copper(II), 5×10^{-3} M TTCT. (○) copper(II) with 0.1 M perchlorate; (●) copper(II) with 1×10^{-3} M picrate; (◑) copper(II) with 1×10^{-3} M tetraphenylborate; (□) TTCT.

Extraction equilibria involving the copper(I)—TTCT complex and ion-pair formation

If the extracted species in the organic phase are represented by $Cu(TTCT)_m Pic_n$, the extraction equilibrium and the extraction constant are given by

$$Cu^+ + mTTCT(o) + nPic^- \overset{K_{ex}}{\rightleftharpoons} Cu(TTCT)_m Pic_n(o) \quad (1)$$

$$K_{ex} = [Cu(TTCT)_m Pic_n]_o / [Cu^+][TTCT]_o^m [Pic^-]^n$$

Figure 4 illustrates the numerous equilibria involved in this extraction system; the relevant equilibrium constants are as follows:

$$K_c = [Cu(TTCT)_m^+] / [Cu^+][TTCT]^m;$$

$$K_{ass} = [Cu(TTCT)_m Pic_n] / [Cu(TTCT)_m^+][Pic^-]^n$$

$$K_{Dc} = [Cu(TTCT)_m Pic_n]_o / [Cu(TTCT)_m Pic_n]; K_{DR} = [TTCT]_o / [TTCT]$$

$$K_a = [H^+][Pic^-] / [HPic]; K_{DA} = [HPic]_o / [HPic]$$

As the extraction proceeds around pH 4—5, the concentration of picrate ion corresponds almost to the initial concentration of picric acid. Consequently, the equilibria involving K_a and K_{DA} can be neglected. If it assumed that hydroxy and other anionic complexes of Cu(I) are absent from the aqueous phase and that the species present in the organic phase is the ion-pair $Cu(TTCT)_m Pic_n$ only, the expression for the distribution ratio of copper(I)

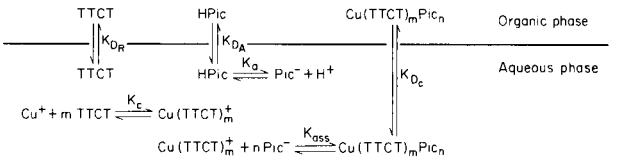

Fig. 4. Equilibria in the liquid—liquid distribution.

is given by

$$D_{Cu(I)} = [Cu(TTCT)_m Pic_n]_o / \{[Cu(TTCT)_m Pic_n] + [Cu^+]\}$$

With appropriate substitutions using the above expressions for K_c, K_{ass}, K_{Dc} and K_{DR}, this becomes

$$D_{Cu(I)} = K_{Dc} / \{1 + K_{DR}^m / K_{ass} K_c [TTCT]_o^m [Pic^-]^n\} \quad (2)$$

and for values $D < K_{Dc}$

$$D_{Cu(I)} = K_{Dc} K_{ass} K_c [TTCT]_o^m [Pic^-]^n / K_{DR}^m \quad (3)$$

Substitution of the expression for K_{ex} into Eqn. (3) leads finally to $D_{Cu(I)} = K_{ex}[TTCT]_o^m[Pic^-]^n$, which gives the logarithmic expression

$$\log D_{Cu(I)} = \log K_{ex} + m \log[TTCT]_o + n \log [Pic^-] \quad (4)$$

The relationship between the logarithmic distribution ratio ($\log D_{Cu(I)}$) and the logarithm of the picrate concentration in the aqueous phase at pH 4.5 is shown in Fig. 5A. A plot of $\log D_{Cu(I)}$ vs. the logarithm of the ligand concentration in the organic phase at pH 4.4 is shown in Fig. 5B. Straight lines with slopes of +1 were obtained in both cases, i.e., $m = 1$ and $n = 1$. Consequently copper(I) ion forms the complex $[Cu(TTCT)]^+$ and then the ion-pair $[Cu(TTCT)]^+Pic^-$. This composition was supported by the results

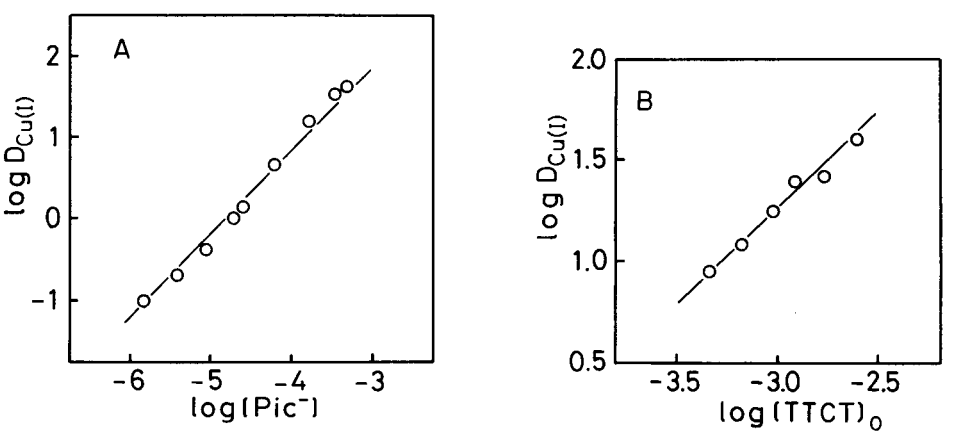

Fig. 5. Plots of (A) $\log D_{Cu(I)}$ vs. $\log[Pic^-]$ at pH 4.5, and (B) $\log D_{Cu(I)}$ vs. $\log[TTCT]_o$ at pH 4.4. Initial concentrations: 5×10^{-5} M copper(I), 5×10^{-3} M TTCT (for A), 5×10^{-4} M picrate (for B). Chloroform as solvent.

TABLE 2

Extraction of copper(I) from aqueous solution containing picrate into various solvents with TTCT[a]

$[Pic^-]^b$ (M)	Log D values			
	CCl_4	$CHCl_3$	$C_2H_4Cl_2$	Nitrobenzene
2×10^{-5}	−2.40	−0.38	−0.16	−0.12
5×10^{-5}	−1.92	0.14	1.38	2.12
2×10^{-4}	−0.47	1.26	2.12	2.40
4×10^{-4}	Ppt.[c]	1.61	2.30	2.40

[a]Initial concentrations: 5×10^{-5} M copper(I), 5×10^{-3} M TTCT, pH 4.5. [b]Initial concentration of picrate in aqueous phase. [c]Precipitation.

of elemental analysis of the compound isolated from the extracted chloroform solution. From Eqn. (4) and the results in Fig. 5, log K_{ex} = 7.3 ± 0.3 was calculated.

Extraction behavior of copper(I) with TTCT in various solvents

The extraction of copper(I) from aqueous solution containing picrate into carbon tetrachloride, chloroform, 1,2-dichloroethane and nitrobenzene with TTCT was examined, with the results shown in Table 2. The extractability of copper(I) decreases in the order of nitrobenzene > 1,2-dichloroethane > chloroform > carbon tetrachloride. This is consistent with the order of

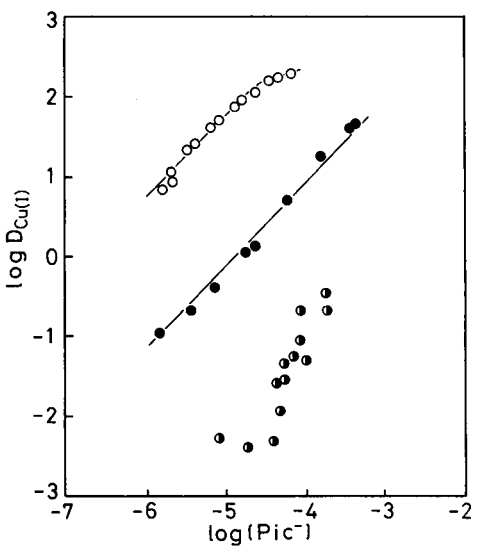

Fig. 6. Plots of log $D_{Cu(I)}$ vs. log[Pic^-] for various organic solvents at pH 4.5. Initial concentration: 5×10^{-5} M copper(I), 5×10^{-3} M TTCT. (○) 1,2-dichloroethane; (●) chloroform; (◑) carbon tetrachloride.

the dielectric constants of the solvents. The order is completely reversed in the case of TTCT extraction. In the case of nitrobenzene, copper(I) is extracted readily even at 5×10^{-5} M picrate, i.e., the same concentration as copper(I). In the case of carbon tetrachloride, yellow precipitates are formed at high picrate concentration, which suggests that the ion-pair is poorly soluble in such solvents of low dielectric constant.

The relationship of log $D_{Cu(I)}$ and log[Pic^-] at constant pH and TTCT concentration for each solvent is shown in Fig. 6. The extraction data for nitrobenzene are not included because the extractability of copper(I) was so high that the determination of copper by atomic absorption spectrometry was difficult at high picrate concentration and the determination of picrate by spectrophotometry was difficult at low picrate concentration. Figure 6 also shows that solvents with high dielectric constant favor the extraction of copper(I) with TTCT. Straight lines with slope of +1, obtained for 1,2-dichloroethane and chloroform, confirm that copper(I) is extracted as the 1:1 ion-pair. A log K_{ex} value of 9.0 ± 0.2 was obtained for 1,2-dichloroethane.

REFERENCES

1 C. J. Pedersen, J. Am. Chem. Soc., 89 (1967) 2495.
2 H. K. Frensdorff, J. Am. Chem. Soc., 93 (1971) 4684.
3 A. Sadakane, T. Iwachido and K. Toei, Bull. Chem. Soc. Jpn., 48 (1975) 60.
4 J. W. Mitchell and D. L. Sanks, Anal. Chem., 47 (1975) 642.
5 J. J. Christensen, D. J. Eatough and R. M. Izatt, Chem. Rev., 74 (1974) 351.
6 S. Ahrland, J. Chatt and N. R. Davies, Quart. Rev., London, 12 (1958) 265.
7 W. Rosen and D. H. Bush, J. Am. Chem. Soc., 91 (1969) 4694.
8 K. Travis and D. H. Bush, Inorg. Chem., 13 (1974) 2591.
9 E. R. Dockal, L. L. Diaddario, M. D. Glick and D. B. Rorabacher, J. Am. Chem. Soc., 99 (1977) 4530.
10 D. Sevdic and H. Mieder, J. Inorg. Nucl. Chem., 39 (1977) 1403.
11 D. Sevdic and H. Mieder, J. Inorg. Nucl. Chem., 39 (1977) 1409.
12 D. Sevdic, L. Fekete and H. Mieder, J. Inorg. Nucl. Chem., 42 (1980) 885.
13 R. G. Pearson, J. Am. Chem. Soc., 85 (1963) 3533.
14 J. O. Edwards, J. Am. Chem. Soc., 76 (1954) 1540.
15 S. Yamada and M. Tanaka, J. Inorg. Nucl. Chem., 37 (1975) 587.

Analytica Chimica Acta, 151 (1983) 457—463
Elsevier Science Publishers B.V., Amsterdam — Printed in The Netherlands

WATER-SOLUBLE PYRIDYLAZOANILINE REAGENTS FOR THE SPECTROPHOTOMETRIC DETERMINATION OF METALS
Determination of Iron(II) with 2-(5-bromo-2-pyridylazo)-5-(*N*-propyl-*N*-sulfopropylamino)aniline

DAIKICHI HORIGUCHI, MIKIHIKO SAITO, TOSHIAKI IMAMURA and KENYU KINA*

Dojindo Laboratories, 2861, Kengun-machi, Kumamoto-shi 862 (Japan)

(Received 13th October 1982)

SUMMARY

Three water-soluble pyridylazoaniline reagents were synthesized and their application as spectrophotometric reagents for iron(II), copper(II), nickel(II) and cobalt(III) was investigated. Of the three reagents, 2-(5-bromo-2-pyridylazo)-5-(*N*-propyl-*N*-sulfopropylamino)aniline (5-Br-PSAA) was found to be very sensitive (ϵ = 8.9 × 10^4 l mol^{-1} cm^{-1} at 558 nm, pH 4.3) and selective for iron(II). The iron(II) complex has a 1:2 metal/reagent ratio and, once formed, is not decomposed by EDTA, whereas the copper(II) and nickel(II) complexes are readily decomposed by EDTA. Thus, 5-Br-PSAA is useful for the determination of traces of iron(II) in biological samples, and is successfully applied to blood serum. The reagent is four times more sensitive than bathophenanthroline for iron(II). High sensitivity is also obtained for cobalt(III) in 3 M hydrochloric acid.

A new class of spectrophotometric reagents with ultra-high sensitivity for metals has been developed over the past 10 years. Most of these reagents are heterocyclic azo compounds with an electron-donating amino group in the *p*-position to the azo linkage of the basic heterocyclic azophenol skeletal structure [1—6]. Recently, water-soluble spectrophotometric reagents have been developed by introducing a sulfoalkyl group into the amino group of the mother reagent without sacrificing the original spectrophotometric sensitivity [7]. Wada and her colleagues [8, 9] have also developed a water-soluble reagent which is highly sensitive and selective for cobalt(III), by introducing a sulfomethyl group into the amino group of thiazolylazoaminobenzoic acid [8, 9].

The metal ion selectivity of heterocyclic azo compounds depends on the nature of the functional group in the *o*-position to the azo linkage of the phenylazo structure, and increases in the order of hydroxyl < carboxyl < amino group [10]. Thus, 2-(2-pyridylazo)-1,5-diaminobenzene derivatives would be expected to show some selectivity for metal ions as well as high sensitivity. This paper describes the syntheses of a series of water-soluble 2-(2-pyridylazo)-1,5-diaminobenzene derivatives.

0003-2670/83/$03.00

EXPERIMENTAL

Syntheses of reagents

Three water-soluble 2-(2-pyridylazo)-1,5-diaminobenzene derivatives were synthesized (Table 1). The procedures were similar for all three reagents and the synthesis of 2-(5-bromo-2-pyridylazo)-5-(*N*-propyl-*N*-sulfopropylamino)-aniline (5-Br-PSAA) is described below as an example.

N-*Propyl*-m-*nitroaniline*. *m*-Nitroaniline (25 g, 0.18 mol) and *n*-propyl bromide (44 g, 0.36 mol) were dissolved in 500 ml of ethanol, to which 20 g of potassium carbonate was added, and the mixture was refluxed for 50 h. After the reaction, the mixture was poured into hot water. The resulting oil was separated and dissolved in 40 ml of 6 M hydrochloric acid to give a white crystalline mass, which was eventually filtered and washed with 3 M hydrochloric acid. The cake was dissolved in 200 ml of water and the solution was neutralized with sodium carbonate to precipitate yellow crystals, which were recrystallized from isopropanol (m.p. 39—41°C; yield 8.4 g, 26%).

N-*Propyl*-N-*sulfopropyl*-m-*nitroaniline*. A mixture of *N*-propyl-*m*-nitroaniline (8 g, 0.044 mol) and propanesultone (5.4 g, 0.044 mol) was heated at 120—140°C for 5 h. The reaction mixture was dissolved in 50 ml of methanol, to which 100 ml of water was added. After extraction of unreacted starting material with ether, *N*-propyl-*N*-sulfopropyl-*m*-nitroaniline was obtained by evaporating the aqueous solution (yield 9.0 g, 63%).

2-(5-Bromo-2-pyridylazo)-5-(N-propyl-N-sulfopropylamino)aniline. *N*-propyl-*N*-sulfopropyl-*m*-nitroaniline (9 g, 0.028 mol) was reduced with tin in hydrochloric acid to obtain the corresponding amino derivative, which was then coupled with 5-bromo-2-aminopyridine diazotate (10 g, 0.045 mol) in the standard manner, by introducing carbon dioxide. The resulting precipitates were recrystallized from water (m.p. 235—40°C, decomp.; yield 3.4 g, 24%). Found 41.5% C, 4.7% H, 14.1% N; calcd. for $C_{17}H_{21}N_5O_3$—NaSBr·H_2O,

TABLE 1

Structure of water-soluble pyridylazoaniline reagents

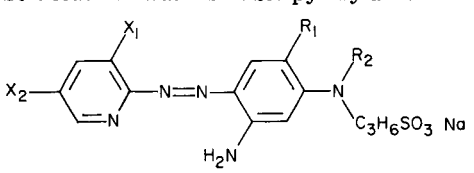

Compound	Abbreviation	Substituents			
		X_1	X_2	R_1	R_2
1	5-Br-PSAA	H	Br	H	n-C_3H_7
2	3,5-diBr-PSAA	Br	Br	H	n-C_3H_7
3	3,5-diBr-MSAA	Br	Br	CH_3	H

41.1% C, 4.7% H, 14.1% N. I.r. $\nu_{C=C(arom)}$ 1610 cm^{-1}, $\nu_{C=N}$ 1340 cm^{-1}, $\nu_{SO_2(asym)}$ 1200, 1140 cm^{-1}, $\nu_{SO_2(sym)}$ 1040 cm^{-1}. δ_{C-H} 830, 780, 710 cm^{-1}. ^{1}H-n.m.r. spectral data supported this structure.

The other reagents were prepared similarly. For 2-(3,5-dibromo-2-pyridylazo)-5-(*N*-propyl-*N*-sulfopropylamino)aniline (3,5-diBr-PSAA): m.p. 240—60°C, decomp.; i.r. $\nu_{C=C}$ 1610 cm^{-1}, $\nu_{C=N}$ 1355 cm^{-1}, $\nu_{SO_2(asym)}$ 1210, 1150 cm^{-1}, $\nu_{SO_2(sym)}$ 1040 cm^{-1}, δ_{C-H} 730 cm^{-1}. For 2-(3,5-dibromo-2-pyridylazo)-4-methyl-5-(*N*-sulfopropylamino)aniline (3,5-diBr-MSAA): m.p. 262—4°C; i.r. $\nu_{C=C}$ 1630 cm^{-1}, $\nu_{C=N}$ 1300 cm^{-1}, $\nu_{SO_2(asym)}$ 1180 cm^{-1}, $\nu_{SO_2(sym)}$ 1040 cm^{-1}. $\delta_{C=H}$ 720 cm^{-1}.

Reagent solutions and apparatus

The 5-Br-PSAA solution was prepared by dissolving 49.74 mg of the reagent in 100 ml of water to give a 1×10^{-3} M (M = mol l^{-1}) solution. Analytical-grade metal salts were dissolved in water to make 1×10^{-2} M stock solutions of the metal ions, which were standardized by complexometry. The stock solutions were diluted to appropriate concentrations as needed. All other reagents were of analytical grade.

A Shimadzu UV-210A recording spectrophotometer and a Horiba F-7LC pH meter were used.

Procedures

Determination of iron(II). Place 0—5 ml of 1×10^{-4} M iron(II) solution in a 50-ml volumetric flask. Add 2 ml of 0.1 M ascorbic acid solution, 5 ml of 1×10^{-3} M 5-Br-PSAA solution, and 2.5 ml of 1.0 M sodium acetate solution, and let the mixture stand for 2 min. To this, add 5 ml of 1.0 M acetic acid or 1.0 M hydrochloric acid and dilute the mixture to volume. Measure the absorbance of the resulting solution at 558 nm or 716 nm against the reagent blank using 1-cm cells.

Determination of iron(II) in human serum. Place 0.5 ml of serum in a centrifuge tube. Add 0.5 ml of water and 1 ml of deproteinizing solution which contains 7.5 g of trichloroacetic acid and 1.5 g of ascorbic acid in 100 ml of water. Mix well and centrifuge at 4000 rpm for 5 min. To a 1-ml aliquot of the supernatant liquid, add 1 ml of 1.0 M sodium acetate and 0.5 ml of 1×10^{-3} M 5-Br-PSAA, and let the mixture stand for 5 min. To this, add 0.5 ml of 0.01 M EDTA solution and measure the absorbance of the resulting solution against the reagent blank using 1-cm cells. Prepare the reagent blank by adding EDTA solution first, and then 5-Br-PSAA.

RESULTS AND DISCUSSION

The water-soluble pyridylazoaniline derivatives which were prepared in this study react with iron(II), cobalt(III), copper(II) and nickel(II) to form red metal complexes. The resulting complexes are soluble in water and these metal ions can be determined spectrophotometrically in aqueous solution

without solvent extraction. The 5-Br-PSAA reagent was studied in detail, as it was found to be the most sensitive among the reagents synthesized.

Visible absorption spectra of metal complexes

The spectral characteristics of the metal complexes with these reagents at their optimum pH ranges are summarized in Table 2. The monobromo derivative is slightly more sensitive than the dibromo derivative, and the absorption maximum of its metal complexes appear at shorter wavelengths.

The introduction of a methyl group to the 4-position of the phenyl ring as in the case of 3,5-DiBr-MSAA, generally results in the decrease of sensitivity. It is well known that the unusually high molar absorptivity of *p*-aminophenylazo reagents is due to the charged quinoid structure of the chromophore. A methyl group ortho to the amino group sterically hinders the coplanarity of the substituted amino group with the phenyl ring, resulting in decreased molar absorptivity. Thus, 5-Br-PSAA proved to be the most sensitive reagent for copper(II), iron(II), cobalt(III) and nickel(II).

Metal complexes with 5-Br-PSAA

The visible absorption spectra of metal complexes with 5-Br-PSAA are illustrated in Fig. 1. Absorption maxima with shoulders are observed in the range 500—600 nm for the complexes with copper(II), cobalt(III) and nickel(II), whereas double maxima are observed at 558 nm and 716 nm for the iron(II) complex. It is clear that iron(II) can be determined selectively at 716 nm where the absorptions by other metal complexes do not overlap. The molar absorptivity of the iron(II) complex at 716 nm is 4.2×10^4 l mol^{-1} cm^{-1}. Iron(III), in the presence of an oxidizing agent such as potassium periodate, does not form a colored complex with 5-Br-PSAA.

The iron(II) and cobalt(III) complexes are so inert that, once formed, they cannot be decomposed by EDTA. Therefore, iron(II) can be determined selectively with high sensitivity at 558 nm in the presence of nickel(II) and copper(II), if EDTA is added after the complex formation with 5-Br-PSAA. The molar absorptivity of iron(II) complex at this wavelength is 8.9×10^4 l mol^{-1} cm^{-1}.

TABLE 2

Spectral characteristics of water-soluble pyridylazoaniline reagents and their metal complexes

Reagents	λ_{max} (ϵ, 10^4 l mol^{-1} cm^{-1}) pH				
	Free reagent	Cu(II)	Fe(II)	Co(III)	Ni(II)
5-Br-PSAA	457(4.7)4.3	577(6.5)4.3	558(8.9)4.3	602(8.8)4.3	568(11.2)7.3
3,5-diBr-PSAA	450(2.8)2.9	595(4.7)2.9	581(8.6)4.3	619(8.6)2.9	591(5.8)7.3
3,5-diBr-MSAA	433(3.0)2.9	575(4.1)2.9	566(7.9)4.3	600(7.4)2.9	572(4.6)7.3

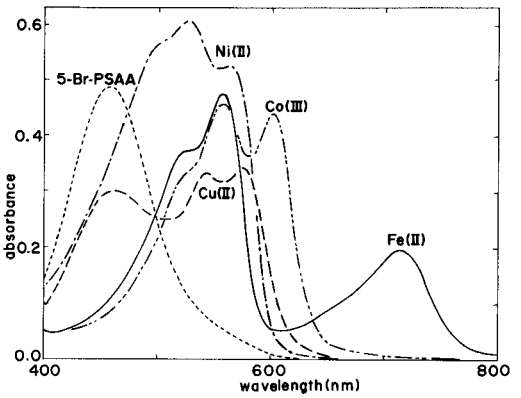

Fig. 1. Absorption spectra of metal complexes of 5-Br-PSAA (5×10^{-6} M metal ion, 1×10^{-5} M reagent, pH as in Table 2).

Effect of pH

The pH dependencies of complex formation with 5-Br-PSAA are illustrated in Fig. 2. It can be seen that the complexes of copper(II) and nickel(II) are completely formed at pH 4—6 and 6.5—9, respectively. The absorbance of the cobalt(III) complex becomes constant at pH 3—4, but increases with increasing acidity; the molar absorptivity becomes as high as 12.4×10^4 l mol^{-1} cm^{-1} (at 618 nm) in 3 M hydrochloric acid. Such an unusually high absorptivity has also been reported [11] for 5-Cl-PADAB, and was attributed by Shibata et al. [11] to the charged quinoid structure of the chromophore.

The iron(II) complex is formed rather slowly at pH <5, and the extent of complexation after 1 h is shown by the broken line in Fig. 2. Yet the complex

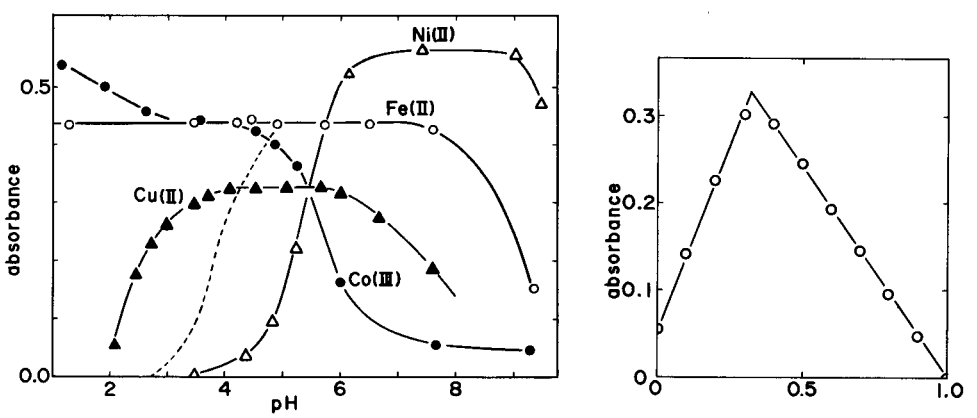

Fig. 2. Effect of pH on the absorbance of metal—5-Br-PSAA complexes (4×10^{-5} M 5-Br-PSAA, 5×10^{-6} M metal).

Fig. 3. Continuous variations study of the iron—5-Br-PSAA complex; (Fe) + (5-Br-PSAA) = 1×10^{-5} M, pH 4.3.

TABLE 3

Influence of diverse ions on the determination of 1×10^{-5} M iron(II)[a]

Ions	Amount (M)	Absorbance (558 nm)	Ions	Amount (M)	Absorbance (558 nm)
None	—	0.888	Ni(II) + EDTA	1×10^{-5}	0.888
None + EDTA[a]	—	0.888	Co(III) + EDTA	1×10^{-5}	1.488
Cu(II) + EDTA	1×10^{-5}	0.891	Zn(II)	1×10^{-3}	0.885

[a] 2×10^{-4} M EDTA, 4×10^{-5} M 5-Br-PSAA, pH 4.3.

formation is very fast in the neutral region, and the complex, once formed, is stable even in strongly acidic solution. The ligand exchange reaction of the iron(II) complex is so slow that it is not decomposed by EDTA. The acid dissociation behavior of 5-Br-PSAA was observed from the pH dependence of the absorption spectra of the reagent itself; the estimated acidity constants are pK_{a_1} and $pK_{a_2} < 2$ and $pK_{a_3} = 6.1$. These values are in good accord with those for a series of pyridylazodiaminobenzene reagents [12].

The continuous variations study of the iron(II)—5-Br-PSAA complex (Fig. 3) shows that the metal/ligand ratio of the complex is 1:2 and that the complex is fairly stable.

Effect of diverse ions

The extent of interferences by diverse ions on the determination of iron(II) is summarized in Table 3. As noted above, the iron(II) and cobalt(III) complexes are not decomposed by EDTA, whereas the copper(II) and nickel(II) complexes are. Accordingly, iron(II) can be determined in the presence of copper(II) and nickel(II), but cobalt must be separated previously by extraction with nitrosophenol reagents [13]. Zinc does not form a complex with 5-Br-PSAA, so that even 100-fold amounts do not interfere. Iron(III) does not react and copper(II) can be determined with 5-Br-PSAA in its presence.

Determination of iron in serum

Iron in human serum was determined spectrophotometrically with 5-Br-PSAA. The mean result of five assays of one serum was 2.27 μg ml^{-1} (r.s.d. 1.8%, $n = 5$) whereas the mean result was 2.15 μg ml^{-1} (r.s.d. 4.0%, $n = 3$) by the bathophenanthroline method which has been adopted as the international standard analytical method for serum iron. The results are in good agreement.

The authors express their gratitude to Professor Keihei Ueno for helpful discussions.

REFERENCES

1 S. Shibata, M. Furukawa and K. Toei, Anal. Chim. Acta, 66 (1973) 397.
2 E. Kiss, Anal. Chim. Acta, 66 (1973) 385.
3 S. Shibata, M. Furukawa and K. Goto, Anal. Chim. Acta, 71 (1974) 85.
4 S. Shibata, M. Furukawa and E. Kamata, Anal. Chim. Acta, 73 (1974) 107.
5 S. Shibata, E. Kamata and R. Nakashima, Anal. Chim. Acta, 82 (1976) 169.
6 D. A. Johnson and T. M. Florence, Talanta, 22 (1975) 253.
7 T. Makino, M. Saito, D. Horiguchi and K. Kina, Clin. Chim. Acta, 120 (1982) 127.
8 T. Ishizuki, H. Wada and G. Nakagawa, Bunseki Kagaku, 28 (1979) 535.
9 H. Wada, T. Ishizuki and G. Nakagawa, Anal. Chim. Acta, 135 (1982) 333.
10 M. Furukawa and S. Shibata, Bunseki, (1980) 330.
11 S. Shibata, M. Furukawa, Y. Ishiguro and S. Sasaki, Anal. Chim. Acta, 55 (1971) 231.
12 S. Shibata and M. Furukawa, Bunseki Kagaku, 23 (1974) 1412.
13 S. Motomizu, Bunseki Kagaku, 20 (1971) 1507.

Analytica Chimica Acta, 151 (1983) 465—472
Elsevier Science Publishers B.V., Amsterdam — Printed in The Netherlands

EXTRACTION—SPECTROPHOTOMETRIC DETERMINATION OF BORON WITH MANDELIC ACID AND MALACHITE GREEN

SHIGEYA SATO

Faculty of Education, Kumamoto University, 2-40-1, Kurokami, Kumamoto 860 (Japan)

(Received 7th December 1982)

SUMMARY

Several α-hydroxy acids are examined as complexing agents for the extraction—spectrophotometric determination of boron. Mandelic acid is the most useful. The boron-complex anion obtained is extracted into benzene with malachite green in a single extraction; boron is determined indirectly by measuring the absorbance of malachite green in the extract at 633 nm. The calibration graph is linear over the range 7.50×10^{-7}—1.50×10^{-5} mol l^{-1} boron; the apparent molar absorptivity is 6.52×10^{4} l mol^{-1} cm^{-1}. The method is applied to the determination of micro amounts of boron in natural waters with satisfactory results.

The analytical chemistry of boron is very important in the fields of nuclear energy, pharmacy and agriculture, and many spectrophotometric methods for its determination have been reported [1]. Many of these methods are very sensitive but tend to be troublesome, and most recent research [2—9] has been concentrated on the extraction of ion-pairs formed between boron-complex anions and large colored cations following the method of Ducret [10—12]. Some boron complexes with α-diols have been tested in such methods. Thus, Vlacil and Drbal [6] extracted boron into butanol with 2,3-dihydroxynaphthalene and diphenylguanizium chloride, and different methods based on α-diols and crystal violet have been investigated [7—9]. When 2,3-dihydroxynaphthalene was used to complex boron, it was extracted along with the boron complex [9], and back-washing with a strongly alkaline solution was needed to remove the excess of reagents; this was also a disadvantage in earlier procedures [2—4]. The hydrobenzoin method [8] did not require the removal of the excess of reagent, but the boron—hydrobenzoin complex anion was unstable.

In further work on these systems, the complex formation of boron with several α-hydroxy acids was investigated because of their solubility in water. It was found that mandelic acid reacted with boric acid in weakly acidic medium at room temperature to form a complex anion which could be extracted with a cationic dye into an organic solvent with less blank absorbance. The extracted species, moreover, was quite stable.

0003-2670/83/$03.00

EXPERIMENTAL

Apparatus and reagents

Hitachi Model 100-10 and Model 624 digital spectrophotometers were used with 10-mm glass cells. An Iwaki Model V-DN Type KM shaker and a Hitachi centrifuge 03P were also used. The pH values were measured with a Hitachi-Horiba M-3 pH meter.

A standard boron stock solution (2.00×10^{-2} mol l^{-1}) was prepared by dissolving boric acid in deionized water; working solutions were prepared by dilution. Cationic dyes were dissolved in deionized water to give 1.0×10^{-3} mol l^{-1} solutions. The 1.0×10^{-1} mol l^{-1} solution of mandelic acid in deionized water was adjusted to pH 3.0 with sodium hydroxide solution. The other α-hydroxy acid solutions were 1.0×10^{-1} or 1.0×10^{-2} mol l^{-1}. Deionized water was used throughout. Other than the dyes, the reagents were of analytical-reagent grade.

Procedures

Preliminary tests. Place an aliquot of the boron solution (1.00×10^{-4} mol l^{-1}) in a stoppered 10-ml test tube. Add 1.0 ml of α-hydroxy acid solution (0.1 or 0.01 mol l^{-1}) and 1.0 ml of cationic dye solution (1.0×10^{-3} mol l^{-1}). Dilute the mixed solution to 4 ml with water and shake the solution with 4 ml of organic solvent for 10 min with a KM shaker. After phase separation, measure the absorbance of the organic phase against solvent as reference.

Recommended procedure with mandelic acid. Place an aliquot of the sample or standard solution containing up to 0.65 μg of boron in a stoppered 10-ml test tube. Add 1.0 ml of the specified mandelic acid solution and 1 ml of malachite green solution (1.0×10^{-3} mol l^{-1}). Dilute the mixed solution to 4 ml with water and shake the solution with 4 ml of benzene for 10 min. After phase separation, measure the absorbance of the organic phase at 633 nm, using a 10-mm glass cell, against benzene as reference.

RESULTS AND DISCUSSION

Complexing agents for boron

Boron reacts with various α-diols to form five-membered monovalent anions, which can be extracted with a cationic dye into an organic solvent, so that boron can be determined indirectly by measuring the absorbance of the extracted dye. When 1,2-dihydroxybenzene (catechol) or 2,3-dihydroxynaphthalene was used, the absorbance of the blank extract was excessive unless the extracted ion-pair of the reagent with the cationic dye was first back-washed from the organic phase. Yet when an aliphatic diol such as pinacol (tetramethylethane-1,2-diol) was used, the complex anion formed [13] could not be extracted into any solvent. When hydrobenzoin (1,2-diphenylethane-1,2-diol) was used, boron could be determined in a single extraction without removal of the excess of reagents, but the extracted

boron complex was unstable. To improve this point, di-(4-pyridyl)-glycol and derivatives of 1,2-diphenylethane-1,2-diol which possessed electron-releasing groups (dimethoxy, methoxy, dichloro and dimethylamino) were synthesized [14, 15]. It was found that these compounds gave more stable extracts but poorer sensitivities. These results indicated that a reagent with a reasonable solubility in water and hydrophobic group was necessary.

α-Hydroxy acids were therefore examined: glycolic acid, lactic acid, 2-hydroxyisobutyric acid, 2-hydroxy-2-methylbutyric acid, 2-hydroxyisocaproic acid, mandelic acid, benzilic acid, *p*-chloromandelic acid, *p*-hydroxymandelic acid and 4-hydroxy-3-methoxymandelic acid. For each of these acids, different combinations of extracting solvents and cationic dyes were examined. From the relationship between the apparent molar absorptivity (ϵ) and the absorbance of the reagent blank obtained, the acids can be classified into four groups. First, the boron complex with glycolic acid and lactic acid cannot be extracted into any solvent. Second, the boron complex can be extracted with an apparently good sensitivity but the absorbance of the reagent blank is very high (0.40); this happened with 4-hydroxy-3-methoxymandelic acid in an ethyl violet—benzene system, and with 2-hydroxyisobutyric acid in a crystal violet—chlorobenzene system. In the third group, the absorbance of the reagent blank is low (0.20); systems of this type were *p*-chloromandelic acid—malachite green—toluene, 2-hydroxy-2-methylbutyric acid—malachite green—chlorobenzene and 2-hydroxyisocaproic acid—malachite green—benzene. The fourth group comprises systems with very low reagent blank absorbances (0.10); these were the mandelic acid—malachite green—benzene and benzilic acid—methylene blue—toluene systems.

Mandelic acid and benzilic acid were the most suitable reagents for boron. In the case of benzilic acid, however, a long time (ca. 60 min) was needed to achieve constant extraction of the boron-complex anion, possibly because of the low solubility of the reagent in water. Accordingly, mandelic acid was preferred as the complexing agent.

Extracting solvent and cationic dye

Various solvents and dyes were examined to achieve the best determination of boron. The solvents examined were 4-methyl-2-pentanone, 1,2-dichloroethane, dichloromethane, *o*-dichlorobenzene, chloroform, toluene, carbon tetrachloride, benzene, n-hexane and cyclohexane; the dyes tested were ethyl violet, crystal violet, malachite green and methylene blue.

The solvents can be classified into three groups: (1) the cationic dye itself is easily extracted without mandelic acid (4-methyl-2-pentanone, 1,2-dichloroethane, dichloromethane, chloroform and *o*-dichlorobenzene); (2) the ion-pair formed between the boron-complex anion and the dye is extracted (chlorobenzene, benzene and toluene); (3) the ion-pair formed between the boron-complex anion and the dye is not extracted (carbon tetrachloride except for the ethyl violet system, n-hexane and cyclohexane). Accordingly, the group 2 solvents and carbon tetrachloride were examined further. Table 1

TABLE 1

The reagent blank and the apparent molar absorptivity (ϵ) with selected solvents and dyes

Solvent		Ethyl violet	Crystal violet	Malachite green	Methylene blue
Chlorobenzene	blank	—[a]	0.46	0.10	0.17
	ϵ		2200	17400	52000
Benzene	blank	—[a]	0.25	0.10	0.20
	ϵ		19000	65200	15000
Toluene	blank	0.13	0.15	0.23	0.08
	ϵ	4500	12000	13000	5000
Carbon tetrachloride	blank	0.18	—[b]	—[b]	—[b]
	ϵ	12000			

[a]The absorbance of the reagent blank was very high. [b]The ion-pair formed between the boron-complex anion and the dye was not extracted.

shows the practical results obtained by using these solvents. It is clear that the method based on malachite green and benzene should be the most suitable for the determination of boron. The method recommended in the Experimental part was therefore worked out.

The absorption spectra of the reagent blank and the ion-pair formed between the boron complex and malachite green in benzene are shown in Fig. 1. Malachite green itself was not extracted into benzene irrespective of the presence or absence of boron, when mandelic acid was absent. The wavelength of maximum absorption of each spectrum occurs at 633 nm.

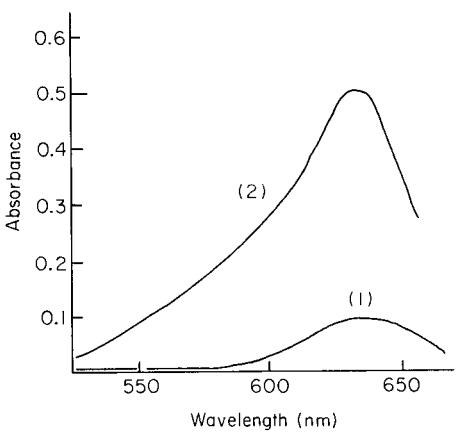

Fig. 1. Absorption spectra: (1) reagent blank; (2) 6.25×10^{-6} mol l^{-1} boric acid. Conditions: 2.5×10^{-4} mol l^{-1} malachite green, 2.5×10^{-2} mol l^{-1} mandelic acid, pH 3.0; benzene as reference.

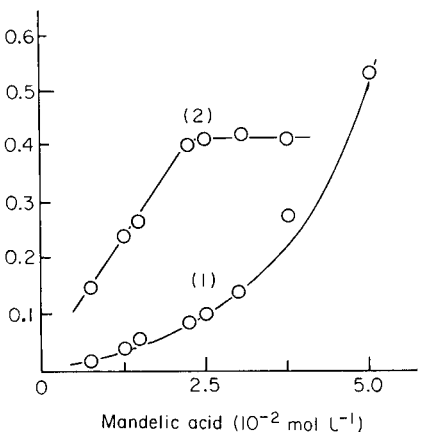

Fig. 2. Effect of mandelic acid concentration: (1) reagent blank; (2) net absorbance for 6.25×10^{-6} mol l^{-1} boric acid. Other conditions as for Fig. 1.

Effects of experimental variables

A series of mandelic acid solutions (0.1 mol l^{-1}) of various pH values were prepared by adding dilute phosphoric acid or sodium hydroxide solution. The results obtained showed that there was maximum constant absorbance in the organic phase over the pH range 2.0—4.5 when the reagent blank solution served as reference. As the mandelic acid solution adjusted to pH 3.0 has some buffering action, it is not necessary to add another buffer. Accordingly, 1 ml of 0.1 mol l^{-1} mandelic acid solution adjusted to pH 3.0 is recommended.

When the malachite green concentration was increased, the absorbance of the reagent blank increased slowly but the net absorbance reached a constant plateau at concentrations exceeding 2.0×10^{-4} mol l^{-1}. The concentration of malachite green was fixed at 2.5×10^{-4} mol l^{-1}.

The effect of the mandelic acid concentration was examined, with the results shown in Fig. 2. Increasing the mandelic acid concentration led to increased absorbance of both reagent blank and sample extracts, but maximum constant extraction was obtained with more than 2.3×10^{-2} mol l^{-1} mandelic acid when the reagent blank served as reference. The concentration of mandelic acid was, therefore, fixed at 2.5×10^{-2} mol l^{-1} to keep the blank low.

An extraction time of about 8 min was necessary to attain constant absorbance. For routine work, it was fixed at 10 min for security.

Calibration graph

The calibration graph obtained by the standard procedure was linear over the range 7.50×10^{-7}—1.50×10^{-5} mol l^{-1} boron (8—162 μg l^{-1}) in the aqueous phase. The apparent molar absorptivity calculated from the slope of the graph was 6.52×10^{4} l mol^{-1} cm^{-1}. It was not affected by the temperature of the extraction over the range 10—25°C, although the absorbance of the reagent blank depended on temperature (0.10 at 25°C, 0.05 at 10°C) against a benzene reference. The coefficient of variation was 3.8% in absorbance for eight runs at 6.25×10^{-6} mol l^{-1} boron. The absorbance of the organic phase did not vary during at least 60 min. Furthermore, when the volume of extracting solvent was halved, the apparent molar absorptivity almost doubled compared to the standard procedure, although the absorbance of the reagent blank was 0.20.

Effect of diverse ions

Table 2 shows the recovery of boron in a series of solutions containing 6.25×10^{-6} mol l^{-1} boron and various ions likely to be present in river and sea water. Perchlorate and thiocyanate caused large positive errors in 10-fold amounts compared to boron, but chloride, nitrate, sulfate and phosphate did not interfere even at high concentrations. Fluoride did not interfere even when added at a high ratio, presumably because of the rapidity of the procedure. Iron(II) did not interfere at quite high concentrations; interferences of

TABLE 2

Effect of diverse ions on the recovery of 6.25×10^{-6} mol l^{-1} boric acid

Ion[a]	Mole ratio	Recovery (%)	Ion	Added as	Mole ratio	Recovery (%)
F^-	500	103	Ca^{2+}	$CaCl_2$	200	102
	1000	74			500	108
Cl^-	2000[b]	101	Mg^{2+}	$MgSO_4$	200	104
Br^-	10[b]	96			500	113
I^-	10[b]	101	Fe^{2+}	Mohr salt	1000[b]	98
ClO_4^-	1	102	Fe^{3+}	Fe-alum	1	100
	10	201			10	90
SCN^-	1	100			1000[c]	101
	10	137	Al^{3+}	Al-alum	1	99
NO_3^-	2000[b]	97			10	113
SO_4^{2-}	1000[b]	102			1000[c]	97
$H_2PO_4^-$	1000[b]	100				

[a]Added as sodium or potassium salts. [b]Maximum concentration tested. [c]In the presence of 1.0×10^{-2} mol l^{-1} EDTA.

iron(III) and aluminum were eliminated by adding EDTA to the sample solution at a concentration of 1.0×10^{-2} mol l^{-1}. Thus no pretreatment of water samples should be needed for this determination of boron.

Application to the determination of boron in natural waters

The proposed method was applied to the determination of boron in river and sea waters in Kumamoto Prefecture, Japan. Samples were filtered through a Millipore filter (0.45 μm), and the filtered sea samples were diluted 10-fold with distilled water. These samples (1.5 ml of river or 0.5 ml of sea samples) were used for the standard procedure. The results obtained are shown in Table 3, together with the data obtained by a well-known methylene blue method [10]. The values obtained are in good agreement. The recovery of boron was examined by adding known amounts of boron (6.25×10^{-6} mol l^{-1}) to the sample solution; the results (Table 3) show that the boron in natural waters is quantitatively extracted into benzene.

CONCLUSION

The evaluation of organic complexing agents, cationic dyes and extracting solvents enabled a sensitive and simpler extraction—spectrophotometric determination method of boron to be developed. The main results are compared in Table 4, together with the results for some α-diols. The new recommended method with malachite green, mandelic acid and benzene seems to be the best for the extraction—spectrophotometric determination method of micro amounts of boron.

TABLE 3

Determination of boron in sea and river water from Kumamoto Prefecture and recovery of boron

Sample[a]	Boron[b] ($\mu g\ l^{-1}$)	Recovery test			Comparative boron value[d] ($\mu g\ l^{-1}$)
		Boron in sample (μg)	Found[c] (μg)	Recovery (%)	
Sea water near the shore					
at Ushibuka	3140 ± 40	0.157	0.425	99	3100
at Misumi	4110 ± 150	0.206	0.468	96	4000
at Oda	4320 ± 160	0.216	0.482	98	4200
River water					
Shirakawa (A)	82.2 ± 3.7	0.123	0.385	97	
Shirakawa (B)	72.6 ± 3.2	0.109	0.384	102	
Midorikawa	25.9 ± 1.3	0.039	0.320	104	

[a]0.5 ml of sea samples diluted 10-fold, and 1.5 ml of river water were taken. [b]Mean of five determinations. [c]0.270 μg of boron was added to each sample. [d]By the methylene blue method [10].

TABLE 4

Comparison of methods for the extraction—spectrophotometric determination of boron

Complexing agent	Mandelic acid	Benzilic acid	Naphthalene 2,3-diol[a]	Hydrobenzoin[b]
Cationic dye	Malachite green	Methylene blue	Crystal violet	Crystal violet
Solvent	Benzene	Toluene	Benzene	Benzene
Apparent molar absorptivity	65200	60300	88000	30000
Reagent blank	0.10	0.09	0.10	0.20
Shaking time (min)	10	60	30	2
Stability of color in the extract	stable	stable	stable	unstable
Washing org. phase	none	none	necessary	none
Interference[c]	none	none	none	Cl^-, Ca^{2+}, Mg^{2+}

[a]Ref. 9. [b]Ref. 8. [c]From diverse ions normally present in natural waters.

The simple, rapid procedure requires only common equipment, and no evaporation to dryness or removal of the excess of reagent is necessary. The procedure is highly selective with little interference from other ions normally present in natural waters. The sensitivity is good (1.7×10^{-4} μg B cm^{-2} for

$\log(I_0/I)$ = 0.001 at 633 nm) and the reagent blank is low. Finally, the reproducibility is good because of the stability of color in the extract.

The author expresses his thanks to Professor Y. Yamamoto of Hiroshima University for his kind guidance and helpful discussions. The author is also indebted to Professor S. Uchikawa of Kumamoto University for his useful suggestions and warm encouragement.

REFERENCES

1 See, e.g., Z. Marczenko, Spectrophotometric Determination of Elements, Horwood, Chichester, 1976.
2 K. Kuwada, S. Motomizu and K. Toei, Anal. Chem., 50 (1978) 1788.
3 T. Korenaga, S. Motomizu and K. Toei, Analyst, 103 (1978) 745.
4 T. Korenaga, S. Motomizu and K. Toei, Anal. Chim. Acta, 120 (1980) 321.
5 M. Oshima, K. Fujimoto, S. Motomizu and K. Toei, Anal. Chim. Acta, 134 (1982) 73.
6 F. Vlacil and K. Drbal, Collect. Czech. Chem. Commun., 41 (1976) 1169.
7 S. Sato and S. Uchikawa, Jpn. Analyst, 29 (1980) 729.
8 S. Sato and S. Uchikawa, Jpn. Analyst, 31 (1982) 479.
9 S. Sato and S. Uchikawa, Anal. Chim. Acta, 143 (1983) 283.
10 L. Ducret, Anal. Chim. Acta, 17 (1957) 213.
11 S. Utsumi, S. Ito and A. Isozaki, Nippon Kagaku Zasshi, 86 (1965) 921.
12 L. Pasztor, J. D. Bode and Q. Fernando, Anal. Chem., 32 (1960) 277.
13 J. Dale, J. Chem. Soc., (1961) 922.
14 L. F. Fieser, Organic Experiments, Maruzen Asian edn., Maruzen, Tokyo, 1959, p. 211.
15 R. Adams and C. S. Marvel, Org. Synth. Coll., 1 (1941) 94.

Analytica Chimica Acta, 151 (1983) 473—477
Elsevier Science Publishers B.V., Amsterdam — Printed in The Netherlands

Short Communication

ENZYMATIC DETERMINATION OF NICOTINAMIDE ADENINE DINUCLEOTIDE PHOSPHATE WITH A SILVER SULFIDE MEMBRANE ELECTRODE

SAAD S. M. HASSAN[a] and G. A. RECHNITZ*

Department of Chemistry, University of Delaware, Newark, DE 19711 (U.S.A.)

(Received 14th September 1982)

Summary. A simple, sensitive and selective method is proposed for the determination of nicotinamide adenine dinucleotide phosphate (NADPH) in the concentration range 10^{-4}—10^{-7} mol l^{-1} (90 μg—90 ng ml^{-1}). The method is based on monitoring with a silver sulfide membrane electrode the concentration of the reduced glutathione released at pH 8 by reaction of oxidized glutathione with NADPH in the presence of glutathione reductase. Calibration data for 10^{-4}—10^{-7} mol l^{-1} range of NADPH yielded a least-squares equation of (ΔE, mV) = (36.65 ± 0.15) log C + 264.93 ± 0.1 with a standard error of 0.4 mV. Other common nucleotides including $NADP^+$ do not interfere.

The determination of pyridine nucleotides is usually approached by spectroscopic methods [1—4]. Some of these techniques are sufficiently sensitive to quantify 10^{-10} mol l^{-1} or less of these nucleotides, but most tend to suffer from complications. Electroanalytical techniques can provide alternative approaches, and amperometric [5], voltammetric [6] and potentiometric [7] methods have been proposed. Of these, the potentiometric method [7] is the simplest and most selective, being based on enzymatic decarboxylation of malate followed by measurement of the rate of carbon dioxide liberation as a function of $NADP^+$ concentration with the pCO_2 electrode [7]. The method is, however, applicable only to the oxidized form of nicotinamide adenine dinucleotide phosphate in the range 2×10^{-4}—5×10^{-6} mol l^{-1}.

In previous work [8], a potentiometric method was suggested for the determination of oxidized glutathione by reaction with glutathione reductase and measurement of the reduced glutathione with a silver sulfide membrane electrode. Because this reaction is selectively initiated by the reduced form of nicotinamide adenine dinucleotide phosphate and the sulfide electrode displays a high sensitivity and fast response for reduced glutathione, the present investigation was undertaken to develop a simple, sensitive and selective determination of NADPH. The reaction and measurement conditions

[a]Present address: Department of Chemistry, Faculty of Science, Ain Shams University, Cairo, Egypt.

0003-2670/83/$03.00

were optimized to permit measurement of NADPH with good accuracy and minimal interferences from other nucleotides at levels of 10^{-7} mol l^{-1}.

Experimental

Reagents. All the reagents used were of reagent grade unless otherwise stated and deionized water was used throughout.

Nicotinamide adenine dinucleotide phosphate (tetrasodium salt, reduced form), reduced and oxidized glutathione and all other nucleotides investigated were from Sigma Chemical Co. Glutathione reductase working solution (138.8 IU ml^{-1}) was prepared by 10-fold dilution of the commercially available enzyme E.C.1.6.4.2 (1388 IU ml^{-1}) from yeast. Aqueous 10^{-2} mol l^{-1} stock solutions of oxidized glutathione and NADPH were freshly prepared daily and stored in crushed ice until used.

Apparatus. A silver sulfide membrane electrode (Orion Model 94-16) was used with a single-junction reference electrode (Orion Model 90-01), a Corning Model 12 pH/mV meter and a Heath-Schlumberger SR-210 strip chart recorder. The reaction cells were thermostated with a Haake Model FS bath.

Procedure. Mixtures of 4 ml of 0.1 mol l^{-1} Tris—HNO_3 buffer of pH 8, 15 μl of glutathione reductase solution (138.8 IU ml^{-1}) and 100 μl of 10^{-2} mol l^{-1} oxidized glutathione were transferred to a 25-ml double-jacketed reaction cell thermostated at 25 ± 0.1°C and containing a small teflon-covered magnet. The silver sulfide and reference electrodes were immersed in the solution and the potential was allowed to reach a stable reading. The speed of the chart recorder was adjusted at 0.25 cm min^{-1}. Then, 10-μl aliquots of 10^{-2}—10^{-4} mol l^{-1} NADPH were added, each in a separate experiment. The potential change was recorded until a steady reading was obtained. A blank experiment was done under identical conditions. The change in potential (ΔE) at 10 min was plotted as a function of the logarithm of NADPH concentration and the plot was used for subsequent measurement of unknown NADPH samples in the concentration range 10^{-4}—10^{-7} mol l^{-1} (90 μg—90 ng ml^{-1}). The electrode was soaked in 0.1 mol l^{-1} Tris—HNO_3 buffer of pH 4 between measurements; this procedure serves to restore the starting potential.

Results and discussion

The reduced glutathione (GSH) released by the action of glutathione reductase on oxidized glutathione (GSSG) [9] was monitored as a function of nicotinamide adenine dinucleotide phosphate:

$$GSSG + NADPH + H^+ \xrightarrow[\text{Reductase}]{\text{Glutathione}} 2\ GSH + NADP^+ \qquad (1)$$

The relationship between the potential change of the electrode system and the concentration of GSH in pure solutions was examined at 25° C in 0.1 mol l^{-1} Tris—HNO_3 buffer solution of pH 4—9. The relation between ΔE and the logarithm of GSH concentration in the range 10^{-4}—10^{-7} mol l^{-1} was linear

with an average slope of 40 mV per concentration decade. It has been reported that the response characteristics of the silver sulfide membrane electrode for thiols depend on both the ratio with which the thiol compounds react with silver ion and the formation constant of the reaction products [10]. This commonly results in non-Nernstian slopes [10]. The response time of the electrode was relatively fast (ca. 5 min) at pH 8—9 without any significant response to GSSG at concentrations of 10^{-3} mol l^{-1}.

Enzyme activity and GSSG concentration. A series of 0.1 mol l^{-1} Tris—HNO_3 buffer solutions of pH 8 containing various mole ratios of NADPH and GSSG in the concentration range 10^{-4}—10^{-7} mol l^{-1} was allowed to react in the presence of 0.5—1.0 IU ml^{-1} glutathione reductase and the potential change at 10 min was measured. Typical recorded signals are shown in Fig. 1. The results showed that 1.8 mol of GSH is reproducibly released per mol of NADPH in the presence of at least 1 mol of GSSG. Thus, 2.5 × 10^{-4} mol l^{-1} GSSG was used throughout this study to quantify the nucleotide up to 10^{-4} mol l^{-1}. Increasing the enzyme activity by a factor of 4 did not significantly affect the overall potential change (Fig. 2) but increased the blank to the equivalent of about 30 ng ml^{-1} GSH. Addition of 10^{-3} mol l^{-1} phosphate or chloride ions to 10^{-4}—10^{-7} mol l^{-1} GSSG solutions affected the starting potential but not the ΔE value obtained after initiation of the enzymatic reaction.

Temperature and pH. The temperature dependence of the reaction was studied in the range 20—40° C with the results shown in Fig. 3. The GSH concentration increased with decreasing temperature with maximum change between 20 and 25° C. The pH profile at 25° C under similar conditions showed maximum change in the pH range 5.5—7.5 (Fig. 4), a finding which agrees well with previous reports [11]. The enzymatic reaction, however,

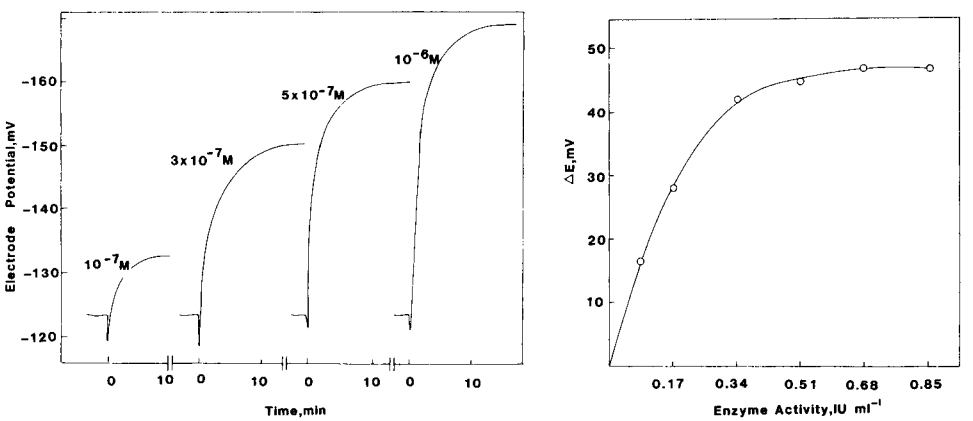

Fig. 1. Typical response curves for NADPH (0.5 IU ml^{-1} glutathione reductase and 2.5 × 10^{-4} mol l^{-1} GSSG at pH 8 and 25° C).

Fig. 2. Effect of glutathione reductase activity on the reaction of 2.5 × 10^{-4} mol l^{-1} GSSG and 10^{-6} mol l^{-1} NADPH at pH 8 and 25° C; ΔE at 10 min.

becomes faster, as indicated by the electrode response, as the pH increases. Subsequent measurements were made at pH 8 in order to take advantage of fast electrode response for reduced glutathione and the maximal buffer capacity.

Sequence of reagent addition. Two series of experiments at pH 8 and 25°C were conducted with identical concentrations of the reactants (2.5×10^{-4} mol l^{-1} GSSG, 10^{-6} mol l^{-1} NADPH, and 0.5 IU ml^{-1} glutathione reductase). The first series involved incubation of the NADPH and enzyme until attainment of a steady potential reading followed by addition of GSSG and measurement of GSH concentration. In the second set of experiments, GSSG and the enzyme were incubated and NADPH was added after establishment of a steady potential. These experiments gave almost identical results but the blank value obtained with the first set was much higher (equivalent to about 5 ng ml^{-1} GSH).

Accuracy and selectivity. For the conditions described above, the relationship between the change of the electrode potential (ΔE) at 10 min and the logarithm of NADPH concentration in the 10^{-4}—10^{-7} mol l^{-1} range was linear. The regression equation for NADPH data is (ΔE, mV) = (36.65 ± 0.15)log C + 264.93 ± 0.1 with a standard error of 0.4 mV and correlation coefficient of 0.9997. The selectivity of the method was demonstrated by measuring 10^{-6} mol l^{-1} NADPH in the presence of 100-fold amounts of various nucleotides. Although $NADP^+$, NAD^+, adenosine-5-triphosphate (ATP), adenosine-3,5-cyclic monophosphate (cAMP), adenosine-2-monophosphate (AMP), and 2-deoxyadenosine-5-phosphate did not interfere, NADH at concentrations

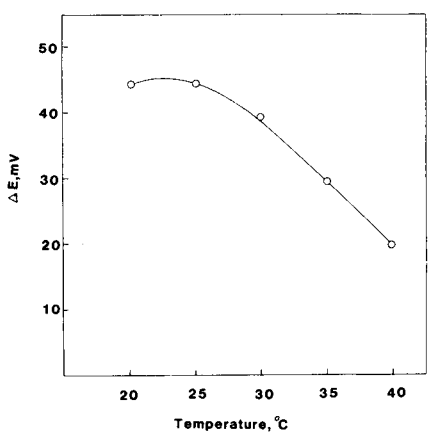

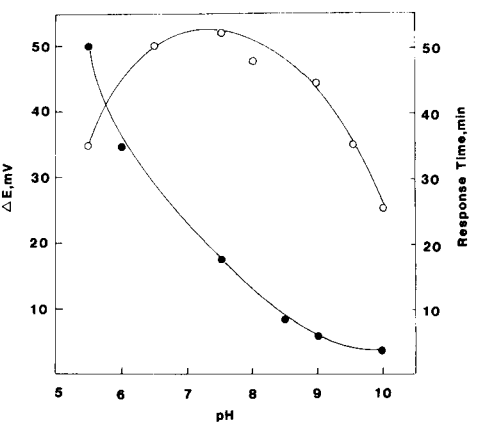

Fig. 3. Effect of temperature on the reaction of 2.5×10^{-4} mol l^{-1} GSSG, 10^{-6} mol l^{-1} NADPH and 0.5 IU ml^{-1} glutathione reductase in 4 ml of buffer pH 8; ΔE at 10 min.

Fig. 4. Effect of pH on the enzymatic reaction and on response time: (○, left scale) the reaction of 2.5×10^{-4} mol l^{-1} GSSG, 10^{-6} mol l^{-1} NADPH and 0.5 IU ml^{-1} glutathione reductase, ΔE at 10 min; (●, right scale) the electrode response time, with 0.1 mol l^{-1} Tris—HNO_3 buffer at 25°C.

higher than 10^{-4} mol l^{-1} produced a relative interference of approximately 1%.

Apart from its inherent simplicity, the proposed method offers lower detection limits and a wider range of applicability than some of the earlier electroanalytical methods [5, 6]. The usefulness of the method for quantifying NADPH in the presence of $NADP^+$ is an advantage over the highly sensitive cyclic methods [1, 2, 4] which require a prior separation step [12].

We are grateful to the National Institutes of Health (Grant GM-25308) for support of this research.

REFERENCES

1 B. M. Jörgensen and H. N. Rasmussen, Anal. Biochem., 99 (1979) 297.
2 C. Cox, P. Camus, J. Buret and J. Duvivier, Anal. Biochem., 119 (1982) 185.
3 D. C. Williams III and W. R. Seitz, Anal. Chem., 48 (1976) 1478.
4 T. Kaneko and J. B. Field, Anal. Biochem., 29 (1969) 193.
5 F. S. Cheng and G. D. Christian, Anal. Chem., 49 (1977) 1785.
6 L. C. Thomas and G. D. Christian, Anal. Chim. Acta, 78 (1975) 271.
7 S. S. M. Hassan and G. A. Rechnitz, Anal. Chem., 54 (1982) 303.
8 S. S. M. Hassan and G. A. Rechnitz, Anal. Chem., 54 (1982) 1972.
9 B. E. Davidson and F. J. R. Hird, Biochem. J., 93 (1964) 232.
10 P. K. C. Tseng and W. F. Gutknecht, Anal. Chem., 47 (1975) 2316.
11 R. van Heyningen and A. Pirie, Biochem. J., 53 (1953) 436.
12 G. C. Davis, K. L. Holland and P. T. Kissinger, J. Liq. Chromatogr., 2 (1979) 663.

Analytica Chimica Acta, 151 (1983) 479—482
Elsevier Science Publishers B.V., Amsterdam — Printed in The Netherlands

Short Communication

THE DETERMINATION OF COPPER AND LEAD IN SEDIMENTS BY POTENTIOMETRIC STRIPPING ANALYSIS

P. PHEIFFER MADSEN*, I. DRABAEK and J. SØRENSEN
Danish Isotope Centre, 2, Skelbækgade, DK-1717 Copenhagen V (Denmark)
(Received 7th December 1982)

Summary. Potentiometric stripping analysis was applied to sediments and sludge for the determination of lead (7—700 $\mu g\ g^{-1}$) and copper (3—110 $\mu g\ g^{-1}$). The precision obtained was in the range 2.5—4.1% for lead and 3.9—4.5% for copper. The accuracy of the method was checked on standard reference materials and found to be typically better than 7%.

Recently, a novel electrochemical method, potentiometric stripping analysis (p.s.a.) [1, 2], has been introduced for determinations of lead, copper, zinc and cadmium. The system has three electrodes, a glassy carbon cathode, a saturated calomel reference electrode, and a platinum counter electrode. The first step in the determination of metal ions in a sample solution is the electrochemical formation of a mercury film on the glassy carbon electrode. Subsequently, the metal ions are reduced and amalgamated in the mercury film during the electrolysis step (plating). When the plating is terminated, the metals are stripped from the mercury film back into the solution by chemical oxidation. During this step the potential of the carbon electrode (against SCE) versus time is recorded. The metals are identified by their stripping potentials and are quantified by measuring the stripping time for each metal.

The number of publications concerning the application of the p.s.a. method is somewhat limited. The sample matrices have been sea water [3], blood and serum [4], mussels and bovine liver [5]. At the Danish Isotope Centre (DIC), the method has been used on a routine basis for the past 2—3 years for the analysis of sea water and sediments. The present communication describes the experience gained in the analysis of sediments.

Experimental

Instrumentation. A Radiometer ISS-820 Ion Scanning System was used; this consists of an REA-120 Ion Scanning Module plugged into an REC-80 Servograph and TTA-80-IS Titration Cell. Three Radiometer standard electrodes were used, i.e., glassy carbon F-3500, SCE K-4040 and platinum P-1312. The entire system has been thoroughly described (see, e.g., [6] and [7]). All the instrumentation was placed on a clean bench with a laminar flow of HEPA-filtered air over the working area.

0003-2670/83/$03.00

Chemicals. All chemicals used were of analytical grade except sodium acetate, sodium chloride and the mineral acids which were of Suprapur grade (Merck). Commercial stock solutions for atomic absorption spectrometry (Merck/BDH) were used as standards.

Procedure for determination of lead and copper in sediments. Approximately 0.5 g of dried (105°C) sediment was decomposed by boiling for 2 h in a mixture of 3 ml of concentrated hydrochloric acid and 1 ml of concentrated nitric acid. After the dissolution, the sample was diluted with 10 ml of redistilled water, filtered (Whatman No. 41) and further diluted with redistilled water to a total volume of 100 ml. To an aliquot (25 ml) were added 1 ml of 10% (w/v) ascorbic acid solution (antioxidant and reductant for iron(III)) and 1 g of sodium chloride (to ensure reproducible ionic activity) together with mercury solution (usually 100 μl of 1000 ppm Hg solution, but depending on metal concentration) and an internal standard (cadmium) to correct for variations in oxidation rate.

To increase precision, especially at the lower concentration levels, preparation, regeneration and precoating of the working electrode were done prior to each set of measurements for Cu and Pb. Adequate cleaning of all the equipment was essential. For mercury plating, the normal procedure described in detail earlier [2] with ten precoating—stripping cycles was employed. Simultaneously, the sample was deaerated by purging with helium. After precoating and deaeration of the sample, an appropriate plating time and plating potential were applied (1—32 min and —0.95 V vs. SCE, respectively).

Lead and copper were quantified by using at least two standard additions. This was done in a cyclic mode and standards were added immediately after the stripping curve had been recorded. When the concentration levels of Pb and Cu were far apart, it was found convenient to determine the two elements separately, using the other element as the internal standard.

Results and discussion

In Fig. 1, the stripping curve for copper determined in 0.5 g of sediment is shown. The plating time was 4 min at —0.95 V vs. SCE; 2.5 μg of copper

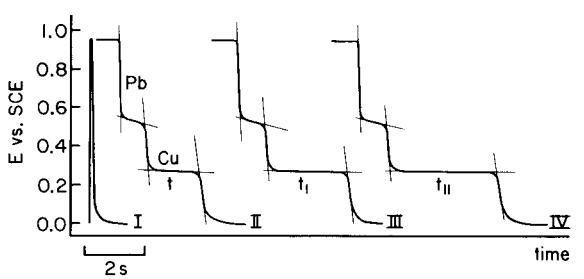

Fig. 1. Potentiometric stripping curve for a 25-ml aliquot of solution from a 0.5-g sediment sample. (I) Background; (II) curve before standard addition; (III, IV) curves after each addition of 2.5 μg of Cu(II).

was added at each standard addition and the natural lead content of the sample was used as the internal standard. The amount of copper in the sample was found to be 36 $\mu g\ g^{-1}$.

Accuracy and precision of the potentiometric stripping determinations of Pb and Cu in sediments were evaluated partly by repetitive analyses of both national and international standard reference materials, and partly by participation in intercalibration runs. In Table 1 are shown the results of repetitive analyses of a Danish marine reference sediment ("Lillebælt" sediment) and SRM 1645 River Sediment from the National Bureau of Standards (U.S.A.). For lead, the precisions found were 4.1% and 2.5% respectively, and for copper, 3.9% and 4.5%, respectively. The values found were in all cases within the certified limits, indicating good accuracy (Pb 3.2% and 1.1%, respectively; Cu 3.2% and 1.8%, respectively). Also in Table 1 are some results from analyses of the NBS SRM 1646 Estuarine Sediment.

Table 2 gives the results obtained during collaboration in the ICES (International Committee for Exploration of the Sea) marine sediment intercali-

TABLE 1

Results from analyses of a national reference sediment, NBS SRM 1645 River Sediment and NBS SRM 1646 Estuarine Sediment

Standard	Metal content ($\mu g\ g^{-1}$)[a]			
	Lead		Copper	
	Found	Certified[b]	Found	Certified[b]
Reference sediment (Lillebælt)	19.6 ± 0.8 (7)	19.0 ± 2.0	25.5 ± 1.0 (6)	24.7 ± 1.7
SRM 1645	722 ± 18 (8)	714 ± 28	111 ± 5 (5)	109 ± 19
SRM 1646	26.5 (1)	28.2 ± 1.8	16.8 (2)	18 ± 3

[a]Dry sediments were processed in all cases. Numbers in parentheses indicate the number of separate determinations used for calculation of the standard deviations shown.
[b]Certified values with 95% confidence intervals.

TABLE 2

Results obtained in the ICES sediment intercalibration. MS1 (NBS SRM 1645 River Sediment), MS2 and MS3 are the three intercalibration samples

Sample	Metal content ($\mu g\ g^{-1}$)			
	Lead		Copper	
	Found	$\bar{x} \pm S^a$	Found	$\bar{x} \pm S^a$
MS1	724	688 ± 59	104	108 ± 7
MS2	64	52 ± 13	35	39 ± 4
MS3	7.5	4.5 ± 0.6	2.6	1.7 ± 0.8

[a]Mean and estimated deviation obtained in the intercalibration tests for the dry sediments. The certified results for MS1 are given in Table 1.

TABLE 3

Results from analysis of intercalibration samples from the 17th Danish Intercalibration arranged by the Danish National Environmental Protection Agency

Sample	Metal content ($\mu g\ g^{-1}$)			
	Lead		Copper	
	Found	$\bar{x} \pm S^a$	Found	$\bar{x} \pm S^a$
Sediment	18.6	21.5 ± 4.0	14.5	18.1 ± 1.0
Sewage sludge[b]	507	554 ± 35	965	1095 ± 97

[a]Mean and estimated deviation obtained in the intercalibration tests for dried samples.
[b]Results certified by EPA with 95% confidence intervals are 519 (305—733) $\mu g\ g^{-1}$ for lead and 1095 (831—1360) $\mu g\ g^{-1}$ for copper.

bration [8]. The sample marked MS1 was identical with NBS SRM 1645 River Sediment. Except for the lead in MS3, agreement is satisfactory. The results of analysis of samples from intercalibration runs on sediments and sewage sludge, arranged by the Danish National Environmental Protection Agency, are listed in Table 3. The sewage sludge employed was one certified by the U.S. Environmental Protection Agency (EPA). There are minor discrepancies between the present results and the intercalibration results for copper in the sediment. For the sewage sludge, the present results are generally a little low but within the limits given by EPA.

Conclusions

Potentiometric stripping analysis provides a simple instrumental approach to accurate and precise determination of lead and copper in sediments. One of the major advantages of the potentiometric stripping technique is the simple instrumentation required and the straightforward calculation of results. The minimization of sample treatment also makes this form of measurement very suitable for trace element determinations. Sediments and sludge can be analysed for zinc and cadmium by using nearly the same procedure as here described. The only modification required is that nitric acid from the dissolution step be boiled off by hydrochloric acid before the potentiometric stripping method is applied.

REFERENCES

1 D. Jagner and A. Granelli, Anal. Chim. Acta, 83 (1976) 19.
2 D. Jagner, Anal. Chem., 50 (1978) 1924.
3 D. Jagner and K. Årén, Anal. Chim. Acta, 107 (1979) 29.
4 D. Jagner, M. Josefson, S. Westerlund and K. Årén, Anal. Chem., 53 (1981) 1406.
5 L. G. Danielsson, D. Jagner, M. Josefson and S. Westerlund, Anal. Chim. Acta, 127 (1981) 147.
6 A. M. Graabaek and O. J. Jensen, Ind. Res., 21 (1979) 124.
7 C. Labar and L. Lambérts, Anal. Chim. Acta, 132 (1981) 23.
8 Centre National Pour L'exploration des Oceans: Metaux-Traces dans les Sediments Marins (1980).

Analytica Chimica Acta, 151 (1983) 483—486
Elsevier Science Publishers B.V., Amsterdam — Printed in The Netherlands

Short Communication

DETERMINATION OF CADMIUM IN THE PRESENCE OF INDIUM BY POLAROGRAPHY WITH ADDITION OF AN ELECTROINACTIVE SURFACTANT

RICHARD MODOLO and OLIVIER VITTORI*

Université Lyon I, Laboratoire de Chimie Analytique III, 43 Boulevard du 11 Novembre 1918, 69622 Villeurbanne Cedex (France)

(Received 5th January 1983)

Summary. Cadmium can be determined in the presence of a large amount of indium when the surfactant, Montanox 80, is added to the bulk solution at pH 2. The indium wave disappears when sufficient Montanox 80 is present, while the cadmium wave is shifted to more negative potentials and becomes more irreversible. Classical, differential pulse and a.c. polarography are compared; all are suitable for routine work. The detection limits are about 10^{-6} M cadmium for 5×10^{-3} M of indium in the presence of 10^{-3} M Montanox 80.

Since the first investigations of Heyrósvky [1], Takagi [2], Tomes [3], and Lingane [4], a great deal of work has been done on the electroreduction of indium in various supporting electrolytes; this work has been reviewed [5]. It has been clearly established that in a non-complexing medium, the indium(III) wave appears at about —1.0 V (vs. SCE) [1—4, 6, 7] and that, when halides are added to the electrolyte, the wave is shifted to more positive potentials by about 400 mV [8—12]. The reason suggested for this shift is the better reversibility of the reduction of halide complexes, but some authors have published inconsistent data for the chloro complexes [8, 9]. The adsorption of halides always plays an important role, depending on its concentration, and the same effect has been noticed for thiocyanate [11]. The indium wave appears to be well developed at about —0.55 V (vs. SCE) but just as the plateau is reached, the current decreases markedly up to —0.9 V and then increases. This apparent negative resistance is caused by reduction through an adsorbed anion and the effect has been measured with an a.c. impedance bridge [13]. The interference of the indium wave with that of cadmium is serious and the problem has been solved in different ways. Surfactants have been studied to suppress the minimum, but gelatine, Triton X-100 or X-305, and dodecylsulphate have uncommon effects [12, 15] and are unsuitable for quantitative work. Several authors have dealt with changes of the electrolyte by addition of ligands or salt mixtures [16—22] whereas others [23, 24] have recommended preliminary liquid—liquid extraction or precipitation steps.

The present communication is concerned with the determination of traces

0003-2670/83/$03.00

of cadmium when indium is the major component, by masking the indium wave completely with a surfactant containing twenty polyoxyethylene groups, Montanox 80.

Experimental

Apparatus. A PRG-5 pulse polarograph and a PRG-3 device for a.c. measurements were used (Tacussel, France). A saturated calomel electrode served as reference and a platinum wire as auxiliary electrode. The dropping mercury electrode (DME) comprised a 20—40-μm i.d. capillary, with hexadistilled mercury (Rhone Alpes Mercure, France). Oxygen was removed by nitrogen and the temperature was fixed at 25 ± 0.2°C. All other precautions required for polarography were observed.

Reagents. Indium chloride, cadmium chloride and potassium chloride were of analytical grade (Prolabo or Merck). The surfactant was Montanox 80 (I; Seppic, France), which is the monooleate ester of polyoxyethylene sorbitan (II).

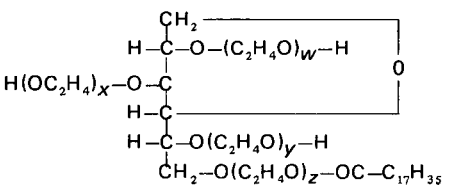

(I)

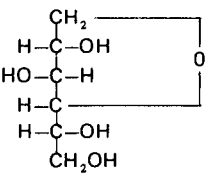

(II)

The total number ($x + y + z + w$) of oxyethylene groups is 20. Montanox 80 is a water-soluble liquid at room temperature and is widely used in drugs and cosmetics as an emulsifying reagent. All solutions of Montanox were obtained by weighing and the pH was adjusted with pure hydrochloric acid.

Results and discussion

As shown in Fig. 1, the indium wave decreases progressively when Montanox 80 is added. Usually surfactants shift the wave towards more negative potentials because the charge-transfer constant is lowered, but the peculiar shape of the indium wave in the absence of any surfactant indicates that the reduction is very complex. At pH 2, the pronounced minimum at —1.0 V is not suppressed by the surfactant and the intensity decreases. At the same time the indium wave is fully suppressed by 2.5×10^{-4} M Montanox 80, a value less than the initial amount of indium. Thus there is no complexation but rather a coverage of the DME sufficient to mask the wave completely. Simao and Von Stackelberg [12] showed that at very low concentrations of polyoxyethylene the indium wave is first shifted to more positive potentials because of acceleration of the reduction process, catalysed by the adsorbed molecules. In the present case, however, at pH 2 in 0.1 M KCl, this effect was not noticed even at very low Montanox 80 concentrations; rather there was a rapid decrease of the current (Fig. 1).

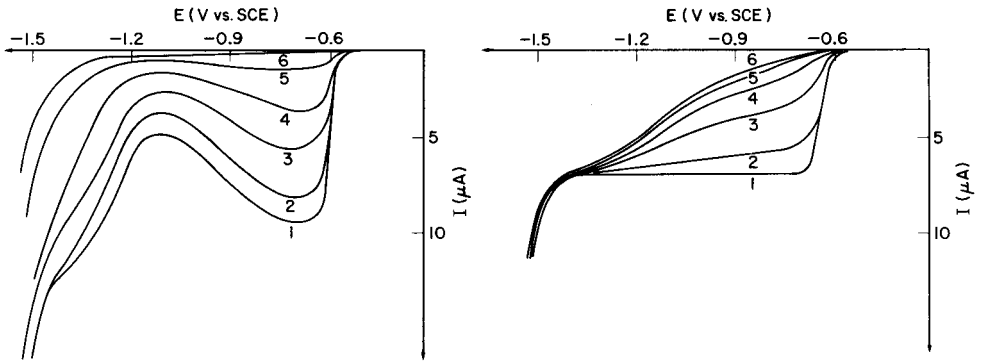

Fig. 1. D.c. polarographic waves for 10^{-3} M indium(III) at pH 2 with increasing concentrations of Montanox 80: (1) 0; (2) 1 × 10^{-5} M; (3) 2.5 × 10^{-5} M; (4) 5 × 10^{-5} M; (5) 1.25 × 10^{-4} M; (6) 2.5 × 10^{-4} M.

Fig. 2. D.c. polarographic waves for 10^{-3} M cadmium(II) at pH 2 with increasing concentrations of Montanox 80: (1) 0; (2) 5 × 10^{-6} M; (3) 1.25 × 10^{-5} M; (4) 2.5 × 10^{-5} M; (5) 3.75 × 10^{-5} M; (6) 5 × 10^{-4} M.

Cadmium, in the same supporting electrolyte at pH 2, behaved as expected. As Montanox 80 is added, the wave decreases progressively and shifts to more negative potentials. Irreversibility becomes accentuated (Fig. 2), but the determination of cadmium is always possible at about −1.2 V by direct current (d.c.) polarography. Variation of the cadmium(II) concentration at a fixed Montanox 80 concentration (10^{-3} M) showed that the calibration graph was linear with a correlation coefficient of 0.999. The limiting concentration is 10^{-5} M with d.c. polarography and 10^{-6} M with differential pulse (d.p.) or alternating current (a.c.) polarography.

When d.p. or a.c. polarography is applied, cadmium(II) exhibits two reduction peaks at about −0.73 and −1.20 V (vs. SCE). With the d.p. technique, the first peak is more interesting than the second because some irregularities appear on the polarogram when the potential is less than −1.2 V, probably because of hydrogen evolution; the first peak is therefore used to prepare calibration graphs. However, the two peaks are regular when a.c. polarography is used; the second peak is 2.7-fold higher than the first and so is used for calibration. For the d.c., d.p. and a.c. methods, all the calibration graphs had correlation coefficients equal to or better than 0.99. The detection limits were 10^{-5} M for d.c. and 10^{-6} M for d.p. or a.c. polarography.

Experiments with 10^{-2} or 10^{-3} M indium(III) in the presence of 10^{-3} M Montanox 80 showed that cadmium can be determined at −1.2 V by d.c. polarography and with the first or second peak when d.p. or a.c. polarography is used. In all cases, the calibration graphs were linear when indium was present, but the currents were about 10% less than in absence of indium. Figure 3 shows a typical set of d.p. polarographic curves. From the detection

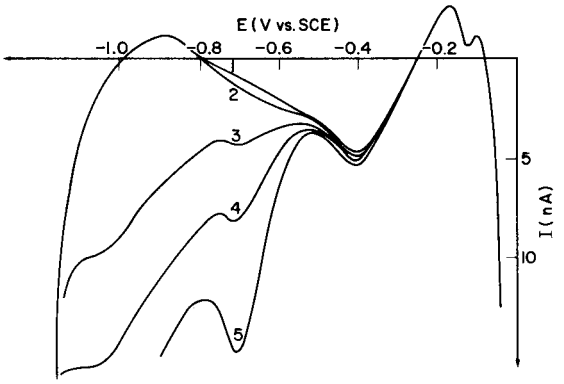

Fig. 3. D.p. polarographic curves for cadmium(II) in the presence of 5×10^{-3} M indium-(III) and 10^{-3} M Montanox 80, in 0.1 M KCl at pH 2. Pulse amplitude: 50 mV, sampling time: 45 ms. Cadmium concentration: (1) 0; (2) 2×10^{-6} M; (3) 1.25×10^{-5} M; (4) 2.5×10^{-5} M; (5) 5×10^{-5} M.

limit to 10^{-5} M for both the d.p. and a.c. techniques, the peak is not well developed and care is needed in subtracting the baseline current. In this range, identification of cadmium is not possible, but the use of the surfactant allows reproducible routine determinations.

REFERENCES

1 J. Heyrόvsky, Chem. Listy, 19 (1925) 168.
2 S. Takagi, J. Chem. Soc., (1928) 301.
3 J. Tomes, Collect. Czech. Chem. Commun., 9 (1937) 12.
4 J. J. Lingane, J. Am. Chem. Soc., 61 (1939) 2099.
5 R. Piercy and N. A. Hampson, J. Appl. Electrochem., 5 (1975) 1.
6 J. V. Lawson and D. A. Aikens, J. Electroanal. Chem., 15 (1967) 193.
7 A. I. Molodov and V. V. Losev, Sov. Electrochem., 1 (1965) 42, 573.
8 J. A. Schufle, M. T. Stubbs and R. E. Witman, J. Am. Chem. Soc., 73 (1951) 1013.
9 E. D. Moorhead and W. M. MacNevin, Anal. Chem., 24 (1962) 269.
10 A. J. Engel, J. Lawson and D. A. Aikens, Anal. Chem., 37 (1965) 203.
11 R. E. Visco, J. Electroanal. Chem., 10 (1965) 82.
12 J. Simao and M. von Stackelberg, J. Electroanal. Chem., 50 (1974) 247.
13 N. Tanaka, T. Tekeuchi and R. Tamamushi, Bull. Chem. Soc. Jpn., 37 (1964) 1435.
14 M. Bulovova, Collect. Czech. Chem. Commun., 19 (1954) 1123.
15 K. Sykut, G. Dalmata, B. Nowicka and J. Saba, Chem. Anal. (Warsaw), 25 (1980) 1109.
16 Suon Kim Nuor and O. Vittori, Anal. Chim. Acta, 91 (1977) 143.
17 K. Keim, H. D. Sommer and F. Umland, Fresenius Z. Anal. Chem., 301 (1980) 207.
18 V. V. Slepushkin, N. N. Kuz'mina and M. G. Yartsev, Zh. Anal. Khim., 32 (1977) 535.
19 M. Kasagi and C. V. Banks, Anal. Chim. Acta, 30 (1964) 248.
20 M. Marczak and J. Biedon, Chem. Anal. (Warsaw), 16 (1971) 945.
21 T. Fuzinaga and B. K. Puri, Talanta, 22 (1975) 71.
22 A. L. Rao and A. Kumar, Analyst, 99 (1974) 439.
23 E. Temmerman and F. Verbeek, Fresenius Z. Anal. Chem., 244 (1969) 25.
24 L. S. Kopanskaya and V. G. Revenko, Zavod. Lab., 41 (1975) 267.

Analytica Chimica Acta, 151 (1983) 487—490
Elsevier Science Publishers B.V., Amsterdam — Printed in The Netherlands

Short Communication

A SIMPLE SOLID-PHASE RADIOIMMUNOASSAY FOR ENKEPHALINS WITH *STAPHYLOCOCCUS AUREUS*

NAVIN C. KHANNA and SHAIL K. SHARMA*

Department of Biochemistry, All India Institute of Medical Sciences, New Delhi-110029 (India)

(Received 11th August 1982)

Summary. The assay utilizes ^{125}I-labelled peptides and *Staphylococcus aureus Cowan I* coated with antienkephalin antibodies. Binding equilibrium is attained in <30 min and the assay takes 1 h.

Radioimmunoassay (r.i.a.) is a highly sensitive and widely used technique for the detection and determination of opiate peptides in biological samples. All the methods currently in use [1—3] for the separation of free and bound label in the r.i.a. of enkephalins fall into two categories. The methods based on charcoal, polyethylene glycol and ammonium sulfate are unselective and give high blank values. The double antibody method, although specific, is expensive and time-consuming. Here, a rapid, simple and sensitive method is described for the separation of free and bound enkephalins based on the bacterium *Staphylococcus aureus Cowan I* strain (*SAC I*) as the solid support. *SAC I* bacteria bearing Protein A endowed with the ability to bind immunoglobulins through their complement-binding fragment [4] have already been employed successfully for the isolation of immune complexes in r.i.a. [5, 6].

Experimental

Preparation of immunogenic conjugates. Conjugates of enkephalins were prepared by the method of Gros et al. [3]. On the basis of isotopic dilution the two conjugates were estimated to contain 24 and 18 residues of met-enkephalin and leu-enkephalin, respectively, per molecule of ovalbumin (Sigma Chemical Co., St. Louis, MO).

Immunization. Two male adult rabbits (New Zealand strain) were injected intradermally at multiple sites with 1 mg of the immunogenic conjugates emulsified with complete Freund's adjuvant. Booster injections of 0.5 mg of the same conjugates emulsified with incomplete Freund's adjuvant were given at fortnightly intervals. Blood samples taken two weeks after the third booster injection showed the presence of sufficient antibodies for use in r.i.a.

Radio-iodination. The tyrosine residues of the two enkephalins were iodinated by the method of Hunter and Greenwood [7]: 5 μg of met- or leu-

0003-2670/83/$03.00

enkephalin (Peninsula Labs., San Carlos, CA), 1 mCi of $Na^{125}I$ (New England Nuclear, Boston, MA) and 25 μg of chloramine-T (Sigma Chemical Co.) were incubated for 20—25 s in 0.5 M sodium phosphate buffer, pH 7.5, in a total volume of 40 μl. Reaction was terminated by the addition of 50 μg of sodium hydrogensulfite (Sigma Chemical Co.) dissolved in 25 μl of the same buffer. The products were immediately loaded on 40 × 0.7 cm columns of Sephadex G-10 (40—120 μm; Pharmacia, Uppsala, Sweden), previously equilibrated with 0.05 M phosphate buffer, pH 7.5, containing bovine serum albumin (0.1%) and sodium azide (0.1%). Fractions of 0.5 ml each were collected and checked for binding with antienkephalin antibodies. Purity of the labelled peptides was checked by t.l.c. on silica gel with butanol:acetic acid:water (4:1:1) as solvent.

Coating of antienkephalin antibodies on SAC I. *SAC I* were harvested in 0.1 M phosphate buffered saline (PBS), pH 7.4, and subsequently killed by heating at 65° C for 30 min. Bacteria were extensively washed with PBS and finally suspended in 0.1 M Tris—maleate buffer, pH 8.6, containing 0.1% each of bovine serum albumin and sodium azide (assay buffer). To the bacterial suspension was added antienkephalin antiserum in the ratio 10:1 (v/v) and thorough mixing was achieved on an end-to-end shaker for 1 h at room temperature (30° C). The bacteria were washed thrice with the assay buffer and suspended in the same buffer at a concentration of 10^7 bacteria ml^{-1}. The suspension was stored at 0—4° C and was stable for more than six months.

Assay procedure. To 10 × 75 mm borosilicate glass tubes were added 100 μl each of the diluted tracer (10^4 cpm), sample or standard, and antibody-coated *SAC I* suspension in the assay buffer. After incubation at room

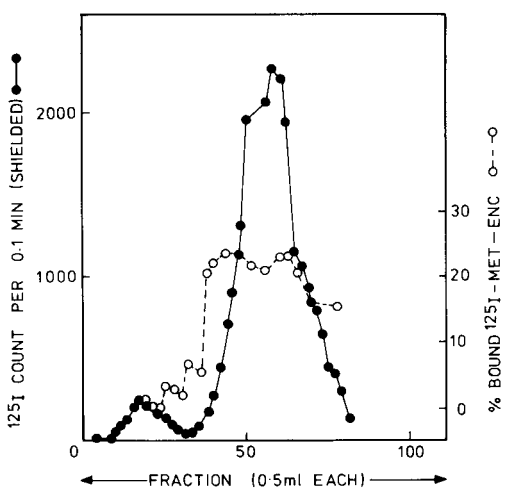

Fig. 1. Elution profile of ^{125}I-labelled met-enkephalin on Sephadex G-10. Each fraction was checked for its binding with antisera.

TABLE 1

Rate of binding of ^{125}I-met-enkephalin (^{125}I-ME) with antibody-coated *SAC I*

Time (min)	0	5	10	15	30	60	1000
Bound ^{125}I-ME (%)	0	27	29	30	30	30	30

temperature for 30 min, the tubes were centrifuged at 1000 *g* for 10 min. Supernatant liquids were discarded and pellets were counted in the same tubes in a Packard γ-counter.

Results and discussion

The elution profile of free iodine and labelled peptide is shown in Fig. 1. Iodine appears first followed by the labelled peptide. This may appear anomalous and is probably due to the affinity of tyrosine residues of enkephalins with Sephadex as has been reported for luteinizing hormone release factor [8]. A similar profile was observed for leu-enkephalin.

Table 1 shows the rate of binding of ^{125}I-met-enkephalin to antibody-coated *SAC I*. Maximum binding was observed after 10—15 min of incubation, compared to 12—18 h required for other methods. This very rapid antigen—antibody reaction may be explained by the high concentration of the antibody that is presented to the antigen on the bacterial surface. Similar results were obtained for leu-enkephalin.

Data presented in Table 2 show the relative efficacies of various methods used for the separation of free and bound enkephalins. As is evident, *SAC I* precipitates most radioactivity, with the minimum non-specific precipitation. Again leu-enkephalin gave similar results.

Figure 2 shows the calibration graph, with no significant cross-reactivity with other known brain peptides. The assay is sensitive to pmol amounts of enkephalin. This method has been used to assay the levels of enkephalins in different regions of rat brain; the values obtained were close to those reported in the literature [9].

TABLE 2

Separation of bound and free met-enkephalin by various separating agents[a]

Separating agent	Percent bound	
	Total	Nonspecific
Ethanol (5 vols.)	31—32	4—5
Ammonium sulfate (50%)	50—52	7—9
Polyethylene glycol (40%)	40—42	2—3
SAC I (10^6 bact./tube)	62—65	1—1.5

[a]100 μl each of the assay buffer, diluted tracer and antiserum were used. After overnight incubation, separating agents were added, and the tube contents centrifuged.

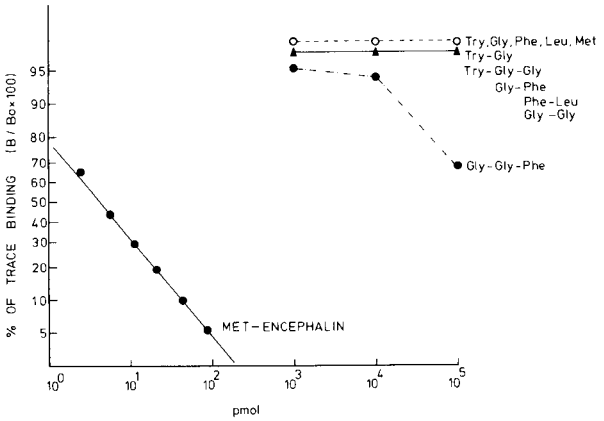

Fig. 2. Cross-reactivity of various compounds with met-enkephalin antiserum. (Each compound, 100—10,000 pmol, was added to the assay tubes, with incubation for 30 min at room temperature. Results are expressed as % for ^{125}I-met-enkephalin bound to antibody-coated *SAC I*.

Thus, experimental conditions are described for a convenient and simple one-step method for r.i.a. of enkephalin. The coating of *SAC I* with antibody permits an effective use of dilute antisera. This also obviates the need of bacitracin, which is often used with such dilute antisera.

This work was supported by an Indian Department of Science and Technology grant (No. 12(36)/76 SERC).

REFERENCES

1 R. J. Miller, K. J. Chang, B. Cooper and P. Cuatrecasas, J. Biol. Chem., 253(2) (1978) 531.
2 R. Simantov, S. R. Childers and S. H. Snyder, Brain Res., 135(2) (1977) 358.
3 C. Gros, P. Pradelles, C. Rouget, O. Bepoldin, F. Dray, M. C. Fournie-Zaluski, B. P. Rooques, H. Pollard, C. Llorens-Cortes and J. C. Schwartz, J. Neurochem., 31 (1978) 29.
4 I. Lind, I. Live and B. Mansa, Acta Pathol. Microbiol. Scand., Sect. B, 78 (1970) 673.
5 S. W. Kessler, J. Immunol., 115 (1975) 1617.
6 P. E. Reddy, S. G. Devare, R. Vasudev and P. S. Sarma, J. Natl. Cancer Inst., 58 (1977) 1859.
7 W. M. Hunter and F. C. Greenwood, Nature, 194 (1962) 495.
8 S. L. Jeffeoate, H. M. Fraser, A. Gunn and D. T. Holland, J. Endocrinol., 57 (1973) 189.
9 R. Simantov and S. H. Snyder, in H. W. Kosterlitz (Ed.), Opiates and Endogenous Opioid Peptides, Elsevier, Amsterdam, 1976.

Analytica Chimica Acta, 151 (1983) 491—495
Elsevier Science Publishers B.V., Amsterdam — Printed in The Netherlands

Short Communication

EXTRACTION—SPECTROPHOTOMETRIC DETERMINATION OF VANADIUM(V) WITH CUPFERRON IN THE PRESENCE OF PHENOLS

YOSIEF ALEM, GEBRAY ASGEDOM and B. S. CHANDRAVANSHI*

Department of Chemistry, Addis Ababa University, P.O. Box 1176, Addis Ababa (Ethiopia)

(Received 10th December 1982)

Summary. Vanadium(V) reacts with cupferron (ammonium *N*-nitrosophenylhydroxylamine) in the presence of phenols to form coloured 1:2:1 complexes, stable at room temperature, which can be extracted into chloroform. The wavelengths of maximum absorption and the molar absorptivities of the ternary complexes depend on the nature of the phenols. The most satisfactory phenol is *p*-chlorophenol, with which the molar absorptivity is 5650 l mol^{-1} cm^{-1} at 590 nm; the linear range is 0.9—8.6 ppm vanadium. The method is applicable to steel samples.

Numerous chelating agents [1] have been used for the extraction and spectrophotometric determination of vanadium(V). These reagents form 1:2 (metal:ligand) complexes which have a basic V=O and an acidic V—OH group in the same molecule. The V=O group reacts with acidic substances (carboxylic acids, phenols) to give hyperchromic and bathochromic shifts [2, 3]. Cupferron (ammonium *N*-nitrosophenylhydroxylamine) reacts with vanadium(V) to form a red 1:2 complex which can be extracted into chloroform [4]. However, the extracted complex is unstable and decomposes rapidly at room temperature. This has necessitated the presence of a stabilizer and the use of lower temperatures for the determination of vanadium [5].

In this communication, vanadium(V) is extracted with cupferron in the presence of phenols, to improve the stability of the complex and the sensitivity and selectivity of the method. It was found that the V=O group reacts with phenols to give a stable complex which provides the basis for a highly sensitive extractive spectrophotometric determination. The reliability of the method was checked by determining vanadium in standard steel samples.

Experimental

Apparatus and reagents. A Beckman model 24 u.v.—visible spectrophotometer equipped with 1-cm matched quartz cells was used.

A stock solution of vanadium(V) was prepared by dissolving reagent-grade ammonium metavanadate in doubly-distilled water; it was standardized titrimetrically [6]. The solutions of foreign ions were prepared from reagent-grade salts [7].

0003-2670/83/$03.00

All other chemicals used were of analytical-reagent grade.

A 0.2% (w/v) solution of cupferron in doubly-distilled water was stored in a refrigerator. Freshly prepared solutions were used. Ethanol-free chloroform was used for the preparation of phenol solutions and for the extraction work.

General procedure. An aliquot of neutral or slightly acidic vanadium(V) solution containing 25—250 μg of the metal was placed in a 100-ml separatory funnel and 5 ml of 0.2% (w/v) solution of cupferron was added. Sufficient concentrated hydrochloric acid and distilled water were added to adjust the acidity to about 1 M and the volume of the aqueous phase to about 10 ml. A 10-ml aliquot of a 0.5 M solution of a particular phenol (*p*-chlorophenol is recommended) in chloroform was added immediately and the mixture was equilibrated for 2 min. The organic phase was collected and the residual aqueous phase was washed with two 4-ml portions of chloroform. The combined chloroform extracts were dried over anhydrous sodium sulphate in a 50-ml beaker, transferred to 25-ml volumetric flasks and diluted to volume with chloroform. The absorbances were measured at the wavelength of maximum absorption against chloroform as a blank.

For calibration, 0.5, 1.0, 1.5, 2.0 and 2.5 ml of a standard solution (100 μg V ml^{-1}) were taken through the procedure.

Determination of vanadium in steel. A weighed quantity of steel (0.1—0.4 g) containing about 2.0 mg of vanadium was transferred to a 400-ml beaker and treated with 10—20 ml of concentrated (1 + 1) nitric acid. The solution was heated gently until brisk reaction had ceased, 5—10 ml of aqua regia was added, and the solution was evaporated to near dryness to expel nitrogen oxides. The cold pasty residue was dissolved in about 25 ml of water by heating. The solution was filtered through a Whatman No. 42 filter paper to remove silicic acid and hydrated tungstic acid, the precipitate being washed several times with hot water. Filtrate and washings were collected in a 100-ml volumetric flask and diluted to volume with water. A suitable aliquot (5—10 ml) of the sample solution was taken for the determination of vanadium as described above.

Results and discussion

Spectra. The absorption spectra of the vanadium(V)—cupferron complex was measured in the absence and presence of various phenols in chloroform. The red complex formed in the absence of phenols showed a broad absorption maximum around 520 nm. When phenols were added to the chloroform solution of the complex the absorbance maximum shifted to longer wavelengths and the absorbances increased with increasing concentration of phenols. Above 0.02 M phenols the wavelength of maximum absorption and the absorbance became constant.

Effect of different phenols. The wavelength of maximum absorption and the molar absorptivity of the adduct depended on the nature of the phenols, as shown in Table 1. The presence of a methyl group in the *m*- or *p*-position, or the presence of two methyl groups in the phenol shifted the absorbance

TABLE 1

Spectral characteristics of some vanadium(V)—cupferron—phenol complexes in chloroform

Phenol	Colour[a] of complex	λ_{max} (nm)	ϵ (l mol^{-1} cm^{-1})	Sandell sensitivity (μg V cm^{-2})
Phenol	V	575	4850	0.0105
m-Cresol	GB	595	4750	0.0107
p-Cresol	BG	610	4820	0.0105
2,3-Xylenol	BG	610	4380	0.0116
2,4-Xylenol	BG	640	5580	0.0091
2,5-Xylenol	G	620	4400	0.0116
2,6-Xylenol	BG	620	[b]	[b]
3,5-Xylenol	G	600	4470	0.0114
p-Chlorophenol	B	590	5650	0.0090

[a]V, violet; GB, greenish blue; BG, bluish green; G, green; B, blue. [b]Very unstable complex.

maximum to longer wavelengths. However, the intensity of the absorption band generally decreased, probably because of the decreased acidity of the phenolic hydroxyl group, although for 2,4-xylenol an unexpected increase was observed. The presence of two methyl groups in the 2,6-position had a steric effect which made the resulting complex unstable. The presence of chlorine in the *p*-position increased both the absorbance and the wavelength of maximum absorbance because of the increased acidity of the phenol.

Effect of conditions. A 6-fold molar excess of cupferron was adequate for the complete extraction of vanadium. Addition of more reagent (up to a 50-fold molar excess) had no adverse effect on the absorbances or the wavelength of maximum absorbance. A 300-fold molar excess of a particular phenol was sufficient for the complete extraction of vanadium. Excess of phenol up to 4000-fold molar excess had no effect in the extraction and determination of vanadium(V). The order of addition of reagents was not critical.

Chloroform was found to be the best solvent for the extraction of the ternary complexes. The acidity of the aqueous phase was maintained with hydrochloric acid; the optimum hydrochloric acid ranges for the extraction of vanadium are shown in Table 2. A period of 2 min was sufficient for the complete extraction of vanadium(V). The extracts were stable for at least 6 h at 25°C. Variation in temperature from 20 to 30°C did not affect the wavelengths and absorbances.

The linear and optimum [8] concentration ranges and the relative standard deviations of the systems are shown in Table 2. On this basis, *p*-chlorophenol is the phenol of choice for applications.

Complex composition. The stoichiometry of the ternary phenol complex was determined by different methods. The ratio of vanadium to cupferron

TABLE 2

The determination of vanadium(V) with cupferron in the presence of phenols

Phenol	HCl range (M)	Linear range (ppm V)	Optimum range[a] (ppm V)	Relative standard deviation[b] (%)
Phenol	0.4—1.8	1.0—10.5	2.0—8.6	0.76
m-Cresol	0.6—2.0	1.1—11.0	2.0—8.8	0.68
p-Cresol	0.2—1.8	1.0—10.2	1.8—8.2	0.72
2,3-Xylenol	0.6—1.4	1.2—12.0	2.3—9.4	0.90
2,4-Xylenol	0.4—1.6	0.9—8.8	1.8—7.8	0.64
2,5-Xylenol	0.2—1.8	1.2—11.6	2.4—9.6	0.85
3,5-Xylenol	0.6—1.6	1.1—10.8	2.2—9.0	0.78
p-Chlorophenol	0.5—1.5	0.9—8.6	1.6—7.4	0.58

[a]From Ringbom plots [8]. [b]10 measurements of 100 μg V in 25 ml.

TABLE 3

Tolerance limits[a] for foreign ions in the determination of 4 ppm of vanadium(V) with cupferron in the presence of *p*-chlorophenol in 1.5 M hydrochloric acid

Tolerance limit (ppm)	Species tested
600	Mn^{2+}, Cd^{2+}, Hg^{2+}, Zn^{2+}, Tl^{+}
400	Co^{2+}, Al^{3+}, Bi^{3+}, Ce^{4+}, Pb^{2+}, W(VI)
300	Ni^{2+}, U(VI)
200	Fe^{3+}, Cr^{3+}, Sn(IV)
60	Ti(IV), Zr(IV), Mo(VI), Cu^{2+}

[a]Maximum concentration causing an error <2%.

was determined by the method of continuous variations [9] and the mole ratio method [10]. The ratio of vanadium to phenol was evaluated by the curve-fitting method [11]. The results obtained indicated the formation of a 1:2:1 (metal:cupferron:phenol) complex.

Effect of other ions and applications. In order to assess possible analytical applications, the effects of other ions on the extraction and determination of vanadium(V) were studied by adding a known amount of the ion in question to a solution containing 100 μg of vanadium and proceeding as described in the recommended procedure, with *p*-chlorophenol as the phenol. Acetate, chloride, bromide, nitrate, phosphate, oxalate, citrate, sulphate, tartrate, ammonium, alkali metals, alkaline earths and lanthanide elements did not interfere up to 1000 ppm in the test solution. The tolerance limits for other ions are given in Table 3.

TABLE 4

Determination of vanadium in B.C.S. steels[a] with cupferron in the presence of *p*-chlorophenol

Steel No.	Vanadium found[b] (%)	Certified value (%)
64a	1.548 ± 1.00	1.57
64b	1.972 ± 0.84	1.99
241/1	1.550 ± 0.92	1.57
252	0.446 ± 1.20	0.46

[a]Obtained from the Bureau of Analyzed Samples Ltd., Middlesborough, Cleveland, U.K.
[b]Mean with relative standard deviation (n = 6).

The accuracy of the method was tested by determining the vanadium contents of standard steel samples. The results of the analyses in Table 4 show good agreement with the certificate values.

The authors are grateful to the Chairman, Department of Chemistry, Addis Ababa University, Addis Ababa, Ethiopia for providing the facilities to conduct the research work.

REFERENCES

1 G. Svehla and G. Tölg, Talanta, 23 (1976) 755.
2 I. Kojima and Y. Miwa, Anal. Chim. Acta, 83 (1976) 329.
3 I. Kojima and M. Tanaka, Anal. Chim. Acta, 75 (1975) 367.
4 D. Bertrand, Bull. Soc. Chim. Fr., 9 (1942) 121.
5 E. B. Sandell, Colorimetric Determination of Traces of Metals, 3rd edn., Wiley-Interscience, New York, 1959.
6 G. Charlot and D. Bezier, Quantitative Inorganic Analysis, Wiley-Interscience, New York, 1957, p. 623.
7 P. W. West, J. Chem. Educ., 18 (1941) 528.
8 A. Ringbom, Z. Anal. Chem., 115 (1938) 332.
9 P. Job, Ann. Chim. (France), 9 (1928) 113.
10 J. H. Yoe and A. L. Jones, Ind. Eng. Chem., Anal. Ed., 16 (1944) 111.
11 L. G. Sillen, Acta Chem. Scand., 10 (1956) 185.

Analytica Chimica Acta, 151 (1983) 497
Elsevier Science Publishers B.V., Amsterdam — Printed in The Netherlands

Errata

Akira Miyazaki, Akira Kimura, Kenji Bansho and Yoshimi Umezaki, Simultaneous Determination of Heavy Metals in Waters by Inductively-coupled Plasma Atomic Emission Spectrometry after Extraction into Diisobutyl Ketone.

Anal. Chim. Acta, 144 (1982) 213—221.

On p. 213, in the last sentence of the Summary, "... the DIBK extract was higher than ..." should read "... the DIBK extract was lower than ..."

On p. 219, Table 2, footnote c should be deleted; superscript c in the Table should be replaced by superscript b.

Klaus R. Koch and Janet E. Yates, The Effect of Tin(II) Chloride on the Liquid—Liquid Extraction of Tetrachloroplatinate(II) Ions by Triphenylphosphine in Dichloromethane.

Anal. Chim. Acta, 147 (1983) 235—245.

Unfortunately, two errors occurred in this paper:

(1) in Table 1, third column, "0.74" should read "0.074";
(2) on page 242, second line of text, "HALTAFAL" should read "HALTAFALL".

ANALYTICA CHIMICA ACTA, VOL. 151 (1983)

AUTHOR INDEX

ɔntinued from outside back cover)

Elsevier Science Publishers B.V., 1983 0003-2670/83/$03.00

nted in The Netherlands.

CONTENTS

(Abstracted, Indexed in: Anal. Abstr.; Biol. Abstr.; Chem. Abstr.; Curr. Contents Phys. Chem. Earth Sci.; Life Sci.; Index Med.; Mass Spectrom. Bull.; Sci. Citation Index; Excerpta Med.)

(continued on inside page of cov